BEILSTEIN JOURNAL OF ORGANIC CHEMISTRY

Modern radical chemistry

Edited by Huan-Ming Huang

Imprint

Beilstein Journal of Organic Chemistry
www.bjoc.org
ISSN 1860-5397
Email: journals-support@beilstein-institut.de

The *Beilstein Journal of Organic Chemistry* is published by the Beilstein-Institut zur Förderung der Chemischen Wissenschaften.

Beilstein-Institut zur Förderung der Chemischen Wissenschaften
Trakehner Straße 7–9
60487 Frankfurt am Main
Germany
www.beilstein-institut.de

BEILSTEIN JOURNAL OF ORGANIC CHEMISTRY

Modern radical chemistry

Huan-Ming Huang

Editorial

Open Access

Address:
School of Physical Science and Technology, ShanghaiTech University, Shanghai 201210, China

Email:
Huan-Ming Huang - huanghm@shanghaitech.edu.cn

Keywords:
catalysis; electrosynthesis; photoredox chemistry; radical chemistry; transition-metal catalysis

Beilstein J. Org. Chem. **2025,** *21,* 945–946.
https://doi.org/10.3762/bjoc.21.77

Received: 17 April 2025
Accepted: 05 May 2025
Published: 15 May 2025

This article is part of the thematic issue "Modern radical chemistry".

Guest Editor: H.-M. Huang

For decades, the synthetic potential of radical chemistry remained largely untapped due to the inherent challenges posed by highly reactive, short-lived radical intermediates. This transient nature led many chemists to favour more predictable ionic pathways, resulting in comparatively slower development of radical methodologies [1]. However, the landscape of organic synthesis has undergone a dramatic transformation in recent years through groundbreaking advances in photoredox chemistry [2-5], transition-metal catalysis [6,7], and electrosynthesis [8]. These innovations have not only overcome historical limitations but have propelled radical chemistry to the forefront of modern synthetic strategy development, which has also appeared as an important synthetic tool in drug discovery, natural product synthesis, and materials science [9,10].

To highlight the cutting-edge developments in this dynamic field, this thematic issue gathers recent reports from leading research groups worldwide. These contributions demonstrate how three key technological advances have reshaped radical chemistry. Piersanti and his team developed an unusual radical decarboxylative cyclization cascade reaction of γ,γ-dimethylallyltryptophan (DMAT) derivatives under visible-light conditions [11]. As a result, various six-, seven-, and eight-membered-ring-3,4-fused tricyclic indoles were afforded, which illustrates the synthetic potential of Ir–polypyridyl complexes as photoredox catalysts. West and co-workers overviewed the concept of radical ligand transfer (RLT) catalysis [12]. Therein, they took a closer look at recent applications in the difunctionalization of alkenes and decarboxylative synthetic transformations, noting that RLT has reemerged as a powerful tool in the design of catalytic radical reactions. Pérez-Luna, Terán, et al. developed an air-promoted radical–polar crossover process involving the 1,4-addition of an alkyl radical, followed by homolytic substitution at the zinc atom of dialkylzinc [13]. In the presence of carbonyl acceptors, aldol condensation occurred, in summary providing a tandem 1,4-addition–aldol process. Yan and team overviewed the radical chemistry in modern polymer science and industry, including radical polymerization, reversible deactivation radical polymerization, and radical depolymerization [14]. Noting that radical chemistry is one of the most important methods used in these fields, they also claimed that a number of powerful emergent radical methodologies are yet to be implemented in polymer science. Lumb and co-worker reviewed the different mechanisms of radical reactions involving *N*-hydroxyphthalimide (NHPI) esters, with an emphasis on recent applications in radical additions, cycliza-

tions, and decarboxylative cross-coupling reactions for complex generation [15]. They suspect that in the future, NHPI esters will be implemented more broadly in radical reactions due to the concomitant development of appropriate new catalysts and increasingly mild reaction conditions. Patureau and colleagues investigated different redox-active phenotellurazine catalysts and their applications in different cross-dehydrogenative couplings [16]. Specifically, they analyzed the effects of various electronic and structural features on the catalytic performance. Ogawa and colleague summarized the addition and cyclization reactions of heteroatom radicals with isocyanides for the construction of nitrogen-containing organic molecules [17]. They noted that a range of useful transformations have been developed, but a current bottleneck is the generation of appropriate heteroatom radicals. Finally, Ogawa, Yamamoto, et al. developed a simple and versatile synthesis of arylboronates by using triarylbismuthines as aryl radical sources under transition-metal-free and open-air conditions [18]. Their method is superior to many existing approaches in the sense that no special setup is required for acyl radical generation from triarylbismuthines.

With this, I extend my sincere appreciation to all authors for their outstanding contributions to this thematic issue. Special thanks goes to the dedicated reviewers and the Editorial Team of the *Beilstein Journal of Organic Chemistry* for their invaluable expertise and support in bringing this collection to fruition.

Huan-Ming Huang

Shanghai, April 2025

Data Availability Statement

Data sharing is not applicable as no new data was generated or analyzed in this study.

References

1. Yan, M.; Lo, J. C.; Edwards, J. T.; Baran, P. S. *J. Am. Chem. Soc.* **2016,** *138,* 12692–12714. doi:10.1021/jacs.6b08856
2. Chan, A. Y.; Perry, I. B.; Bissonnette, N. B.; Buksh, B. F.; Edwards, G. A.; Frye, L. I.; Garry, O. L.; Lavagnino, M. N.; Li, B. X.; Liang, Y.; Mao, E.; Millet, A.; Oakley, J. V.; Reed, N. L.; Sakai, H. A.; Seath, C. P.; MacMillan, D. W. C. *Chem. Rev.* **2022,** *122,* 1485–1542. doi:10.1021/acs.chemrev.1c00383
3. Skubi, K. L.; Blum, T. R.; Yoon, T. P. *Chem. Rev.* **2016,** *116,* 10035–10074. doi:10.1021/acs.chemrev.6b00018
4. Juliá, F.; Constantin, T.; Leonori, D. *Chem. Rev.* **2022,** *122,* 2292–2352. doi:10.1021/acs.chemrev.1c00558
5. Bellotti, P.; Huang, H.-M.; Faber, T.; Glorius, F. *Chem. Rev.* **2023,** *123,* 4237–4352. doi:10.1021/acs.chemrev.2c00478
6. Wang, F.; Chen, P.; Liu, G. *Acc. Chem. Res.* **2018,** *51,* 2036–2046. doi:10.1021/acs.accounts.8b00265
7. Li, Z.-L.; Fang, G.-C.; Gu, Q.-S.; Liu, X.-Y. *Chem. Soc. Rev.* **2020,** *49,* 32–48. doi:10.1039/c9cs00681h
8. Yan, M.; Kawamata, Y.; Baran, P. S. *Chem. Rev.* **2017,** *117,* 13230–13319. doi:10.1021/acs.chemrev.7b00397
9. Campos, K. R.; Coleman, P. J.; Alvarez, J. C.; Dreher, S. D.; Garbaccio, R. M.; Terrett, N. K.; Tillyer, R. D.; Truppo, M. D.; Parmee, E. R. *Science* **2019,** *363,* eaat0805. doi:10.1126/science.aat0805
10. Plesniak, M. P.; Huang, H.-M.; Procter, D. J. *Nat. Rev. Chem.* **2017,** *1,* 0077. doi:10.1038/s41570-017-0077
11. Regni, A.; Bartoccini, F.; Piersanti, G. *Beilstein J. Org. Chem.* **2023,** *19,* 918–927. doi:10.3762/bjoc.19.70
12. Nemoto, D. T., Jr.; Bian, K.-J.; Kao, S.-C.; West, J. G. *Beilstein J. Org. Chem.* **2023,** *19,* 1225–1233. doi:10.3762/bjoc.19.90
13. Palillero-Cisneros, A.; Gordillo-Guerra, P. G.; García-Alvarez, F.; Jackowski, O.; Ferreira, F.; Chemla, F.; Terán, J. L.; Perez-Luna, A. *Beilstein J. Org. Chem.* **2023,** *19,* 1443–1451. doi:10.3762/bjoc.19.103
14. Wang, Z.; Cui, F.; Sui, Y.; Yan, J. *Beilstein J. Org. Chem.* **2023,** *19,* 1580–1603. doi:10.3762/bjoc.19.116
15. Azpilcueta-Nicolas, C. R.; Lumb, J.-P. *Beilstein J. Org. Chem.* **2024,** *20,* 346–378. doi:10.3762/bjoc.20.35
16. Paffen, A.; Cremer, C.; Patureau, F. W. *Beilstein J. Org. Chem.* **2024,** *20,* 1292–1297. doi:10.3762/bjoc.20.112
17. Ogawa, A.; Yamamoto, Y. *Beilstein J. Org. Chem.* **2024,** *20,* 2114–2128. doi:10.3762/bjoc.20.182
18. Yamamoto, Y.; Konakazawa, Y.; Fujiwara, K.; Ogawa, A. *Beilstein J. Org. Chem.* **2024,** *20,* 2577–2584. doi:10.3762/bjoc.20.216

License and Terms

BEILSTEIN JOURNAL OF ORGANIC CHEMISTRY

Photoredox catalysis enabling decarboxylative radical cyclization of γ,γ-dimethylallyltryptophan (DMAT) derivatives: formal synthesis of 6,7-secoagroclavine

Alessio Regni, Francesca Bartoccini and Giovanni Piersanti*

Full Research Paper

Open Access

Address:
Department of Biomolecular Sciences, University of Urbino, Carlo Bo Piazza Rinascimento 6, 61029 Urbino, PU, Italy

Email:
Giovanni Piersanti* - giovanni.piersanti@uniurb.it

* Corresponding author

Keywords:
decarboxylative cyclization; DMAT; ergot alkaloids; photoredox catalysis; radicals

Beilstein J. Org. Chem. **2023,** *19,* 918–927.
https://doi.org/10.3762/bjoc.19.70

Received: 15 February 2023
Accepted: 15 June 2023
Published: 26 June 2023

This article is part of the thematic issue "Modern radical chemistry".

Guest Editor: H.-M. Huang

Abstract

An unusual photoredox-catalyzed radical decarboxylative cyclization cascade reaction of γ,γ-dimethylallyltryptophan (DMAT) derivatives containing unactivated alkene moieties has been developed, providing green and efficient access to various six-, seven-, and eight-membered ring 3,4-fused tricyclic indoles. This type of cyclization, which was hitherto very difficult to comprehend in ergot biosynthesis and to accomplish by more conventional procedures, enables the synthesis of ergot alkaloid precursors. In addition, this work describes a mild, environmentally friendly method to activate, reductively and oxidatively, natural carboxylic acids for decarboxylative C–C bond formation by exploiting the same photocatalyst.

Introduction

Visible-light photoredox catalysis is rapidly changing the way organic chemists approach the design and synthesis of molecules by offering new synthetic disconnection opportunities that are usually more convergent, enabling a more diverse chemical space in a rapid fashion [1-15]. Currently, increasing numbers of synthetic chemists are developing photocatalytic processes to make molecules efficiently and in an environmentally friendly manner due to their intrinsic mildness and broad substrate compatibility [16-20]. This transformative synthetic tool often utilizes direct single-electron transfer (SET) between an electronically excited photoredox catalyst and an organic substrate, resulting in oxidation or reduction, to easily generate reactive open-shell radical species and/or intermediates. The substrate is consequently activated for bond cleavage, atom abstraction, or nucleophilic or electrophilic attack. After quenching, the oxidized or reduced photocatalyst regains or loses an electron to return to the starting ground state catalyst [21-26].

While early research has focused on methods for the functionalization of relatively simple hydrocarbons [27-30], develop-

ments in photoredox catalysis have gained traction recently as a viable strategy for the total synthesis of natural products [31-33], modification of biomacromolecules [34], and relatively complex pharmaceutical agents [35-38]. Photocatalysis tremendously enriches the synthetic compound library, providing a precious alternative to directly modify abundant natural substrates, including biomass, which usually requires a multistep process in conventional chemical synthesis [39-41]. Among the various widely available and abundant substrates for photocatalyzed reactions, natural and unnatural α-amino acids play a very important role, given their paramount importance across several chemistry fields as well as their ability to participate in either redox step of the catalytic cycle [42-45]. For example, the main use of α-amino acids in syntheses via photoredox catalysis is as readily available precursors of regioselective α-amino radicals by decarboxylative transformations, by oxidation of the carboxylate anion and/or reduction of the corresponding *N*-hydroxyphthalimide- (NHPI)-derived redox-active ester, although it destroys their stereochemical information [46-51]. In addition, the side-chains of aromatic amino acids (mainly electron-rich tryptophan and tyrosine) can be selectively targeted by photoredox catalysis to enable unprecedented modification of the amino acid. In this context, it is worth mentioning that the single-electron oxidation of the indole moiety in tryptophan provides the radical cation, which enables selective C-radical generation at the weaker benzylic position via a sequential electron transfer–proton transfer (ET/PT) [52-59].

With our ongoing interest of establishing new methods for the asymmetric synthesis of nonproteinogenic tryptophan derivatives as well as their associated indole alkaloid natural products [60-67], we became fascinated in exploring whether photoredox catalysis could be applied for the activation of such unnatural amino acids to expedite the development of completely new synthetic pathways. In particular, 4-dimethylallyltryptophan (DMAT) is of interest for the following reasons: 1) it functions as the central intermediate in the biosynthetic pathways leading to numerous prenylated indole alkaloids, such as ergot alkaloids in normal biosynthesis and clavicipitic acid in derailment biosynthesis [68-71]; and 2) the mechanism of the fundamental central C-ring formation of all ergot alkaloids, specifically the decarboxylative cyclization of DMAT, is still a puzzle even though a radical mechanism has been proposed (Figure 1a) [72,73].

Results and Discussion

Herein, we propose that visible light irradiation of the cationic iridium photocatalyst Ir[dF(CF$_3$)ppy]$_2$(dtbbpy)PF$_6$ ($E_{1/2}^{*III/II}$ = +1.21 V, $E_{1/2}^{III/II}$ = −1.37; $E_{1/2}^{IV/*III}$ = −0.89, $E_{1/2}^{IV/III}$ = +1.69 V) [74] would permit efficient radical generation and

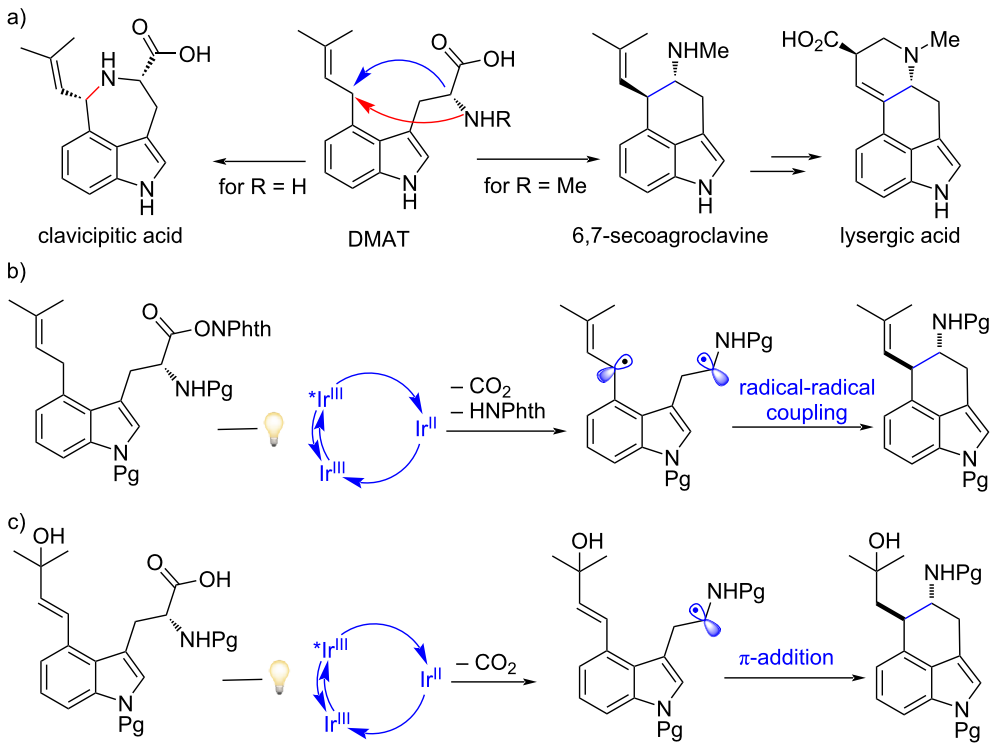

Figure 1: (a) Transformations of DMAT to different classes of ergot alkaloids. (b) and (c) Strategies for the photoredox-catalyzed radical decarboxylative cyclization cascade reaction of DMAT derivatives (this work).

$C(sp^3)$–$C(sp^3)$ bond formation either by challenging selective radical–radical cross-coupling or by radical addition to a π-bond, enabling a rare example of intramolecular decarboxylative cyclization with the formation of the 3,4-fused indole carbocycle rings (Figure 1b,c). In detail, the photocatalytic strategy for accessing the two $C(sp^3)$ radicals of DMAT derivatives envision the formation of a relatively stabilized allylic-benzylic carbon-centered radical by proton transfer from the oxidized indole radical cation [75], generated by SET from the activated photocatalyst. The α-amino radical generated by reductive decarboxylation of a DMAT derivative with a redox-active ester (−1.26 V to −1.37 V vs a saturated calomel electrode) would enable turnover of the photoredox cycle (Figure 1b). Alternatively, we envisioned a more established approach expecting the direct oxidative photoredox decarboxylation of the carboxylic acid/carboxylate (by SET from the activated photocatalyst) of DMAT to generate the α-aminoalkyl radical that might readily be captured/trapped intramolecularly with the C4-pendant prenyl side-chain previously oxidized [76]. Closure of the photoredox catalytic cycle would then involve SET reduction, and protonation would deliver the desired carbocyclic ring (Figure 1c). If this cyclization reaction could be realized in either way, it would shorten the synthetic route of ergot alkaloids and may offer new opportunities for drug discovery and biochemistry applications.

As natural and unnatural tryptophan-derived redox-active *N*-hydroxyphthalimide esters have already been used in photoredox catalysis, we decided to use them as the initial substrates [77-85]. To test this concept, we turned our attention to the synthesis of key intermediate **5** (Scheme 1). The synthesis began with protection of the indole nitrogen of the known compound **1**, which is readily available from commercially available 4-bromoindole in one step [62]. Regioselective palladium-catalyzed prenylation of **2** with prenylboronic acid pinacol ester and subsequent hydrolysis with LiOH provided the linear prenylated acid **4** in good yield. Coupling acid **4** with *N*-hydroxyphthalimide using DCC and a catalytic amount of DMAP afforded the key intermediate **5** in 59% yield.

With compound **5** in hand, the required radical–radical coupling was investigated next, and some of the representative results are shown in Table S1 (see Supporting Information File 1). Irradiation from blue light-emitting diodes (LEDs) in the presence of 2 mol % of the photocatalyst $[Ir(dF(CF_3)ppy)_2(dtbpy)]PF_6$ in CH_2Cl_2 at room temperature using our integrated photoreactor enabled efficient cyclization to give a decarboxylated compound with the correct mass (*m*/*z* 426.2) after 16 h. While we were delighted to find that the proposed radical–radical coupling in the synthesis of extracyclic fused indoles was feasible under these conditions, the observed reaction efficiency was poor (14–33% yield). However, on the ^1H NMR spectrum, some unexpected signals were observed. The appearance of equilibrating species such as rotamers in the ^1H NMR spectrum (see the variable-temperature NMR experiments in Supporting Information File 1, Figure S1) due to the protecting groups complicates the analysis of the reaction products. However, the olefinic signals were a pair of two doublets representing two vicinal vinylic protons [6.48 (d, *J* = 8.0 Hz, 1H), 6.29 (d, *J* = 8.0 Hz, 1H), 5.31 (d, *J* = 8.0 Hz, 1H), and 5.28 (d, *J* = 8.0 Hz, 1H)], strongly indicating that this product is not the desired structure **6'** but the eight-membered cycloalkene structure **6**, shown in Scheme 2. Based on these results and previous reports on the benzylic and allylic C–H bond functionalization enabled by metallaphotoredox catalysis [86], we propose a tentative mechanism (Figure 2).

First, the radical cation **I** was generated via the oxidation of indole **5** by the excited Ir-based photocatalyst, followed by sequential regioselective proton transfer on the benzylic

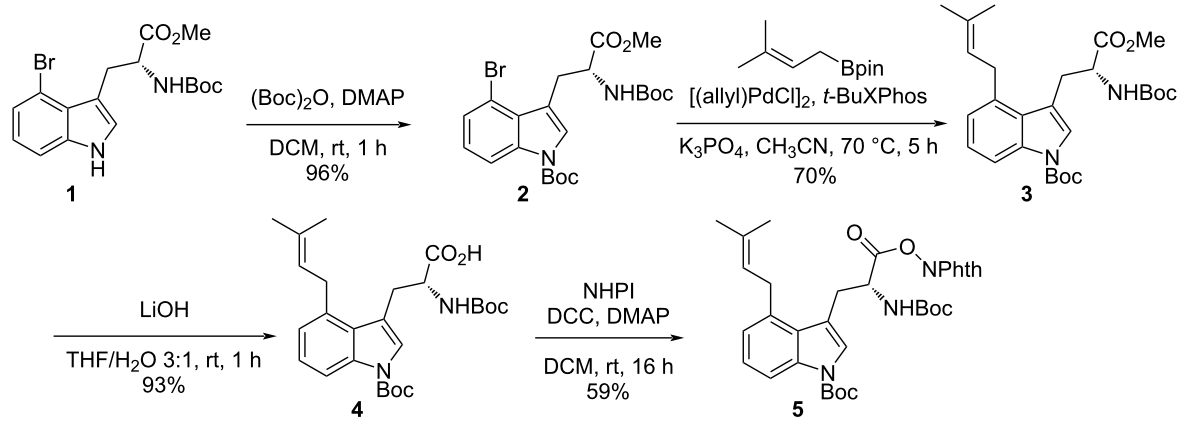

Scheme 1: Synthesis of compound **5**.

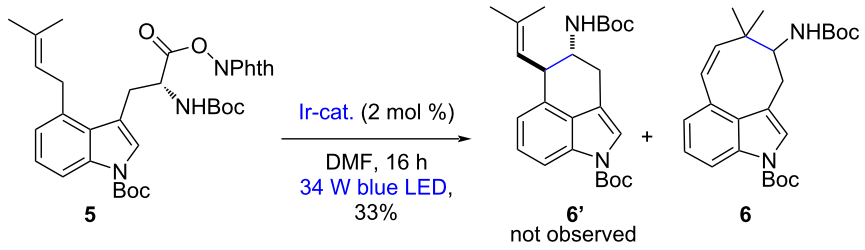

Scheme 2: Photoredox-catalyzed radical decarboxylative cyclization of **5**.

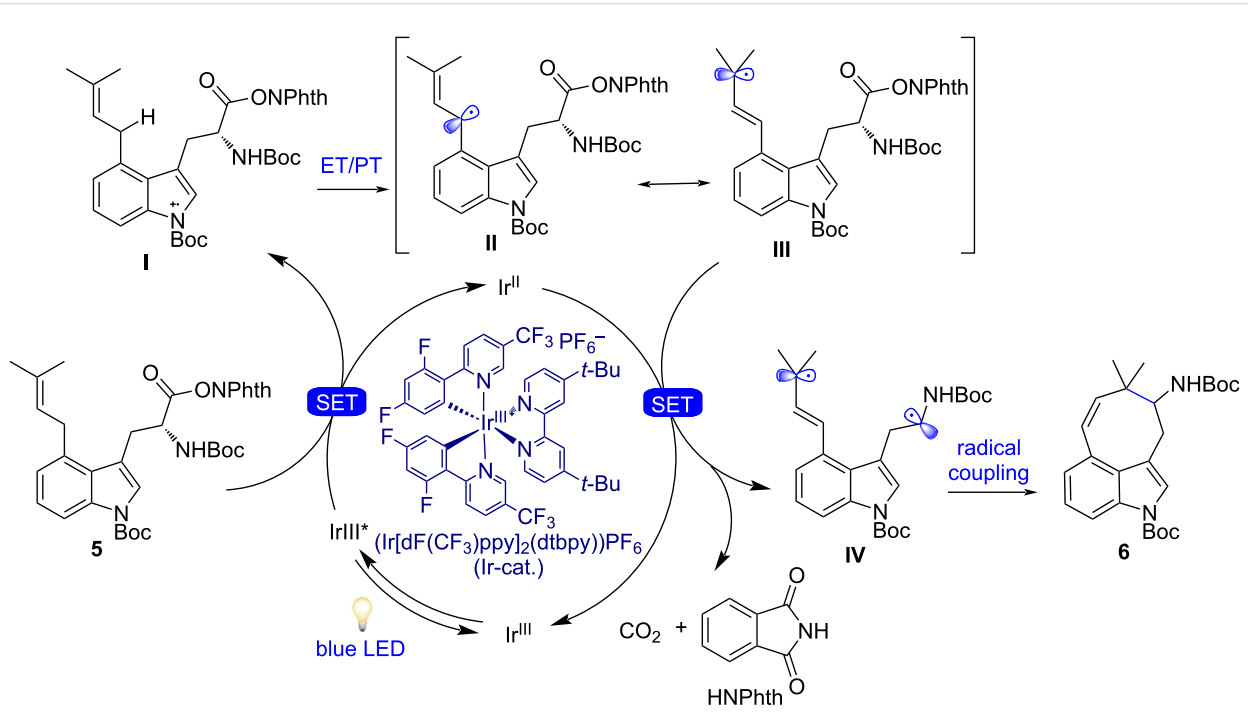

Figure 2: Proposed reaction mechanism for photoredox-catalyzed radical decarboxylative cyclization.

dimethylallyl unit C–H bond of the C4 side-chain, thereby generating **II**. Here, the radical is stabilized by both the indole ring and the Δ2-olefin. Next, the resonance-stabilized radical intermediate **III** was trapped by the active α-aminoalkyl radical, generated by reductive decarboxylation by Ir(II) produced in the photocatalytic cycle (which undergoes oxidation to afford the Ir(III) complex and to close the cycle), thus furnishing compound **6** comprised of an eight-membered ring. The related stabilization effect of the conjugated product **6** might be the thermodynamic driving force for this radical coupling. An alternative route (not showen) would be that, the α-amidoalkyl radical generated by reductive decarboxylation, could add in an 8-*endo*-trig manner (common in radical chemistry) to the alkene and the resulting radical could be oxidized to the cation by the oxidized form of the photocatalyst to close the photocatalytic cycle, followed by formation of the double bond. Even though no desired cyclized product was observed, an interesting aspect of this reaction was the access of an attractive, unusual, and highly functionalized 3,4-fused eight-membered tricyclic indole, whose ring closure would not have been possible or at least very difficult in the ground state [87-89].

Although not yet completely clarified, some previous studies on the detailed mode of closure of the C ring in ergot alkaloids from DMAT have been shown to involve, before decarboxylative cyclization, oxidation on the C4-prenyl chain to give the stable rearranged allyl alcohol and/or the relatively unstable diene [90,91]. In addition, these results support the hypothesis that the decarboxylative cyclization can occur through subsequent selective 6-*exo*-trig radical addition. It also has been reported that it is difficult to detect which intermediate is really involved, since they are easily interconvertible to each other by

hydration or dehydration, i.e., a plausible precursor of the allylic alcohol would be the diene, and vice versa [90]. Since both **8** and **10** are easily obtainable from **2** by Mozoroki–Heck coupling with commercially available 2-methyl-3-buten-2-ol, ester hydrolysis (LiOH in THF/H_2O), and, finally for **10**, dehydration of the tertiary alcohol (mesylation and elimination) (Scheme 3), we decided to test their roles in the photoredox-catalyzed decarboxylative cyclization. With **8** and **10** in hand with the C4-prenyl side-chain already oxidized/functionalized, we recognized that this cyclization event would be triggered using their innate functionality, namely the α-amino carboxylate, through photoredox-mediated oxidative activation and CO_2 extrusion, without the need for acid prefunctionalization to the redox-activated ester. Consequently, a technique involving direct generation of α-aminoalkyl radicals from free carboxylic acids of **8** and **10** under mild conditions would make the approach even more efficient and more biosimilar; nevertheless, issues regarding the regioselectivity of the ring formation could be raised, since both the 6-*exo*-trig and 7-*endo*-trig cyclization are both favorable, according to the Baldwin rules [92].

We began our investigation of the proposed decarboxylative cyclization by exposing the *N*-Boc derivative **8**, Ir catalyst, and K_2HPO_4 in DMF to a 34 W blue LED lamp at room temperature (Table 1) [93-97]. To our delight, cyclization was observed under these preliminary conditions, albeit in low yield (35% yield) and low regioselectivity (1:1) (Table 1, entry 1). No regiocontrol was observed; but remarkably, the regioisomers exhibited distinct retention factors on silica gel, allowing **11** and **12** to be isolated separately in good yield as single *trans* diastereomers [98]. Reducing the substrate concentration increased efficiency while assisting in avoiding the oligomerization pathways (Table 1, entries 2 and 3). Higher photocatalyst loadings resulted in an increased yield (Table 1, entry 4). Control experiments showed that both the photocatalyst and light were essential for product production (Table 1, entries 6 and 7), despite the fact that the removal of base did not result in a significantly reduced efficiency (Table 1, entry 5). The regioselectivity outcome was explained by the relative stability of the intermediate radicals involved, with strong evidence of the importance of steric effects [99]. Indeed, while the addition of the nucleophilic α-amino radical to the α-styrenyl position affords the 6-membered ring (kinetic product via intramolecular 6-*exo*-trig ring closure) [100] the resulting radical is unstabilized, the 7-membered ring (obtained via intramolecular 7-*endo*-trig ring closure) may well be the thermodynamic product based on the more stabilized benzylic radical that is produced [101].

As largely reported in the literature [102,103], radicals generated next to alcohols do not normally undergo β-elimination to give alkene/carbon–carbon double-bond formation and a hydroxyl radical (•OH). However, it is possible to transform an alcohol into a leaving group, in the radical sense, by converting it into a halide or pseudohalide derivative [104,105]. For alcohol **8**, all attempts to make a better leaving group, including phenyl sulfone derivative, to have radical addition–fragmentation on the latter and most likely to shift the regioselectivity towards 6-*exo*-trig by a favorable interplay of polar effects [99] failed and furnished only the 1,3-diene **10**. Unfortunately, when substrate **10** was subjected to the reaction conditions shown above, only tarry compounds were obtained; this result was probably due to the competitive cycloaddition and polymeriza-

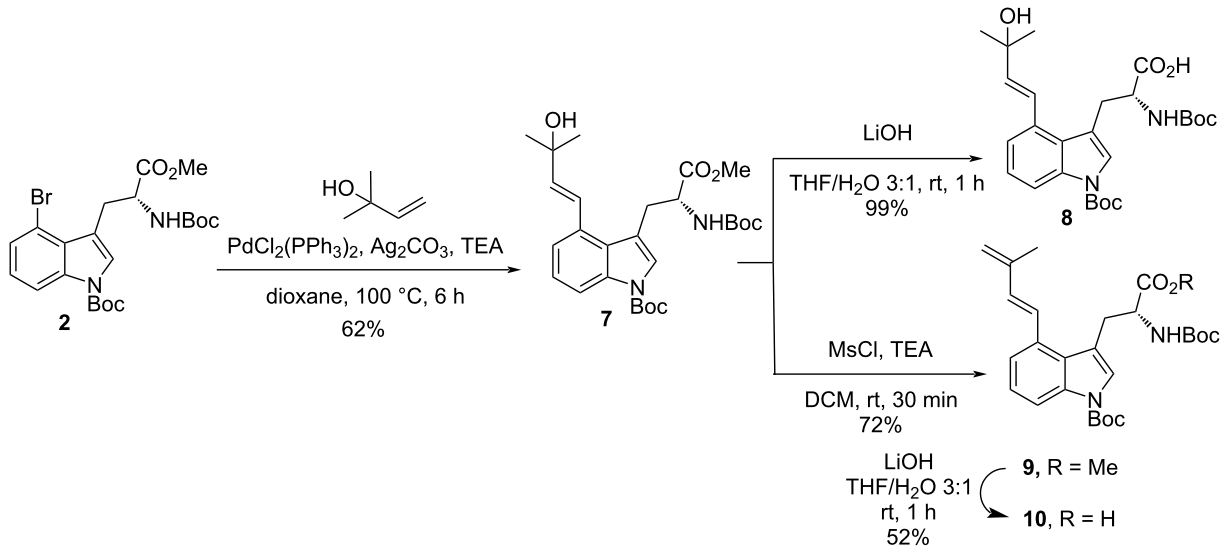

Scheme 3: Synthesis of tryptophan derivatives **8** and **10**.

Table 1: Photoredox-catalyzed radical decarboxylative cyclization of **8**.[a]

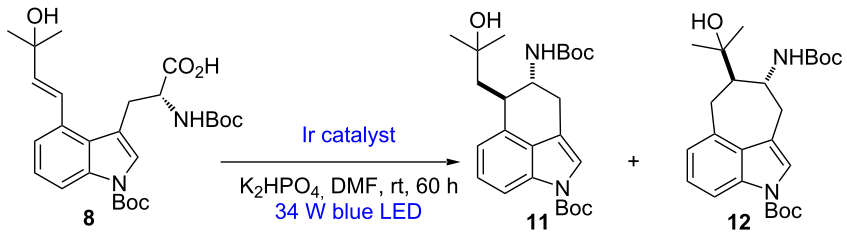

Entry	Conditions	Concentration of **8**	Ir catalyst (mol %)	Ratio of **11**/**12**[b]	Yield of **11** and **12**[c]
1	as shown	10 mM	2	1:1	35%
2	as shown	5 mM	2	1:0.7	39%
3	as shown	2.5 mM	2	1:0.6	42%
4	as shown	2.5 mM	4	1:0.7	59%
5	no base	2.5 mM	4	1:0.7	53%
6	no photocatalyst	2.5 mM	–	–	N.D.[d]
7	no light	2.5 mM	4	–	N.D.[d]
8	DMSO instead of DMF	2.5 mM	4	0.7:1	33%
9	DCE instead of DMF	2.5 mM	4	1:0.7	40%

[a]Reaction conditions: **8** (0.1 mmol), K_2HPO_4 (0.12 mmol), catalyst (*x* mol %), solvent (4 mL), irradiation with 34 W blue LEDs for 60 h. [b]Ratio of **11**/**12** was determined by ^{1}H NMR analysis. [c]Isolated yields. [d]N.D., not detected.

tion reactions and decomposition of the diene moiety, which is unstable and very sensitive to acidic and basic conditions [106].

As shown in Figure 3 and anticipated above, our proposed mechanism begins with visible-light irradiation of the photoredox catalyst $[Ir(dF(CF_3)ppy)_2(dtbpy)]PF_6$ to access the excited state $*[Ir(dF(CF_3)ppy)_2(dtbpy)]PF_6$, which can trigger SET oxidation of **8**. Rapid decarboxylation leads to α-amino radical **V** (and the reduced photocatalyst), which is intercepted by the pendant double bond to forge the desired six-membered ring through a key C–C bond formation while furnishing secondary radical **VI** and the undesired seven-membered-ring compound **VII**. Closure of the photoredox catalytic cycle would then involve either SET reduction of the radical **VI** and **VII** (which upon protonation would deliver the desired product **11** and the undesired product **12**), or an hydrogen-atom-transfer

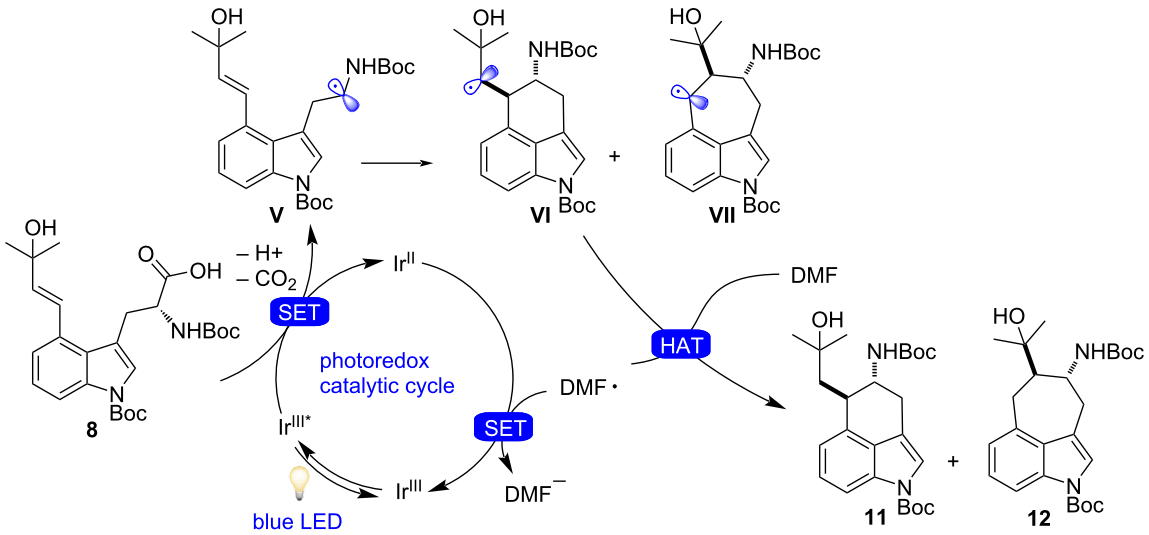

Figure 3: Proposed reaction mechanism for photoredox-catalyzed radical decarboxylative cyclization.

(HAT) process (which would not place a formal negative charge onto the molecule), where the hydrogen atom required for this possible final HAT step originates from the solvent (DMF) itself [107]. Therefore, we tested the reaction in *N*,*N*-dimethylformamide-d_7 (DMF-d_7), which showed almost quantitative deuterium incorporation. While this result was surprising, further studies into this complex mechanism are ongoing and will be reported in due course.

The synthetic potential and utility of this method was further demonstrated by the formal total synthesis of (±)-6,7-secoagroclavine (Scheme 4) [108-114]. Towards this end, compound **11** was methylated efficiently and selectively at the secondary amide by treatment with methyl iodide in DMF to afford compound **13**. In additional two steps, intermediate **13** was transformed to (±)-6,7-secoagroclavine in enantiopure form, as reported previously by the Bisai group in 2018 [115]. All the spectroscopic data of **13** were in agreement with those reported in the literature, confirming that the radical addition reaction provided the *trans* amino group due to steric hindrance.

Conclusion

In summary, this work illustrates, once more, the synthetic potential of an Ir-polypyridyl complex as a photoredox catalyst that can efficiently convert visible light into chemical energy. In addition, this catalyst was applied to demonstrate the proposed radical mechanism involved in the biosynthetic formation of the central C ring of several DMAT derivatives. The results presented here lend strong credence to decarboxylation and cyclization to form the six-membered ring as well as the nature of the stable oxidized intermediates concerned. Moreover, unprecedented and functionalized 3,4-fused tricyclic indoles with medium-sized rings (seven and eight), which have been largely neglected in previous studies, can be synthesized by this new protocol. Notably, the reaction has been successfully applied in the formal synthesis of (±)-6,7-secoagroclavine, a key intermediate for a common synthetic route to ergot alkaloids, providing an advantageous synthetic method for this class of natural products. Further studies on the utility of the decarboxylative radical cyclization and their applications are currently being investigated in our laboratory.

Supporting Information

Supporting Information File 1

Experimental and copies of spectra.
[https://www.beilstein-journals.org/bjoc/content/supplementary/1860-5397-19-70-S1.pdf]

Acknowledgements

The authors thank Dott. Michele Retini for helpful discussion. We also thank Dott. Vittorio Ciccone, an undergraduate student in the Piersanti group, for preliminary exploratory studies. Prof. Michele Menotta and Federica Biancucci for assistance with HRMS analysis.

Funding

This work was supported by the Italian Ministry for University and Research (MUR, PRIN 2020, 2020AEX4TA project) and University of Urbino grants (DISB_PIERSANTI_PROG_SIC_ALIMENTARE).

ORCID® iDs

Alessio Regni - https://orcid.org/0000-0002-2188-1789
Francesca Bartoccini - https://orcid.org/0000-0003-0400-7771
Giovanni Piersanti - https://orcid.org/0000-0003-0418-7143

References

1. Nicewicz, D. A.; MacMillan, D. W. C. *Science* **2008,** *322,* 77–80. doi:10.1126/science.1161976
2. Ischay, M. A.; Anzovino, M. E.; Du, J.; Yoon, T. P. *J. Am. Chem. Soc.* **2008,** *130,* 12886–12887. doi:10.1021/ja805387f
3. Narayanam, J. M. R.; Tucker, J. W.; Stephenson, C. R. J. *J. Am. Chem. Soc.* **2009,** *131,* 8756–8757. doi:10.1021/ja9033582
4. Narayanam, J. M. R.; Stephenson, C. R. J. *Chem. Soc. Rev.* **2011,** *40,* 102–113. doi:10.1039/b913880n
5. Xuan, J.; Xiao, W.-J. *Angew. Chem., Int. Ed.* **2012,** *51,* 6828–6838. doi:10.1002/anie.201200223

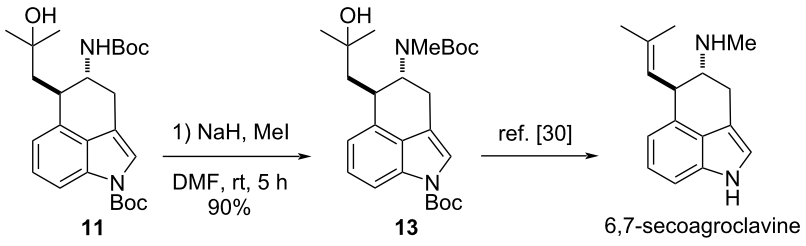

Scheme 4: Methylation of **11** and the formal total synthesis of (±)-6,7-secoagroclavine.

6. Prier, C. K.; Rankic, D. A.; MacMillan, D. W. C. *Chem. Rev.* **2013,** *113,* 5322–5363. doi:10.1021/cr300503r
7. Schultz, D. M.; Yoon, T. P. *Science* **2014,** *343,* 1239176. doi:10.1126/science.1239176
8. Ravelli, D.; Protti, S.; Fagnoni, M. *Chem. Rev.* **2016,** *116,* 9850–9913. doi:10.1021/acs.chemrev.5b00662
9. Shaw, M. H.; Twilton, J.; MacMillan, D. W. C. *J. Org. Chem.* **2016,** *81,* 6898–6926. doi:10.1021/acs.joc.6b01449
10. Tellis, J. C.; Kelly, C. B.; Primer, D. N.; Jouffroy, M.; Patel, N. R.; Molander, G. A. *Acc. Chem. Res.* **2016,** *49,* 1429–1439. doi:10.1021/acs.accounts.6b00214
11. Marzo, L.; Pagire, S. K.; Reiser, O.; König, B. *Angew. Chem., Int. Ed.* **2018,** *57,* 10034–10072. doi:10.1002/anie.201709766
12. McAtee, R. C.; McClain, E. J.; Stephenson, C. R. J. *Trends Chem.* **2019,** *1,* 111–125. doi:10.1016/j.trechm.2019.01.008
13. Zhu, C.; Yue, H.; Chu, L.; Rueping, M. *Chem. Sci.* **2020,** *11,* 4051–4064. doi:10.1039/d0sc00712a
14. Stephenson, C.; Yoon, T.; MacMillan, D. W. C. *Visible Light Photocatalysis in Organic Chemistry;* Wiley-VCH: Weinheim, Germany, 2018. doi:10.1002/9783527674145
15. König, B., Ed. *Chemical Photocatalysis,* 2nd ed.; De Gruyter: Berlin, Germany, 2020. doi:10.1515/9783110576764
16. Yoon, T. P.; Ischay, M. A.; Du, J. *Nat. Chem.* **2010,** *2,* 527–532. doi:10.1038/nchem.687
17. Oelgemöller, M. *Chem. Rev.* **2016,** *116,* 9664–9682. doi:10.1021/acs.chemrev.5b00720
18. Cambié, D.; Bottecchia, C.; Straathof, N. J. W.; Hessel, V.; Noël, T. *Chem. Rev.* **2016,** *116,* 10276–10341. doi:10.1021/acs.chemrev.5b00707
19. Zhou, L.; Lokman Hossain, M.; Xiao, T. *Chem. Rec.* **2016,** *16,* 319–334. doi:10.1002/tcr.201500228
20. Crisenza, G. E. M.; Melchiorre, P. *Nat. Commun.* **2020,** *11,* 803. doi:10.1038/s41467-019-13887-8
21. Romero, N. A.; Nicewicz, D. A. *Chem. Rev.* **2016,** *116,* 10075–10166. doi:10.1021/acs.chemrev.6b00057
22. Capaldo, L.; Ravelli, D.; Fagnoni, M. *Chem. Rev.* **2022,** *122,* 1875–1924. doi:10.1021/acs.chemrev.1c00263
23. Cao, H.; Tang, X.; Tang, H.; Yuan, Y.; Wu, J. *Chem Catal.* **2021,** *1,* 523–598. doi:10.1016/j.checat.2021.04.008
24. Bell, J. D.; Murphy, J. A. *Chem. Soc. Rev.* **2021,** *50,* 9540–9685. doi:10.1039/d1cs00311a
25. Buzzetti, L.; Crisenza, G. E. M.; Melchiorre, P. *Angew. Chem., Int. Ed.* **2019,** *58,* 3730–3747. doi:10.1002/anie.201809984
26. Arias-Rotondo, D. M.; McCusker, J. K. *Chem. Soc. Rev.* **2016,** *45,* 5803–5820. doi:10.1039/c6cs00526h
27. Ciamician, G. *Science* **1912,** *36,* 385–394. doi:10.1126/science.36.926.385
28. Klán, P.; Wirz, J. *Photochemistry of Organic Compounds: From Concepts to Practice;* John Wiley & Sons: Chichester, UK, 2009. doi:10.1002/9781444300017
29. Hu, A.; Guo, J.-J.; Pan, H.; Zuo, Z. *Science* **2018,** *361,* 668–672. doi:10.1126/science.aat9750
30. Laudadio, G.; Deng, Y.; van der Wal, K.; Ravelli, D.; Nuño, M.; Fagnoni, M.; Guthrie, D.; Sun, Y.; Noël, T. *Science* **2020,** *369,* 92–96. doi:10.1126/science.abb4688
31. Nicholls, T. P.; Leonori, D.; Bissember, A. C. *Nat. Prod. Rep.* **2016,** *33,* 1248–1254. doi:10.1039/c6np00070c
32. Liu, X.-Y.; Qin, Y. *Acc. Chem. Res.* **2019,** *52,* 1877–1891. doi:10.1021/acs.accounts.9b00246
33. Pitre, S. P.; Overman, L. E. *Chem. Rev.* **2022,** *122,* 1717–1751. doi:10.1021/acs.chemrev.1c00247
34. Lechner, V. M.; Nappi, M.; Deneny, P. J.; Folliet, S.; Chu, J. C. K.; Gaunt, M. J. *Chem. Rev.* **2022,** *122,* 1752–1829. doi:10.1021/acs.chemrev.1c00357
35. Capaldo, L.; Quadri, L. L.; Ravelli, D. *Green Chem.* **2020,** *22,* 3376–3396. doi:10.1039/d0gc01035a
36. Douglas, J. J.; Sevrin, M. J.; Stephenson, C. R. J. *Org. Process Res. Dev.* **2016,** *20,* 1134–1147. doi:10.1021/acs.oprd.6b00125
37. Li, P.; Terrett, J. A.; Zbieg, J. R. *ACS Med. Chem. Lett.* **2020,** *11,* 2120–2130. doi:10.1021/acsmedchemlett.0c00436
38. Candish, L.; Collins, K. D.; Cook, G. C.; Douglas, J. J.; Gómez-Suárez, A.; Jolit, A.; Keess, S. *Chem. Rev.* **2022,** *122,* 2907–2980. doi:10.1021/acs.chemrev.1c00416
39. Nguyen, S. T.; Murray, P. R. D.; Knowles, R. R. *ACS Catal.* **2020,** *10,* 800–805. doi:10.1021/acscatal.9b04813
40. Zhang, J. *ChemSusChem* **2018,** *11,* 3071–3080. doi:10.1002/cssc.201801370
41. Scott, E.; Peter, F.; Sanders, J. *Appl. Microbiol. Biotechnol.* **2007,** *75,* 751–762. doi:10.1007/s00253-007-0932-x
42. Liu, J.-Q.; Shatskiy, A.; Matsuura, B. S.; Kärkäs, M. D. *Synthesis* **2019,** *51,* 2759–2791. doi:10.1055/s-0037-1611852
43. Bottecchia, C.; Noël, T. *Chem. – Eur. J.* **2019,** *25,* 26–42. doi:10.1002/chem.201803074
44. Aguilar Troyano, F. J.; Merkens, K.; Anwar, K.; Gómez-Suárez, A. *Angew. Chem., Int. Ed.* **2021,** *60,* 1098–1115. doi:10.1002/anie.202010157
45. King, T. A.; Mandrup Kandemir, J.; Walsh, S. J.; Spring, D. R. *Chem. Soc. Rev.* **2021,** *50,* 39–57. doi:10.1039/d0cs00344a
46. Zuo, Z.; MacMillan, D. W. C. *J. Am. Chem. Soc.* **2014,** *136,* 5257–5260. doi:10.1021/ja501621q
47. Schwarz, J.; König, B. *Green Chem.* **2016,** *18,* 4743–4749. doi:10.1039/c6gc01101b
48. Liao, L.-L.; Cao, G.-M.; Jiang, Y.-X.; Jin, X.-H.; Hu, X.-L.; Chruma, J. J.; Sun, G.-Q.; Gui, Y.-Y.; Yu, D.-G. *J. Am. Chem. Soc.* **2021,** *143,* 2812–2821. doi:10.1021/jacs.0c11896
49. Li, Y.; Dai, C.; Xie, S.; Liu, P.; Sun, P. *Org. Lett.* **2021,** *23,* 5906–5910. doi:10.1021/acs.orglett.1c02014
50. Xuan, J.; Zhang, Z.-G.; Xiao, W.-J. *Angew. Chem., Int. Ed.* **2015,** *54,* 15632–15641. doi:10.1002/anie.201505731
51. Rahman, M.; Mukherjee, A.; Kovalev, I. S.; Kopchuk, D. S.; Zyryanov, G. V.; Tsurkan, M. V.; Majee, A.; Ranu, B. C.; Charushin, V. N.; Chupakhin, O. N.; Santra, S. *Adv. Synth. Catal.* **2019,** *361,* 2161–2214. doi:10.1002/adsc.201801331
52. Schmittel, M.; Burghart, A. *Angew. Chem., Int. Ed. Engl.* **1997,** *36,* 2550–2589. doi:10.1002/anie.199725501
53. Roth, H. G.; Romero, N. A.; Nicewicz, D. A. *Synlett* **2016,** *27,* 714–723. doi:10.1055/s-0035-1561297
54. Yu, Y.; Zhang, L.-K.; Buevich, A. V.; Li, G.; Tang, H.; Vachal, P.; Colletti, S. L.; Shi, Z.-C. *J. Am. Chem. Soc.* **2018,** *140,* 6797–6800. doi:10.1021/jacs.8b03973
55. Laroche, B.; Tang, X.; Archer, G.; Di Sanza, R.; Melchiorre, P. *Org. Lett.* **2021,** *23,* 285–289. doi:10.1021/acs.orglett.0c03735
56. Rahimidashaghoul, K.; Klimánková, I.; Hubálek, M.; Matoušek, V.; Filgas, J.; Slavíček, P.; Slanina, T.; Beier, P. *ChemPhotoChem* **2021,** *5,* 43–50. doi:10.1002/cptc.202000214
57. Lima, R. N.; Delgado, J. A. C.; Bernardi, D. I.; Berlinck, R. G. S.; Kaplaneris, N.; Ackermann, L.; Paixão, M. W. *Chem. Commun.* **2021,** *57,* 5758–5761. doi:10.1039/d1cc01822a

58. Weng, Y.; Ding, B.; Liu, Y.; Song, C.; Chan, L.-Y.; Chiang, C.-W. *Org. Lett.* **2021,** *23,* 2710–2714. doi:10.1021/acs.orglett.1c00609
59. Hoopes, C. R.; Garcia, F. J.; Sarkar, A. M.; Kuehl, N. J.; Barkan, D. T.; Collins, N. L.; Meister, G. E.; Bramhall, T. R.; Hsu, C.-H.; Jones, M. D.; Schirle, M.; Taylor, M. T. *J. Am. Chem. Soc.* **2022,** *144,* 6227–6236. doi:10.1021/jacs.1c10536
60. Bartoccini, F.; Regni, A.; Retini, M.; Piersanti, G. *Eur. J. Org. Chem.* **2022,** e202200315. doi:10.1002/ejoc.202200315
61. Bartoccini, F.; Regni, A.; Retini, M.; Piersanti, G. *Org. Biomol. Chem.* **2021,** *19,* 2932–2940. doi:10.1039/d1ob00353d
62. Bartoccini, F.; Fanini, F.; Retini, M.; Piersanti, G. *Tetrahedron Lett.* **2020,** *61,* 151923. doi:10.1016/j.tetlet.2020.151923
63. Bartoccini, F.; Venturi, S.; Retini, M.; Mari, M.; Piersanti, G. *J. Org. Chem.* **2019,** *84,* 8027–8034. doi:10.1021/acs.joc.9b00879
64. Bartoccini, F.; Bartolucci, S.; Mari, M.; Piersanti, G. *Org. Biomol. Chem.* **2016,** *14,* 10095–10100. doi:10.1039/c6ob01791f
65. Bartoccini, F.; Casoli, M.; Mari, M.; Piersanti, G. *J. Org. Chem.* **2014,** *79,* 3255–3259. doi:10.1021/jo500245s
66. Lucarini, S.; Bartoccini, F.; Battistoni, F.; Diamantini, G.; Piersanti, G.; Righi, M.; Spadoni, G. *Org. Lett.* **2010,** *12,* 3844–3847. doi:10.1021/ol101527j
67. Bartoccini, F.; Piersanti, G. *Synthesis* **2021,** *53,* 1396–1408. doi:10.1055/a-1340-3423
68. Tasker, N. R.; Wipf, P. Biosynthesis, Total Synthesis, and Biological Profiles of Ergot Alkaloids. *The Alkaloids: Chemistry and Biology;* Academic Press: Cambridge, MA, USA, 2021; Vol. 85, pp 1–112. doi:10.1016/bs.alkal.2020.08.001
69. Liu, H.; Jia, Y. *Nat. Prod. Rep.* **2017,** *34,* 411–432. doi:10.1039/c6np00110f
70. McCabe, S. R.; Wipf, P. *Org. Biomol. Chem.* **2016,** *14,* 5894–5913. doi:10.1039/c6ob00878j
71. Jakubczyk, D.; Cheng, J. Z.; O'Connor, S. E. *Nat. Prod. Rep.* **2014,** *31,* 1328–1338. doi:10.1039/c4np00062e
72. Yao, Y.; An, C.; Evans, D.; Liu, W.; Wang, W.; Wei, G.; Ding, N.; Houk, K. N.; Gao, S.-S. *J. Am. Chem. Soc.* **2019,** *141,* 17517–17521. doi:10.1021/jacs.9b10217
73. Ma, Y.; Yan, J.; Yang, L.; Yao, Y.; Wang, L.; Gao, S.-S.; Cui, C. *Front. Bioeng. Biotechnol.* **2022,** *10,* 1095464. doi:10.3389/fbioe.2022.1095464 And references cited therein.
74. Lowry, M. S.; Goldsmith, J. I.; Slinker, J. D.; Rohl, R.; Pascal, R. A.; Malliaras, G. G.; Bernhard, S. *Chem. Mater.* **2005,** *17,* 5712–5719. doi:10.1021/cm051312+
75. Walden, S. E.; Wheeler, R. A. *J. Phys. Chem.* **1996,** *100,* 1530–1535. doi:10.1021/jp951838p
76. Ge, Y.; Wang, H.; Wang, H.-N.; Yu, S.-S.; Yang, R.; Chen, X.; Zhao, Q.; Chen, G. *Org. Lett.* **2021,** *23,* 370–375. doi:10.1021/acs.orglett.0c03867
77. Yang, J.; Zhang, J.; Qi, L.; Hu, C.; Chen, Y. *Chem. Commun.* **2015,** *51,* 5275–5278. doi:10.1039/c4cc06344a
78. Jin, Y.; Jiang, M.; Wang, H.; Fu, H. *Sci. Rep.* **2016,** *6,* 20068. doi:10.1038/srep20068
79. Cheng, W.-M.; Shang, R.; Fu, Y. *ACS Catal.* **2017,** *7,* 907–911. doi:10.1021/acscatal.6b03215
80. Cheng, W.-M.; Shang, R.; Fu, M.-C.; Fu, Y. *Chem. – Eur. J.* **2017,** *23,* 2537–2541. doi:10.1002/chem.201605640
81. Liu, X.; Liu, Y.; Chai, G.; Qiao, B.; Zhao, X.; Jiang, Z. *Org. Lett.* **2018,** *20,* 6298–6301. doi:10.1021/acs.orglett.8b02791
82. Proctor, R. S. J.; Davis, H. J.; Phipps, R. J. *Science* **2018,** *360,* 419–422. doi:10.1126/science.aar6376
83. Xiao, Z.; Wang, L.; Wei, J.; Ran, C.; Liang, S. H.; Shang, J.; Chen, G.-Y.; Zheng, C. *Chem. Commun.* **2020,** *56,* 4164–4167. doi:10.1039/d0cc00451k
84. He, S.; Li, H.; Chen, X.; Krylov, I. B.; Terent'ev, A. O.; Qu, L.; Yu, B. *Chin. J. Org. Chem.* **2021,** *41,* 4661–4689. doi:10.6023/cjoc202105041
85. Dong, W.; Yen-Pon, E.; Li, L.; Bhattacharjee, A.; Jolit, A.; Molander, G. A. *Nat. Chem.* **2022,** *14,* 1068–1077. doi:10.1038/s41557-022-00979-0
86. Yue, H.; Zhu, C.; Huang, L.; Dewanji, A.; Rueping, M. *Chem. Commun.* **2022,** *58,* 171–184. doi:10.1039/d1cc06285a
87. Nemoto, T.; Harada, S.; Nakajima, M. *Asian J. Org. Chem.* **2018,** *7,* 1730–1742. doi:10.1002/ajoc.201800336
88. Yuan, K.; Jia, Y. *Chin. J. Org. Chem.* **2018,** *38,* 2386–2399. doi:10.6023/cjoc201705058
89. Connon, R.; Guiry, P. J. *Tetrahedron Lett.* **2020,** *61,* 151696. doi:10.1016/j.tetlet.2020.151696
90. Kozikowski, A. P.; Chen, C.; Wu, J. P.; Shibuya, M.; Kim, C. G.; Floss, H. G. *J. Am. Chem. Soc.* **1993,** *115,* 2482–2488. doi:10.1021/ja00059a051
91. Wong, G.; Lim, L. R.; Tan, Y. Q.; Go, M. K.; Bell, D. J.; Freemont, P. S.; Yew, W. S. *Nat. Commun.* **2022,** *13,* 712. doi:10.1038/s41467-022-28386-6
92. Jasperse, C. P.; Curran, D. P.; Fevig, T. L. *Chem. Rev.* **1991,** *91,* 1237–1286. doi:10.1021/cr00006a006
93. Chu, L.; Ohta, C.; Zuo, Z.; MacMillan, D. W. C. *J. Am. Chem. Soc.* **2014,** *136,* 10886–10889. doi:10.1021/ja505964r
94. Noble, A.; McCarver, S. J.; MacMillan, D. W. C. *J. Am. Chem. Soc.* **2015,** *137,* 624–627. doi:10.1021/ja511913h
95. Xiao, T.; Li, L.; Zhou, L. *J. Org. Chem.* **2016,** *81,* 7908–7916. doi:10.1021/acs.joc.6b01620
96. Ernouf, G.; Chirkin, E.; Rhyman, L.; Ramasami, P.; Cintrat, J.-C. *Angew. Chem., Int. Ed.* **2020,** *59,* 2618–2622. doi:10.1002/anie.201908951
97. Li, J.-T.; Luo, J.-N.; Wang, J.-L.; Wang, D.-K.; Yu, Y.-Z.; Zhuo, C.-X. *Nat. Commun.* **2022,** *13,* 1778. doi:10.1038/s41467-022-29464-5
98. It should be mentioned that racemization was found in products **11** and **12** from the chiral intermediate **V**, which is common in this radical coupling reaction. See reference [76].
99. McCarver, S. J.; Qiao, J. X.; Carpenter, J.; Borzilleri, R. M.; Poss, M. A.; Eastgate, M. D.; Miller, M. M.; MacMillan, D. W. C. *Angew. Chem., Int. Ed.* **2017,** *56,* 728–732. doi:10.1002/anie.201608207
100. Blackwell, J. H.; Harris, G. R.; Smith, M. A.; Gaunt, M. J. *J. Am. Chem. Soc.* **2021,** *143,* 15946–15959. doi:10.1021/jacs.1c07402
101. Lovett, G. H.; Sparling, B. A. *Org. Lett.* **2016,** *18,* 3494–3497. doi:10.1021/acs.orglett.6b01712
102. Renaud, P.; Sibi, M. P., Eds. *Radicals in Organic Synthesis;* Wiley-VCH: Weinheim, Germany, 2001; Vol. 1 and 2. doi:10.1002/9783527618293
103. Zard, S. Z. *Radicals Reactions in Organic Synthesis;* Oxford University Press: Oxford, UK, 2003.
104. Beckwith, A. L. J.; Crich, D.; Duggan, P. J.; Yao, Q. *Chem. Rev.* **1997,** *97,* 3273–3312. doi:10.1021/cr950207o
105. Crich, D.; Brebion, F.; Suk, D.-H. *Top. Curr. Chem.* **2006,** *263,* 1–38. doi:10.1007/128_024
106. Hurtley, A. E.; Lu, Z.; Yoon, T. P. *Angew. Chem., Int. Ed.* **2014,** *53,* 8991–8994. doi:10.1002/anie.201405359

107. Capaldo, L.; Ravelli, D. *Eur. J. Org. Chem.* **2017,** 2056–2071. doi:10.1002/ejoc.201601485
108. Yamada, F.; Makita, Y.; Somei, M. *Heterocycles* **2007,** *72,* 599–620. doi:10.3987/com-06-s(k)55
109. Somei, M.; Yamada, F.; Ohnishi, H.; Makita, Y.; Kuriki, M. *Heterocycles* **1987,** *26,* 2823–2828. doi:10.3987/r-1987-11-2823
110. Somei, M.; Ohnishi, H.; Shoken, Y. *Chem. Pharm. Bull.* **1986,** *34,* 677–681. doi:10.1248/cpb.34.677
111. Oppolzer, W.; Grayson, J. I.; Wegmann, H.; Urrea, M. *Tetrahedron* **1983,** *39,* 3695–3705. doi:10.1016/s0040-4020(01)88608-7
112. Somei, M.; Tsuchiya, M. *Chem. Pharm. Bull.* **1981,** *29,* 3145–3157. doi:10.1248/cpb.29.3145
113. Somei, M.; Yamada, F.; Karasawa, Y.; Kaneko, C. *Chem. Lett.* **1981,** *10,* 615–618. doi:10.1246/cl.1981.615
114. Natsume, M.; Muratake, H. *Heterocycles* **1980,** *14,* 1101–1105. doi:10.3987/r-1980-08-1101
115. Chaudhuri, S.; Bhunia, S.; Roy, A.; Das, M. K.; Bisai, A. *Org. Lett.* **2018,** *20,* 288–291. doi:10.1021/acs.orglett.7b03683

License and Terms

BEILSTEIN JOURNAL OF ORGANIC CHEMISTRY

Radical ligand transfer: a general strategy for radical functionalization

David T. Nemoto Jr, Kang-Jie Bian, Shih-Chieh Kao and Julian G. West*

Perspective

Open Access

Address:
Department of Chemistry, Rice University, 6100 Main St MS 602, Houston, TX 77005, USA

Email:
Julian G. West* - jgwest@rice.edu

* Corresponding author

Keywords:
catalysis; cooperative catalysis; earth abundant elements; photocatalysis; radicals

Beilstein J. Org. Chem. **2023,** *19,* 1225–1233.
https://doi.org/10.3762/bjoc.19.90

Received: 22 June 2023
Accepted: 04 August 2023
Published: 15 August 2023

This article is part of the thematic issue "Modern radical chemistry".

Guest Editor: H.-M. Huang

Abstract

The place of alkyl radicals in organic chemistry has changed markedly over the last several decades, evolving from challenging-to-generate “uncontrollable” species prone to side reactions to versatile reactive intermediates enabling construction of myriad C–C and C–X bonds. This maturation of free radical chemistry has been enabled by several advances, including the proliferation of efficient radical generation methods, such as hydrogen atom transfer (HAT), alkene addition, and decarboxylation. At least as important has been innovation in radical functionalization methods, including radical–polar crossover (RPC), enabling these intermediates to be engaged in productive and efficient bond-forming steps. However, direct engagement of alkyl radicals remains challenging. Among these functionalization approaches, a bio-inspired mechanistic paradigm known as radical ligand transfer (RLT) has emerged as a particularly promising and versatile means of forming new bonds catalytically to alkyl radicals. This development has been driven by several key features of RLT catalysis, including the ability to form diverse bonds (including C–X, C–N, and C–S), the use of simple earth abundant element catalysts, and the intrinsic compatibility of this approach with varied radical generation methods, including HAT, radical addition, and decarboxylation. Here, we provide an overview of the evolution of RLT catalysis from initial studies to recent advances and provide a conceptual framework we hope will inspire and enable future work using this versatile elementary step.

Introduction

The behavior of alkyl radicals has been studied rigorously for decades, though only recently have these come to be widely viewed as selective and useful synthetic intermediates [1-4]. This sea change has been driven by innovations in both the generation and functionalization of alkyl radicals, with successful synthetic reactions requiring efficiency and selectivity in both of these processes and inherent compatibility between each. Radical generation has benefitted from many general mechanistic approaches, including hydrogen atom transfer (HAT) [5], alkene addition [6], and decarboxylation [7], enabling these

intermediates to be easily accessed from diverse starting materials. Functionalization methods have also seen significant development, with elementary steps such as radical–polar crossover (RPC) finding significant purchase [8]; however, these steps are not amenable to all radical generation approaches/substrate classes nor can they form all desired bonds from alkyl radical intermediates, limiting the toolkit of radical reactions.

Recently, radical ligand transfer (RLT) [9-11] has emerged as a radical functionalization paradigm with the potential to overcome the challenges faced by other strategies (Scheme 1). At its core, RLT involves the outer sphere transfer of an anionic, X-type ligand coordinated to a redox-active metal to a radical intermediate, resulting in formation of a new C–ligand bond with concomitant single electron reduction of the metal center. Subsequent reoxidation of the metal with coordination of a new equivalent of anionic ligand allows for the RLT complex to be regenerated, making this strategy inherently compatible with catalysis.

Building on this, one of the most important examples of catalytic RLT can be found in the human body's own cytochrome P450 enzymes. These catalysts exhibit unique "radical rebound" reactivity at their heme active sites (Scheme 1) [12], a mechanism proposed by Groves and co-workers and heavily explored beginning in the 1970s [13,14]. This two-step functionalization sequence begins with HAT from an alkyl C–H bond to a high valent iron oxo species, resulting in formation of iron hydroxo and alkyl radical intermediates [15]. Subsequent RLT of the hydroxo ligand to the alkyl radical produces a hydroxylated

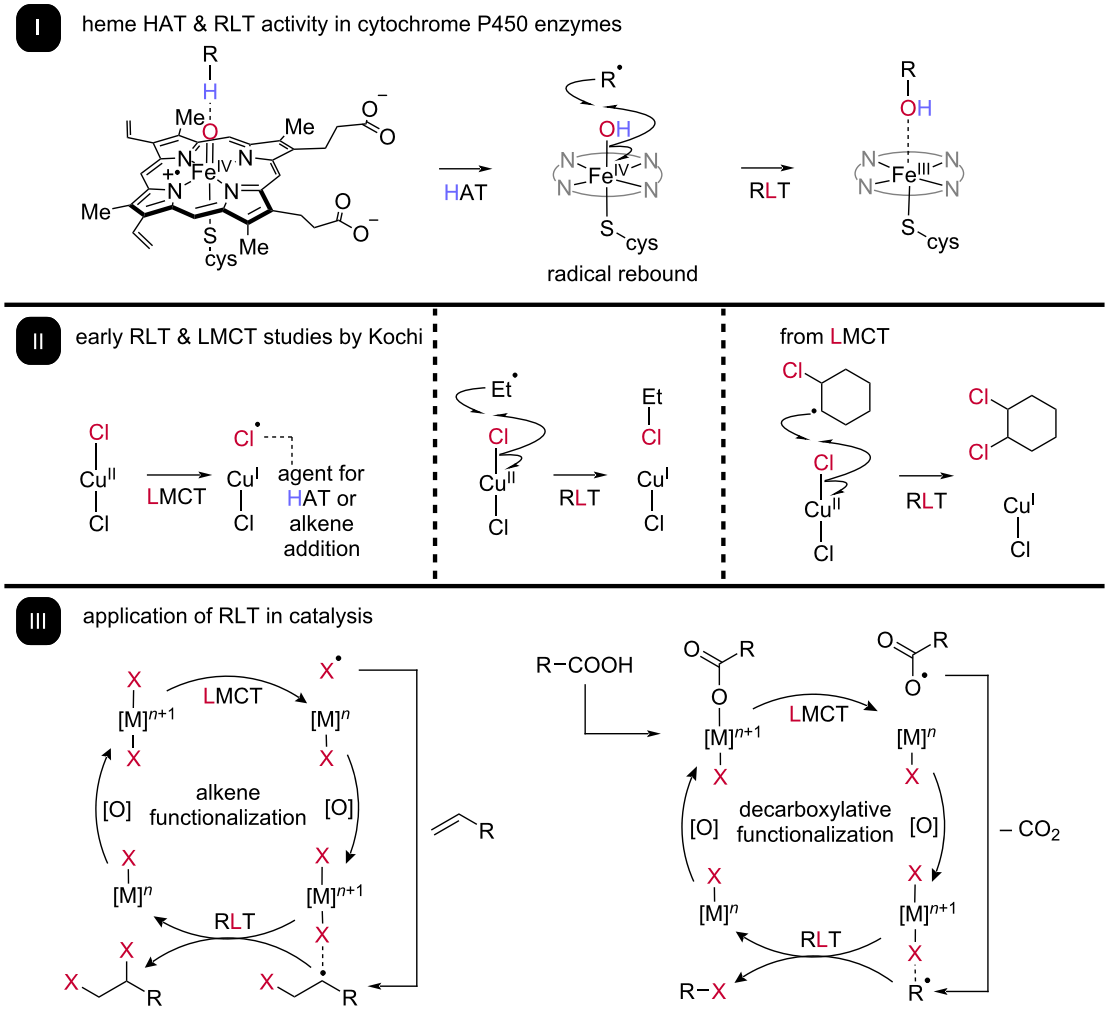

Scheme 1: Overview of the RLT mechanism in nature and in literature. I: The radical rebound mechanism in cytochrome P450 enzymes consists of HAT on a C–H bond, followed by RLT with a hydroxy ligand. II: Kochi reported the oxidation of alkyl radicals through LMCT of copper(II) chloride and subsequent radical chlorine ligand transfer [26]. 1-Cyclohexene was also reported to be oxidized to the vicinal dichlorinated product through a similar mechanism. III: RLT has become more prevalent in reported catalytic cycles involving radical-based transformations including alkene difunctionalization and decarboxylative functionalization. Many of these transformations have also utilized LMCT as a means of generating reactive radical species.

product, allowing for metabolism and excretion of previously diverse bioactive compounds. Similar RLT "rebound" steps have been implicated in non-heme oxygenase and halogenase enzymes as well [16-19], hinting that this strategy might be general; however, enzymatic examples outside of hydroxo and halide ligand transfer are scarce.

Groves' initial discovery of the radical rebound behavior of P450 oxygenases encouraged early work on site-selective C–H functionalization [20]. Throughout their studies, it was found that manganese could perform the same HAT and RLT steps as iron at heme active sites. Groves developed the manganese tetramesitylporphine catalyst **V** (Scheme 2), which was found to be capable of functionalizing specific C–H bonds to numerous functionalities, including C–F [21,22], C–N_3 [23], and C–Cl bonds [24,25]. Upon these remarkable observations, methodologies involving manganese–porphyrin catalysts have been developed over the years. These methods take advantage of the power of RLT to install a variety of medicinally relevant groups, largely mirroring the selectivity of CYP450s. Intriguingly, studies by Groves have revealed earth abundant iron and manganese to be particularly privileged for this application of RLT, a major advantage for sustainable method development.

Outside of bioinorganic chemistry, the concept of radical ligand transfer was investigated in early work by Jay Kochi in purely synthetic systems (Scheme 1) [26,27]. Studies on the oxidation of alkyl radicals with earth abundant cupric salts uncovered the

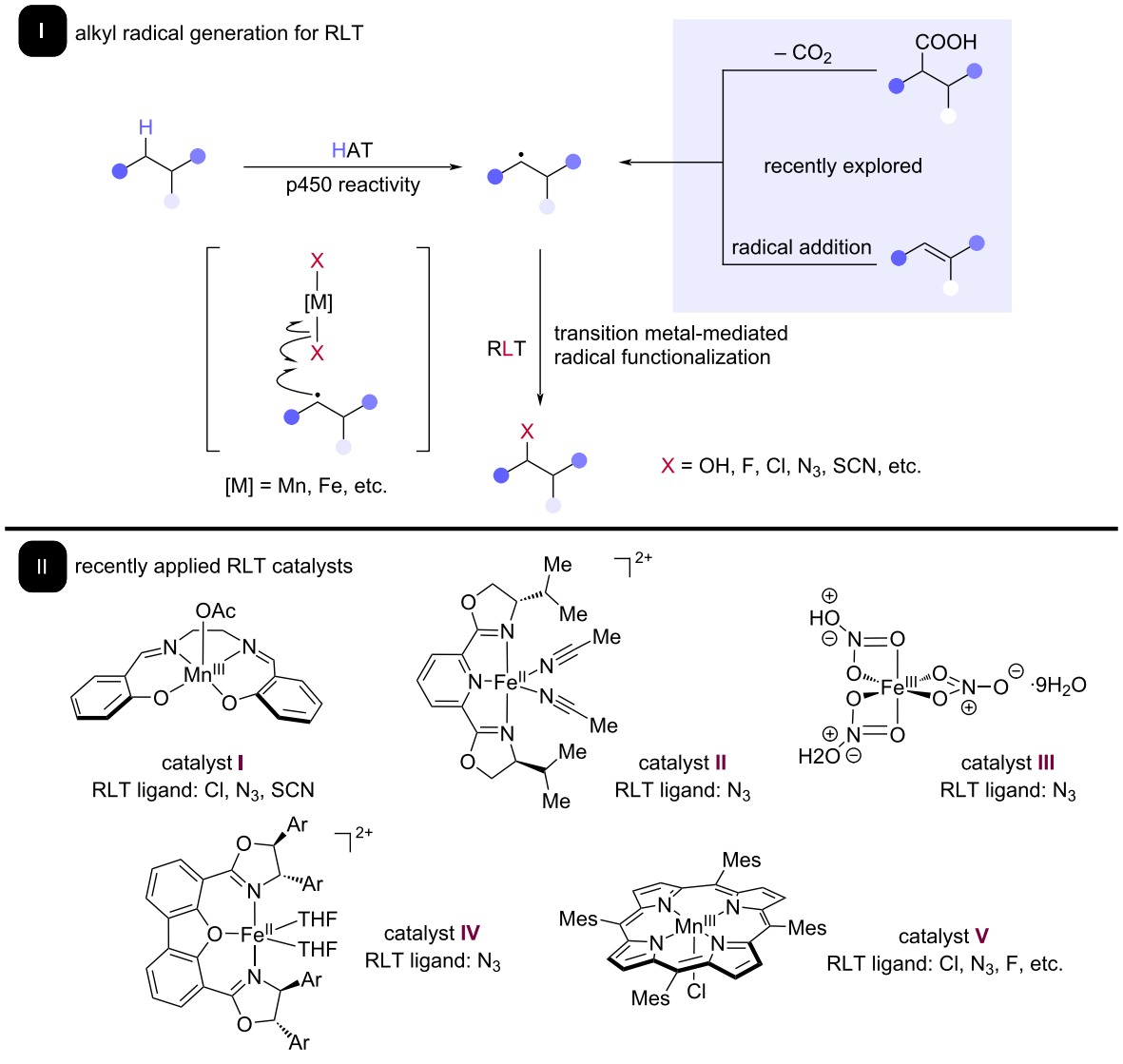

Scheme 2: Areas of recent work on RLT development and application in catalysis. I: Reported RLT pathways often involve the generation of alkyl radicals from selective HAT on C–H bonds and, more recently, radial decarboxylation and radical addition onto π systems. Generated alkyl radicals are simultaneously quenched and functionalized through RLT. II: Modern catalysts developed for RLT catalysis.

ability of simple Cu(II) chloride to form new C–Cl bonds in the presence of transient alkyl radicals, with mechanistic studies implicating homolytic abstraction of a chlorine ligand from the intermediate copper complex. Outside of the substitution products which could be generated from the RLT pathway, alkyl radicals could also undergo an elimination-like pathway to afford unsaturated C–C bonds in the presence of copper(II) sulfate, presumably via competitive RPC to the carbocation followed by E_1 olefination.

Kochi also demonstrated that RLT can be combined with other radical generation strategies to enable new, non-biomimetic reactions to be achieved (Scheme 1), showing that photolysis of stoichiometric Cu(II) chloride in the presence of unactivated alkenes allows for direct formation of vicinal dichloride products. The mechanistic study implicated initial formation of a chlorine radical through homolysis of a Cu–Cl bond via ligand-to-metal charge transfer (LMCT) which, following cage escape, could add to the alkene to generate an alkyl radical. This alkyl radical could then be chlorinated via RLT from a second Cu(II) chloride species, furnishing the dichlorinated product. While copper was unable to be used catalytically in this early report, it augured the potential of RLT to be a general strategy in synthetic method development, with modern examples including new alkene addition reactions and decarboxylative functionalizations (Scheme 2).

Recent applications of RLT in catalysis

Upon the discovery and initial exploration of the RLT paradigm by Groves and Kochi, many groups have adopted and characterized new ways of using RLT to form valuable carbon–heteroatom bonds from a diverse pool of simple starting materials. RLT has been especially present in modern catalysis, where complexes of earth abundant iron and manganese have been demonstrated to be particularly privileged in delivery of various ligands to alkyl radicals (Scheme 2). These developments have been supported by discovery of the compatibility of RLT with many different reaction paradigms leading to alkyl radical intermediates under catalytic conditions, including radical addition to alkenes and radical decarboxylation, with many of these being driven by light energy.

RLT in alkene functionalization

Outside of the realm of C–H activation, RLT has been leveraged to afford complex medicinal scaffolds in alkene difunctionalization. A recent example can be found in the merger of RLT with photoredox-catalyzed atom transfer radical addition (ATRA) (Scheme 3). ATRA results in the net addition of a C–X bond across an alkene, forming both valuable C–C and C–X bonds in a single reaction. While ATRA-type reactions were first reported in the 1940s by Kharasch [28], interest in the area was revitalized the early 2010s with the advent of Stephenson's photoredox catalytic methods which dramatically simplified reaction conditions [29,30], driving ongoing interest in this mechanistic approach [31].

Our group recently devised a dual catalytic method which combines the RLT paradigm with photocatalytic ATRA to enable the modular difunctionalization of alkenes under reagent control (Scheme 3). In Stephenson's photocatalytic ATRA reports, the C–X bond in the product was proposed to be formed through both direct quenching of a transient alkyl radical by halogen atom transfer (XAT) from the alkyl halide reagent and further oxidation of the transient radical to a carbocation by radical polar crossover (RPC), providing two mechanistic pathways to form the ATRA products [32]. While powerful, this approach is inherently incompatible with introducing alternative functionality instead of the halide included in the alkyl halide reagent, limiting the ability to form different difunctionalization products. Taking inspiration from Groves' bio-inspired manganese tetradentate manganese catalysts, we found we could instead functionalize the transient alkyl radical via RLT from a simplified manganese salen complex **I**, allowing for the identity of the carbon–heteroatom bond to be controlled based on added nucleophile and enabling C–Cl, C–N, and C–S bonds to be formed directly while completely suppressing traditional ATRA products [9]. In mechanistic studies, rearrangement products indicative of a carbocationic pathway are not observed, suggesting that RPC does not occur. Further, the inability of ATRA products to undergo S_N2 with the added nucleophiles under our reaction conditions is inconsistent with a tandem ARTA/nucleophilic displacement alternative mechanism. Finally, a functionalization via the canonical organometallic steps of oxidative addition/reductive elimination was ruled out via catalytic reaction of the macrocyclic Groves-type porphyrin catalyst **V**, a species that is unable to accommodate the mutual cis-orientation of ligands for metal-centered reductive elimination. The system was found to be compatible with unactivated alkenes bearing a wide range of functionalities, including more-substituted alkenes, and a wide range of alkyl halide reagents, permitting a library of difunctionalized products to be prepared from a single alkene.

RLT can also be used to deliver valuable homodifunctionalized products using unactivated alkenes. Vicinal diazides (and to a lesser extent dihalides) have been popular targets for modern method development. Both photochemical [33] and electrochemical [34-36] methods have been effective in delivering products containing these molecular motifs. Intriguingly, several recent alkene diazidation methods have made RLT a key design criterion, with both thermal and photochemical driving forces [37].

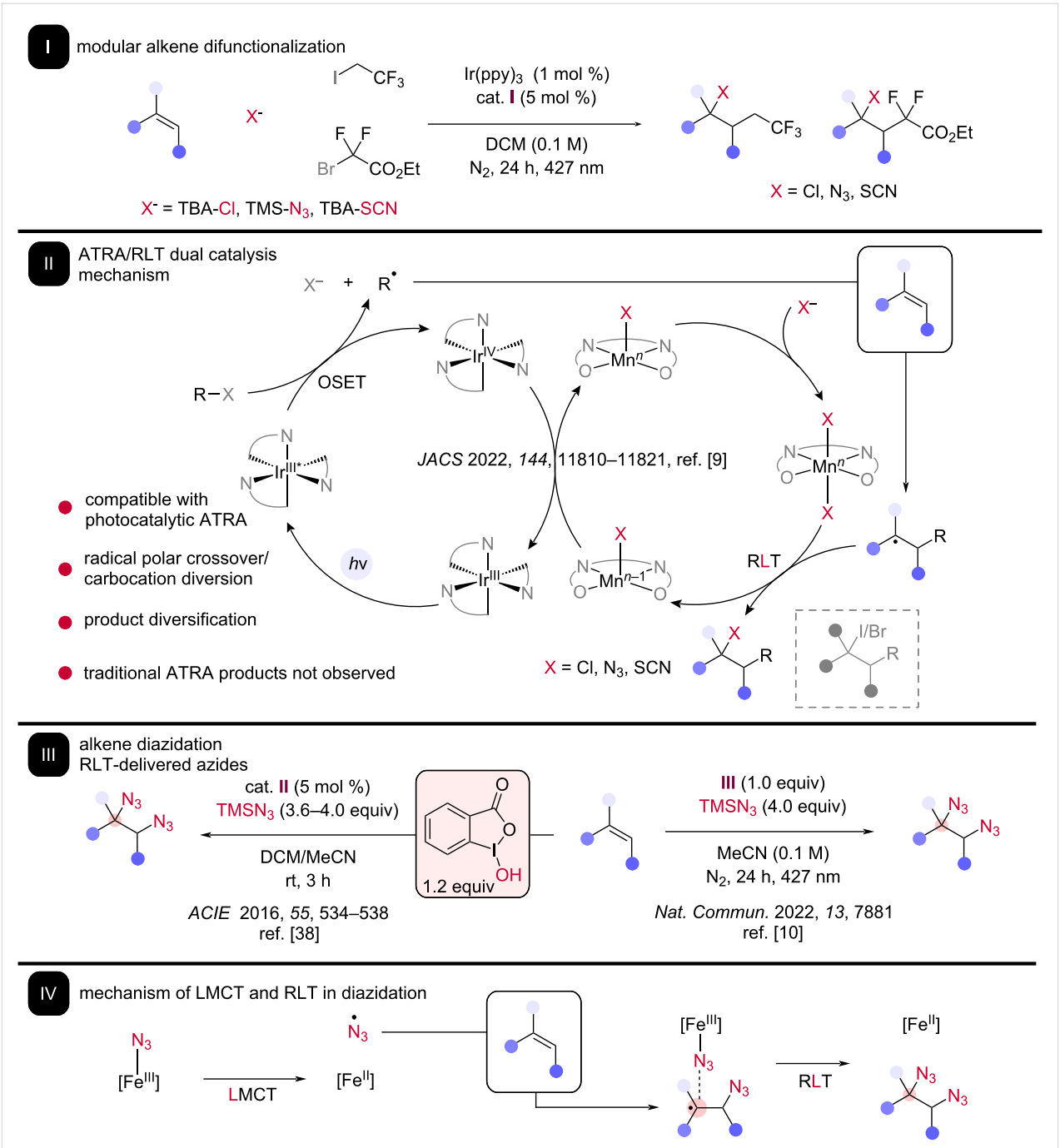

Scheme 3: The incorporation of RLT catalysis in ATRA photocatalysis. I: The reported method is compatible with nucleophilic sources of chlorine groups, azide groups, and thioisocyanate groups. II: The proposed mechanism for the dual catalytic ATRA-RLT cycle. III: Our lab and Xu reported photochemical diazidation of alkenes carried out using iron and trimethylsilyl azide. IV: The proposed mechanism for photoinduced LMCT between iron and azide ligands as well as RLT on azidoalkyl radical intermediates.

Recent interest in alkene diazidation was accelerated by a 2016 report from Xu detailing alkene diazidation using low loadings of a molecular iron catalyst **II** and stoichiometric hydroxyiodinane as a terminal oxidant [38]. It is proposed that an azidoiodinane is generated in situ and serves as the radical initiator, generating an azido radical which adds to the less substituted position on the alkene. The resultant transient radical is captured via RLT from an in-situ generated iron–azide complex, resulting in net reduction of iron. The competent RLT species can then be regenerated through oxidation by the iodinane species and coordination of another equivalent of azide. This reaction was particularly notable for the wide alkene

scope, including terminal aliphatic alkenes, internal (cyclic) styrenes, and one example of a nonconjugated diene, suggesting RLT to be compatible with many functionalities. The diastereoselectivity of the reaction varies, with high anti-selectivity being achieved with cyclic styrenes and low diastereoselectivity in linear internal alkenes.

Building on this key iron catalysis result, our group and that of Shi contemporaneously reported the photochemical diazidation of alkenes using stoichiometric iron and no external oxidant or ancillary ligand, providing a simple protocol for the preparation of vicinal diamines with excellent functional group compatibility (Scheme 3) [10,39]. In both reports, it is proposed that photoinduced LMCT of an in-situ generated Fe(III) azide species furnishes an azido radical, compatible with unactivated alkene addition. These steps provide the reactive carbon-centered radical intermediate. RLT to this radical from another azide ligand leads to a diazidated product. The overall scope of both reports suggests that the diazidation of simple to complex drugs/natural product-derived alkene substrates is readily achievable, including highly substituted and cyclic aliphatic alkenes. Further, we demonstrated that diazidation could be rendered catalytic using Fe(III) nitrate hydrate **III** as the iron source and performing the reaction under continuous flow conditions. Interestingly, this mechanism bears some similarity to Lin's electrocatalytic diazidation, where azido radical generation is proposed via thermal homolysis of a Mn(III) azide species and RLT from a second equivalent of Mn(III) azide furnishes the desired organic diazide, providing a strong demonstration of the applicability of RLT to not only photochemical but electrochemical conditions as well [35].

RLT in decarboxylative functionalization

Aside from its strategic application in alkene difunctionalization methods, RLT has also found synthetic utility in radical decarboxylative reactions. Radical decarboxylative functionalization reactions to form C–X bonds have been demonstrated, with bond construction being proposed to follow one of two pathways: formation of a carbocation through RPC followed by nucleophilic attack or direct RLT from a redox-active metal complex.

Preliminary evidence for a radical decarboxylation/RLT cascade was reported in 1965, when Kochi demonstrated decarboxylative chlorination of various acids with lead(IV) tetraacetate in the presence of lithium chloride (Scheme 4) [40,41]. Nucleophilic lithium chloride was used as the chlorine atom source for this transformation. In the representative scope of this transformation, primary and secondary chlorides could be formed in relatively high yields from their respective acids, a result incompatible with a carbocation RPC mechanism. This Kochi decarboxylative chlorination separated itself from other pioneering methods of decarboxylative functionalization (i.e., Barton and Hunsdiecker) because of its inclusion of RLT as a key element of the mechanism.

In 2015, the Groves group reported their manganese porphin-based catalyst **V** and related species being capable of participating in decarboxylation reactions (Scheme 4) [42]. The activated Mn(V) species is proposed to perform HAT carboxylic acid O–H bond, directly forming a carboxyl radical and Mn(IV) species which can exchange its hydroxo ligand for a fluoride from triethylamine tris(hydrofluoride) (Scheme 4). Rapid decarboxylation of this intermediate produces the alkyl radical species which could be fluorinated via RLT from the Mn(IV)–F complex, generating a Mn(III) intermediate. To close the cycle and reform the oxo ligand on the Mn(V) species, a stoichiometric amount of iodosylbenzene is used in the reaction.

While initial development of this reaction focused on incorporating the stable ^{19}F, subsequent study expanded the scope to RLT of the unstable ^{18}F radioisotope, an important medical radioisotope used for positron emission tomography (PET) [43]. Optimized conditions of both isotopes included fast reaction times of under two hours; in the case of the ^{18}F radioisotope, reactions were carried out in 10 minutes and resulted in moderate to high yields, demonstrating the potential of RLT reactions to be rapid and efficient. In both cases, benzylic carboxylic acids were most amenable as substrates, with alkyl carboxylic acids such as adamantane and dicyclohexylmethane providing fluorinated aliphatic products in low to moderate yields.

Asymmetric RLT catalysis has also been of recent interest, with exciting preliminary decarboxylative azidation results obtained under thermal conditions by Hongli Bao and co-workers [44]. An asymmetric iron (NON) pincer catalyst **IV** was employed to decarboxylate benzylic peroxyesters and form enantiomerically enriched benzylic azides. An Fe(II/III) cycle is proposed, where a single electron transfer from Fe(II) reduces the peroxyester and produces a carboxyl radical and Fe(III), which can coordinate an azide ligand. Rapid decarboxylation produces the transient alkyl radical which can be asymmetrically azidated by RLT from an Fe(III) azide complex, reducing the iron catalyst back to the starting Fe(II) state. Organic azides can be formed in moderate to high enantioselectivity using this approach; however, the scope is largely limited to benzylic products, a result in line with Groves' finding that benzylic acid substrates perform much more efficiently in decarboxylative RLT reactions than aliphatic acids [42]. Outside of decarboxylation, X. Peter Zhang recently reported the enantioselective synthesis of allylic amines through coupled HAT and RLT on allylic C–H bonds [45],

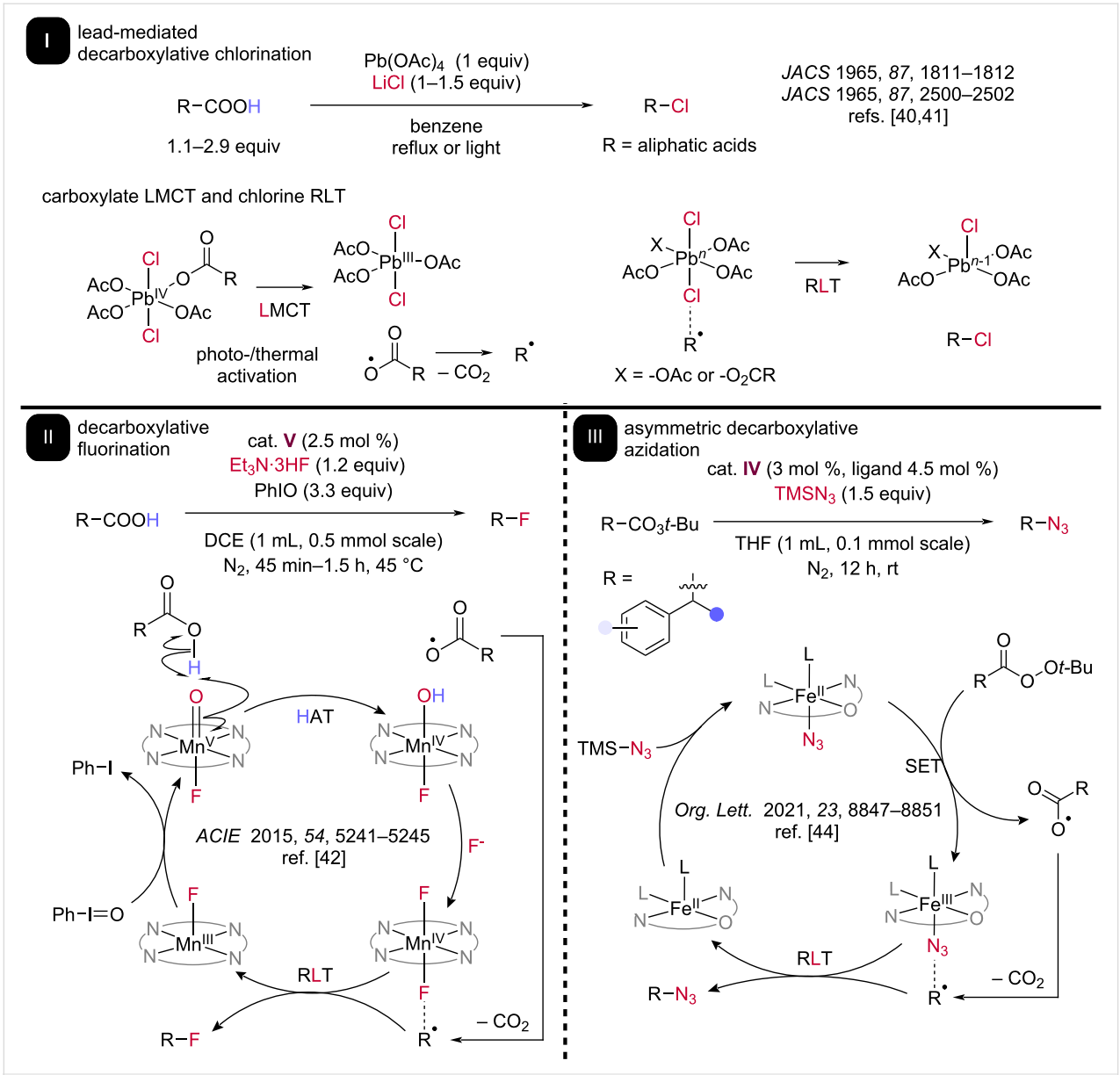

Scheme 4: Pioneering and recent work on decarboxylative functionalization involving a posited RLT pathway. I: In 1965, Kochi reported thermal and photochemical decarboxylative chlorination using stoichiometric lead(IV) acetate. LMCT on the carboxylate substrate and RLT on a Pb–Cl bond are supported by mechanistic studies. II: Groves reported decarboxylative fluorination employing catalyst **V**. III: Bao reported asymmetric decarboxylative azidation through use of BOX-derived iron catalyst **IV**.

using a bulky cobalt porphyrin complex developed and utilized to perform both HAT and RLT. While many challenges remain for achieving general asymmetric induction in RLT catalysis, this advance represents an important step toward this aspirational goal with many lessons to build upon.

Our group has recently leveraged iron photochemistry to build on these beautiful decarboxylative azidation examples, combining iron-mediated photodecarboxylation via LMCT and azide RLT (Scheme 5) [11]. Irradiating a substoichiometric amount of iron(III) nitrate hydrate **III** in the presence of carboxylic acid, TMS azide, and sodium carbonate allows for direct synthesis of alkyl azides for a wide range of both activated (benzylic) and unactivated carboxylic acids. Control reactions support the intermediacy of alkyl radicals and the absence of carbocation rearrangements in a variety of probe substrates disfavor the reaction proceeding via RPC.

Intriguingly, no additional oxidant is required for this process, implicating the nitrate counterion functioning as an internal oxidant to regenerate the active Fe(III) species capable of LMCT and RLT. This result is consistent with our finding that

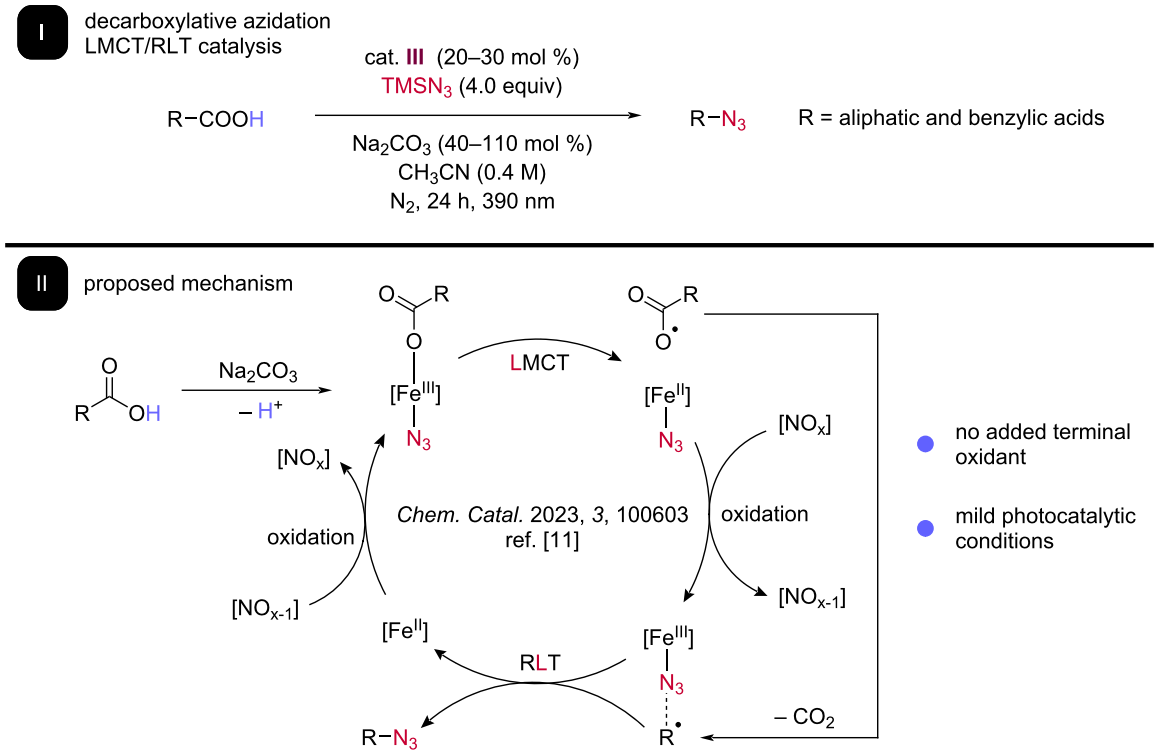

Scheme 5: Our lab reported decarboxylative azidation of aliphatic and benzylic acids. I: The reaction proceeds via LMCT and RLT catalysis without the addition of terminal oxidant. II: The proposed mechanism includes reoxidation of the iron catalyst through inner-sphere electron transfer by anionic nitrate.

iron nitrate can catalytically diazidate alkenes in flow with no additional oxidant and literature examples of nitrate oxidation of different transition metals, such as palladium. Control reactions further supported this proposal, including the inability of alternative Fe(III) salts (e.g., $FeCl_3$) to form more than stoichiometric azide product in the absence of added nitrate. We believe this adventitious discovery of nitrate functioning as a mild and selective oxidant in RLT catalytic systems presents many opportunities for future method development and are avidly pursuing this area of research.

Outlook

After scant exploration following its elucidation in early mechanistic studies of bioinorganic and synthetic systems, radical ligand transfer (RLT) has reemerged as a powerful tool in the design of catalytic radical reactions. This development has been fueled by the unique aspects of RLT, with its ability to functionalize radicals with diverse nucleophilic reagents and inherent compatibility with different elementary steps, including hydrogen atom transfer (HAT) and ligand-to-metal charge transfer (LMCT), enabling new transformations to be unlocked with unprecedented modularity. Further, the privileged position of earth abundant elements such as iron and manganese in RLT has made reactions using this step appealing from a sustainability standpoint. While exciting progress has been made, many opportunities remain using this mechanistic approach. Two key areas that could yield exciting advances are combining RLT with new radical-generating elementary steps and the further development of asymmetric RLT processes. We hope that this perspective provides a useful framework for understanding RLT reactivity and inspires new advances using this versatile and intriguing elementary step.

Funding

J.G.W. acknowledges financial support from CPRIT (RR190025), NIH NIGMS (R35GM142738), Research Corporation for Science Advancement (CS-CSA-2023-007), and the Welch Foundation (C-2085).

ORCID® iDs

David T. Nemoto Jr - https://orcid.org/0000-0002-8596-6909
Julian G. West - https://orcid.org/0000-0002-3715-7883

References

1. Yan, M.; Kawamata, Y.; Baran, P. S. *Chem. Rev.* **2017,** *117,* 13230–13319. doi:10.1021/acs.chemrev.7b00397
2. Yan, M.; Lo, J. C.; Edwards, J. T.; Baran, P. S. *J. Am. Chem. Soc.* **2016,** *138,* 12692–12714. doi:10.1021/jacs.6b08856

3. Crespi, S.; Fagnoni, M. *Chem. Rev.* **2020,** *120,* 9790–9833. doi:10.1021/acs.chemrev.0c00278
4. Corcé, V.; Ollivier, C.; Fensterbank, L. *Chem. Soc. Rev.* **2022,** *51,* 1470–1510. doi:10.1039/d1cs01084k
5. Capaldo, L.; Ravelli, D.; Fagnoni, M. *Chem. Rev.* **2022,** *122,* 1875–1924. doi:10.1021/acs.chemrev.1c00263
6. Yao, H.; Hu, W.; Zhang, W. *Molecules* **2021,** *26,* 105. doi:10.3390/molecules26010105
7. Chen, H.; Liu, Y. A.; Liao, X. *Synthesis* **2021,** *53,* 1–29. doi:10.1055/s-0040-1707273
8. Sharma, S.; Singh, J.; Sharma, A. *Adv. Synth. Catal.* **2021,** *363,* 3146–3169. doi:10.1002/adsc.202100205
9. Bian, K.-J.; Nemoto, D., Jr.; Kao, S.-C.; He, Y.; Li, Y.; Wang, X.-S.; West, J. G. *J. Am. Chem. Soc.* **2022,** *144,* 11810–11821. doi:10.1021/jacs.2c04188
10. Bian, K.-J.; Kao, S.-C.; Nemoto, D., Jr.; Chen, X.-W.; West, J. G. *Nat. Commun.* **2022,** *13,* 7881. doi:10.1038/s41467-022-35560-3
11. Kao, S.-C.; Bian, K.-J.; Chen, X.-W.; Chen, Y.; Martí, A. A.; West, J. G. *Chem Catal.* **2023,** *3,* 100603. doi:10.1016/j.checat.2023.100603
12. Meunier, B.; de Visser, S. P.; Shaik, S. *Chem. Rev.* **2004,** *104,* 3947–3980. doi:10.1021/cr020443g
13. Groves, J. T.; Van Der Puy, M. *J. Am. Chem. Soc.* **1976,** *98,* 5290–5297. doi:10.1021/ja00433a039
14. Groves, J. T.; McClusky, G. A. *J. Am. Chem. Soc.* **1976,** *98,* 859–861. doi:10.1021/ja00419a049
15. Groves, J. T. *Nat. Chem.* **2014,** *6,* 89–91. doi:10.1038/nchem.1855
16. Krebs, C.; Galonić Fujimori, D.; Walsh, C. T.; Bollinger, J. M., Jr. *Acc. Chem. Res.* **2007,** *40,* 484–492. doi:10.1021/ar700066p
17. Vaillancourt, F. H.; Yeh, E.; Vosburg, D. A.; Garneau-Tsodikova, S.; Walsh, C. T. *Chem. Rev.* **2006,** *106,* 3364–3378. doi:10.1021/cr050313i
18. Kojima, T.; Leising, R. A.; Yan, S.; Que, L., Jr. *J. Am. Chem. Soc.* **1993,** *115,* 11328–11335. doi:10.1021/ja00077a035
19. Costas, M.; Mehn, M. P.; Jensen, M. P.; Que, L. *Chem. Rev.* **2004,** *104,* 939–986. doi:10.1021/cr020628n
20. Huang, X.; Groves, J. T. *J. Biol. Inorg. Chem.* **2017,** *22,* 185–207. doi:10.1007/s00775-016-1414-3
21. Liu, W.; Huang, X.; Cheng, M.-J.; Nielsen, R. J.; Goddard, W. A., III; Groves, J. T. *Science* **2012,** *337,* 1322–1325. doi:10.1126/science.1222327
22. Liu, W.; Huang, X.; Placzek, M. S.; Krska, S. W.; McQuade, P.; Hooker, J. M.; Groves, J. T. *Chem. Sci.* **2018,** *9,* 1168–1172. doi:10.1039/c7sc04545j
23. Huang, X.; Bergsten, T. M.; Groves, J. T. *J. Am. Chem. Soc.* **2015,** *137,* 5300–5303. doi:10.1021/jacs.5b01983
24. Liu, W.; Groves, J. T. *J. Am. Chem. Soc.* **2010,** *132,* 12847–12849. doi:10.1021/ja105548x
25. Liu, W.; Groves, J. T. *Acc. Chem. Res.* **2015,** *48,* 1727–1735. doi:10.1021/acs.accounts.5b00062
26. Kochi, J. K. *J. Am. Chem. Soc.* **1962,** *84,* 2121–2127. doi:10.1021/ja00870a025
27. Kochi, J. K. *Science* **1967,** *155,* 415–424. doi:10.1126/science.155.3761.415
28. Kharasch, M. S.; Jensen, E. V.; Urry, W. H. *Science* **1945,** *102,* 128. doi:10.1126/science.102.2640.128.a
29. Nguyen, J. D.; Tucker, J. W.; Konieczynska, M. D.; Stephenson, C. R. J. *J. Am. Chem. Soc.* **2011,** *133,* 4160–4163. doi:10.1021/ja108560e
30. Wallentin, C.-J.; Nguyen, J. D.; Finkbeiner, P.; Stephenson, C. R. J. *J. Am. Chem. Soc.* **2012,** *134,* 8875–8884. doi:10.1021/ja300798k
31. Courant, T.; Masson, G. *J. Org. Chem.* **2016,** *81,* 6945–6952. doi:10.1021/acs.joc.6b01058
32. Williams, T. M.; Stephenson, C. R. J. Atom Transfer Radical Addition using Photoredox Catalysis. In *Visible Light Photocatalysis in Organic Chemistry;* Stephenson, C. R. J.; Yoon, T. P.; MacMillan, D. W. C., Eds.; Wiley-VCH: Weinheim, Germany, 2018; pp 73–92. doi:10.1002/9783527674145.ch3
33. Lian, P.; Long, W.; Li, J.; Zheng, Y.; Wan, X. *Angew. Chem., Int. Ed.* **2020,** *59,* 23603–23608. doi:10.1002/anie.202010801
34. Fu, N.; Sauer, G. S.; Lin, S. *J. Am. Chem. Soc.* **2017,** *139,* 15548–15553. doi:10.1021/jacs.7b09388
35. Fu, N.; Sauer, G. S.; Saha, A.; Loo, A.; Lin, S. *Science* **2017,** *357,* 575–579. doi:10.1126/science.aan6206
36. Dong, X.; Roeckl, J. L.; Waldvogel, S. R.; Morandi, B. *Science* **2021,** *371,* 507–514. doi:10.1126/science.abf2974
37. Ge, L.; Chiou, M.-F.; Li, Y.; Bao, H. *Green Synth. Catal.* **2020,** *1,* 86–120. doi:10.1016/j.gresc.2020.07.001
38. Yuan, Y.-A.; Lu, D.-F.; Chen, Y.-R.; Xu, H. *Angew. Chem., Int. Ed.* **2016,** *55,* 534–538. doi:10.1002/anie.201507550
39. Zhang, M.; Zhang, J.; Li, Q.; Shi, Y. *Nat. Commun.* **2022,** *13,* 7880. doi:10.1038/s41467-022-35344-9
40. Kochi, J. K. *J. Am. Chem. Soc.* **1965,** *87,* 2500–2502. doi:10.1021/ja01089a041
41. Kochi, J. K. *J. Am. Chem. Soc.* **1965,** *87,* 1811–1812. doi:10.1021/ja01086a046
42. Huang, X.; Liu, W.; Hooker, J. M.; Groves, J. T. *Angew. Chem., Int. Ed.* **2015,** *54,* 5241–5245. doi:10.1002/anie.201500399
43. Shields, A. F.; Grierson, J. R.; Dohmen, B. M.; Machulla, H.-J.; Stayanoff, J. C.; Lawhorn-Crews, J. M.; Obradovich, J. E.; Muzik, O.; Mangner, T. J. *Nat. Med.* **1998,** *4,* 1334–1336. doi:10.1038/3337
44. Wang, K.; Li, Y.; Li, X.; Li, D.; Bao, H. *Org. Lett.* **2021,** *23,* 8847–8851. doi:10.1021/acs.orglett.1c03355
45. Xu, P.; Xie, J.; Wang, D.-S.; Zhang, X. P. *Nat. Chem.* **2023,** *15,* 498–507. doi:10.1038/s41557-022-01119-4

License and Terms

BEILSTEIN JOURNAL OF ORGANIC CHEMISTRY

α-(Aminomethyl)acrylates as acceptors in radical–polar crossover 1,4-additions of dialkylzincs: insights into enolate formation and trapping

Angel Palillero-Cisneros[1,2], Paola G. Gordillo-Guerra[1,2,3], Fernando García-Alvarez[1,2], Olivier Jackowski[1], Franck Ferreira[1], Fabrice Chemla[1], Joel L. Terán[*2] and Alejandro Perez-Luna[*1]

Full Research Paper

Open Access

Address:
[1]Sorbonne Université, CNRS, Institut Parisien de Chimie Moléculaire, IPCM. 4 place Jussieu, 75005 Paris, France, [2]Benemérita Universidad Autonóma de Puebla, Instituto de Ciencias, ICUAP, Edificio IC-9, Complejo de Ciencias, C.U., 72570, Puebla, México and [3](current adress) Universidad Autónoma Metropolitana, Unidad Xochimilco, Departamento de Sistemas Biológicos, Ciudad de México, C.P., 04690, México

Email:
Joel L. Terán[*] - joel.teran@correo.buap.mx; Alejandro Perez-Luna[*] - alejandro.perez_luna@sorbonne-universite.fr

* Corresponding author

Keywords:
β-amino acids; tandem reactions; radical–polar crossover; *tert*-butanesulfinamide; zinc radical transfer

Beilstein J. Org. Chem. **2023,** *19,* 1443–1451.
https://doi.org/10.3762/bjoc.19.103

Received: 27 July 2023
Accepted: 12 September 2023
Published: 21 September 2023

This article is part of the thematic issue "Modern radical chemistry".

Guest Editor: H.-M. Huang

Abstract

We demonstrate that α-(aminomethyl)acrylates are suitable acceptors for 1,4-additions of dialkylzincs in aerobic conditions. The air-promoted radical–polar crossover process involves the 1,4-addition of an alkyl radical followed by homolytic substitution at the zinc atom of dialkylzinc. Coordination of the nitrogen atom to zinc enables this S_H2 process which represents a rare example of alkylzinc-group transfer to a tertiary α-carbonyl radical. The zinc enolate thus formed readily undergoes β-fragmentation unless it is trapped by electrophiles in situ. Enolates of substrates having free N–H bonds undergo protodemetalation to provide ultimately the 1,4-addition adduct. In the presence of carbonyl acceptors, aldol condensation occurs providing overall a tandem 1,4-addition–aldol process. When a *tert*-butanesulfinyl moiety is present on the nitrogen atom, these electrophilic substitution reactions occur with good levels of chiral induction, paving the way to enantioenriched β^2-amino acids and $\beta^{2,2}$-amino acids.

Introduction

Dialkylzinc reagents react in aerobic medium with a range of α,β-unsaturated carbonyl compounds to provide the corresponding zinc enolates (Scheme 1) [1,2]. While simple, this reaction offers attractive features: 1) it proceeds under mild conditions in the absence of any transition-metal catalyst; 2) the 1,4-addition step can be combined with condensation reactions of the zinc

enolate with electrophiles in protocols wherein all the reactive partners can be introduced from the start, given that dialkylzinc reagents offer a large functional group tolerance; and 3) the radical character of the process allows for the use of alkyl iodides as alkyl source in multicomponent reactions. Trialkylboranes can react in a similar way with enones [3] whereas, distinctively, suitable acceptors for the reaction with dialkylzinc reagents also include α,β-unsaturated carboxylic acid derivatives such as α,β-unsaturated (di)esters [4,5], *N*-enoyloxazolidinones [6,7], *N*-enoyloxazolidines [8], or alkylidenemalonates [9-11]. These reactions follow a free-radical chain process wherein alkyl radicals (R•) add across the C–C double bond of the 1,4-acceptor, activated by complexation with the dialkylzinc, to deliver an enoxyl radical that undergoes homolytic substitution at zinc (S_H2) to produce a zinc enolate and a new R• that propagates the radical chain (Scheme 1). Initiation occurs upon oxidation of the dialkylzinc reagent by oxygen.

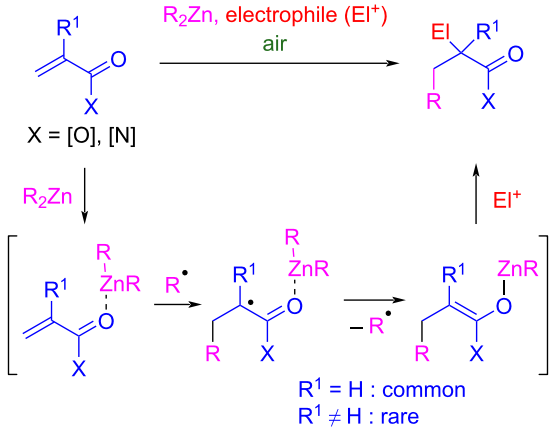

Scheme 1: Air-promoted radical chain reaction of dialkylzinc reagents with α,β-unsaturated carbonyl compounds.

The feasibility of such 1,4-addition reactions is fully reliant on the ease of the intermediate enoxyl radical to undergo alkylzinc-group transfer. Secondary α-carbonyl radicals (Scheme 1, R^1 = H) undergo readily homolytic substitution. By contrast, tertiary α-carbonyl radicals (Scheme 1, $R^1 \neq$ H) are less prone, making additions to α-substituted 1,4-acceptors more challenging. Typically, ethyl methacrylate does not react with dialkylzinc reagents [12]. Notwithstanding, 1,4-additions of dialkylzinc reagents have been reported with dehydroamino ester derivatives [13,14] and α-bromoacrylates [15], which both involve an S_H2 at zinc of tertiary α-alkoxycarbonyl radicals (Scheme 2, top). Here, the key to unlock the reactivity is the presence of a Lewis-basic substituent coordinated to the zinc atom: this offers a gain in enthalpy associated to the formation of zinc enolates stabilized by chelation and increases the spin density delocalized at the oxygen atom involved in the chelate. Note that the reported 1,4-additions of dialkylzinc reagents to alkylidenemalonates could benefit from a similar effect, even though in this case, the direct formation of an intermediate enolate remains uncertain [11].

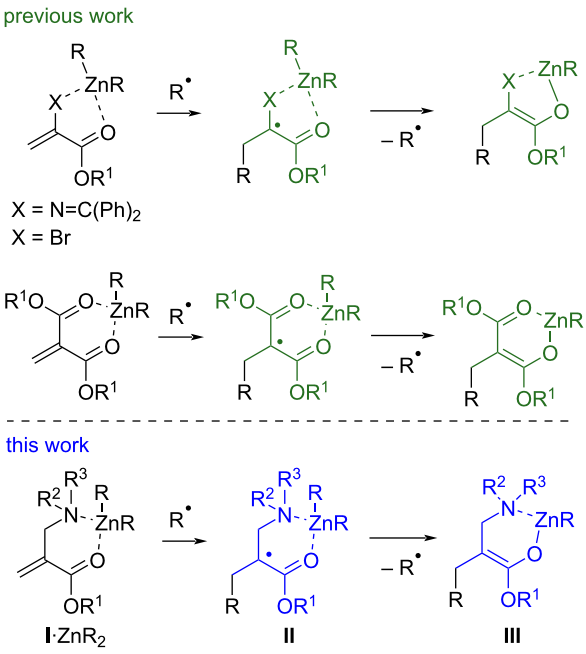

Scheme 2: Enolate formation by zinc radical transfer (S_H2 on dialkylzinc reagents).

With this context in mind, we surmised that β-aminoenoates **I** could be suitable 1,4-acceptors (Scheme 2, bottom). We previously reported tandem reactions of such substrates wherein the intermediate enoxyl radical **II** arising from the addition step evolves via intramolecular addition to tethered alkenes [16,17] or alkynes [18]. We wondered if, in the absence of the pending radical acceptor, the presence of the β-nitrogen atom could nevertheless promote zinc enolate formation. Trapping of this enolate would lead to β-amino acid units, a class of compounds that has attracted a great deal of attention [19-24]. An obvious possible shortcoming that had to be considered was still that the generated zinc enolate **III** having a β-amino group could undergo β-elimination, thereby precluding its synthetic exploitation.

Results and Discussion

Preparation of α-(aminomethyl)acrylates

We commenced our study by preparing a selection of α-(aminomethyl)acrylates with variations of the nitrogen protecting group and the ester substituent. Towards this end, the direct allylation of primary amines **1**–**3** with methyl α-(bromo-

methyl)acrylate was contemplated first under several typical conditions that all afforded non-synthetically useful mixtures of mono- and diallylation, even if excess of the nitrogen nucleophiles was used. An alternative strategy was thus developed relying on the allylation of lithium (trimethylsilyl)amides prepared in situ from the parent amines by a lithiation/silylation/lithiation sequence (Table 1). Using this protocol, α-(aminomethyl)acrylates **5** and **6** derived from benzhydrylamine and aniline were prepared in high yields (Table 1, entries 1 and 2). The procedure was poorly efficient with tosylamine, leading to product **7** in low 20% yield [25].

With the aim to develop asymmetric variants, we also considered the synthesis of *N*-(*tert*-butanesulfinyl) α-(aminomethyl)acrylates **8a**–**c**. For this purpose, the application of the same protocol with (±)-*tert*-butanesulfinamide (**4**) and the requisite α-(bromomethyl)acrylates gave satisfactory yields as well. Finally, *N*-benzyl-*N*-(*tert*-butanesulfinyl) α-(aminomethyl)acrylate **10** was prepared by allylation of lithiated *N*-benzyl *tert*-butanesulfinamide **9** (Scheme 3).

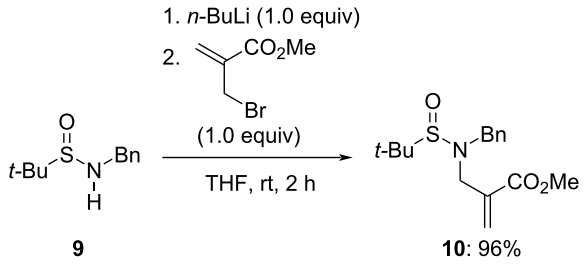

Scheme 3: Preparation of α-(aminomethyl)acrylate **10**.

1,4-Addition reactions

Having the requisite α-(aminomethyl)acrylates in hands, we carried out an initial survey of their reaction with Et_2Zn in CH_2Cl_2 at −33 °C on addition of air. In these conditions, acrylate **10** led to the recovery (following aqueous work-up) of sulfinamide **9** without traces of formation of the 1,4-adduct (Scheme 4).

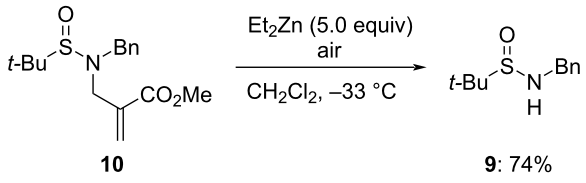

Scheme 4: Reaction of α-(aminomethyl)acrylate **10** with Et_2Zn in the presence of air.

By contrast, 1,4-addition without subsequent fragmentation was observed starting from α-(aminomethyl)acrylates having free N–H bonds (Table 2). The reaction of Et_2Zn with acrylates **5**–**7** afforded the desired 1,4-addition products **11**–**13** in 42–55% yield. Better results were obtained starting from **8a**, which delivered adduct **14a** in 79% yield and 70:30 dr. We also noted that in the absence of deliberately added air, these reactions proceeded only with low conversion. For instance, starting from **8a**, product **14a** was obtained in only 25% yield along with ≈70% of starting material recovery.

These results are relevant in the sense that not only they demonstrate that the oxygen-promoted 1,4-addition of α-(aminomethyl)acrylates with free N–H bonds is a productive process,

Table 1: Preparation of α-(aminomethyl)acrylates with free N–H bonds.

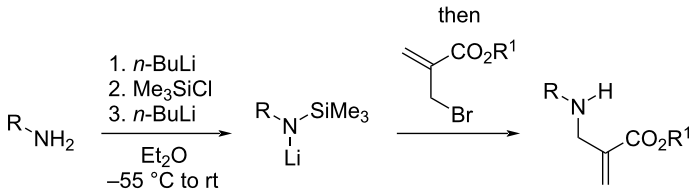

Entry	Substrate (R)	R^1	Product	Yield[a]
1	**1** ($CH(Ph)_2$)	Me	**5**	81
2	**2** (Ph)	Me	**6**	80
3	**3** (Ts)	Me	**7**	20
4	**4** (S(O)*t*-Bu)	Me	**8a**	69
5	**4** (S(O)*t*-Bu)	*t*-Bu	**8b**	50
6	**4** (S(O)*t*-Bu)	Bn	**8c**	36

[a]Isolated yield.

Table 2: Air-promoted 1,4-addition of Et_2Zn onto α-(aminomethyl)acrylates having free N–H bonds.[a]

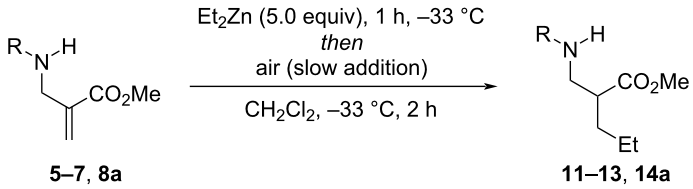

5–7, **8a** **11–13**, **14a**

Entry	Substrate (R)	Product	Yield[b]	dr[c]
1	**5** ($CH(Ph)_2$)	**11**	42	
2	**6** (Ph)	**12**	55	
3	**7** (Ts)	**13**	55	
4	**8a** (S(O)*t*-Bu)	**14a**	76	70:30
5	**8a** (S(O)*t*-Bu)	**14a**	25[d]	50:50

[a]General conditions: α-(aminomethyl)acrylate (0.2 mmol), Et_2Zn (1.0 mmol), CH_2Cl_2 (6 mL), air (20 mL introduced via syringe at 0.5 mL·min^{-1} rate). [b]Isolated yield. [c]Ratio of diastereomers measured by ^{1}H NMR spectroscopy prior to purification. [d]No air was added.

but also that the *tert*-butanesulfinyl moiety is well tolerated and that 1,4-stereoinduction can be achieved. Hence, in order to improve the levels of diastereoselectivity, we investigated further the reaction conditions starting with enoate **8a** as model substrate (Table 3).

Carrying out the reaction at −78 °C instead of −33 °C was deleterious both for the yield and the selectivity (Table 3, entry 2). By contrast, we rapidly learned that leaving diethylzinc in contact with the starting acrylate for 1 h prior to the addition of air had a significant impact on the stereoselectivity. When air was

Table 3: Optimization of the air-promoted 1,4-addition of dialkylzinc reagents onto *N*-(*tert*-butanesulfinyl) α-(aminomethyl)acrylates.

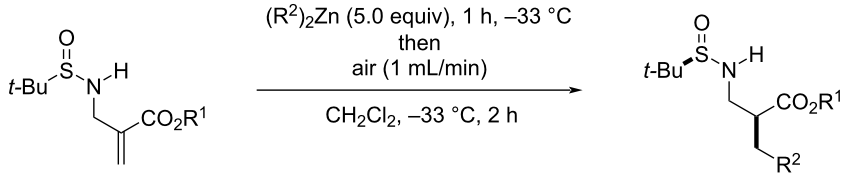

8a–c **14a–c**, **15a**, **16a**

Entry	Substrate (R^1)	R^2	Product	Variation of conditions[a]	Yield[b]	dr[c,d]
1	**8a** (Me)	Et	**14a**	none	76	70:30
2	**8a** (Me)	Et	**14a**	–78 °C instead of –33 °C	60	57:43
3	**8a** (Me)	Et	**14a**	oxygen (5 mL) was added at once immediately after Et_2Zn	83	59:41
4	**8a** (Me)	Et	**14a**	toluene instead of CH_2Cl_2	82	75:25
5	**8a** (Me)	Et	**14a**	hexane instead of CH_2Cl_2	82	85:15
6	**8b** (*t*-Bu)	Et	**14b**	hexane instead of CH_2Cl_2	88	85:15
7	**8c** (Bn)	Et	**14c**	none	76	70:30
8	**8a** (Me)	Bu	**15a**	none	71	67:33
9	**8a** (Me)	Me	**16a**	none	n.r.[e]	
10	**8a** (Me)	Me	**16a**	hexane instead of CH_2Cl_2	n.r.[e]	

[a]All reactions were conducted at a 0.2 mmol scale using 20 mL of air. [b]Isolated yield (mixture of diastereoisomers). [c]Measured by ^{1}H or ^{13}C NMR spectroscopy prior to purification. [d]The relative configuration of the major diastereomer is shown in the scheme; it was determined by chemical correlation for **14b** (see below) and inferred by analogy for **14a** and **14c**. [e]No reaction.

introduced directly after Et_2Zn (Table 3, entry 3) a much lower 59:41 dr was observed. This behavior was suggestive of the need for coordination of diethylzinc both to the carbonyl and sulfinyl unit to achieve good levels of selectivity. Hence, to reinforce Lewis pair formation, the reaction was also carried out in apolar solvents such as toluene and hexane (entries 4 and 5 in Table 3). In hexane, an 88% yield with 85:15 dr was obtained, which constituted the best conditions. Importantly, the protocol was found to be similarly applicable with enoates **8b** (Table 3, entry 6) and **8c** (entry 7) having *tert*-butyl and benzyl ester groups, which, as the methyl ester unit, are typical in the context of amino acid synthesis. $ZnBu_2$ was also amenable to 1,4-addition (Table 3, entry 8), but not $ZnMe_2$ (entries 9 and 10). This difference can be ascribed to a less favorable homolytic substitution reaction of $ZnMe_2$ in relation to its higher analogues and is in line with previous literature observations [11].

The configuration of the major diastereomer was determined by chemical correlation (Scheme 5). Product (R_S)-**14b** (85:15 dr), i.e., a mixture of two enantiomerically pure diastereomers, was obtained from (R_S)-*tert*-butylsulfinamide upon allylation with *tert*-butyl α-(bromomethyl)acrylate followed by 1,4-addition with Et_2Zn. It was then converted into the known β^2-amino acid **17** by TFA-promoted concomitant deprotection of the nitrogen and the ester groups. The sample was found to have a negative optical rotation, thereby indicating that the major enantiomer present had *S* configuration [26]. This allowed to establish that the configuration of the major diastereomer present in (R_S)-**14b** was (R_S,*S*), and thus the sense of chiral induction for the 1,4-addition reactions reported in Table 2.

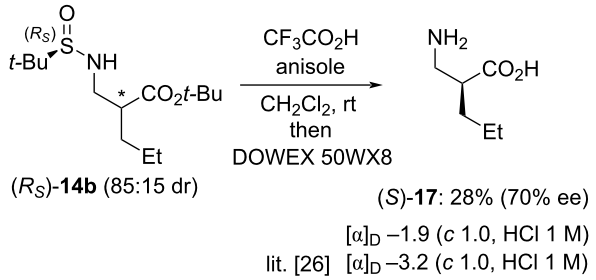

Scheme 5: Chemical correlation to determine the configuration of the major diastereomer of (R_S)-**14b**.

Tandem 1,4-addition–aldol condensation reactions

We then went on to consider tandem 1,4-addition–aldol condensation reactions (Scheme 6), which offer the interesting prospect of generating an all-carbon quaternary stereocenter. α-(Aminomethyl)acrylates **5**–**7** reacted smoothly at −33 °C within 2 h with Et_2Zn in the presence of cyclohexanone to afford amino alcohols **18**–**20** in quite good yields (63–68%). Even better yields were obtained with enoates **8a** and **8b** both with cyclohexanone and acetone as carbonyl partners. Starting from **8a** and carrying out the reaction in CH_2Cl_2, product **21a** was obtained in 86% yield with 75:25 dr. Alike for the 1,4-addition protocol, better stereoinduction was obtained by performing the reaction in hexane: **8b** was converted into **21b** and **22** in 77–84% yield with higher than 90:10 dr. It is also interesting to note that the levels of induction for the 1,4-addition–aldol condensations are somewhat higher than those obtained for the 1,4-additions. Aldehydes also proved competent terminal electrophiles for the tandem sequence. Illustratively, adducts **23** and **24** were obtained from α-(aminomethyl)acrylates **5** and **8a** in 77–88% yields, albeit as poorly selective mixtures of diastereoisomers. This lack of stereocontrol is not surprising, given the well-known difficulty to control the relative configuration between the two adjacent stereocenters created during aldol condensations with zinc enolates.

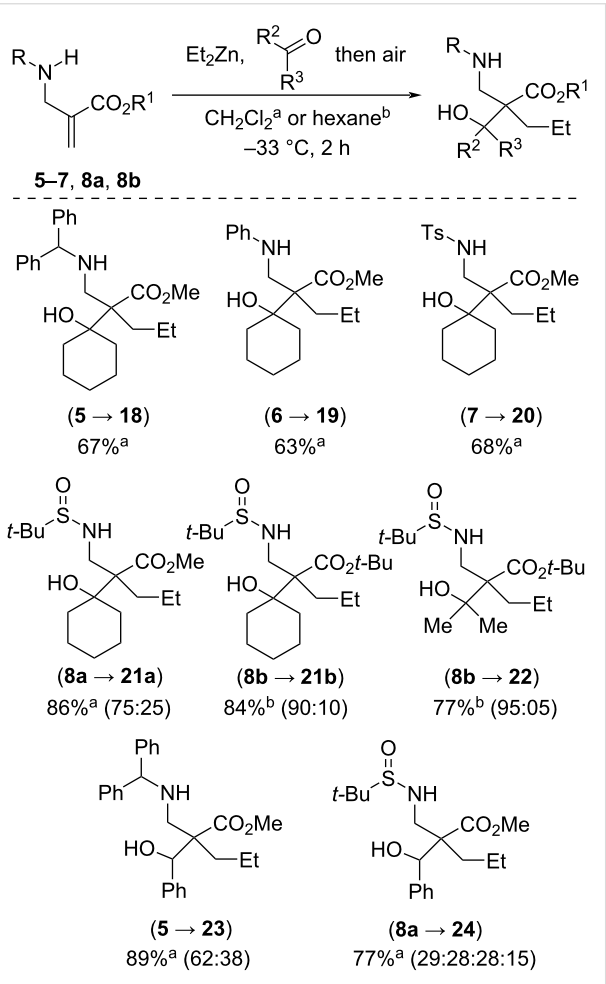

Scheme 6: Air-promoted tandem 1,4-addition–aldol condensation reactions of Et_2Zn with α-(aminomethyl)acrylates.

Mechanistic insights

The last part of our work was devoted to gain mechanistic insight for the developed reaction protocols through several diagnostic experiments. Regarding the 1,4-addition process, the lower reactivity noted in the absence of air (Table 2, entry 5) represents already a strong indication for a radical addition mechanism. This is further supported by the result of an I-atom transfer experiment (Scheme 7, top). In the presence of two equivalents of iPrI, the reaction of **8a** with Et_2Zn leads to a mixture of product **14a** and product **25a**, incorporating an iPr moiety, in a **14a**/**25a** 30:70 mixture. Product **25a** is formed on addition of an iPr radical generated by I-atom transfer from iPrI to the Et radical, and is diagnostic for the formation of the latter in the reaction medium.

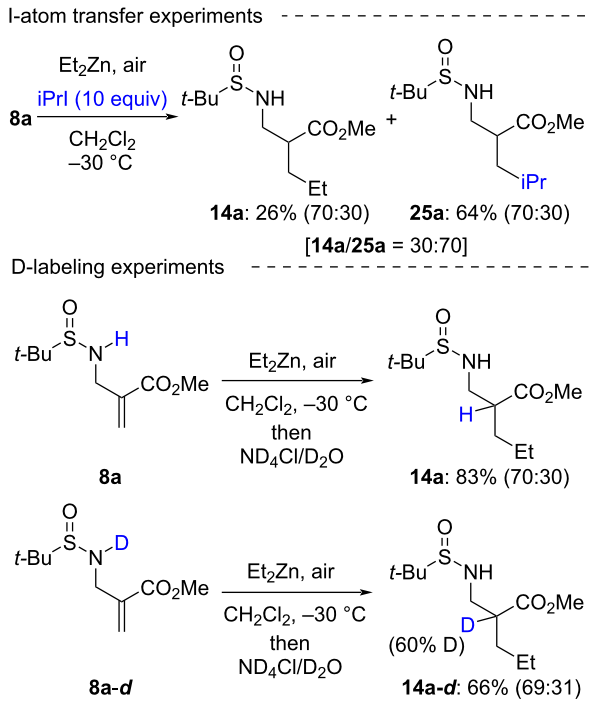

Scheme 7: Diagnostic experiments for a radical mechanism and for enolate formation.

Deuterium labeling experiments were then performed to substantiate the formation of a zinc enolate following radical addition (Scheme 7, bottom). Much to our surprise however, no deuterium incorporation is observed on quenching with ND_4Cl/D_2O the reaction between **8a** and Et_2Zn. By contrast, a significant deuterium incorporation is obtained when deuterated starting material (**8a-*d***) is engaged. The combination of these two results is in agreement with the formation of a zinc enolate that undergoes proto- (or deuterio)demetalation with the N–H (or N–D) as proton (or deuterium) source.

To further analyze the influence of the presence of an N–H function, we performed other reactions with *N*-benzyl enoate **10** which proved highly informative. As discussed previously (Scheme 4), application of the developed protocol for 1,4-addition to **10** only yields *N*-benzyl-*N*-*tert*-butylsulfinamide following β-elimination. By contrast, in the presence of benzaldehyde, 1,4-addition–aldol condensation is predominant, yielding **26** in 56% yield as a 49:25:23:3 diastereomeric mixture (Scheme 8). When **10** is exposed to Et_3B in the presence of iPrI, benzaldehyde, and O_2, which are conditions known to promote radical 1,4-addition, only formation of telomers [7] is noted. This lends clear evidence that the intermediate enoxyl radical does not intervene neither in the β-fragmentation (Scheme 4) nor in the addition across the carbonyl bonds.

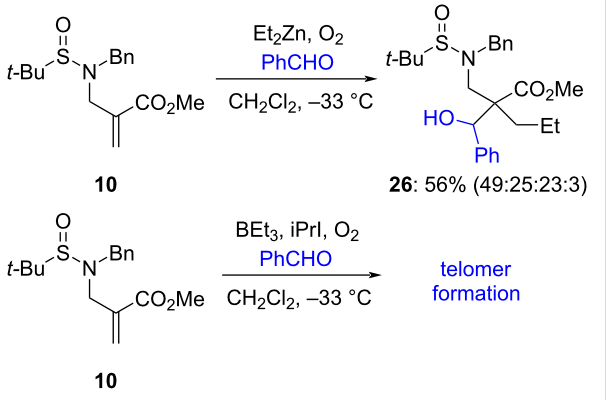

Scheme 8: Diagnostic experiments with *N*-benzyl enoate **10**.

Overall, the mechanistic investigations support the scenario depicted in Scheme 9. Oxygen (in air) triggers a free-radical chain reaction between α-(aminomethyl)acrylates and dialkylzinc reagents that entails 1,4-addition and S_H2 of the formed enoxyl radical facilitated by coordination of nitrogen to zinc. The zinc enolate thus formed evolves following different pathways according to the type of substrate and reaction conditions. In the absence of a carbonyl electrophile, enolates of substrates with trisubstituted nitrogen groups undergo β-fragmentation. By contrast, those derived from substrates having N–H bonds undergo protodemetalation to provide ultimately the 1,4-addition adduct. In the presence of carbonyl acceptors, these two competitive reactions are superseded and the enolate engages in aldol condensation regardless of its nitrogen substitution; the outcome of the reaction is a tandem 1,4-addition–aldol process. When the *tert*-butanesulfinyl moiety is present on the nitrogen atom, electrophilic substitution of the intermediate enolates (protodemetalation or aldol condensation) occurs with decent levels of chiral induction. It should be mentioned here that our attempts to trap the intermediate enolate with a carbon electrophile other than carbonyl acceptors (i.e., iodomethane) were not

successful and protodemetalation of the enolate outcompeted methylation.

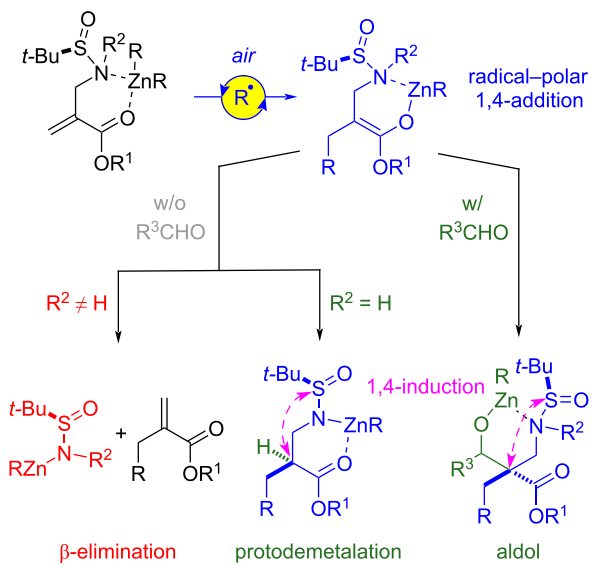

Scheme 9: Reactivity manifolds for the air-promoted tandem 1,4-addition–electrophilic substitution reaction between dialkylzinc reagents and α-(aminomethyl)acrylates (*N*-(*tert*-butanesulfinyl) derivatives shown).

Conclusion

In conclusion, we have demonstrated that α-(aminomethyl)acrylates are suitable acceptors for 1,4-additions with dialkylzincs in aerobic conditions. Coordination of the nitrogen atom to zinc is crucial to enable the S_H2 step of the tertiary α-carbonyl radical that follows radical 1,4-addition in order to deliver a zinc enolate. The latter is poised to undergo β-fragmentation, but this process can be outcompeted by in situ electrophilic substitution reactions which offer synthetically useful procedures: 1,4-addition (for substrates having N–H bonds) or tandem 1,4-addition–aldol reactions (in the presence of carbonyl electrophiles). Asymmetric variants of these transformations are possible using the *tert*-butanesulfinyl chiral auxiliary on the nitrogen atom. The levels of 1,4-stereoinduction are significant but a convincing model to account for it cannot be put forward at this point. Nonetheless, from a synthetic methodology point of view, the reported protocols are relevant as they offer a new, direct and modular route to enantioenriched α-mono- and α,α-disubstituted β-amino acids (β^2-amino acids and $\beta^{2,2}$-amino acids), with, for the latter, the noteworthy stereocontrolled construction of an all-carbon quaternary stereocenter. Furthermore, our protocol provides a complement to existing literature, as none of the previously reported methods to convert α-(aminomethyl)acrylates into enantioenriched β-amino acids is applicable for the preparation of $\beta^{2,2}$-amino acids [27-31].

Experimental

1. Procedure for the monoallylation of primary amines and *tert*-butylsulfinamide (preparation of compounds 5–7 and 8a–c). In a round-bottomed flask under argon, *n*-BuLi (1.0 equiv, soln. in heptane) was added dropwise to a THF (0.2 mol·L^{-1}) solution of the appropriate primary amine or *tert*-butylsulfinamide (1.0 equiv) at −55 °C. The mixture was then stirred at rt for 30 min, cooled to −55 °C, and trimethylsilyl chloride (1.0 equiv) was added. The mixture was then stirred at rt for 30 min, cooled to −55 °C, and *n*-BuLi (1.0 equiv, soln. in heptane) was added dropwise. The mixture was stirred at rt for 30 min, cooled to −78 °C, and the corresponding α-(bromomethyl)acrylate (1.0 equiv) was added. The reaction mixture was then stirred for 2 h letting the temperature rise to rt and quenched with aq 1 M NH_4Cl. The aqueous layer was extracted with EtOAc (3×) and the combined organic layer was washed (brine), dried ($MgSO_4$), and concentrated under reduced pressure to provide the crude product which was then purified by column chromatography on silica gel.

2. Procedure for the air-promoted 1,4-addition of dialkylzinc reagents to α-(aminomethyl)acrylates (preparation of compounds 11–13, 14a–c, and 15a). In a Schlenk-tube under argon, the appropriate α-(aminomethyl)acrylate (0.2 mmol) was dissolved in the indicated reaction solvent (3 mL) and the solution was cooled to −33 °C. Then, Et_2Zn (1 M in hexanes, 1.0 mL, 1.0 mmol) was added dropwise and the solution was stirred for 1 h. Air (20 mL) was introduced directly into the solution via a syringe fitted with a $CaCl_2$ pad at a 0.5 mL/min rate (syringe pump). After the end of the air addition, the mixture was stirred for an additional 80 min at −33 °C and then quenched with aq NH_4Cl (5 mL) at 0 °C. The aqueous layer was extracted with CH_2Cl_2 (2×). The combined organic layer was washed (brine), dried ($MgSO_4$), and concentrated under reduced pressure to provide the crude product which was then purified by column chromatography on silica gel.

3. Procedure for the air-promoted tandem 1,4-addition–aldol reaction between dialkylzinc reagents, α-(aminomethyl)acrylates and carbonyl derivatives (preparation of compounds 18–20, 21a–b, 22–24). In a Schlenk-tube under argon, the appropriate α-(aminomethyl)acrylate (0.2 mmol) was dissolved in the indicated reaction solvent (3 mL) and the solution was cooled to −33 °C. The carbonyl electrophile (1.0 mmol) and then Et_2Zn (1 M in hexanes, 1.0 mL, 1.0 mmol) were added dropwise and the solution was stirred for 1 h. Air (20 mL) was introduced directly into the solution via a syringe fitted with a $CaCl_2$ pad at a 0.5 mL/min rate (syringe pump). After the end of the air addition, the mixture was stirred for an additional 80 min at −33 °C and then quenched with aq NH_4Cl (5 mL) at 0 °C. The aqueous layer was extracted with CH_2Cl_2

(2×). The combined organic layer was washed (brine), dried ($MgSO_4$), and concentrated under reduced pressure to provide the crude product which was then purified by column chromatography on silica gel.

Supporting Information

Supporting Information File 1

General information, characterization data, chemical correlation, and copies of NMR spectra.
[https://www.beilstein-journals.org/bjoc/content/supplementary/1860-5397-19-103-S1.pdf]

Acknowledgements

The authors acknowledge MS3U of Sorbonne Université for HRMS analysis.

Funding

A. P.-C. (207839), P. G.-G. (226571) and F. G.-A. (360237) are thankful to CONACyT for scholarships.

ORCID® iDs

Fernando García-Alvarez - https://orcid.org/0000-0002-4833-9420
Olivier Jackowski - https://orcid.org/0000-0001-9162-3294
Franck Ferreira - https://orcid.org/0000-0002-7571-1830
Joel L. Terán - https://orcid.org/0000-0002-4055-4353
Alejandro Perez-Luna - https://orcid.org/0000-0002-5578-9024

References

1. Bazin, S.; Feray, L.; Bertrand, M. P. *Chimia* **2006,** *60,* 260–265. doi:10.2533/000942906777674679
2. Chemla, F.; Pérez-Luna, A. Radical-Polar Crossover Reactions. In *Free Radicals: Fundamentals and Applications in Organic Synthesis 2;* Fensterbank, L.; Ollivier, C., Eds.; *Science of Synthesis*; Thieme: Stuttgart, Germany, 2021; pp 209–357. doi:10.1055/sos-sd-233-00075
3. Brown, H. C.; Midland, M. M. *Angew. Chem., Int. Ed. Engl.* **1972,** *11,* 692–700. doi:10.1002/anie.197206921
4. Bazin, S.; Feray, L.; Vanthuyne, N.; Siri, D.; Bertrand, M. P. *Tetrahedron* **2007,** *63,* 77–85. doi:10.1016/j.tet.2006.10.049
5. Maury, J.; Mouysset, D.; Feray, L.; Marque, S. R. A.; Siri, D.; Bertrand, M. P. *Chem. – Eur. J.* **2012,** *18,* 3241–3247. doi:10.1002/chem.201102366
6. Bazin, S.; Feray, L.; Vanthuyne, N.; Bertrand, M. P. *Tetrahedron* **2005,** *61,* 4261–4274. doi:10.1016/j.tet.2005.02.042
7. Bazin, S.; Feray, L.; Siri, D.; Naubron, J.-V.; Bertrand, M. P. *Chem. Commun.* **2002,** 2506–2507. doi:10.1039/b206695e
8. Zelocualtecatl-Montiel, I.; García-Álvarez, F.; Juárez, J. R.; Orea, L.; Gnecco, D.; Mendoza, A.; Chemla, F.; Ferreira, F.; Jackowski, O.; Aparicio, D. M.; Perez-Luna, A.; Terán, J. L. *Asian J. Org. Chem.* **2017,** *6,* 67–70. doi:10.1002/ajoc.201600501
9. Yamada, K.-i.; Konishi, T.; Nakano, M.; Fujii, S.; Cadou, R.; Yamamoto, Y.; Tomioka, K. *J. Org. Chem.* **2012,** *77,* 5775–5780. doi:10.1021/jo300944f
10. Yamada, K.-i.; Matsumoto, Y.; Fujii, S.; Konishi, T.; Yamaoka, Y.; Takasu, K. *J. Org. Chem.* **2016,** *81,* 3809–3817. doi:10.1021/acs.joc.6b00485
11. Lingua, H.; Dwadnia, N.; Siri, D.; Bertrand, M. P.; Feray, L. *Tetrahedron* **2018,** *74,* 7507–7515. doi:10.1016/j.tet.2018.11.029
12. Bertrand, M. P.; Feray, L.; Nouguier, R.; Perfetti, P. *J. Org. Chem.* **1999,** *64,* 9189–9193. doi:10.1021/jo9912404
13. Miyabe, H.; Asada, R.; Yoshida, K.; Takemoto, Y. *Synlett* **2004,** 540–542. doi:10.1055/s-2004-815407
14. Miyabe, H.; Asada, R.; Takemoto, Y. *Tetrahedron* **2005,** *61,* 385–393. doi:10.1016/j.tet.2004.10.104
15. Vibert, F.; Maury, J.; Lingua, H.; Besson, E.; Siri, D.; Bertrand, M. P.; Feray, L. *Tetrahedron* **2015,** *71,* 8991–9002. doi:10.1016/j.tet.2015.09.045
16. Denes, F.; Chemla, F.; Normant, J. F. *Angew. Chem., Int. Ed.* **2003,** *42,* 4043–4046. doi:10.1002/anie.200250474
17. Denes, F.; Cutri, S.; Pérez-Luna, A.; Chemla, F. *Chem. – Eur. J.* **2006,** *12,* 6506–6513. doi:10.1002/chem.200600334
18. Beniazza, R.; Romain, E.; Chemla, F.; Ferreira, F.; Jackowski, O.; Perez-Luna, A. *Eur. J. Org. Chem.* **2015,** 7661–7665. doi:10.1002/ejoc.201501173
19. Cheng, R. P.; Gellman, S. H.; DeGrado, W. F. *Chem. Rev.* **2001,** *101,* 3219–3232. doi:10.1021/cr000045i
20. Liu, M.; Sibi, M. P. *Tetrahedron* **2002,** *58,* 7991–8035. doi:10.1016/s0040-4020(02)00991-2
21. Lelais, G.; Seebach, D. *Biopolymers* **2004,** *76,* 206–243. doi:10.1002/bip.20088
22. Seebach, D.; Gardiner, J. *Acc. Chem. Res.* **2008,** *41,* 1366–1375. doi:10.1021/ar700263g
23. Seebach, D.; Beck, A. K.; Capone, S.; Deniau, G.; Groselj, U.; Zass, E. *Synthesis* **2009,** 1–32. doi:10.1055/s-0028-1087490
24. Noda, H.; Shibasaki, M. *Eur. J. Org. Chem.* **2020,** 2350–2361. doi:10.1002/ejoc.201901596
25. Xuan, J.; Daniliuc, C. G.; Studer, A. *Org. Lett.* **2016,** *18,* 6372–6375. doi:10.1021/acs.orglett.6b03267
26. Gutiérrez-García, V. M.; Reyes-Rangel, G.; Muñoz-Muñiz, O.; Juaristi, E. *Helv. Chim. Acta* **2002,** *85,* 4189–4199. doi:10.1002/hlca.200290004
27. Sibi, M. P.; Tatamidani, H.; Patil, K. *Org. Lett.* **2005,** *7,* 2571–2573. doi:10.1021/ol050630b
28. Qiu, L.; Prashad, M.; Hu, B.; Prasad, K.; Repič, O.; Blacklock, T. J.; Kwong, F. Y.; Kok, S. H. L.; Lee, H. W.; Chan, A. S. C. *Proc. Natl. Acad. Sci. U. S. A.* **2007,** *104,* 16787–16792. doi:10.1073/pnas.0704461104
29. Guo, Y.; Shao, G.; Li, L.; Wu, W.; Li, R.; Li, J.; Song, J.; Qiu, L.; Prashad, M.; Kwong, F. Y. *Adv. Synth. Catal.* **2010,** *352,* 1539–1553. doi:10.1002/adsc.201000122
30. Li, L.; Chen, B.; Ke, Y.; Li, Q.; Zhuang, Y.; Duan, K.; Huang, Y.; Pang, J.; Qiu, L. *Chem. – Asian J.* **2013,** *8,* 2167–2174. doi:10.1002/asia.201300339
31. Sibi, M. P.; Patil, K. *Angew. Chem., Int. Ed.* **2004,** *43,* 1235–1238. doi:10.1002/anie.200353000

BEILSTEIN JOURNAL OF ORGANIC CHEMISTRY

Radical chemistry in polymer science: an overview and recent advances

Zixiao Wang, Feichen Cui, Yang Sui and Jiajun Yan*

Review

Open Access

Address:
School of Physical Science and Technology, ShanghaiTech University, 393 Middle Huaxia Rd., Shanghai, 201210, China

Email:
Jiajun Yan* - yanjj@shanghaitech.edu.cn

* Corresponding author

Keywords:
crosslinking; polymer surface modification; post-polymerization modification; radical chemistry; radical polymerization

Beilstein J. Org. Chem. **2023,** *19,* 1580–1603.
https://doi.org/10.3762/bjoc.19.116

Received: 09 June 2023
Accepted: 05 October 2023
Published: 18 October 2023

This article is part of the thematic issue "Modern radical chemistry".

Guest Editor: H.-M. Huang

Abstract

Radical chemistry is one of the most important methods used in modern polymer science and industry. Over the past century, new knowledge on radical chemistry has both promoted and been generated from the emergence of polymer synthesis and modification techniques. In this review, we discuss radical chemistry in polymer science from four interconnected aspects. We begin with radical polymerization, the most employed technique for industrial production of polymeric materials, and other polymer synthesis involving a radical process. Post-polymerization modification, including polymer crosslinking and polymer surface modification, is the key process that introduces functionality and practicality to polymeric materials. Radical depolymerization, an efficient approach to destroy polymers, finds applications in two distinct fields, semiconductor industry and environmental protection. Polymer chemistry has largely diverged from organic chemistry with the fine division of modern science but polymer chemists constantly acquire new inspirations from organic chemists. Dialogues on radical chemistry between the two communities will deepen the understanding of the two fields and benefit the humanity.

Introduction

Early last century, with the groundbreaking macromolecular hypothesis by Hermann Staudinger [1], polymer science was born out of organic chemistry. Since then, polymer science has evolved into an important branch of physical science and a fundament of the modern life. Like many other organic methodologies, radical chemistry was applied to polymer science and nowadays, radical chemistry plays a critical role in both the production of a major portion of industrial polymers and the research on novel materials [2]. In this minireview, we discuss several aspects of radical chemistry found in polymer science.

Section 1 focuses on the best-established radical chemistry – radical polymerization, including radical polymerization in nature, conventional radical polymerization, and a new class of

radical polymerization, reversible deactivation radical polymerization, which emerged late last century. To continue with the discussion on polymer construction, section 2 explores some emergent polymer synthesis techniques via a radical process but other than a chain-growth mechanism by addition of radical species to vinyl monomers. In section 3, we cover radical chemistry approaches used in post-polymerization modification, including chemical crosslinking of polymers and polymer surface modification. Radicals are powerful tools for post-polymerization processes because of their exceptional reactivity. In contrast to the previous sections, we set the topic of section 4 on the radical degradation of polymers, both in nanofabrication and polymer upcycling.

Review

1 Radical polymerization

Radical polymerization has long been an effective and inexpensive method in the synthesis of polymers since it was invented, making it the most important industrial polymerization technique. Polymers produced by radical polymerization represent a major fraction of all industrial polymers.

1.1 Radical polymerization in nature

In addition to well-established processes in modern industry, examples of radical polymerization exist in nature. The principle of the two cases in the following text is based on the radical polymerization of catechol derivatives. Catechols are known as easily oxidizable compounds and are prone to undergo oxidation by losing one or two electrons [3]. This way, either semiquinone radicals or *o*-quinones are formed by single or double-electron oxidation, respectively [4]. The semiquinone radicals formed during the oxidation of catechol can undergo a cross-coupling reaction to form polymers (Scheme 1).

One example is the radical polymerization of urushiol. The earliest recorded application of natural radical polymerization can be traced back to the manufacture of lacquerwares several thousand years ago [5]. The surface coating of lacquerwares was made up of a sap from a lacquer tree growing in Asia. The lacquer sap obtained from *Rhus vernicifera* lacquer tree mainly consists of urushiol (60–65%), water (20–30%), lacquer polysaccharide (3–7%), water-insoluble glycoprotein (≈1–2%), laccase (≈0.2%), and stellacyanin (≈0.02%) [6,7]. Urushiol is the main active coating-forming ingredient of the resin. A typical urushiol is shown in Scheme 2. In a humid and warm environment, urushiol absorbs oxygen from air and is oxidized to a phenolic oxygen free radical under the action of laccase enzymes [5]. The radical then rearranges to form a semiquinone radical and reacts rapidly with a neighboring urushiol molecule to produce a biphenyl dimer. The dimers further polymerize to form the polymer [8].

Radical processes also occur in oceans. The mussel attachment system consists of a bundle of disc-tipped acellular thread called *byssus,* which connect the mussel to the surfaces of substrates [10]. A family of proteins called mussel foot proteins (mfp's) distribute throughout the whole length of *byssus* while there is an extremely high concentration of mfp's at the plaque–substrate interface. The mfp's contain up to 27 mol % of DOPA (L-3,4-dihydroxyphenylalanine), which plays a crucial role on mussel adhesion [11]. Although the crucial role of DOPA in mussel adhesion is not fully understood, a prevailing view suggests that DOPA can be oxidized to *o*-quinones at an acidic pH and the quinones react with unoxidized catechols to form *o*-semiquinone radicals afterwards [12]. The semiquinone radicals can help DOPA adhere onto organic surfaces. At a basic pH, the system is cured and mechanically stabilized through the formation of DOPA-metal coordination bonds. The

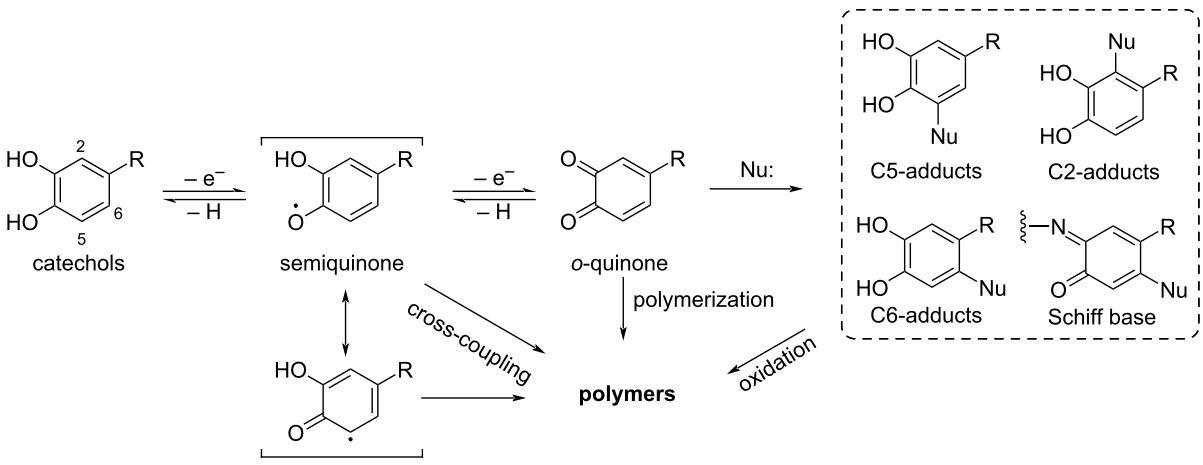

Scheme 1: Oxidation of catechol and subsequent cross-linking. Scheme 1 redrawn from [3].

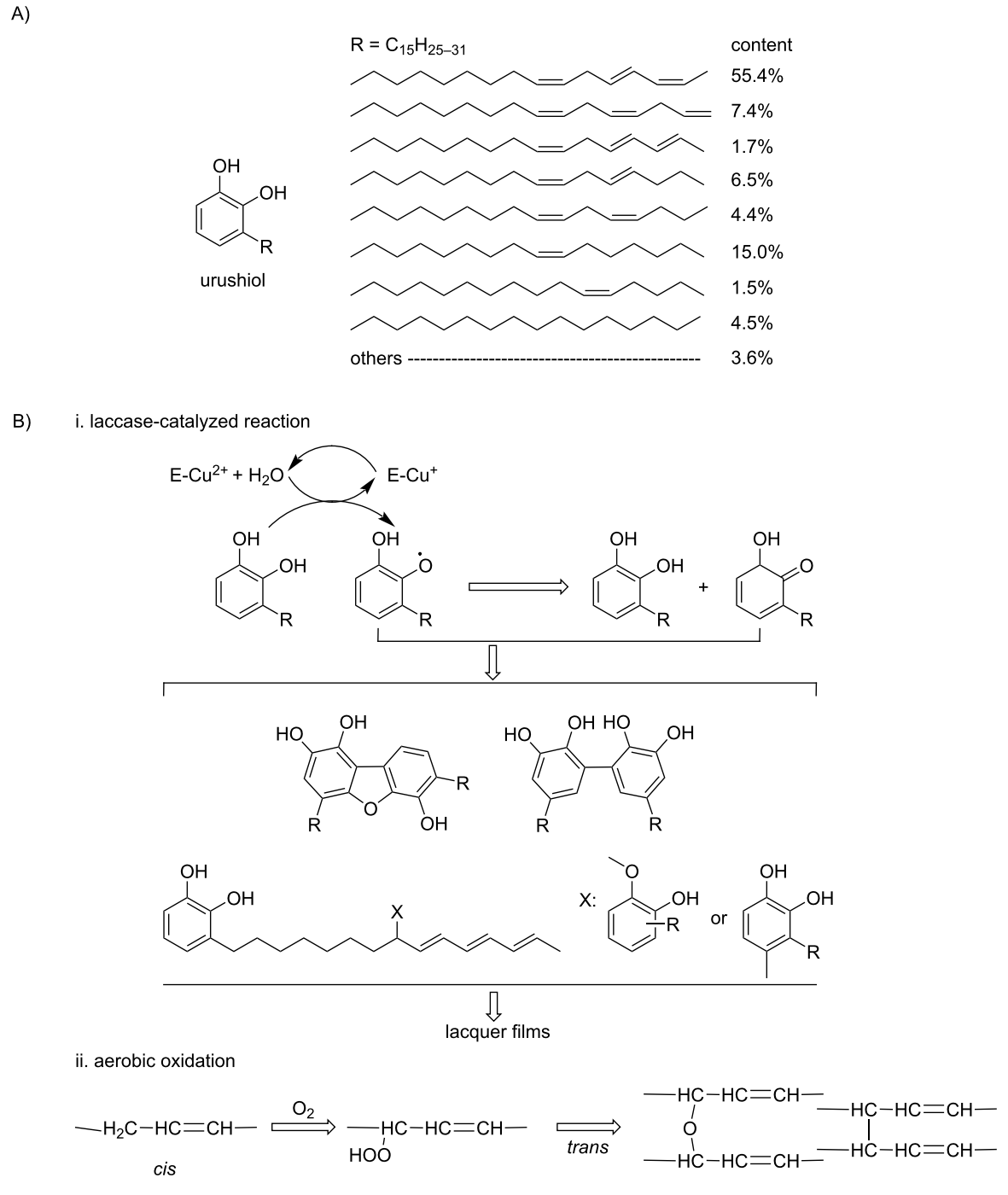

Scheme 2: (A) Structure of typical urushiol in Chinese lacquer, and (B) schematic process of laccase-catalyzed oxidation polymerization of Chinese lacquer and autoxidation reaction on the long aliphatic unsaturated side chain. Scheme 2 redrawn from [9].

cohesion of the DOPA-metal complex helps mussel adhere onto inorganic surfaces (Scheme 3).

1.2 Conventional radical polymerization

Radical polymerization, which IUPAC defines as 'A chain polymerization in which the kinetic-chain carriers are radicals' [13], is the most widely used reaction in polymer industry. As far back as the 1950s, the basic theory and comprehension of radical polymerization was established. In the past decades, radical polymerization was introduced to be an efficient industrial synthesis method to produce numerous chemicals such as low-density polyethylene (LDPE), polystyrene (PS), and

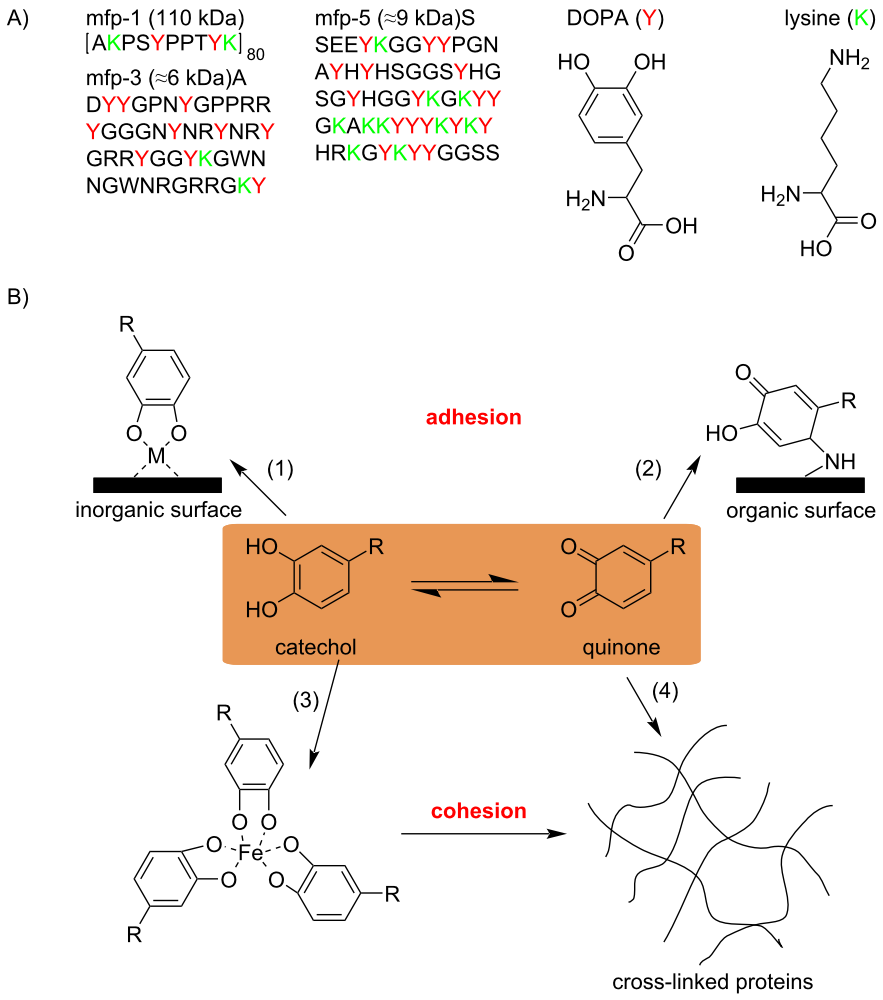

Scheme 3: A) Primary amino acid sequence of mfp-1, mfp-3, and mfp-5 (Y: DOPA, K: lysine). B) Scheme showing examples of the adhesive and cohesive properties of catechol-containing proteins. R represents the remainder of the mfp's. Scheme 3 redrawn from [10].

poly(vinyl chloride) (PVC) [14]. About half of the industrial polymers manufactured worldwide are produced by radical polymerization [15,16].

1.2.1 Key features of radical polymerization: Radical polymerization, which has a classical chain reaction process, usually analyzed kinetically on the assumption of a steady state with respect to the concentration of chain carriers (radicals) [17]. Radical polymerization is a complex mechanism. The basic reactions have been known for quite some time now. They can be simply described by 8 equations (Equations 1–8) as follows. In the equations, I_2 represents an initiator molecule; M represents a monomer molecule; P_i represents a polymer chain with *i* repeating units; S represents a solvent molecule; and a dot indicates free radical species. These reactions are classified into four elementary steps: initiation, propagation, termination, and transfer. The initiation step includes Equation 1 and Equation 2, when the thermal initiator decomposes into two small-molecule radical species and the first monomer adds to the growing chain to form the first repeating unit. The propagation step is depicted in Equation 3 when monomers take turns to undergo radical addition. The termination step occurs by either disproportionation (radical β-elimination, Equation 4) or biradical coupling (Equation 5). Chain transfer (Equations 6–8) is usually considered as a type of side effect in radical polymerization [18]. It occurs between the growing chain and a transfer agent, which can be the monomer (Equation 6), the solvent (Equation 7), the polymer itself (Equation 8), or a chain-transfer agent intentionally added to tune the molecular weight or to introduce chain-end functionalities. When chain transfer happens, the originally growing chain halts while a new chain launches from the radical species formed from the chain transfer agent. In the case when a

growing chain-end radical transfers to its own backbone, i.e., backbiting occurs, a branching point forms as propagation continues in the middle of the backbone.

$$I_2 \xrightarrow{k_d} 2I^{\bullet} \quad (1)$$

$$I^{\bullet} + M \xrightarrow{k_d} P_1^{\bullet} \quad (2)$$

$$P_n^{\bullet} + M \xrightarrow{k_p} P_{n+1}^{\bullet} \quad (3)$$

$$P_n^{\bullet} + P_m^{\bullet} \xrightarrow{k_{td}} P_n^{=} + P_m \quad (4)$$

$$P_n^{\bullet} + P_m^{\bullet} \xrightarrow{k_{tc}} P_{n+m} \quad (5)$$

$$P_n^{\bullet} + M \xrightarrow{k_{tr}^{mon}} P_n + M^{\bullet} \quad (6)$$

$$P_n^{\bullet} + S \xrightarrow{k_{tr}^{sol}} P_n + S^{\bullet} \quad (7)$$

$$P_n^{\bullet} + P_m \xrightarrow{k_{tr}^{pol}} P_n + P_m^{\bullet} \quad (8)$$

Radical polymerization is applicable to a large number of vinylic monomers and is tolerant toward many solvents, functional groups, and impurities common in industrial systems, which makes it an ideal choice for industrial production [19]. Vinylic monomers should be thermodynamically and kinetically polymerizable. The former requires a sufficiently negative free energy of polymerization and the latter an adequate reactivity of the monomer, stability of the derived free radical, and a low proportion of side reactions.

A slow rate of chain initiation, a fast rate of chain propagation, and a rapid rate of chain termination are key features of conventional radical polymerization. Most free radicals have an extremely short lifetime due to a diffusion-controlled termination process between two free radicals. The inevitable termination between radicals makes the synthesis of well-defined polymers and co-polymers very difficult. In addition, polymers obtained from conventional radical polymerization are commonly linear polymers, though transfer to polymer may induce branching.

1.2.2 Radical polymerization in modern industry: In the commercial production of high-molecular-weight polymers, radical polymerization is a widely used method. Its main advantages are (i) the universality to a wide range of monomers such as (meth)acrylates, (meth)acrylamides, dienes, vinyl ethers/esters, etc.; (ii) tolerance to unprotected functionalities in monomers and the solvent including –OH, –COOH, $–SO_3H$, etc.; (iii) different reaction conditions, including bulk, solution, emulsion, and suspension; and (iv) inexpensive and facile setups compared to other polymerization techniques [20].

There are four common industrial methods of radical polymerization [2] as shown in Table 1.

The only components of a bulk polymerization mixture are monomers, the initiator, and optionally, a chain-transfer agent [21]. Products obtained from bulk polymerization have high optical clarity and are usually very pure [2]. The mechanism and equipment are relatively simple for a large-scale production in a short time. However, heat and mass transfer become difficult as the viscosity of the reaction mixture increases. This may lead to autoacceleration, also known as the Trommsdorff–Norrish effect, or even a violent explosive polymerization. At the same time, heat acquisition may cause a broad molecular weight distribution.

Solution polymerization can effectively mitigate problems of bulk polymerization. The use of a solvent can lower the viscosity of the polymerization system, leading to better mass and heat transfer. Good heat transfer can reduce the Trommsdorff–Norrish effect [22]. Meanwhile, the inhibited

Table 1: Common ways of radical polymerization in industry.

method	contains	where polymerization happens
bulk polymerization	monomer, initiator	in bulk
solution polymerization	monomer, initiator, solvent	in solution
suspension polymerization	hydrophobic monomer, hydrophilic initiator, water, suspending agents	in monomer droplet
emulsion polymerization	hydrophobic monomer, hydrophilic initiator, water, surfactants	in latex/colloid particles

termination reactions cause a significant increase in the overall yield.

Polyacrylonitrile (PAN), polyacrylic acid (PAA), and polyacrylamide (PAM), for instance, are obtained by solution polymerization in the polymer industry [23-25]. In addition to the reduced reaction rate due to lower monomer and initiator concentrations, one of the major disadvantages of solution polymerization is that it is difficult to completely rule out chain transfer to the solvent. Therefore, obtaining very high molecular weight product through solution polymerization is tough.

Suspension polymerization is a heterogeneous process and requires the use of a mechanical agitation to mix monomers and dissolved initiators in the liquid phase during the process. A suspending agent, e.g., polyvinyl alcohol (PVA), is added to the system to prevent coalescence. The viscosity in suspension polymerization is low throughout the process which brings good heat transfer and temperature control, and therefore well-defined and high-molecular-weight polymers. PVC, PS, and poly(methyl methacrylate) (PMMA) are industrially produced through suspension polymerization [2]. Nonetheless, the Trommsdorff–Norrish effect exists in suspension polymerization processes, and the residual suspending agent becomes an impurity.

Emulsion polymerization is also a widely-used method in radical polymerization. It is applied to produce several commercially important polymers such as acrylic rubber, nitrile rubber, and polytetrafluoroethylene (PTFE). Polymerization happens in latex or colloid particles that are formed under the action of surfactants, which are also called emulsifiers within the first few minutes [26]. Emulsifiers such as sodium lauryl sulfate, sodium or potassium salts of fatty acids (soaps), salts of alkylbenzene sulfonates, and *O*-polyoxyethyleneated long-chain alcohols are used to change the two incompatible water phase and oil phase into an emulsion phase. The simultaneous presence of a hydrophobic head and a hydrophilic tail on emulsifiers provides the ability to combine water and oil phase into an emulsion. In emulsion polymerization, high molecular weights can be achieved at fast polymerization rates, because both the rate of polymerization and the molecular weight depends on the number of particles. A small latex particle only rooms a single propagating radical at a time. Thus, the chain keeps growing until another radical enters to terminate it. Due to the enormous number of particles, the overall radical concentration in the latex is greatly higher than in a typical bulk polymerization. Meanwhile, the polymerization rate is higher in emulsion polymerization compared to bulk or suspension polymerization. Radicals are divided in different particles also allows for longer lifetimes, which results in a higher degree of polymerization. As the frequency of radical entry decreases with the particle number at a certain initiator concentration, the rate of polymerization and molecular weight can be boosted by raising the number of particles, e.g. by tuning the monomer to surfactant ratio.

The final product can be used as is and does not generally need to be altered or processed. Drawbacks of emulsion polymerization include residual surfactants, significant chain transfer to polymer, and difficulty to dry polymers.

1.3 Reversible deactivation radical polymerization

A key drawback of conventional radical polymerization is that a limited control of molecular weights and architectures can be achieved due to the slow initiation and rapid termination. In 1956, Szwarc coined the term “living polymerization” in an anionic system [27]. Since then, polymer chemists have been in pursuit for a comparable “living radical polymerization”. Despite the fact that radical polymerization is never as “living” as the anionic counterpart, RDRP as per the IUPAC definition, or more commonly named controlled radical polymerization (CRP) has made a booming progress and attracted great attention in the past three decades [28].

1.3.1 Deactivation by reversible coupling: In 1982, Otsu and Yoshida [29] successfully polymerized styrene and MMA using dithiocarbamate compounds, and in 1986, Solomon et al. [30] published a patent entitled "Polymerization Processes and Polymers Produced Thereby", which led to the successful nitroxide-mediated polymerization (NMP). In 1993, Georges et al. used benzoyl peroxide (BPO) as the initiator and 2,2,6,6-tetramethyl-1-piperidinyloxyl (TEMPO) as the control agent. It was called a bicomponent initiating system containing both stable free nitroxide and a conventional thermal initiator. Polystyrene of different molecular weights was obtained with low M_w/M_n and active chain ends [31].

Although a bicomponent initiating system is economical and practical, the traditional initiators have many problems such as the poor initiation efficiency. It is difficult to control the molecular weight and polymerization rate precisely. In order to solve these problems, Hawker et al. [32-34] proposed the concept of the unimolecular initiation system. In this system, an alkoxyamine compound is used instead of the original nitroxide radical/initiator combination. These unimolecular initiators can decompose to produce a stoichiometric pair of the primary initiating radical and a nitroxide radical, thus combining the roles of a conventional initiator and a control agent. The mechanism is shown in Scheme 4 [35].

Due to the steric effect of TEMPO, the dissociation rate constant, k_d, of the corresponding alkoxyamine is very low and it

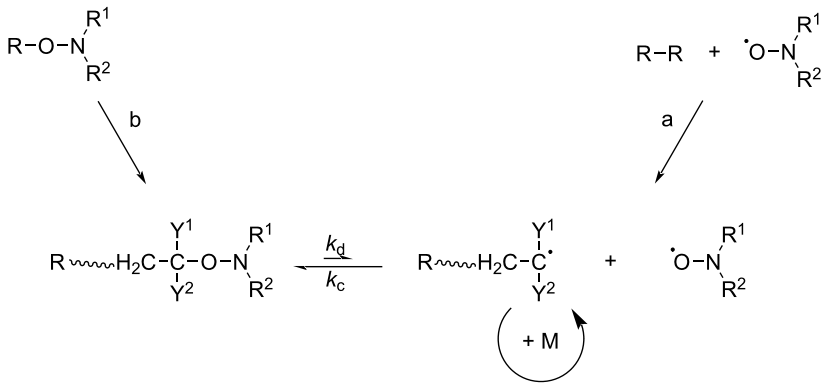

Scheme 4: Activation–deactivation equilibrium in nitroxide-mediated polymerizations. Bicomponent initiating system (a) and unicomponent initiating system (b). Scheme 4 redrawn from [35].

tends to undergo β-elimination in acrylic systems. Thus, TEMPO is only suitable for the polymerization of styrenic monomers at a high temperature and for long time [36]. Functionalized TEMPO was therefore developed for the polymerization of other monomers, such as acrylates, under milder conditions [37-39]. Grimaldi et al. [40] achieved NMP of styrene and *n*-butyl acrylate using SG1-type nitroxide radical (*N*-*tert*-butyl-*N*-(1-diethylphosphono-2,2-dimethylpropyl)nitroxide). Compared with TEMPO, SG1 was considered that it initiated the truly "living"/controlled polymerization at that time and the rate of propagation was much faster than with TEMPO under the same conditions.

1.3.2 Deactivation by atom transfer: Atom transfer radical polymerization (ATRP) was independently reported by the teams of Matyjaszewski [41] and Sawamoto [42] in 1995. The efficient conduct of ATRP relies on the establishment of a reversible activation/deactivation equilibrium reaction between an alkyl halide or halide-like initiator (RX) and a radical species ($R^{\cdot}$) [43]. During the activation process, the organohalides quickly lose their terminal halogen atoms in the presence of the liganded low-valent metal complex (activator, Mt^z/L, typically Cu^I/L) to form the active radical species ($R^{\cdot}$), which in turn initiates polymerization to form the active polymer chain species ($P_n^{\cdot}$). On the other hand, the termination reactions always present in the system causing the liganded high-valent metal complex (deactivator, X–Mt^{z+1}/L, typically X–Cu^{II}/L) to accumulate. When the accumulation reaches a certain level, the deactivator interacts with the active radical chain species ($P_n^{\cdot}$), so that the radical chain species gets into the dormant state (P_nX) via a halogen atom transfer process. This is the deactivation process. Activation and deactivation reactions are always present throughout the process, and the rate of deactivation must be sufficiently high in order to maintain a low radical concentration to effectively inhibit the termination [44]. The mechanism of ATRP is shown in Scheme 5 [14].

Compared with the earlier ATRP techniques (normal ATRP [41], reverse ATRP [45], SR&NI ATRP [46], and AGET ATRP [47]), the recently proposed ATRP techniques (ICAR ATRP [48], ARGET ATRP [49], SARA ATRP [50], *e*ATRP [51,52], photoATRP [53,54], and ultrasonic ATRP [55]) require a much

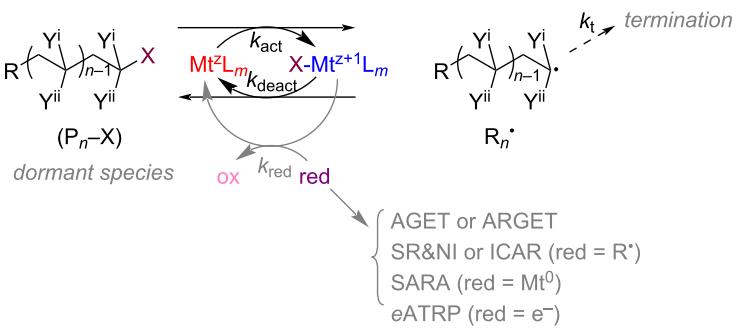

Scheme 5: Mechanism of a transition metal complex-mediated ATRP. Scheme 5 redrawn from [14].

lower catalyst dosage, even down to 10 ppm [56], which to some extent, solves the problem of metal impurities. Meanwhile, the presence of external stimuli in *e*ATRP, photoATRP, and ultrasonic ATRP, allows spatial and temporal control over the polymerization [57]. Hawker et al. proposed a metal-free ATRP in 2014 using an organic photoredox catalyst mediated by light to overcome the challenge of metal contamination in the precipitated polymers [58]. After the ATRP reaction, a reactive chain end retains as a stable alkyl halide moiety. Therefore, ATRP is particularly suitable for the synthesis of polymers with complex architectures [59,60].

1.3.3 Deactivation by degenerative transfer: Reversible addition-fragmentation chain transfer (RAFT) polymerization is one of the most well-established RDRP technique. It was first proposed in 1998 by Commonwealth Scientific and Industrial Research Organization (CSIRO) researchers Chiefari et al. [61]. Due to the presence of chain-transfer agents (CTAs), such as thiocarbonylthio compounds, in RAFT polymerizations, the chain propagating radical species can add to CTAs to form intermediate radical species. RAFT can rely on reversible chain-transfer reactions between the propagating radical species and the dormant chains to achieve controlled polymerization of the monomers, allowing all polymer chains to grow nearly simultaneously.

The product of RAFT polymerization has a preserved thiocarbonylthio chain end. The polymerization reaction can be continued by adding more monomers. Therefore, RAFT is often used to perform chain expansion reactions or to synthesize functionalized multi-block copolymers [62-64]. Boyer and co-workers developed a photocatalytically mediated RAFT polymerization, PET-RAFT, which removes the requirement for conventional radical initiators. The reaction is oxygen tolerant and can be carried out in a milder environment [65,66]. Pan and co-workers recently further advanced the RAFT techniques by allowing them to be fueled by oxygen [67]. The mechanism of a RAFT polymerization is shown in Scheme 6 [68].

Organometallic-mediated radical polymerization (OMRP) is also a commonly used polymerization method, which uses transition-metal complexes such as titanium and vanadium for coordination polymerization [69]. However, due to the high cost of these complexes and their post-processing, OMRP is not widely

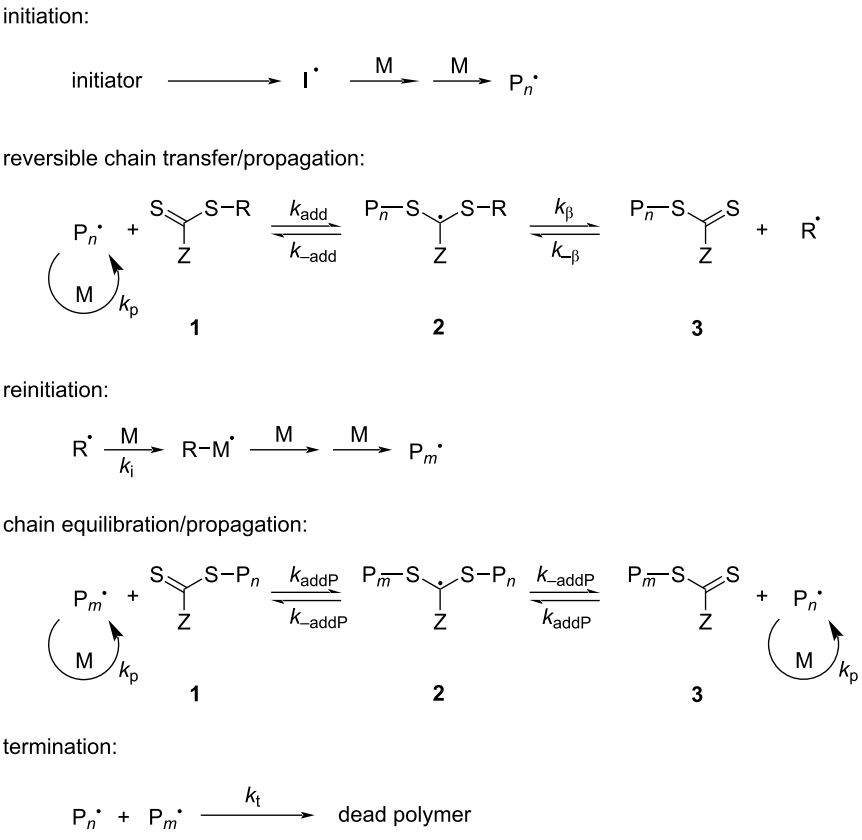

Scheme 6: Mechanism of RAFT polymerization. Scheme 6 redrawn from [68].

used. The chain termination reaction of OMRP is considered to have two mechanisms, degenerative transfer and reversible termination, which are comparable to RAFT and NMP, respectively (Scheme 7) [70].

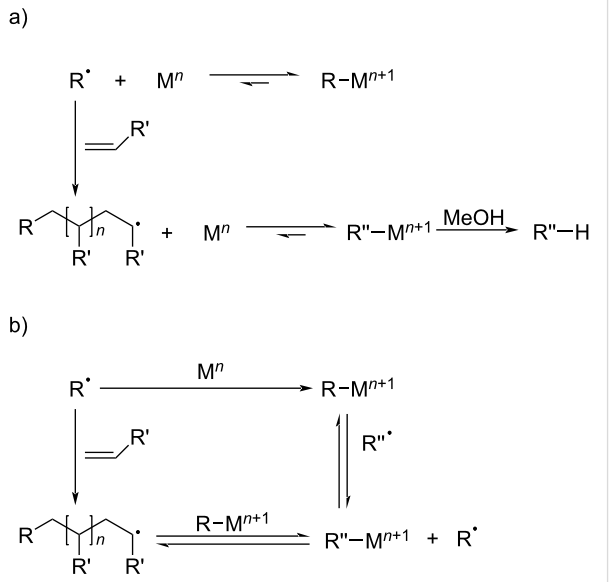

Scheme 7: Degenerative transfer (a) and reversible termination (b) mechanism of OMRP. Scheme 7 redrawn from [70].

Iodine transfer polymerization (ITP) is also a commonly used degenerate chain-transfer method. Its origin can be traced back to the 1970s [71] and it is mostly used for the polymerization of fluorinated olefins. However, the C–I bond of iodoalkyl compounds used as chain-transfer agents is weak and unstable during storage [21]. Therefore, Lacroix-Desmazes et al. [72] used iodine molecules to synthesize iodine chain transfer agents in situ, a process known as reverse iodine transfer polymerization (RITP), which is similar to reverse ATRP. The mechanism of the RITP is shown in Scheme 8.

RDRP is applicable to a wide range of monomers and the reaction conditions become milder and more versatile with emerging techniques, such as oxygen tolerance or even oxygen initiation [73]. Compared with the conventional radical polymerization, RDRP has shown fascinating advantage in complex polymer polymerization. However, RDRP is currently less applied in industry due to cost and process obstacles. It is expected that future technical innovation will allow RDRP to be more widely employed.

2 Other polymerization techniques involving radical chemistry

As discussed in section 1, chain-growth polymerization via radical addition to vinyl monomers is the most broadly applied polymerization technique. However, radical chemistry is used in other polymerization systems. In this section, we cover these techniques excluded from our previous discussion.

2.1 Oxidative synthesis of conductive polymers

The breaking accomplishments of Shirakawa, MacDiarmid, and Heeger have changed our view of organic polymers, from insulating polymers to electrically (semi)conducting materials [74]. In 2000, they received the Nobel Prize in Chemistry. Typical conductive polymer structures have π-conjugation (Scheme 9A) [75]. They can be synthesized by various methods such as electrochemical and chemical methods. Oxidative polymerization and chain-growth polymerization are also good ways to produce conductive polymers (Scheme 9B) [76].

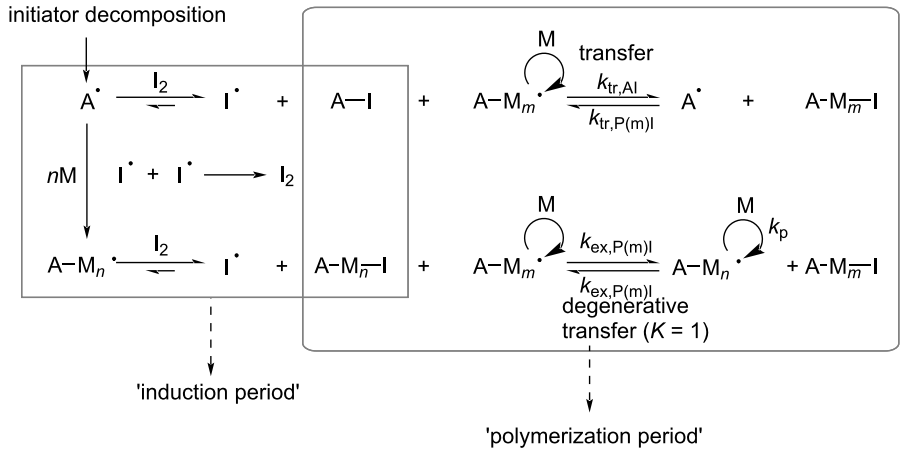

Scheme 8: Simplified mechanism of a RITP. Scheme 8 redrawn from [21].

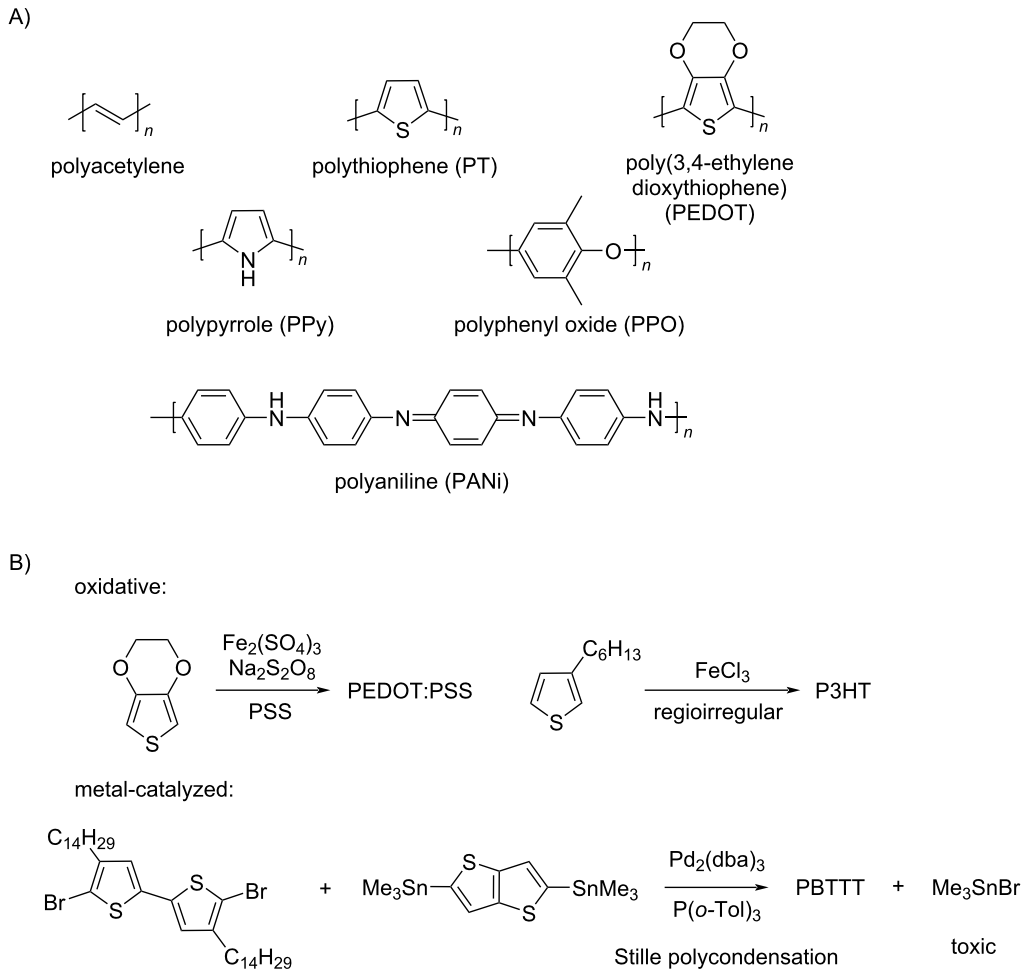

Scheme 9: (A) Structures of π-conjugated conductive polymers. (B) Examples of conductive polymer synthesis via chain-growth polymerization. Scheme 9 redrawn from [76].

Nowadays, most conductive polymers are prepared via metal-catalyzed cross-coupling reactions [77]. However, radical polymerization is also an effective way to synthesize conductive polymers at a relatively low cost. Niemi et al. [78] used $FeCl_3$ as catalyst to produce radicals at the 2- and 5-positions of thiophene and synthesized four types of poly(3-alkylthiophene)s (PATs) with different linking ways (Scheme 10).

2.2 Polymerization by thiol–ene chemistry

The thiol–ene reaction (also called alkene hydrothiolation) is the anti-Markovnikov addition of a thiol to a C–C double bond and was first reported in 1905 [80]. It is considered as a click chemistry reaction due to its high yield, stereoselectivity, rate, and thermodynamic driving force.

Generally, the thiol–ene reaction is conducted under radical conditions, often photochemically induced [81]. In a typical thiol–ene system, the polymerization undergoes a free-radical chain mechanism, involving an initiation step from a thiol group via radical transfer or homolysis (Scheme 11, initiation), radical addition of the thiyl radical to the ene functionality (propagation 1), transfer from the carbon-centered radical to another thiol group (propagation 2), and biradical termination between either carbon-centered or thiyl radicals (termination).

Polymerization by thiol–ene coupling is a step-growth polymerization, which means it can produce polymers with no theoretical upper-limited molecular weight. The simple setup, mild conditions, absence of unfavored byproducts, orthogonality with other reactions, and high yields (nearly full conversion) [82] made thiol–ene polymerizations an ideal way to produce high-molecular-weight cross-linked polymers, optical polymers, biomacromolecules, and materials used in additive manufacturing. It is also compatible to a photopolymerization process. For example, it can be applied to the photo-3D-printing of silicone resin [83]. The refractive index is one of the most impor-

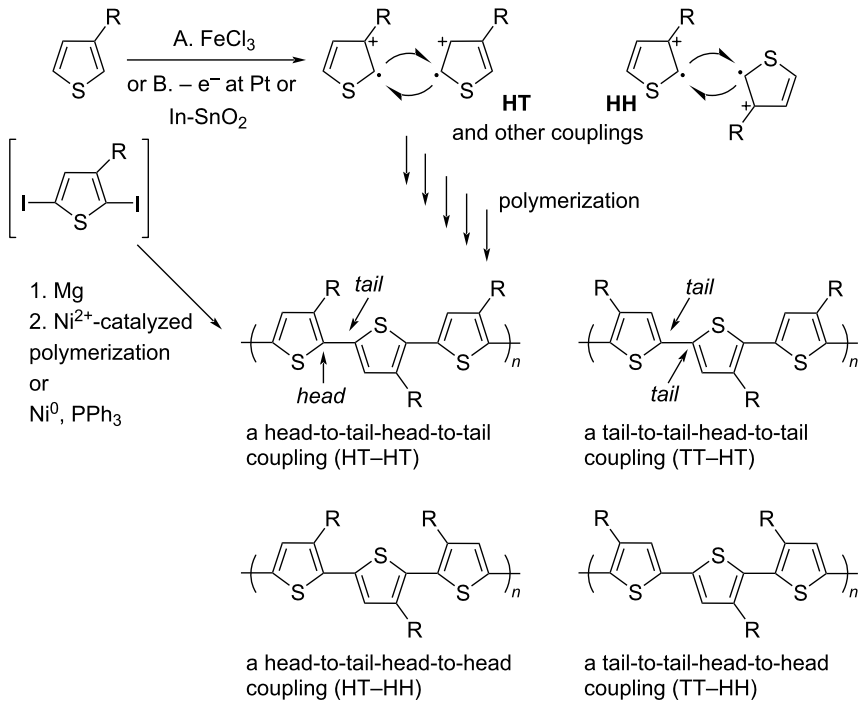

Scheme 10: Possible regiochemical couplings in PATs. Scheme 10 redrawn from [79].

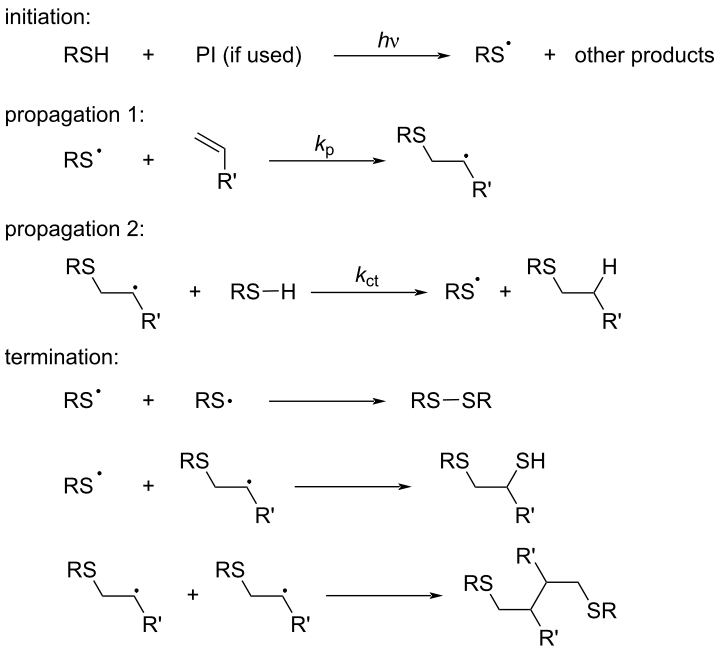

Scheme 11: General thiol-ene photopolymerization process. Scheme 11 redrawn from [81].

tant optical properties and researchers have invested plenty of effort to develop high refractive-index polymers. A common approach is to incorporate atoms or groups with high polarizability and sulfur is a typical constituent with high molar refractivity and is widely used in optical polymers. For example, Bhagat et al. [84] produced polymers with high cross-linking

density and refractive index from tetravinylsilane, ethanedithiol, and benzenedithiol. Polymers made by thiol–ene polymerization usually have well-ordered molecular networks. This character gives thiol–ene polymers highly tunable mechanical response hence it shows great application potential in additive manufacturing. Cook et al. [85] presented the first report of volumetric additive manufacturing-printed thiol–ene resins and showed the potential of the thiol–ene system.

In addition to thiol–ene chemistry, radical hydrosilylation was also used to prepare linear, branched, or cross-linked polymers via a step-growth mechanism (cf. section 3.2) [86].

2.3 Metal-free ring opening metathesis polymerization (MF-ROMP)

ROMP is a powerful and broadly applicable technique for synthesizing polymers. Traditional ROMP systems are initiated by transition-metal complexes and Ru-based alkylidene complexes, which are also known as Grubbs catalysts (Scheme 12A), are the most popular ones [87]. However, Ru-based catalysts are expensive making them less attractive for industrial applications. Living ROMP is commonly terminated by adding a special chemical which can remove the transition metal from the chain end and deactivate it from propagation. However, removing this residue from the product by tradi-

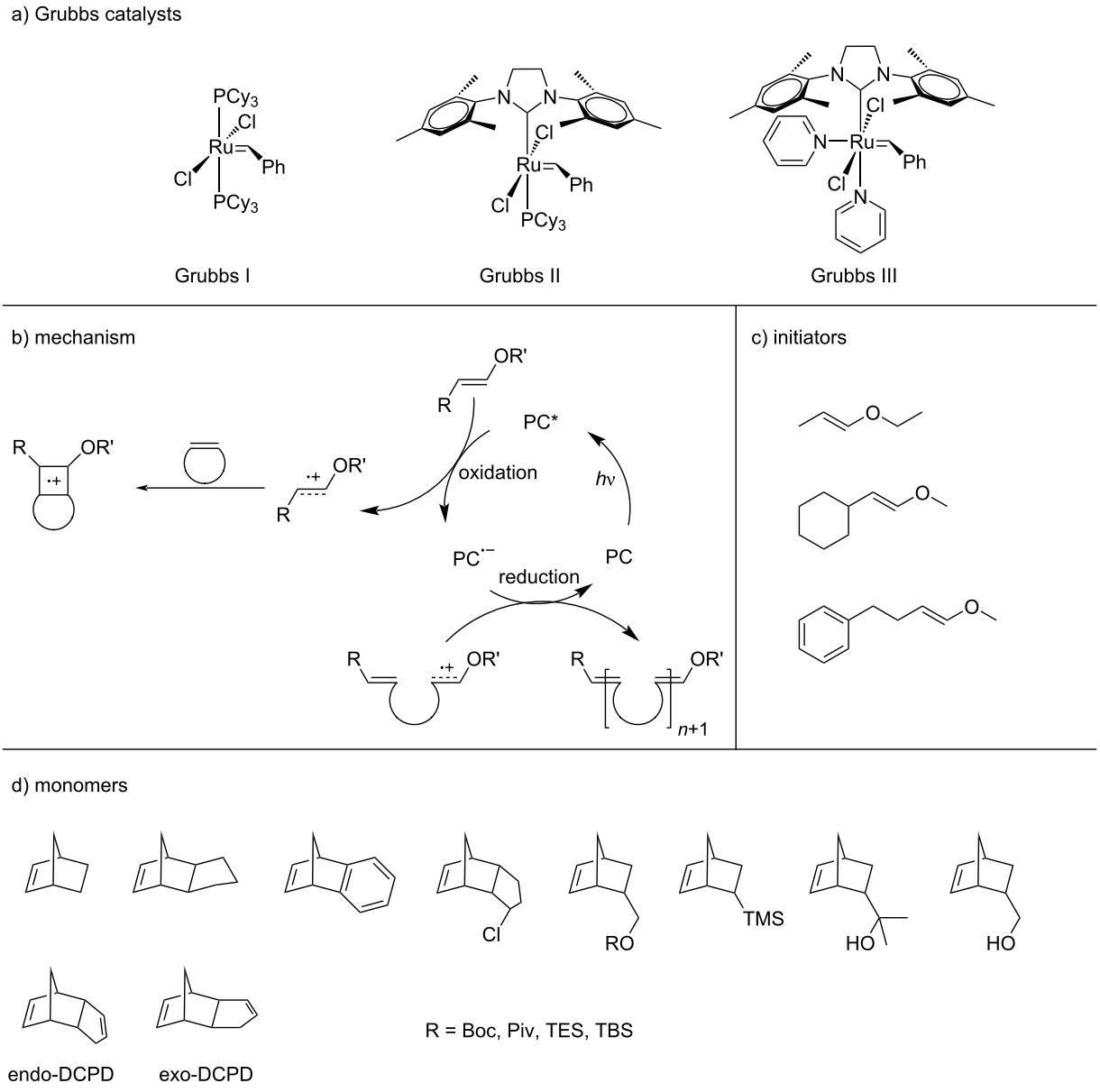

Scheme 12: (a) Three generations of Grubbs catalysts. (b) Proposed mechanism for photo-ROMP via a reductive quenching pathway and (c, d) chemical structures of the (c) initiators and (d) monomers used in photo-ROMP. Scheme 12 redrawn from [89].

tional chromatographic methods can be a challenging task and limits the application of ROMP-produced polymers in biomedical and microelectronic fields [88]. To avoid such drawbacks, the development of a metal-free (MF) procedures is necessary.

MF-ROMP, also termed photo-ROMP, is a novel technique to polymerize cyclic olefins. It begins with the reductive quenching of an photoexcited photocatalyst (PC) at an enol ether initiator to produce a radical cation carrier [90]. Then, the carrier undergoes cyclic addition with a cyclic olefin monomer to generate a cyclobutene radical cation intermediate. The thermodynamically instable intermediate subsequently forms the propagating radical cation species via a ring-opening process. The reduced $PC^{\bullet-}$ terminates the catalytic loop by reducing the propagating species to provide a polymer chain (Scheme 12B). Boydston and co-workers [91], systematically studied various pyrylium and thiopyrylium PCs (Scheme 13). It is necessary for these PCs having a high excited-state redox potential to oxidize the enol ether initiators. A range of enol ether initiators that has been successfully applied in metal-free ROMP are shown in Scheme 12C.

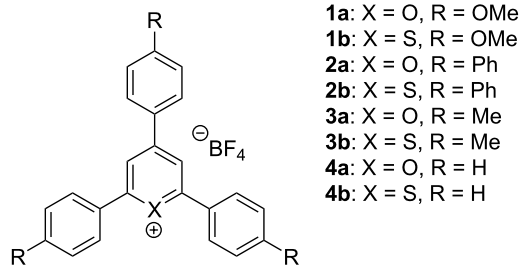

Scheme 13: Pyrylium and thiopyrylium salts studied by Boydston et al. Scheme 13 redrawn from [91].

Meanwhile, metal-free ROMP is applied to monomers like functionalized norbornenes and dicyclopentadienes (DCPD) (Scheme 12D) to synthesize polymers and block copolymers [88,92,93].

3 Post-polymerization radical chemistry

Post-polymerization modification is a chemical process that introduces functionalities to backbones or side-groups of pre-synthesized polymers [94,95]. It typically takes place in polymer solutions. On the other hand, surface modification of polymers is a special case of post-polymerization on polymeric solids. Radical chemistry is overwhelmingly more common in the latter because there are other more selective and efficient solution chemistry methods for post-polymerization modification, such as nucleophilic substitution [94,96]. In this section, we discuss the radical chemistry used in both processes.

3.1 Post-polymerization modification

Radical addition is a popular technique for post-polymerization modification of double-bond-containing polymers (Scheme 14). Thiol–ene and thiol–yne "click chemistry" are highly efficient radical processes well-adopted in synthetic chemistry, material fabrication, and chemical biology (cf. section 2.2) [97,98]. The $S^{\cdot}$ radical is typically generated using a thermal initiator or a photochemical process [99,100]. 1,3-Diene polymers are most commonly modified via thiol–ene chemistry through the pendant vinyl after the polymerization [101] and this technique can be traced back to 1948 [102]. The excellent temporal and spatial control of the available photochemical approach makes the technique especially viable for non-solution processes [103]. When a multifunctional thiol is used with diene-functionalized polymers, the approach becomes suitable for chemical cross-linking [103,104], vide infra. It has been used to cure a liquid isoprene polymer in precise digital light processing 3D printing [105]. Recently, Kanbayashi et al. reported that thiol–ene chemistry would not cause racemization of an asymmetric center linked to a pendant vinyl group, which can be particularly valuable for functionalization of optically active polymers [106]. Theato and co-workers introduced vinyl/alkyne-bearing poly(vinyl ether)s [107], poly(vinylcyclopropanes) [108], and poly(allyl 2-ylideneacetate) [109] as promising new platforms compatible to thiol–ene chemistry. Atom transfer radical addition (ATRA) is another process that usually qualifies for a definition of "click chemistry" [44]. A similar radical addition to vinyl groups takes place in ATRA despite the halogen atom transfer is mediated by a metal complex. Post-polymerization modification by ATRA was pioneered by Jérôme and co-workers [110,111]. In 2014, Xu et al. demonstrated that it can be extended to a milder photochemical process as well [112].

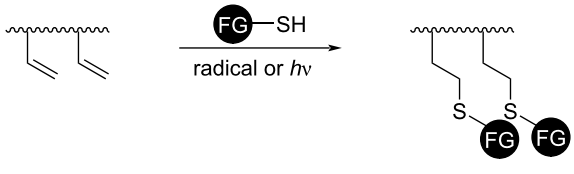

Scheme 14: A general illustration of post-polymerization modification by thiol–ene chemistry.

Radical coupling may also be used to introduce functional groups into polymer backbones. In this context, rapid radical trapping with stable nitroxide radicals is an efficient way [113]. However, this technique requires radical generation on the polymer backbone. A typical approach involves hydrogen abstraction by organic oxidants such as oxygen radicals from peroxide initiators [114], which is similar to the radical cross-

linking process, vide infra. Radicals may also be generated thermally, through photoinduction, or by ATRP initiators incorporated in the polymer backbones [115-117]. TEMPO and its derivatives have a long history of application as radical trapping agents. Commercially available HO-TEMPO is a particularly useful platform for post-polymerization modification via radical coupling because of the chemical versatility of the hydroxy moiety (Scheme 15). Site-selective radical C–H activation has been proven to be a useful tool to functionalize relatively inert polymer backbones and upcycling of polymer waste (cf. section 4) [118,119]. Radical chain-end modification as a highly specific type of post-polymerization modification introduces or removes functionalities at polymer chain ends [120].

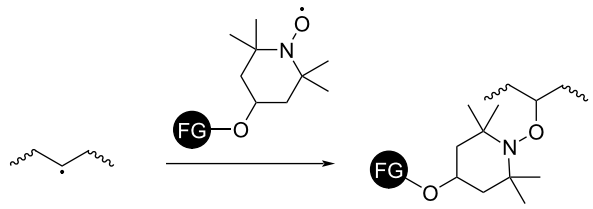

Scheme 15: Introduction of functionalities by nitroxide radical coupling of HO-TEMPO derivatives.

3.2 Chemical crosslinking of polymers

Chemical crosslinking is a suitable approach to increase chemical resistance [121], mechanical strength [122], and other properties [123] of polymers. In 1830s, Charles Goodyear invented vulcanized rubber. By heating natural rubber with lead oxide and sulfur, the temperature-sensitive rubber became a more stable material, even at high and low temperatures, while keeping the elasticity, plasticity, insulation, and other excellent characteristics [124]. During the vulcanization of natural rubber, elemental sulfur was heated to form sulfur radicals which then react with natural rubber crosslinking two independent polymer molecules [125]. This is a typical example of polymer crosslinking by a radical mechanism.

As the traditional vulcanization process, an initiator is needed to start the radical crosslinking. Besides sulfur, peroxides such as di-*tert*-butylcumyl peroxide (BCUP) and dicumyl peroxide (DCP) are often used in radical crosslinking. Free radicals are generated at the peroxides' decomposition temperature and attack the polymer chains to achieve crosslinking (Scheme 16). In dry crosslinking processing of crosslinked polyethylene (XLPE) used in power delivery system, a blend of DCP in low-density polyethylene (LDPE) is extruded at its melting point. In comparison to LDPE, the operational temperature and the short-circuit permissible temperature of XLPE cables are increased from 70 °C to 90 °C and 150 °C to 230 °C, respectively. Besides that, XLPE shows a more rubber-like behavior [126]. As the peroxide crosslinking process is industrially important, multiple kinetic models have been established to understand the reaction between polymers, peroxides, and monomers [127-129].

Polysiloxanes are another class of crosslinkable polymers. Modern silicone industry typically uses Pt-catalyzed hydrosilylation to crosslink multi-vinyl polysiloxane with silicon hydride compounds to manufacture silicone rubbers [130]. However, hydrosilylation may also be achieved via a radical mechanism (Scheme 17). In comparison to the Pt-catalyzed system, the radical-induced hydrosilylation has a lower cost, better toler-

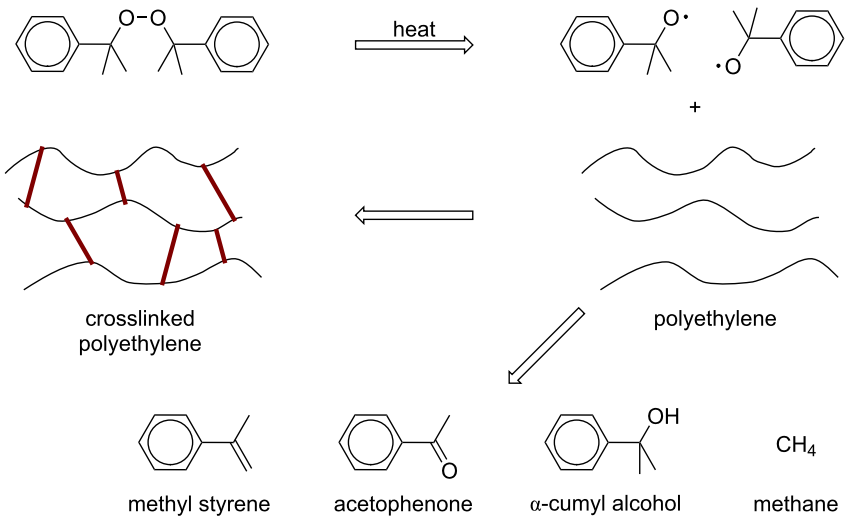

Scheme 16: Chemical reaction process scheme of DCP-induced crosslinking of LDPE. Scheme 16 redrawn from [126].

ance to coordinating functionalities, and yields products without metal residues, but its efficiency is inferior to transition-metal catalyzed methods. Silicone rubber was prepared in such a process [131]. Pan and co-workers recently reported a photoredox hydrosilylation process compatible to both electron-sufficient and -deficient vinyl species [86], and applicable to both post-polymerization modification and crosslinking of polymers bearing pendant vinyl groups [132], demonstrating a promising new orientation of radical hydrosilylation. It is noteworthy, that since the 1940s, polysiloxanes were crosslinked via hydrogen abstraction from Si–CH_3 and a radical coupling mechanism like polyolefins, vide supra [133].

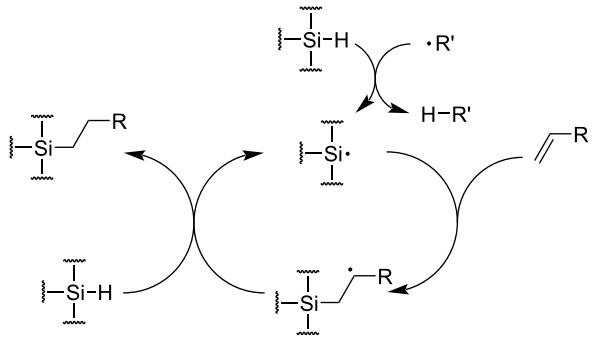

Scheme 17: A probable mechanism of radical-induced hydrosilylation.

Irradiation can also lead to the crosslinking of polymers. Polymeric materials may become brittle or colored after being exposed to sunlight for a long time, which was called 'photoageing' [134]. In fact, the light sensitivity of many polymers results from some impurities or additives remaining in polymer materials, which can form radical species through irradiation. This photooxidation process can lead to the generation of some small molecules or chain scissoring. At the same time, the photooxidation process can also result in crosslinking of polymer backbones [135]. Bousquet and Fouassier [135] investigated the photooxidation and crosslinking of photosensitized elastomers. Samples of an EPDM (ethylene-propenebutadiene) terpolymer were prepared with different additives. Observable crosslinking products were obtained through irradiation of different wavelengths. Besides the side reactions induced during photoageing, rational photocrosslinking of polymers is also feasible in the presence of photoinitiators or photoresponsive moieties [136-138]. Sophisticatedly designed photocrosslinking of polymers finds broad applications in modern 3D printing/additive manufacturing [139-142].

Radical chemistry has been demonstrated as a powerful tool for polymer crosslinking and preparation of materials with enhanced properties.

3.3 Polymer surface modification

When modifying the surface of polymers, chemical selectivity typically plays a minor role, while harsh reaction conditions are useful for the modification of chemically inert substrates. Here, radical chemistry comes into play. When polymer surfaces are modified by radical chemistry, radicals are either generated directly on the polymers or on modifiers. In the latter case, a radical addition, substitution, or coupling reaction takes place to complete the modification. Radicals can be generated by a broader selection of homogeneous and heterogeneous approaches, including hydrogen atom abstraction, decomposition of immobilized initiators, electrochemical redox reaction, or irradiation because the reactions only need to take place at the surface.

Small-molecule oxidants, such as organic peroxides, hydrogen peroxide, persulfates undergo homolysis of O–O bonds generating radicals that can break C–H bonds followed by a hydrogen abstraction reaction. Phenolic compounds can be oxidized by molecular oxygen in the presence of laccase, and the resulting phenolic radical reacts with poly(ethersulfone) [143]. Highly reactive gaseous species may also generate radicals on polymer surfaces. For example, atomic oxygen radical anions emitted from $12CaO{\cdot}7Al_2O_3$ crystals [144] were used to modify PVC and polystyrene [145,146]. Plasma is also a powerful gas-phase tool for polymer surface modification and radical generation [147,148]. It can even generate radicals on otherwise inert fluoropolymer surfaces [149].

Electrochemical reactions are another approach to generate radicals at polymer surfaces. Hydroxyl radicals generated via the electro-Fenton reaction from H_2O_2 in the presence of the Fe^{3+} were used to functionalize polypropylene surfaces [150,151]. Using a scanning electrochemical microscope, highly oxidative Ag(II) and $NO_3^{\cdot}$ species were generated at a polymer surface [152], and oxidized the organic surface via a radical process. The homolytic dediazonation of diazonium salts produces highly reactive aryl radicals (Scheme 18) [153]. The chemical conversion can be initiated by electrochemical reduction [154], a reducing agent [155-157], a base [158], heating [159], or photochemically [160]. Aryl radicals may act as a halogen abstractor for alkyl halides and generate alkyl radicals for surface modification [161]. Electrochemical surface modification also works for inert PTFE surfaces in the presence of a 2,2'-dipyridyl redox mediator [162].

Photons and high-energy charged particles can transfer their energy to bound electrons in atoms, exciting the electron to a higher energy level or even the vacuum, generating radical species. The energy of UV photons is comparable to the energy of chemical bonds [163], and therefore photons are particularly

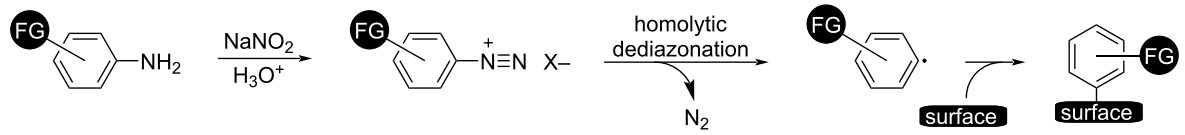

Scheme 18: Polymer surface modification by homolytic dediazonation of diazonium salts.

suitable for driving chemical reactions on polymer surfaces. Benzophenone is the best-established source of radicals on polymer surfaces. Its photoexcitation and subsequent reaction with polymers have been studied for decades [164-166]. When irradiated at around 360 nm, benzophenone undergoes excitation to a triplet state with biradical behavior. It then abstracts a hydrogen atom from the polymer resulting in a $Ph_2C^{\cdot}$ species and a radical on the polymer (Scheme 19). This reaction may complete in radical coupling or proceed with radical polymerization from the surface [167-169], resulting in crosslinked polymers, surface-functionalized polymers, or surface-grafted polymers. RDRP was used to graft well-defined polymer brushes from polymer surfaces [170,171]. Photoinduced processes, including photoATRP and PET-RAFT were used [172-175]. Poly(aryl ether ketone)s such as poly(ether ether ketone), bearing a diaryl ketone moiety resembling that of benzophenone, can generate biradicals upon UV irradiation without a photoinitiator [176,177]. Grafted polymers and untethered polymers are generated simultaneously in the presence of a monomer.

Ionizing radiation including high-energy photons (X-rays and γ-rays) and charged α- or β-particles generate charged particles, especially electrons, emitted from the surface of polymers [178]. When a high-energy photon impacts an atomic electron, part of the photon energy is transferred to the electron leading to excitation or ionization and radical formation, and a deflected photon with lower energy is emitted, ready to impact another electron. This process is called Compton scattering [179]. One of the major purposes of radiation modification of polymer surfaces is grafting. The surface grafting can be simply tuned by the dose of radiation [180]. Radiation grafting on polymer surfaces is also compatible with RDRP for high density and well-defined polymer grafts [181-184]. Polymer surfaces can also be modified using electron and ion beams [185,186]. Komatsu et al. reported surface-initiated ATRP from electron-beam irradiated polymer surfaces [187].

The radical chemistry used for post-polymerization modification, crosslinking, and polymer surface modification has many

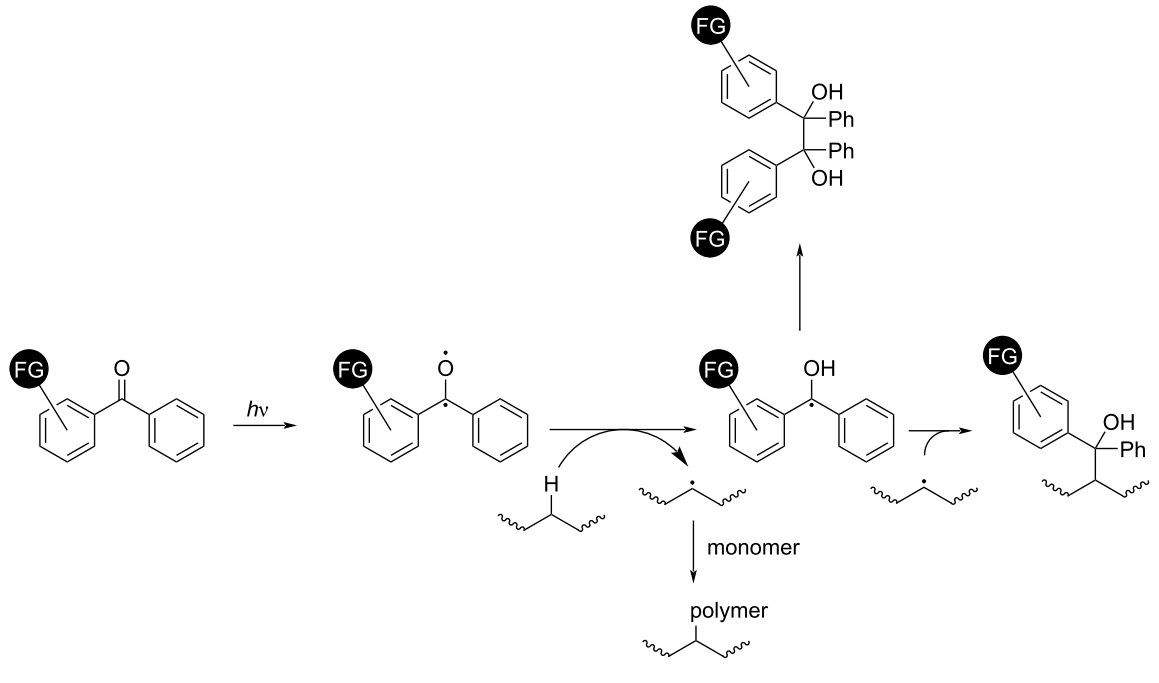

Scheme 19: Photoinduced polymer surface modification or surface grafting using benzophenone.

aspects in common. The key is to activate chemically unreactive polymer backbones with highly reactive radical species to construct new chemical bonds.

4 Radical depolymerization

Radical destruction of polymer chains is an undesirable side reaction sometimes observed in the post-polymerization modification. However, it is also an important chemical process in several circumstances.

Photoresist is one of the bedrocks of the semiconductor industry [188,189]. There are two types of photoresists, positive and negative photoresists, and they become more or less soluble upon radiation, respectively. Some early negative photoresists undergo a photochemical crosslinking process of 1,3-diene cyclic polymers [190] (cf. section 3.2), but such systems are no longer studied due to the poor resolution and sensitivity. On the other hand, positive resists based on decomposition of polymers, especially upon radiation with an electron beam, because of its narrow wavelengths, are still regarded as a promising alternative. Poly(methyl methacrylate) has a long history of being used as a positive resist [191,192]. It undergoes a scission by a Norrish-type I reaction followed by radical unzipping depolymerization under photon or β-irradiation (Scheme 20a). Similarly, poly(olefin sulfone) undergoes depolymerization upon irradiation of light or electron beams [193,194]. It is an alternating copolymer of 1-olefins and SO_2, and therefore the decomposition products are mostly gaseous [195]. While the depolymerization in both systems has a thermodynamic origin [196], the mechanism of poly(olefin sulfone) depolymerization is much more complex. Bowmer et al. proposed a simultaneous radical/cationic process (Scheme 20b) [197]. Meanwhile, an anionic process is also possible in the presence of a photogenerated base [198].

Thanks to their low cost, light weight, and durability, polymeric materials are ubiquitous in modern life. However, over the past decades, people have become aware of the environmental impact of polymeric wastes [199]. One of the approaches to tackle this crisis is upcycling of polymeric wastes, i.e., chemical conversion of polymeric wastes into high-value raw materials [200]. Upcycling of polyesters has been extensively studied in recent years [201]. Nevertheless, upcycling of vinyl polymers, which comprise a major portion of commercial

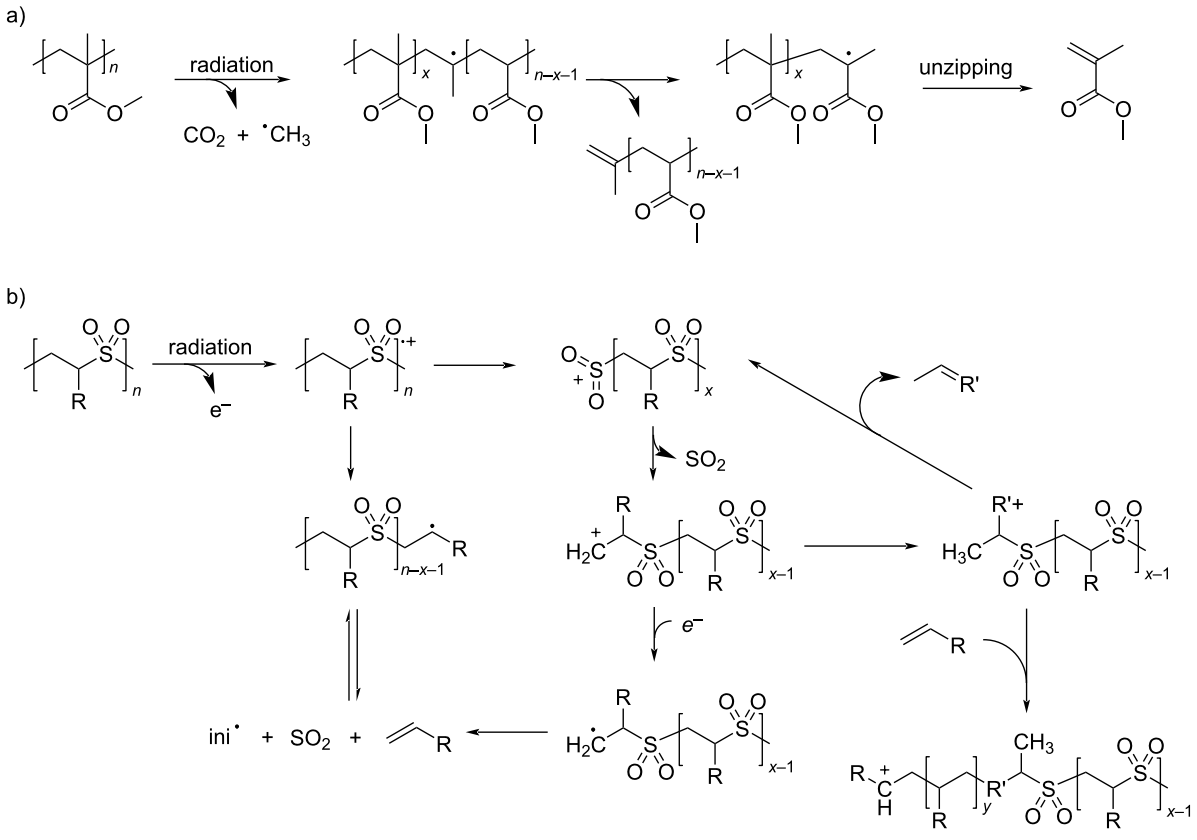

Scheme 20: Depolymerization mechanism of common photoresists. (a) A possible mechanism of radiation decomposition of poly(methyl methacrylate). (b) A proposed mechanism of simultaneous radical/cationic decomposition of poly(olefin sulfone) upon radiation [197].

polymers, remains a great challenge because of their relatively unreactive backbones. Pyrolysis of such polymers is currently experimented by the industry to recover a variety of small molecules. Researchers have introduced radical depolymerization of vinyl polymers as a promising candidate for this task. Oh and Stache reported the photooxidation of polystyrene in the presence of $FeCl_3$ as a radical source (Scheme 21a) [202]. A molar yield of 23% benzoyl small molecules was achieved. Reisner and co-workers employed a similar approach but using aromatic ketones as photocatalyst (Scheme 21b) [203]. Benzoic acid and other aromatic small molecules were recovered at a yield of ≈40% and ≈20%, respectively. Both processes were carried out under relatively mild conditions, paving a route toward a greener future of vinyl polymer upcycling. However, the yield and value of the small molecules produced in photooxidative depolymerization are still relatively low. Thermodynamics dominates the depolymerization of methacrylates [204,205]. Therefore, pyrolysis of PMMA gives a relatively high conversion to its monomer and the purification is straightforward [206,207].

Polyethylene and polypropylene make up a major fraction of commercial polymers. However, their upcycling is much more challenging. Uncontrolled radical depolymerization of these polymers in thermal processes typically gives low-value fuels and wax [208-210]. Kong et al. recently demonstrated a photothermal radical process for the conversion of polyethylene and polypropylene into blending compatibilizers [211]. Radical depolymerization capability can be incorporated at synthesis. Wang et al. introduced photodegradability to polyolefins by copolymerization of carbon monoxide [212]. Nevertheless, radical depolymerization is an essential tool to tackle the problem of polymer wastes.

Conclusion

Radical chemistry has been deeply intertwined with the development of polymer science. Conventional free radical polymerization contributes to a major portion of modern polymer industry while novel polymerization techniques involving radicals emerged in the past decades to enable a rich selection of precisely controlled, high-value polymeric materials. The extremely high reactivity of radical species enabled efficient polymer modifications and depolymerizations with applications in many aspects essential to the advancement of the human society. Since the dawn of polymer science, it has been inextricably linked to organic chemistry. However, the two fields took divergent paths over the past century. Many emergent radical chemistries in the organic chemistry community has not yet found a place in the polymer science. We believe this gap will narrow with a broader use of chemical informatics tools and in-depth dialogs between the organic and polymer communities. Therefore, future opportunities for polymer science evolution lie in the collaboration of radical chemists in both communities.

Used abbreviations in the text and their explanations are collected in Table 2.

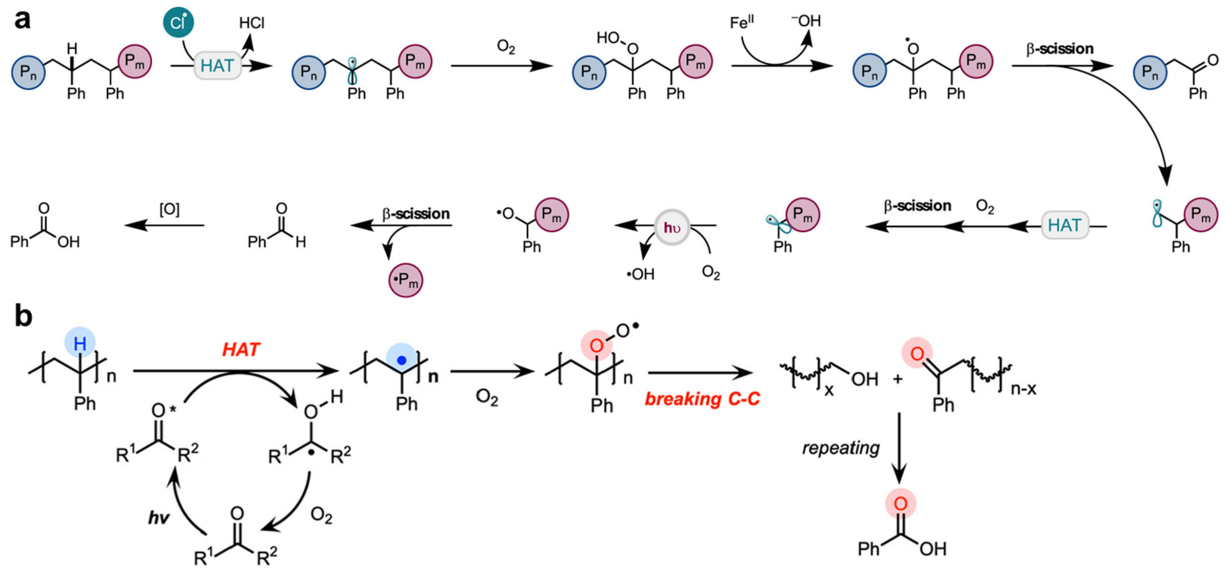

Scheme 21: Proposed mechanisms of photooxidative depolymerization of polystyrene. (a) Scheme 21a was reprinted with permission from [202], Copyright 2022 American Chemical Society. This content is not subject to CC BY 4.0. (b) Scheme 21b was adapted from [203] (© 2022 T. Li et al., published by American Chemical Society, distributed under the terms of the Creative Commons Attribution 4.0 International License, https://creativecommons.org/licenses/by/4.0/).

Table 2: Abbreviations used.

Abbreviation	Explanation
ATRA	atom transfer radical addition
ATRP	atom transfer radical polymerization
BCUP	di-*tert*-butylcumyl peroxide
BPO	benzoyl peroxide
CRP	controlled radical polymerization
CSIRO	Commonwealth Scientific and Industrial Research Organization
CTAs	chain transfer agents
DCP	dicumyl peroxide
DCPD	dicyclopentadiene
DOPA	L-3,4-dihydroxyphenylalanine
HO-TEMPO	4-hydroxy-2,2,6,6-tetramethylpiperidine-1-oxyl
ITP	iodine transfer polymerization
IUPAC	International Union of Pure and Applied Chemistry
LDPE	low-density polyethylene
mfp	mussel foot protein
MMA	methyl methacrylate
MF-ROMP	metal-free ring opening metathesis polymerization
NMP	nitroxide-mediated polymerization
OMRP	organometallic-mediated radical polymerization
PAA	polyacrylic acid
PAN	polyacrylonitrile
PAM	polyacrylamide
PAT	poly(3-alkylthiophene)
PC	photocatalyst
PET-RAFT	photoinduced electron/energy transfer reversible addition–fragmentation chain transfer (polymerization)
PMMA	poly(methyl methacrylate)
PS	polystyrene
PTFE	polytetrafluoroethylene
PVA	poly(vinyl alcohol)
PVC	poly(vinyl chloride)
RAFT	reversible addition-fragmentation chain transfer
RDRP	reversible deactivation radical polymerization
RITP	reverse iodine transfer polymerization
ROMP	ring opening metathesis polymerization
TEMPO	2,2,6,6-tetramethylpiperidine-1-oxyl
UV	ultraviolet
XLPE	crosslinked polyethylene

Funding

This work is sponsored by Science and Technology Commission of Shanghai Municipality (Grant No. 22YF1428200) and the start-up fund at ShanghaiTech University.

Acknowledgements

We thank Prof. Yifan Li for his constructive discussions.

ORCID® iDs

Zixiao Wang - https://orcid.org/0000-0003-2627-6630
Feichen Cui - https://orcid.org/0009-0001-0763-7536
Yang Sui - https://orcid.org/0009-0009-5396-6769
Jiajun Yan - https://orcid.org/0000-0003-3286-3268

References

1. Staudinger, H. *Ber. Dtsch. Chem. Ges.* **1920,** *53,* 1073–1085. doi:10.1002/cber.19200530627
2. Nesvadba, P. Radical Polymerization in Industry. In *Encyclopedia of Radicals in Chemistry, Biology and Materials;* Chatgilialoglu, C.; Studer, A., Eds.; John Wiley & Sons, 2012. doi:10.1002/9781119953678.rad080
3. Lyu, Q.; Hsueh, N.; Chai, C. L. L. *ACS Biomater. Sci. Eng.* **2019,** *5,* 2708–2724. doi:10.1021/acsbiomaterials.9b00281
4. Yang, J.; Cohen Stuart, M. A.; Kamperman, M. *Chem. Soc. Rev.* **2014,** *43,* 8271–8298. doi:10.1039/c4cs00185k
5. Yang, J.; Chen, N.; Zhu, J.; Cai, J.; Deng, J.; Pan, F.; Gao, L.; Jiang, Z.; Shen, F. *Sci. Rep.* **2020,** *10,* 12867. doi:10.1038/s41598-020-69823-0
6. Kumanotani, J. *Prog. Org. Coat.* **1995,** *26,* 163–195. doi:10.1016/0300-9440(95)00559-5
7. Snyder, D. M. *J. Chem. Educ.* **1989,** *66,* 977. doi:10.1021/ed066p977
8. Kumanotani, J. *Prog. Org. Coat.* **1998,** *34,* 135–146. doi:10.1016/s0300-9440(97)00115-x
9. Xia, J.; Lin, J.; Xu, Y.; Chen, Q. *ACS Appl. Mater. Interfaces* **2011,** *3,* 482–489. doi:10.1021/am1010578
10. Krogsgaard, M.; Nue, V.; Birkedal, H. *Chem. – Eur. J.* **2016,** *22,* 844–857. doi:10.1002/chem.201503380
11. Priemel, T.; Palia, G.; Förste, F.; Jehle, F.; Sviben, S.; Mantouvalou, I.; Zaslansky, P.; Bertinetti, L.; Harrington, M. J. *Science* **2021,** *374,* 206–211. doi:10.1126/science.abi9702
12. Yu, M.; Hwang, J.; Deming, T. J. *J. Am. Chem. Soc.* **1999,** *121,* 5825–5826. doi:10.1021/ja990469y
13. Jenkins, A. D.; Kratochvíl, P.; Stepto, R. F. T.; Suter, U. W. *Pure Appl. Chem.* **1996,** *68,* 2287–2311. doi:10.1351/pac199668122287
14. Matyjaszewski, K.; Tsarevsky, N. V. *J. Am. Chem. Soc.* **2014,** *136,* 6513–6533. doi:10.1021/ja408069v
15. Sugihara, S. *Polym. J.* **2022,** *54,* 1407–1418. doi:10.1038/s41428-022-00698-w
16. Abreu, C. M. R.; Fonseca, A. C.; Rocha, N. M. P.; Guthrie, J. T.; Serra, A. C.; Coelho, J. F. J. *Prog. Polym. Sci.* **2018,** *87,* 34–69. doi:10.1016/j.progpolymsci.2018.06.007
17. Jenkins, A. D.; Jones, R. G.; Moad, G. *Pure Appl. Chem.* **2009,** *82,* 483–491. doi:10.1351/pac-rep-08-04-03
18. Pirman, T.; Ocepek, M.; Likozar, B. *Ind. Eng. Chem. Res.* **2021,** *60,* 9347–9367. doi:10.1021/acs.iecr.1c01649
19. Tsarevsky, N. V.; Matyjaszewski, K. *Chem. Rev.* **2007,** *107,* 2270–2299. doi:10.1021/cr050947p
20. Moad, G.; Rizzardo, E.; Thang, S. H. *Acc. Chem. Res.* **2008,** *41,* 1133–1142. doi:10.1021/ar800075n

21. Lacroix-Desmazes, P.; Tonnar, J. Degenerative Transfer with Alkyl Iodide. In *Polymer Science: A Comprehensive Reference;* Matyjaszewski, K.; Möller, M., Eds.; Elsevier: Amsterdam, Netherlands, 2012; pp 159–180. doi:10.1016/b978-0-444-53349-4.00065-0
22. Norrish, R. G. W.; Smith, R. R. *Nature* **1942,** *150,* 336–337. doi:10.1038/150336a0
23. Dong, H.; Tang, W.; Matyjaszewski, K. *Macromolecules* **2007,** *40,* 2974–2977. doi:10.1021/ma070424e
24. Odell, P. G.; Veregin, R. P. N.; Michalak, L. M.; Brousmiche, D.; Georges, M. K. *Macromolecules* **1995,** *28,* 8453–8455. doi:10.1021/ma00128a073
25. Jones, G. R.; Li, Z.; Anastasaki, A.; Lloyd, D. J.; Wilson, P.; Zhang, Q.; Haddleton, D. M. *Macromolecules* **2016,** *49,* 483–489. doi:10.1021/acs.macromol.5b01994
26. Slomkowski, S.; Alemán, J. V.; Gilbert, R. G.; Hess, M.; Horie, K.; Jones, R. G.; Kubisa, P.; Meisel, I.; Mormann, W.; Penczek, S.; Stepto, R. F. T. *Pure Appl. Chem.* **2011,** *83,* 2229–2259. doi:10.1351/pac-rec-10-06-03
27. Szwarc, M.; Levy, M.; Milkovich, R. *J. Am. Chem. Soc.* **1956,** *78,* 2656–2657. doi:10.1021/ja01592a101
28. Parkatzidis, K.; Wang, H. S.; Truong, N. P.; Anastasaki, A. *Chem* **2020,** *6,* 1575–1588. doi:10.1016/j.chempr.2020.06.014
29. Otsu, T.; Yoshida, M. *Makromol. Chem., Rapid Commun.* **1982,** *3,* 127–132. doi:10.1002/marc.1982.030030208
30. Solomon, D. H.; Rizzardo, E.; Cacioli, P. Polymerization process and polymers produced thereby. U.S. Patent US4581429, July 11, 1986.
31. Georges, M. K.; Veregin, R. P. N.; Kazmaier, P. M.; Hamer, G. K. *Macromolecules* **1993,** *26,* 2987–2988. doi:10.1021/ma00063a054
32. Hawker, C. J.; Barclay, G. G.; Orellana, A.; Dao, J.; Devonport, W. *Macromolecules* **1996,** *29,* 5245–5254. doi:10.1021/ma951905d
33. Hawker, C. J. *J. Am. Chem. Soc.* **1994,** *116,* 11185–11186. doi:10.1021/ja00103a055
34. Hawker, C. J. *Angew. Chem., Int. Ed. Engl.* **1995,** *34,* 1456–1459. doi:10.1002/anie.199514561
35. Nicolas, J.; Guillaneuf, Y.; Lefay, C.; Bertin, D.; Gigmes, D.; Charleux, B. *Prog. Polym. Sci.* **2013,** *38,* 63–235. doi:10.1016/j.progpolymsci.2012.06.002
36. Moad, G.; Rizzardo, E. *Macromolecules* **1995,** *28,* 8722–8728. doi:10.1021/ma00130a003
37. Chang, C.-C.; Siegenthaler, K. O.; Studer, A. *Helv. Chim. Acta* **2006,** *89,* 2200–2210. doi:10.1002/hlca.200690206
38. Siegenthaler, K. O.; Studer, A. *Macromolecules* **2006,** *39,* 1347–1352. doi:10.1021/ma0513463
39. Miura, Y.; Nakamura, N.; Taniguchi, I.; Ichikawa, A. *Polymer* **2003,** *44,* 3461–3467. doi:10.1016/s0032-3861(03)00275-1
40. Grimaldi, S.; Finet, J.-P.; Le Moigne, F.; Zeghdaoui, A.; Tordo, P.; Benoit, D.; Fontanille, M.; Gnanou, Y. *Macromolecules* **2000,** *33,* 1141–1147. doi:10.1021/ma9913414
41. Wang, J.-S.; Matyjaszewski, K. *J. Am. Chem. Soc.* **1995,** *117,* 5614–5615. doi:10.1021/ja00125a035
42. Kato, M.; Kamigaito, M.; Sawamoto, M.; Higashimura, T. *Macromolecules* **1995,** *28,* 1721–1723. doi:10.1021/ma00109a056
43. Matyjaszewski, K. *Macromolecules* **2012,** *45,* 4015–4039. doi:10.1021/ma3001719
44. Pintauer, T.; Matyjaszewski, K. *Chem. Soc. Rev.* **2008,** *37,* 1087–1097. doi:10.1039/b714578k
45. Xia, J.; Matyjaszewski, K. *Macromolecules* **1997,** *30,* 7692–7696. doi:10.1021/ma9710085
46. Gromada, J.; Matyjaszewski, K. *Macromolecules* **2001,** *34,* 7664–7671. doi:10.1021/ma010864k
47. Min, K.; Gao, H.; Matyjaszewski, K. *J. Am. Chem. Soc.* **2005,** *127,* 3825–3830. doi:10.1021/ja0429364
48. Matyjaszewski, K.; Jakubowski, W.; Min, K.; Tang, W.; Huang, J.; Braunecker, W. A.; Tsarevsky, N. V. *Proc. Natl. Acad. Sci. U. S. A.* **2006,** *103,* 15309–15314. doi:10.1073/pnas.0602675103
49. Jakubowski, W.; Matyjaszewski, K. *Angew. Chem., Int. Ed.* **2006,** *45,* 4482–4486. doi:10.1002/anie.200600272
50. Matyjaszewski, K.; Tsarevsky, N. V.; Braunecker, W. A.; Dong, H.; Huang, J.; Jakubowski, W.; Kwak, Y.; Nicolay, R.; Tang, W.; Yoon, J. A. *Macromolecules* **2007,** *40,* 7795–7806. doi:10.1021/ma0717800
51. Chmielarz, P.; Fantin, M.; Park, S.; Isse, A. A.; Gennaro, A.; Magenau, A. J. D.; Sobkowiak, A.; Matyjaszewski, K. *Prog. Polym. Sci.* **2017,** *69,* 47–78. doi:10.1016/j.progpolymsci.2017.02.005
52. Magenau, A. J. D.; Strandwitz, N. C.; Gennaro, A.; Matyjaszewski, K. *Science* **2011,** *332,* 81–84. doi:10.1126/science.1202357
53. Kwak, Y.; Matyjaszewski, K. *Macromolecules* **2010,** *43,* 5180–5183. doi:10.1021/ma100850a
54. Pan, X.; Tasdelen, M. A.; Laun, J.; Junkers, T.; Yagci, Y.; Matyjaszewski, K. *Prog. Polym. Sci.* **2016,** *62,* 73–125. doi:10.1016/j.progpolymsci.2016.06.005
55. Mohapatra, H.; Kleiman, M.; Esser-Kahn, A. P. *Nat. Chem.* **2017,** *9,* 135–139. doi:10.1038/nchem.2633
56. Schröder, K.; Mathers, R. T.; Buback, J.; Konkolewicz, D.; Magenau, A. J. D.; Matyjaszewski, K. *ACS Macro Lett.* **2012,** *1,* 1037–1040. doi:10.1021/mz3003787
57. Pan, X.; Fantin, M.; Yuan, F.; Matyjaszewski, K. *Chem. Soc. Rev.* **2018,** *47,* 5457–5490. doi:10.1039/c8cs00259b
58. Treat, N. J.; Sprafke, H.; Kramer, J. W.; Clark, P. G.; Barton, B. E.; Read de Alaniz, J.; Fors, B. P.; Hawker, C. J. *J. Am. Chem. Soc.* **2014,** *136,* 16096–16101. doi:10.1021/ja510389m
59. Matyjaszewski, K.; Tsarevsky, N. V. *Nat. Chem.* **2009,** *1,* 276–288. doi:10.1038/nchem.257
60. Matyjaszewski, K. *Adv. Mater. (Weinheim, Ger.)* **2018,** *30,* 1706441. doi:10.1002/adma.201706441
61. Chiefari, J.; Chong, Y. K.; Ercole, F.; Krstina, J.; Jeffery, J.; Le, T. P. T.; Mayadunne, R. T. A.; Meijs, G. F.; Moad, C. L.; Moad, G.; Rizzardo, E.; Thang, S. H. *Macromolecules* **1998,** *31,* 5559–5562. doi:10.1021/ma9804951
62. Mayadunne, R. T. A.; Rizzardo, E.; Chiefari, J.; Krstina, J.; Moad, G.; Postma, A.; Thang, S. H. *Macromolecules* **2000,** *33,* 243–245. doi:10.1021/ma991451a
63. Chong, Y. K.; Le, T. P. T.; Moad, G.; Rizzardo, E.; Thang, S. H. *Macromolecules* **1999,** *32,* 2071–2074. doi:10.1021/ma981472p
64. Barner-Kowollik, C.; Quinn, J. F.; Morsley, D. R.; Davis, T. P. *J. Polym. Sci., Part A: Polym. Chem.* **2001,** *39,* 1353–1365. doi:10.1002/pola.1112
65. Xu, J.; Jung, K.; Atme, A.; Shanmugam, S.; Boyer, C. *J. Am. Chem. Soc.* **2014,** *136,* 5508–5519. doi:10.1021/ja501745g
66. Allegrezza, M. L.; Konkolewicz, D. *ACS Macro Lett.* **2021,** *10,* 433–446. doi:10.1021/acsmacrolett.1c00046
67. Lv, C.; He, C.; Pan, X. *Angew. Chem., Int. Ed.* **2018,** *57,* 9430–9433. doi:10.1002/anie.201805212
68. Moad, G.; Rizzardo, E.; Thang, S. H. *Aust. J. Chem.* **2006,** *59,* 669–692. doi:10.1071/ch06250

69. Hurtgen, M.; Detrembleur, C.; Jerome, C.; Debuigne, A. *Polym. Rev. (Philadelphia, PA, U. S.)* **2011,** *51,* 188–213. doi:10.1080/15583724.2011.566401
70. Allan, L. E. N.; Perry, M. R.; Shaver, M. P. *Prog. Polym. Sci.* **2012,** *37,* 127–156. doi:10.1016/j.progpolymsci.2011.07.004
71. Tatemoto, M.; Suzuki, T.; Tomoda, M.; Furukawa, Y.; Ueta, Y. Cross linkable fluorine-containing polymer and its production. U.S. Patent US4,243,770, Jan 6, 1981.
72. Lacroix-Desmazes, P.; Severac, R.; Boutevin, B. *Macromolecules* **2005,** *38,* 6299–6309. doi:10.1021/ma050056j
73. Li, N.; Pan, X.-C. *Chin. J. Polym. Sci.* **2021,** *39,* 1084–1092. doi:10.1007/s10118-021-2597-9
74. *Chem. Commun.* **2003,** 1–4. doi:10.1039/b210718j
75. Nezakati, T.; Seifalian, A.; Tan, A.; Seifalian, A. M. *Chem. Rev.* **2018,** *118,* 6766–6843. doi:10.1021/acs.chemrev.6b00275
76. Guo, X.; Facchetti, A. *Nat. Mater.* **2020,** *19,* 922–928. doi:10.1038/s41563-020-0778-5
77. Xu, C.; Dong, J.; He, C.; Yun, J.; Pan, X. *Giant* **2023,** *14,* 100154. doi:10.1016/j.giant.2023.100154
78. Niemi, V. M.; Knuuttila, P.; Österholm, J.-E.; Korvola, J. *Polymer* **1992,** *33,* 1559–1562. doi:10.1016/0032-3861(92)90138-m
79. McCullough, R. D. *Adv. Mater. (Weinheim, Ger.)* **1998,** *10,* 93–116. doi:10.1002/(sici)1521-4095(199801)10:2<93::aid-adma93>3.0.co;2-f
80. Posner, T. *Ber. Dtsch. Chem. Ges.* **1905,** *38,* 646–657. doi:10.1002/cber.190503801106
81. Hoyle, C. E.; Lee, T. Y.; Roper, T. *J. Polym. Sci., Part A: Polym. Chem.* **2004,** *42,* 5301–5338. doi:10.1002/pola.20366
82. Sticker, D.; Geczy, R.; Häfeli, U. O.; Kutter, J. P. *ACS Appl. Mater. Interfaces* **2020,** *12,* 10080–10095. doi:10.1021/acsami.9b22050
83. Sirrine, J. M.; Meenakshisundaram, V.; Moon, N. G.; Scott, P. J.; Mondschein, R. J.; Weiseman, T. F.; Williams, C. B.; Long, T. E. *Polymer* **2018,** *152,* 25–34. doi:10.1016/j.polymer.2018.02.056
84. Bhagat, S. D.; Chatterjee, J.; Chen, B.; Stiegman, A. E. *Macromolecules* **2012,** *45,* 1174–1181. doi:10.1021/ma202467a
85. Cook, C. C.; Fong, E. J.; Schwartz, J. J.; Porcincula, D. H.; Kaczmarek, A. C.; Oakdale, J. S.; Moran, B. D.; Champley, K. M.; Rackson, C. M.; Muralidharan, A.; McLeod, R. R.; Shusteff, M. *Adv. Mater. (Weinheim, Ger.)* **2020,** *32,* 2003376. doi:10.1002/adma.202003376
86. Huang, Z.; Chen, Z.; Jiang, Y.; Li, N.; Yang, S.; Wang, G.; Pan, X. *J. Am. Chem. Soc.* **2021,** *143,* 19167–19177. doi:10.1021/jacs.1c09263
87. Grubbs, R. H.; Carr, D. D.; Hoppin, C.; Burk, P. L. *J. Am. Chem. Soc.* **1976,** *98,* 3478–3483. doi:10.1021/ja00428a015
88. Kensy, V. K.; Tritt, R. L.; Haque, F. M.; Murphy, L. M.; Knorr, D. B., Jr.; Grayson, S. M.; Boydston, A. J. *Angew. Chem., Int. Ed.* **2020,** *59,* 9074–9079. doi:10.1002/anie.202000434
89. Wu, C.; Corrigan, N.; Lim, C.-H.; Liu, W.; Miyake, G.; Boyer, C. *Chem. Rev.* **2022,** *122,* 5476–5518. doi:10.1021/acs.chemrev.1c00409
90. Ogawa, K. A.; Goetz, A. E.; Boydston, A. J. *J. Am. Chem. Soc.* **2015,** *137,* 1400–1403. doi:10.1021/ja512073m
91. Pascual, L. M. M.; Dunford, D. G.; Goetz, A. E.; Ogawa, K. A.; Boydston, A. J. *Synlett* **2016,** *27,* 759–762. doi:10.1055/s-0035-1561330
92. Goetz, A. E.; Boydston, A. J. *J. Am. Chem. Soc.* **2015,** *137,* 7572–7575. doi:10.1021/jacs.5b03665
93. Goetz, A. E.; Pascual, L. M. M.; Dunford, D. G.; Ogawa, K. A.; Knorr, D. B., Jr.; Boydston, A. J. *ACS Macro Lett.* **2016,** *5,* 579–582. doi:10.1021/acsmacrolett.6b00131
94. Gauthier, M. A.; Gibson, M. I.; Klok, H.-A. *Angew. Chem., Int. Ed.* **2009,** *48,* 48–58. doi:10.1002/anie.200801951
95. Günay, K. A.; Theato, P.; Klok, H.-A. *J. Polym. Sci., Part A: Polym. Chem.* **2013,** *51,* 1–28. doi:10.1002/pola.26333
96. Larsen, M. B.; Herzog, S. E.; Quilter, H. C.; Hillmyer, M. A. *ACS Macro Lett.* **2018,** *7,* 122–126. doi:10.1021/acsmacrolett.7b00896
97. Hoyle, C. E.; Bowman, C. N. *Angew. Chem., Int. Ed.* **2010,** *49,* 1540–1573. doi:10.1002/anie.200903924
98. Fairbanks, B. D.; Scott, T. F.; Kloxin, C. J.; Anseth, K. S.; Bowman, C. N. *Macromolecules* **2009,** *42,* 211–217. doi:10.1021/ma801903w
99. Cramer, N. B.; Scott, J. P.; Bowman, C. N. *Macromolecules* **2002,** *35,* 5361–5365. doi:10.1021/ma0200672
100. Xu, J.; Boyer, C. *Macromolecules* **2015,** *48,* 520–529. doi:10.1021/ma502460t
101. Soares, F. A.; Steinbüchel, A. *Macromol. Biosci.* **2021,** *21,* 2100261. doi:10.1002/mabi.202100261
102. Serniuk, G. E.; Banes, F. W.; Swaney, M. W. *J. Am. Chem. Soc.* **1948,** *70,* 1804–1808. doi:10.1021/ja01185a046
103. Decker, C.; Viet, T. N. T. *Macromol. Chem. Phys.* **1999,** *200,* 1965–1974. doi:10.1002/(sici)1521-3935(19990801)200:8<1965::aid-macp1965>3.0.co;2-w
104. Thielke, M. W.; Bruckner, E. P.; Wong, D. L.; Theato, P. *Polymer* **2014,** *55,* 5596–5599. doi:10.1016/j.polymer.2014.09.002
105. Strohmeier, L.; Frommwald, H.; Schlögl, S. *RSC Adv.* **2020,** *10,* 23607–23614. doi:10.1039/d0ra04186f
106. Kanbayashi, N.; Miyamoto, S.; Ishido, Y.; Okamura, T.-a.; Onitsuka, K. *Polym. Chem.* **2017,** *8,* 985–994. doi:10.1039/c6py01946c
107. Butzelaar, A. J.; Schneider, S.; Molle, E.; Theato, P. *Macromol. Rapid Commun.* **2021,** *42,* 2100133. doi:10.1002/marc.202100133
108. Ntoukam, D. H. S.; Mutlu, H.; Theato, P. *Eur. Polym. J.* **2020,** *122,* 109319. doi:10.1016/j.eurpolymj.2019.109319
109. Krappitz, T.; Brauer, D.; Theato, P. *Polym. Chem.* **2016,** *7,* 4525–4530. doi:10.1039/c6py00818f
110. Riva, R.; Rieger, J.; Jérôme, R.; Lecomte, P. *J. Polym. Sci., Part A: Polym. Chem.* **2006,** *44,* 6015–6024. doi:10.1002/pola.21674
111. Riva, R.; Lenoir, S.; Jérôme, R.; Lecomte, P. *Polymer* **2005,** *46,* 8511–8518. doi:10.1016/j.polymer.2005.03.105
112. Xu, J.; Atme, A.; Marques Martins, A. F.; Jung, K.; Boyer, C. *Polym. Chem.* **2014,** *5,* 3321–3325. doi:10.1039/c4py00193a
113. Coiai, S.; Passaglia, E.; Cicogna, F. *Polym. Int.* **2019,** *68,* 27–63. doi:10.1002/pi.5664
114. Miller, J. L.; Lawrence, J.-M. I. A.; Rodriguez del Rey, F. O.; Floreancig, P. E. *Chem. Soc. Rev.* **2022,** *51,* 5660–5690. doi:10.1039/d1cs01169c
115. Mardyukov, A.; Studer, A. *Macromol. Rapid Commun.* **2013,** *34,* 94–101. doi:10.1002/marc.201200595
116. Wang, G.; Zhang, Y.; Huang, J. *J. Polym. Sci., Part A: Polym. Chem.* **2010,** *48,* 1633–1640. doi:10.1002/pola.23929
117. Amamoto, Y.; Higaki, Y.; Matsuda, Y.; Otsuka, H.; Takahara, A. *J. Am. Chem. Soc.* **2007,** *129,* 13298–13304. doi:10.1021/ja075447n

118. Hodges, M. N.; Elardo, M. J.; Seo, J.; Dohoda, A. F.; Michael, F. E.; Golder, M. R. *Angew. Chem., Int. Ed.* **2023,** *62,* e202303115. doi:10.1002/anie.202303115
119. Zhang, Z.; Li, X.; Zhou, D.; Ding, S.; Wang, M.; Zeng, R. *J. Am. Chem. Soc.* **2023,** *145,* 7612–7620. doi:10.1021/jacs.3c01100
120. Li, N.; Yang, S.; Huang, Z.; Pan, X. *Macromolecules* **2021,** *54,* 6000–6005. doi:10.1021/acs.macromol.1c00996
121. Gardel, M. L.; Shin, J. H.; MacKintosh, F. C.; Mahadevan, L.; Matsudaira, P.; Weitz, D. A. *Science* **2004,** *304,* 1301–1305. doi:10.1126/science.1095087
122. Zhang, X.; Wang, S.; Jiang, Z.; Li, Y.; Jing, X. *J. Am. Chem. Soc.* **2020,** *142,* 21852–21860. doi:10.1021/jacs.0c10244
123. Chen, J.; Garcia, E. S.; Zimmerman, S. C. *Acc. Chem. Res.* **2020,** *53,* 1244–1256. doi:10.1021/acs.accounts.0c00178
124. Fisher, H. L. *Ind. Eng. Chem.* **1939,** *31,* 1381–1389. doi:10.1021/ie50359a015
125. Coran, A. Y. Vulcanization. In *The Science and Technology of Rubber,* 4th ed.; Mark, J. E.; Erman, B.; Roland, C. M., Eds.; Academic Press: Boston, MA, USA, 2013; pp 337–381. doi:10.1016/b978-0-12-394584-6.00007-8
126. Huang, X. *High Voltage* **2020,** *5,* 229–230. doi:10.1049/hve.2020.0196
127. Likozar, B. *React. Funct. Polym.* **2011,** *71,* 11–22. doi:10.1016/j.reactfunctpolym.2010.11.004
128. Likozar, B.; Krajnc, M. *Polym. Eng. Sci.* **2009,** *49,* 60–72. doi:10.1002/pen.21218
129. Likozar, B.; Krajnc, M. *Chem. Eng. Process.* **2011,** *50,* 200–210. doi:10.1016/j.cep.2010.12.007
130. Hofmann, R. J.; Vlatković, M.; Wiesbrock, F. *Polymers (Basel, Switz.)* **2017,** *9,* 534. doi:10.3390/polym9100534
131. Deriabin, K. V.; Dobrynin, M. V.; Islamova, R. M. *Dalton Trans.* **2020,** *49,* 8855–8858. doi:10.1039/d0dt01061h
132. Huang, Z.; Liu, K.; Liu, M.; Yun, J.; Dong, J.; Chen, Z.; Xie, Z.; Pan, X. *Chin. J. Chem.* **2023,** *41,* 2275–2281. doi:10.1002/cjoc.202300158
133. Wang, D.; Klein, J.; Mejía, E. *Chem. – Asian J.* **2017,** *12,* 1180–1197. doi:10.1002/asia.201700304
134. Rånby, B. G.; Rabek, J. F. *Photodegradation, Photo-oxidation, and Photostabilization of Polymers: Principles and Applications;* John Wiley & Sons: New York, NY, USA, 1975.
135. Bousquet, J. A.; Fouassier, J. P. *Polym. Degrad. Stab.* **1987,** *18,* 163–185. doi:10.1016/0141-3910(87)90029-2
136. Decker, C. *Prog. Polym. Sci.* **1996,** *21,* 593–650. doi:10.1016/0079-6700(95)00027-5
137. Lai, H.; Peng, X.; Li, L.; Zhu, D.; Xiao, P. *Prog. Polym. Sci.* **2022,** *128,* 101529. doi:10.1016/j.progpolymsci.2022.101529
138. Decker, C. *Macromol. Rapid Commun.* **2002,** *23,* 1067–1093. doi:10.1002/marc.200290014
139. Li, J.; Boyer, C.; Zhang, X. *Macromol. Mater. Eng.* **2022,** *307,* 2200010. doi:10.1002/mame.202200010
140. Bagheri, A.; Jin, J. *ACS Appl. Polym. Mater.* **2019,** *1,* 593–611. doi:10.1021/acsapm.8b00165
141. Zhang, J.; Xiao, P. *Polym. Chem.* **2018,** *9,* 1530–1540. doi:10.1039/c8py00157j
142. Bao, Y. *Macromol. Rapid Commun.* **2022,** *43,* 2200202. doi:10.1002/marc.202200202
143. Nady, N.; Schroën, K.; Franssen, M. C. R.; Lagen, B. v.; Murali, S.; Boom, R. M.; Mohyeldin, M. S.; Zuilhof, H. *ACS Appl. Mater. Interfaces* **2011,** *3,* 801–810. doi:10.1021/am101155e
144. Li, Q. X.; Hayashi, K.; Nishioka, M.; Kashiwagi, H.; Hirano, M.; Torimoto, Y.; Hosono, H.; Sadakata, M. *Appl. Phys. Lett.* **2002,** *80,* 4259–4261. doi:10.1063/1.1476958
145. Wang, L.; Yan, L.; Zhao, P.; Torimoto, Y.; Sadakata, M.; Li, Q. *Appl. Surf. Sci.* **2008,** *254,* 4191–4200. doi:10.1016/j.apsusc.2008.01.035
146. Zhao, E.; Wang, L.; Yan, L.; Torimoto, Y.; Li, Q. *J. Appl. Polym. Sci.* **2008,** *110,* 39–48. doi:10.1002/app.28464
147. Felix, T.; Trigueiro, J. S.; Bundaleski, N.; Teodoro, O. M. N. D.; Sério, S.; Debacher, N. A. *Appl. Surf. Sci.* **2018,** *428,* 730–738. doi:10.1016/j.apsusc.2017.09.147
148. Förster, F. *Plasma Processes Polym.* **2022,** *19,* 2100240. doi:10.1002/ppap.202100240
149. Okubo, M.; Tahara, M.; Saeki, N.; Yamamoto, T. *Thin Solid Films* **2008,** *516,* 6592–6597. doi:10.1016/j.tsf.2007.11.033
150. Brillas, E.; Sirés, I.; Oturan, M. A. *Chem. Rev.* **2009,** *109,* 6570–6631. doi:10.1021/cr900136g
151. Bureau, C.; Pinson, J. Method for the modification of polymer surfaces, such as the hydroxylation of polymer surfaces, and products thus obtained. Eur. Pat. Appl. EP1937759 A1, July 2, 2008.
152. Ktari, N.; Poncet, P.; Sénéchal, H.; Malaquin, L.; Kanoufi, F.; Combellas, C. *Langmuir* **2010,** *26,* 17348–17356. doi:10.1021/la1028564
153. Zollinger, H. Applications of Heterolytic and Homolytic Dediazoniations in Organic Syntheses: Sections 10.1–10.9. *Diazo Chemistry I;* Wiley-VCH: Weinheim, Germany, 1994; pp 221–253. doi:10.1002/3527601724.ch10a
154. Santos, L. M.; Ghilane, J.; Fave, C.; Lacaze, P.-C.; Randriamahazaka, H.; Abrantes, L. M.; Lacroix, J.-C. *J. Phys. Chem. C* **2008,** *112,* 16103–16109. doi:10.1021/jp8042818
155. Liu, X.; Wang, M.; Jia, Y.-x. *Sep. Sci. Technol.* **2016,** *51,* 2823–2832. doi:10.1080/01496395.2016.1210643
156. Chehimi, M. M.; Lamouri, A.; Picot, M.; Pinson, J. *J. Mater. Chem. C* **2014,** *2,* 356–363. doi:10.1039/c3tc31492h
157. Bastekova, K.; Guselnikova, O.; Postnikov, P.; Elashnikov, R.; Kunes, M.; Kolska, Z.; Švorčík, V.; Lyutakov, O. *Appl. Surf. Sci.* **2017,** *397,* 226–234. doi:10.1016/j.apsusc.2016.11.062
158. Troian-Gautier, L.; Martínez-Tong, D. E.; Hubert, J.; Reniers, F.; Sferrazza, M.; Mattiuzzi, A.; Lagrost, C.; Jabin, I. *J. Phys. Chem. C* **2016,** *120,* 22936–22945. doi:10.1021/acs.jpcc.6b06143
159. Benoit, C.; Demeter, D.; Bélanger, D.; Cougnon, C. *Angew. Chem., Int. Ed.* **2016,** *55,* 5318–5321. doi:10.1002/anie.201601395
160. Bouriga, M.; Chehimi, M. M.; Combellas, C.; Decorse, P.; Kanoufi, F.; Deronzier, A.; Pinson, J. *Chem. Mater.* **2013,** *25,* 90–97. doi:10.1021/cm3032994
161. Hetemi, D.; Kanoufi, F.; Combellas, C.; Pinson, J.; Podvorica, F. I. *Langmuir* **2014,** *30,* 13907–13913. doi:10.1021/la503833j
162. Combellas, C.; Kanoufi, F.; Nunige, S. *Chem. Mater.* **2007,** *19,* 3830–3839. doi:10.1021/cm070438z
163. Blanksby, S. J.; Ellison, G. B. *Acc. Chem. Res.* **2003,** *36,* 255–263. doi:10.1021/ar020230d
164. Horie, K.; Mita, I. *Chem. Phys. Lett.* **1982,** *93,* 61–65. doi:10.1016/0009-2614(82)85056-2
165. Kinstle, J. F.; Watson, S. L., Jr. Photoassisted Modification of and Grafting to Polyethylene. In *Polymer Alloys. Polymer Science and Technology;* Klempner, D.; Frisch, K. C., Eds.; Springer: Boston, MA, USA, 1977; Vol. 10, pp 461–478. doi:10.1007/978-1-4684-0874-4_33
166. Williams, J. L. R.; Daly, R. C. *Prog. Polym. Sci.* **1977,** *5,* 61–93. doi:10.1016/0079-6700(77)90005-3

167. Lin, X.; Fukazawa, K.; Ishihara, K. *ACS Appl. Mater. Interfaces* **2015,** *7,* 17489–17498. doi:10.1021/acsami.5b05193
168. Kato, K.; Uchida, E.; Kang, E.-T.; Uyama, Y.; Ikada, Y. *Prog. Polym. Sci.* **2003,** *28,* 209–259. doi:10.1016/s0079-6700(02)00032-1
169. Chen, Y. L.; Rånby, B. *Polym. Adv. Technol.* **1990,** *1,* 103–107. doi:10.1002/pat.1990.220010112
170. Barbey, R.; Lavanant, L.; Paripovic, D.; Schüwer, N.; Sugnaux, C.; Tugulu, S.; Klok, H.-A. *Chem. Rev.* **2009,** *109,* 5437–5527. doi:10.1021/cr900045a
171. Zoppe, J. O.; Ataman, N. C.; Mocny, P.; Wang, J.; Moraes, J.; Klok, H.-A. *Chem. Rev.* **2017,** *117,* 1105–1318. doi:10.1021/acs.chemrev.6b00314
172. Zhou, J.; Huang, Z.; Sun, Y.; Cui, M.; Luo, Z.; Yu, B.; Zou, X.; Hu, H. *Colloids Surf., B* **2021,** *203,* 111718. doi:10.1016/j.colsurfb.2021.111718
173. Zain, G.; Bučková, M.; Mosnáčková, K.; Doháňošová, J.; Opálková Šišková, A.; Mičušík, M.; Kleinová, A.; Matúš, P.; Mosnáček, J. *Polym. Chem.* **2021,** *12,* 7073–7084. doi:10.1039/d1py01322j
174. Ng, G.; Li, M.; Yeow, J.; Jung, K.; Pester, C. W.; Boyer, C. *ACS Appl. Mater. Interfaces* **2020,** *12,* 55243–55254. doi:10.1021/acsami.0c15221
175. Rong, L.-H.; Cheng, X.; Ge, J.; Krebs, O. K.; Capadona, J. R.; Caldona, E. B.; Advincula, R. C. *ACS Appl. Polym. Mater.* **2022,** *4,* 6449–6457. doi:10.1021/acsapm.2c00868
176. Kyomoto, M.; Ishihara, K. *ACS Appl. Mater. Interfaces* **2009,** *1,* 537–542. doi:10.1021/am800260t
177. Kyomoto, M.; Moro, T.; Takatori, Y.; Kawaguchi, H.; Nakamura, K.; Ishihara, K. *Biomaterials* **2010,** *31,* 1017–1024. doi:10.1016/j.biomaterials.2009.10.055
178. Kabanov, V. Y.; Feldman, V. I.; Ershov, B. G.; Polikarpov, A. I.; Kiryukhin, D. P.; Apel', P. Y. *High Energy Chem.* **2009,** *43,* 1–18. doi:10.1134/s0018143909010019
179. Tsoulfanidis, N.; Landsberger, S. *Measurement & Detection of Radiation,* 5th ed.; CRC Press: Boca Raton, FL, USA, 2021. doi:10.1201/9781003009849
180. Flores-Rojas, G. G.; Bucio, E. *Radiat. Phys. Chem.* **2016,** *127,* 21–26. doi:10.1016/j.radphyschem.2016.05.015
181. Barner, L.; Quinn, J. F.; Barner-Kowollik, C.; Vana, P.; Davis, T. P. *Eur. Polym. J.* **2003,** *39,* 449–459. doi:10.1016/s0014-3057(02)00247-1
182. Barsbay, M.; Güven, O. *Radiat. Phys. Chem.* **2020,** *169,* 107816. doi:10.1016/j.radphyschem.2018.04.009
183. Sawada, S.-i.; Hasegawa, S.; Zhao, Y.; Maekawa, Y. *J. Membr. Sci.* **2017,** *532,* 105–114. doi:10.1016/j.memsci.2017.03.016
184. Chen, Q.; Zhang, Z.; Zhou, N.; Cheng, Z.; Zhu, J.; Zhang, W.; Zhu, X. *J. Polym. Sci., Part A: Polym. Chem.* **2011,** *49,* 3588–3594. doi:10.1002/pola.24797
185. Dong, H.; Bell, T. *Surf. Coat. Technol.* **1999,** *111,* 29–40. doi:10.1016/s0257-8972(98)00698-7
186. Burkert, S.; Kuntzsch, M.; Bellmann, C.; Uhlmann, P.; Stamm, M. *Appl. Surf. Sci.* **2009,** *255,* 6256–6261. doi:10.1016/j.apsusc.2009.01.096
187. Komatsu, M.; Kawakami, T.; Kanno, J.-i.; Sasaki, T. *J. Appl. Polym. Sci.* **2011,** *119,* 2533–2538. doi:10.1002/app.33071
188. Xu, H.; Kosma, V.; Giannelis, E. P.; Ober, C. K. *Polym. J.* **2018,** *50,* 45–55. doi:10.1038/pj.2017.64
189. Inoue, S.; Amano, T.; Itani, T.; Watanabe, H.; Mori, I.; Watanabe, T.; Kinoshita, H.; Miyai, H.; Hatakeyama, M. *Adv. Opt. Technol.* **2012,** *1,* 269–278. doi:10.1515/aot-2012-0029
190. Clecak, N. J.; Cox, R. J.; Moreau, W. M. *Polym. Eng. Sci.* **1974,** *14,* 491–493. doi:10.1002/pen.760140705
191. Lin, B. J. *J. Vac. Sci. Technol. (N. Y., NY, U. S.)* **1975,** *12,* 1317–1320. doi:10.1116/1.568527
192. Emoto, F.; Gamo, K.; Namba, S.; Samoto, N.; Shimizu, R. *Jpn. J. Appl. Phys., Part 1* **1985,** *24,* L809. doi:10.1143/jjap.24.l809
193. Pacansky, J.; Waltman, R. J.; Pacansky, G. *Chem. Mater.* **1993,** *5,* 1526–1532. doi:10.1021/cm00034a024
194. Lawrie, K.; Blakey, I.; Blinco, J.; Gronheid, R.; Jack, K.; Pollentier, I.; Leeson, M. J.; Younkin, T. R.; Whittaker, A. K. *Radiat. Phys. Chem.* **2011,** *80,* 236–241. doi:10.1016/j.radphyschem.2010.07.038
195. Bowmer, T. N.; O'Donnell, J. H. *J. Polym. Sci., Polym. Chem. Ed.* **1981,** *19,* 45–50. doi:10.1002/pol.1981.170190105
196. Dainton, F. S.; Ivin, K. J. *Q. Rev., Chem. Soc.* **1958,** *12,* 61–92. doi:10.1039/qr9581200061
197. Bowmer, T. N.; O'Donnell, J. H.; Wells, P. R. *Makromol. Chem., Rapid Commun.* **1980,** *1,* 1–6. doi:10.1002/marc.1980.030010101
198. Sasaki, T.; Yaguchi, H. *J. Polym. Sci., Part A: Polym. Chem.* **2009,** *47,* 602–613. doi:10.1002/pola.23179
199. Borrelle, S. B.; Ringma, J.; Law, K. L.; Monnahan, C. C.; Lebreton, L.; McGivern, A.; Murphy, E.; Jambeck, J.; Leonard, G. H.; Hilleary, M. A.; Eriksen, M.; Possingham, H. P.; De Frond, H.; Gerber, L. R.; Polidoro, B.; Tahir, A.; Bernard, M.; Mallos, N.; Barnes, M.; Rochman, C. M. *Science* **2020,** *369,* 1515–1518. doi:10.1126/science.aba3656
200. Stadler, B. M.; de Vries, J. G. *Philos. Trans. R. Soc., A* **2021,** *379,* 20200341. doi:10.1098/rsta.2020.0341
201. Payne, J.; Jones, M. D. *ChemSusChem* **2021,** *14,* 4041–4070. doi:10.1002/cssc.202100400
202. Oh, S.; Stache, E. E. *J. Am. Chem. Soc.* **2022,** *144,* 5745–5749. doi:10.1021/jacs.2c01411
203. Li, T.; Vijeta, A.; Casadevall, C.; Gentleman, A. S.; Euser, T.; Reisner, E. *ACS Catal.* **2022,** *12,* 8155–8163. doi:10.1021/acscatal.2c02292
204. Wang, H. S.; Truong, N. P.; Pei, Z.; Coote, M. L.; Anastasaki, A. *J. Am. Chem. Soc.* **2022,** *144,* 4678–4684. doi:10.1021/jacs.2c00963
205. Martinez, M. R.; De Luca Bossa, F.; Olszewski, M.; Matyjaszewski, K. *Macromolecules* **2022,** *55,* 78–87. doi:10.1021/acs.macromol.1c02246
206. Godiya, C. B.; Gabrielli, S.; Materazzi, S.; Pianesi, M. S.; Stefanini, N.; Marcantoni, E. *J. Environ. Manage.* **2019,** *231,* 1012–1020. doi:10.1016/j.jenvman.2018.10.116
207. Braido, R. S.; Borges, L. E. P.; Pinto, J. C. *J. Anal. Appl. Pyrolysis* **2018,** *132,* 47–55. doi:10.1016/j.jaap.2018.03.017
208. Shabtai, J.; Xiao, X.; Zmierczak, W. *Energy Fuels* **1997,** *11,* 76–87. doi:10.1021/ef960076+
209. Liu, Y.; Chandra Akula, K.; Phani Raj Dandamudi, K.; Liu, Y.; Xu, M.; Sanchez, A.; Zhu, D.; Deng, S. *Chem. Eng. J.* **2022,** *446,* 137238. doi:10.1016/j.cej.2022.137238
210. Lal, S.; Anisia, K. S.; Jhansi, M.; Kishore, L.; Kumar, A. *J. Mol. Catal. A: Chem.* **2007,** *265,* 15–24. doi:10.1016/j.molcata.2006.09.027
211. Kong, S.; He, C.; Dong, J.; Li, N.; Xu, C.; Pan, X. *Macromol. Chem. Phys.* **2022,** *223,* 2100322. doi:10.1002/macp.202100322

212. Wang, C.; Xia, J.; Zhang, Y.; Hu, X.; Jian, Z. *Natl. Sci. Rev.* **2023,** *10,* nwad039. doi:10.1093/nsr/nwad039

BEILSTEIN JOURNAL OF ORGANIC CHEMISTRY

Mechanisms for radical reactions initiating from *N*-hydroxyphthalimide esters

Carlos R. Azpilcueta-Nicolas and Jean-Philip Lumb*

Perspective

Open Access

Address:
Department of Chemistry, McGill University, 801 Sherbrooke Street West, Montreal, Quebec H3A 0B8, Canada

Email:
Jean-Philip Lumb* - jean-philip.lumb@mcgill.ca

* Corresponding author

Keywords:
decarboxylative couplings; mechanisms; NHPI-esters; radical reactions

Beilstein J. Org. Chem. **2024,** *20,* 346–378.
https://doi.org/10.3762/bjoc.20.35

Received: 11 September 2023
Accepted: 29 January 2024
Published: 21 February 2024

This article is part of the thematic issue "Modern radical chemistry".

Guest Editor: H.-M. Huang

Abstract

Due to their ease of preparation, stability, and diverse reactivity, *N*-hydroxyphthalimide (NHPI) esters have found many applications as radical precursors. Mechanistically, NHPI esters undergo a reductive decarboxylative fragmentation to provide a substrate radical capable of engaging in diverse transformations. Their reduction via single-electron transfer (SET) can occur under thermal, photochemical, or electrochemical conditions and can be influenced by a number of factors, including the nature of the electron donor, the use of Brønsted and Lewis acids, and the possibility of forming charge-transfer complexes. Such versatility creates many opportunities to influence the reaction conditions, providing a number of parameters with which to control reactivity. In this perspective, we provide an overview of the different mechanisms for radical reactions involving NHPI esters, with an emphasis on recent applications in radical additions, cyclizations and decarboxylative cross-coupling reactions. Within these reaction classes, we discuss the utility of the NHPI esters, with an eye towards their continued development in complexity-generating transformations.

Introduction

The historical challenges of using radicals in synthetic chemistry is well documented [1,2]. Traditional approaches for radical generation relied on hazardous reagents and harsh conditions, resulting in low reaction efficiency and undesired byproduct formation [3-6]. As a consequence, the utility of radicals in organic synthesis remained limited for many years and in the past, they were perceived as fleeting reaction intermediates.

Recent progress in photoredox catalysis [6-8], electrochemistry [9,10], and the use of transition-metal (TM) catalysts in radical cross-coupling reactions [11] have dramatically expanded the use of radicals in synthesis, leading to their strategic incorporation as "synthons" in modern organic chemistry, with complementary reactivity to more common polar reaction manifolds [12-15]. The utility of radicals has also been expanded through the recent development of transformations involving radical-

polar crossover, which incorporate both radical and ionic bond-forming steps into a single synthetic operation [16,17].

The success of radical reactions is intimately linked to the mechanisms of their initiation and the radical progenitor employed. Amongst the many progenitors that are available, carboxylic acids are one of the most extensively used, owing to their structural diversity and widespread commercial availability [18,19]. Carboxylic acids **1** can generate radicals under oxidative conditions, as in classical decarboxylative halogenation reactions (Hunsdiecker reaction) that proceed via a radical mechanism [20,21]. More recent approaches have leveraged photoinduced ligand-to-metal charge transfer to generate radicals from aliphatic [22] and aromatic [23,24] carboxylic acids.

However, more broadly used approaches involve carefully designed activated esters. Barton esters **2** emerged in the early 1980s [25,26] (Scheme 1) and have found applications in a number of functional group interconversions mediated by radical chain decarboxylation [27]. However, their widespread use in synthesis, especially in complex molecular settings, suffers from significant disadvantages. These include thermal and photochemical instability, as evidenced by their low N–O bond dissociation energy (BDE ≈ 42 kcal/mol) [28], the reliance on toxic tin hydrides as reductants and the undesired radical recombination with reactive 2-pyridylthiyl radicals that leads to (alkylthio)pyridine byproducts [26]. More recently, *N*-hydroxyphthalimide (NHPI) esters (**3**) have emerged as convenient alternatives to Barton esters (Scheme 1) due in part to their ease of synthesis and greater stability (N–O BDE ≈ 75 kcal/mol) [28]. Their use as radical precursors was first described by Okada and colleagues in 1988 [29], who showed that C(sp^3)-centered radicals were successfully generated by subjecting NHPI esters to light irradiation in the presence of the photoreductant 1,6-bis(dimethylamino)pyrene (BDMAP). Following their initial discovery, multiple studies have shown their versatility as radical progenitors under thermal, photochemical, and electrochemical conditions [30,31].

Due to their propensity towards single-electron reduction, NHPI esters, and similar derivatives such as *N*-hydroxytetrachlorophthalimide (TCNHPI) esters, are collectively referred to as "redox-active esters" (RAEs). The versatility of RAEs stems, in part, to the sensitivity of their reduction half peak potentials ($E_{p/2}$) to their environment. For instance, a recent study by Cornella and co-workers, showed that RAEs derived from phenylacetic acid exhibited varying reduction half peak potentials ($E_{p/2}$) ranging from −2.0 V for the NHPI ester **4** to −1.2 V for the corresponding TCNHPI ester **5** (measured in MeCN vs Fc^0/Fc^+, see Scheme 2A) [32]. Based solely on their redox potentials, single-electron reduction of RAEs is only possible in the presence of a sufficiently strong reducing agent. However, the reduction of RAEs can also be facilitated through the formation of charge transfer complexes with a donor species **6** or via LUMO lowering activation with Brønsted and Lewis acids **7** (Scheme 2B), collectively offering a number of variables to influence their reactivity.

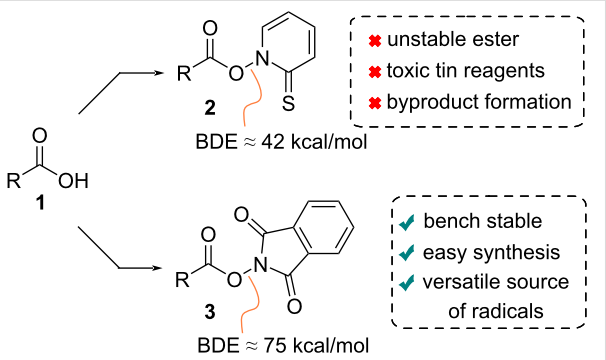

Scheme 1: Comparison between Barton and NHPI ester radical precursors.

Upon reduction, RAEs give rise to a radical anion **8** with a weakened N–O bond (BDE < 70 kcal/mol) [33]. While fragmentation of **8** affords a radical species **9** in a constructive step towards initiating the radical reaction, a principal competing step is back-electron transfer (BET) to return the closed shell starting materials (Scheme 2B). A recent study showed comparable rates for fragmentation ($8 \pm 5 \times 10^5$ s^{-1}) and BET (3.15 to 2.06×10^5 s^{-1}) [34] when employing catalytic Ir^{III} excited state reductants with moderate reducing potentials ($E_{1/2}^{red}[Ir^{IV}/*Ir^{III}] \approx -1.13$ V vs Fc^0/Fc^+ in MeCN) [35]. This suggests that in the absence of a sufficiently strong driving force, BET and fragmentation compete to influence the resulting concentration of radicals. In such instances, opting for a stronger catalytic reductant or utilizing a stoichiometric electron donor can greatly improve the efficiency of radical generation. On the other hand, additional factors such as the ability of Brønsted and Lewis acid additives to promote the fragmentation step can be considered. Importantly, the diverse mechanisms in which RAEs engage in radical reactions can be exploited to modulate the reactivity of the resulting substrate radicals. For example, under net-reductive conditions, the radical intermediates are typically terminated via hydrogen atom transfer (HAT) or sequential electron transfer and proton transfer (ET/PT) steps. Alternatively, redox-neutral transformations can be envisioned using catalytic reductants, which can enable a complementary scope of downstream functionalizations (Scheme 2B).

In this perspective, we present an overview of the diverse mechanisms that have been proposed for radical based transformat-

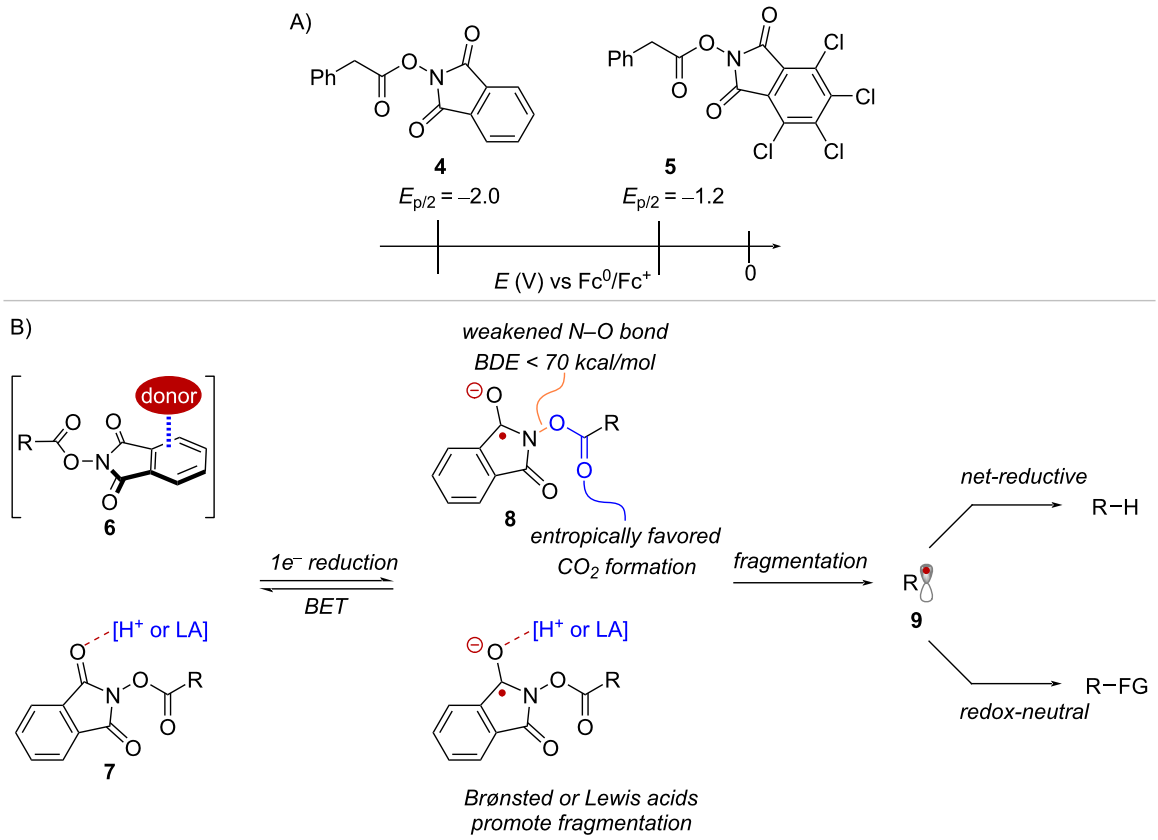

Scheme 2: Overview of the mechanisms and activation modes involved in radical generation from RAEs.

ions initiating from NHPI esters. The discussion is organized into four sections: (i) mechanisms under photochemical conditions, (ii) initiation by metal catalysis and stoichiometric reductants, (iii) *N*-heterocyclic carbene (NHC)-catalyzed radical relay, and (iv) mechanisms under electrochemical activation.

By discussing selected literature examples, we illustrate how the activation mode of NHPI esters, and the reactivity of the resulting radical species, can vary depending upon the choice of catalytic or stoichiometric electron donors, the presence of a TM catalyst, the formation of a charge-transfer complex, and the overall reaction conditions. While we hope that this discussion will spur the continued development of NHPI esters in complexity-generating transformations, it is not comprehensive, and we refer readers to recently published review articles for additional discussion [30,31].

Discussion

Mechanism under photochemical conditions

In this section we provide a summary of the various conditions and activation modes employed in radical reactions of NHPI esters using visible-light irradiation. Upon absorption of light, an excited photocatalyst (***PC**) engages in single-electron transfer (SET) with either donor (**D**) or acceptor (**A**) molecules (Scheme 3) [8,36]. Accordingly, a reductive quenching mechanism (path a) will operate when an excited photocatalyst effects the one-electron oxidation of a sacrificial donor giving rise to a strongly reducing catalytic species ($\mathbf{PC}^{n-1}$). On the other hand, in an oxidative quenching mechanism (path b) the excited photocatalyst directly induces the one-electron reduction of an acceptor substrate. Alternatively, the photocatalyst can mediate the formation of an electronically excited substrate (***S**) through an energy transfer (EnT) mechanism (path c).

In addition to these mechanistic blueprints, the formation of charge-transfer complexes involving NHPI esters, as well as examples of photoinduced transition metal-catalyzed activation will be discussed. Depending on the specific activation mechanism, both net reductive and redox neutral transformations can be implemented.

Photocatalytic reductive quenching mechanism

Among the most common reactions of NHPI esters are radical additions to electron-deficient olefins under net-reductive conditions, often referred to as Giese type addition reactions

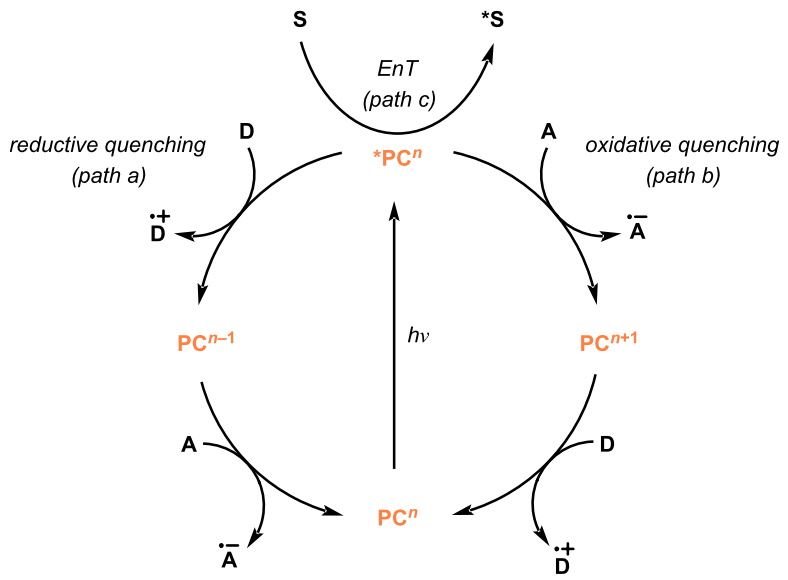

Scheme 3: Common mechanisms in photocatalysis.

(Scheme 4A). In 1991, Okada and co-workers reported the addition of alkyl radicals to α,β-unsaturated ketones, by subjecting NHPI esters to visible-light irradiation in the presence of the photocatalyst $[Ru(bpy)_3]Cl_2$ and the reductant 1-benzyl-1,4-dihydronicotinamide (BNAH) [37]. Two decades later, in 2012 the Overman group demonstrated the utility of this transformation in the total synthesis of (–)-aplyviolene, involving the diastereoselective coupling of a tertiary radical and an enone acceptor [38]. Further developments of this chemistry resulted in the general use of NHPI esters for the construction of quaternary carbons via conjugate addition of 3° radicals [39,40]. In general, this transformation operates under a reductive quenching photocatalytic cycle, requiring a stoichiometric reductant (Scheme 4A). Both TM complexes, and organic dyes such as eosin Y [41-43], have been employed as suitable photocatalysts (Scheme 4B). Under visible light irradiation the photocatalyst (**PC**) is excited into its corresponding excited state (***PC**), where it can be reduced by a suitable electron donor such as DIPEA or Hantzsch ester to generate the reduced form of the photocatalyst ($\mathbf{PC}^{\bullet-}$) (Scheme 4A). This strong reducing agent mediates the one-electron reduction of the NHPI ester **10**, forming radical anion intermediate **11**. Fragmentation of **11** via N–O bond homolysis and decarboxylation forms the key tertiary radical **12** with concomitant formation of phthalimidyl anion ($^{-}$Nphth) and CO_2. Radical **12** undergoes intermolecular addition to the olefin acceptor **13** to form radical intermediate **14**. Finally, under reductive conditions radical **14** can undergo hydrogen atom transfer (HAT) or sequential electron transfer and proton transfer (ET/PT) to form the conjugate addition product **15**.

With this mechanistic blueprint as a backdrop, Phipps and co-workers developed an enantioselective Minisci-type addition, under dual photoredox and chiral Brønsted acid catalysis [44] (Scheme 5A). In their proposed mechanism, the activation of the NHPI ester radical precursor was proposed to occur via a reductive quenching mechanism. However, since the overall transformation is redox-neutral, no stoichiometric reductant was employed. Instead, fluorescence-quenching studies suggested that the reductive quenching of the iridium excited state ($*Ir^{III}$) was taking place "off-cycle" via oxidation of the chiral phosphate co-catalyst (Scheme 5B). This event leads to the generation of a potent Ir^{II} reductant that begins the photocatalytic cycle by reducing **16** into radical anion **17** while regenerating the ground state of the Ir^{III} photocatalyst. After fragmentation, α-amino radical **18** was proposed to undergo addition to the heterocyclic radical acceptor **19** through a ternary transition state **20** involving hydrogen bonding interactions with the chiral phosphate co-catalyst. Notably, a follow-up report revealed that the radical addition is reversible, and that the selectivity determining step involves the deprotonation of **21** to provide radical intermediate **22** [45]. Finally, the iridium excited state ($*Ir^{III}$) formed under blue light irradiation oxidizes **22** to form product **23** and the corresponding reduced Ir^{II} complex, beginning a new photocatalytic cycle.

Photocatalytic oxidative quenching mechanism

The activation of NHPI esters under a photocatalytic oxidative quenching mechanism was reported for the first time by Glorius and co-workers in 2017 [46]. This activation mode was applied

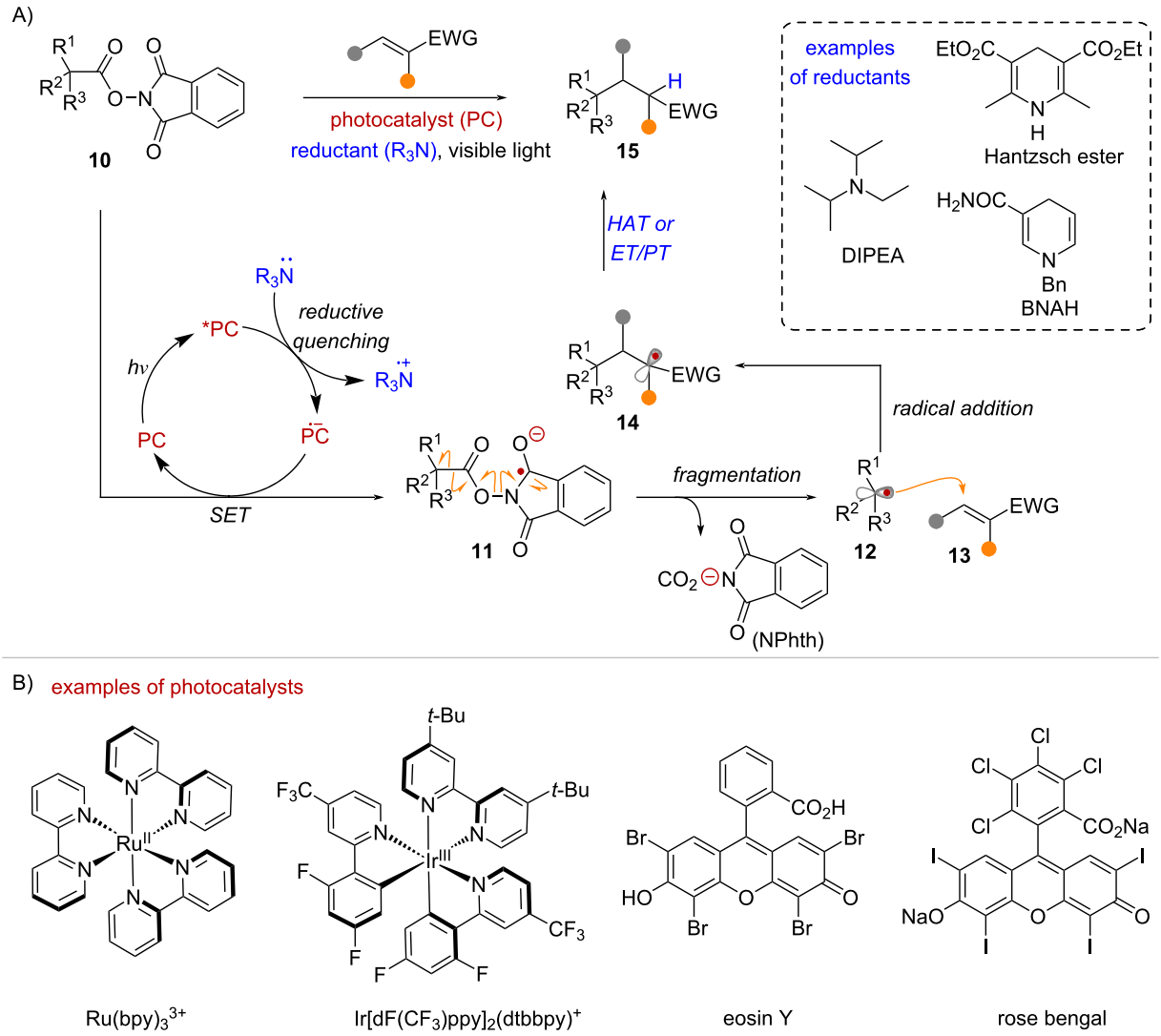

Scheme 4: A) Giese-type radical addition of NHPI esters mediated by a reductive quenching photocatalytic cycle. B) Examples of common photocatalysts.

in the functionalization of styrenes using an Ir-photocatalyst and a diverse range of nucleophiles that are H-bond donors (Scheme 6A). Stern–Volmer analysis revealed that quenching of the photocatalyst's excited state by the NHPI ester occurred only in presence of a hydrogen bond donor such as water (H_2O) or methanol (MeOH). This supported the hypothesis that activation of NHPI esters towards photoinduced electron transfer can occur through hydrogen bonding. In the proposed mechanism (Scheme 6B), hydrogen bonded complex **24** undergoes single electron reduction via oxidative quenching of the excited state $*Ir^{III}$, resulting in the formation of radical anion **25** (presumably H-bonded to H_2O) and the corresponding Ir^{IV} complex. Radical intermediate **9** formed upon fragmentation of **25**, adds to the styrene acceptor forming radical **26**. Finally, a radical-polar crossover event between **26** and the Ir^{IV} complex regenerates the Ir^{III} ground state while delivering cation **27** that is then trapped by the oxygen-nucleophile to form the oxyalkylation product **28**.

Li and co-workers described the activation of NHPI esters towards SET using a Lewis acid catalyst, allowing for the functionalization of styrene radical acceptors with nucleophiles that do not necessarily engage in hydrogen-bonding interactions, such as electron-rich (hetero)arenes [47] (Scheme 7A). Cyclic voltammetry measurements of a model NHPI ester showed a shift in its reduction potential from –1.79 V to –1.51 V (vs SCE in MeCN) in the presence of $In(OTf)_3$. As such, it was hypothesized that the Lewis acid lowers the LUMO of the NHPI ester via interaction with the oxygen lone pair in the phthalimide moiety (Scheme 7B). Thus, the excited state reductant $*Ir^{III}$

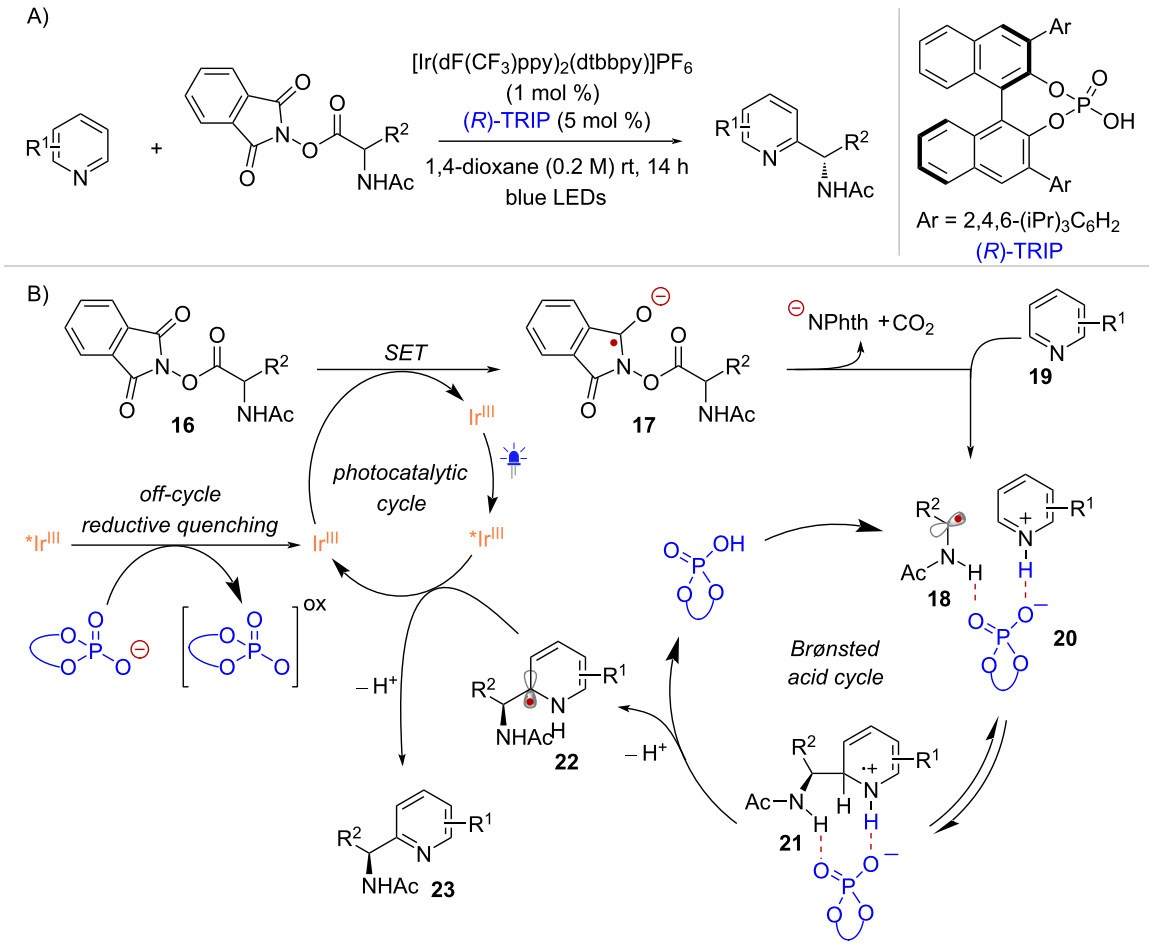

Scheme 5: A) Minisci-type radical addition of NHPI esters. B) Reaction mechanism involving an "off-cycle" reductive quenching.

reduces the activated substrate **29** to form the stabilized radical anion **30**. Fragmentation into radical **9**, followed by radical addition to styrene gives benzyl radical intermediate **26**. Turnover of the catalytic cycle through radical-polar crossover affords cation **27** that delivers functionalized product **31** upon nucleophilic addition.

The Doyle and Knowles groups reported the use of NHPI esters as radical precursors in the context of a radical redox annulation method [48] (Scheme 8A). This transformation occurs through an oxidative quenching photocatalytic cycle employing Ir-based photoreductants and a Brønsted acid additive. While the interaction between the RAE **32** and diphenyl phosphoric acid involves hydrogen bonding, in analogy to the Glorius proposal, it is thought that the substrate activation occurs through proton-coupled electron transfer (PCET), forming neutral radical species **33** and the corresponding phosphate conjugate base (Scheme 8B). The hypothesis is supported by an observed increase in the luminescence quenching of *Ir(p-CF_3-ppy)$_3$ by **32** in the presence of diphenyl phosphoric acid, as quantified by the Stern–Volmer constant (K_{sv} = 1146 M^{-1} with acid vs K_{sv} = 603 M^{-1} without acid). The reaction mechanism continues with the fragmentation of **33** into radical **34**. From radical **34** the annulation reaction initiates via intermolecular radical addition, resulting in the formation of intermediate **35**. After oxidation of **35** to **36**, the photocatalyst is regenerated and product **37** is formed through intramolecular nucleophilic cyclization facilitated by the phosphate base. Importantly, the activation of NHPI esters through PCET may also play a role in transformations mediated by the cyanoarene-based donor–acceptor photocatalyst 4CzIPN, which typically requires the use of strong H^+ donors such as trifluoroacetic acid [49-52]. While many reports, including Okada's original work, have suggested that a proton donor can accelerate the fragmentation rate of RAEs [29,49,53], specific values comparing the fragmentation rate constants or the N–O bond dissociation energies of radical anions and neutral radicals derived from RAEs are not available in the literature.

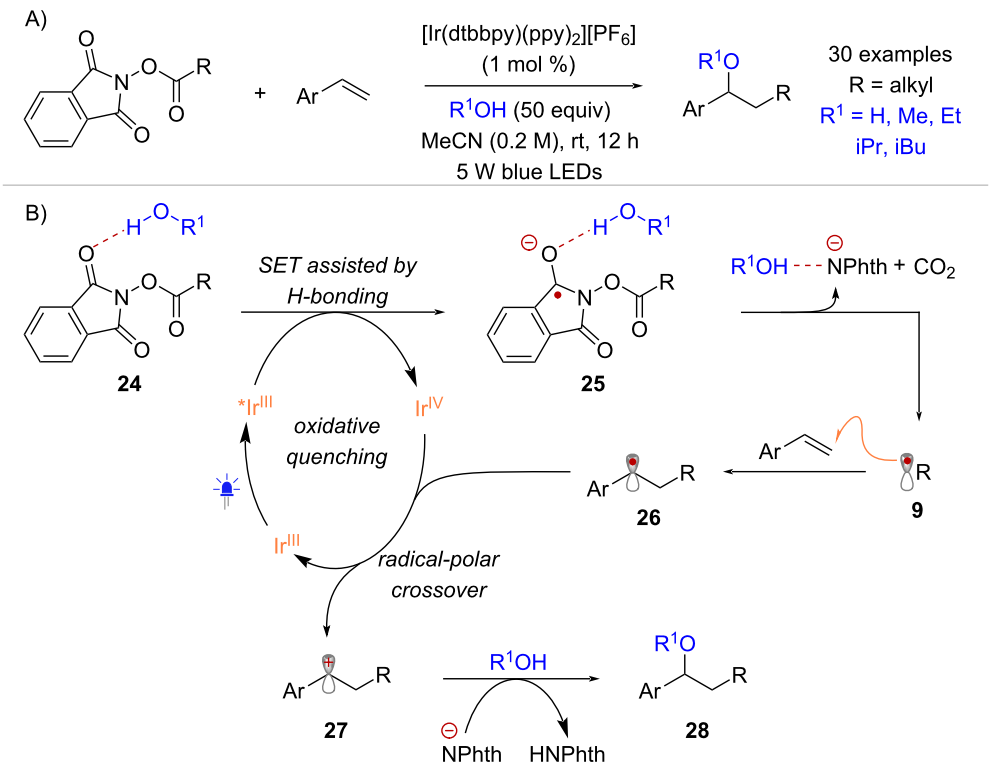

Scheme 6: Activation of NHPI esters through hydrogen-bonding in an oxidative quenching photocatalytic cycle.

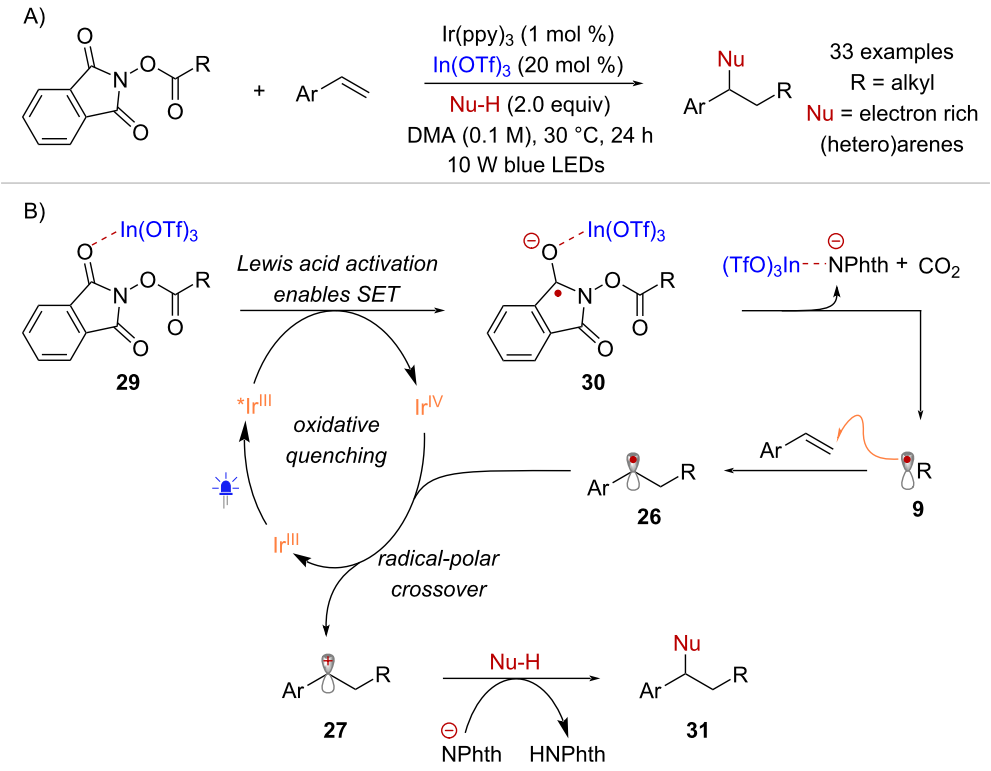

Scheme 7: SET activation of RAE facilitated by a Lewis acid catalyst.

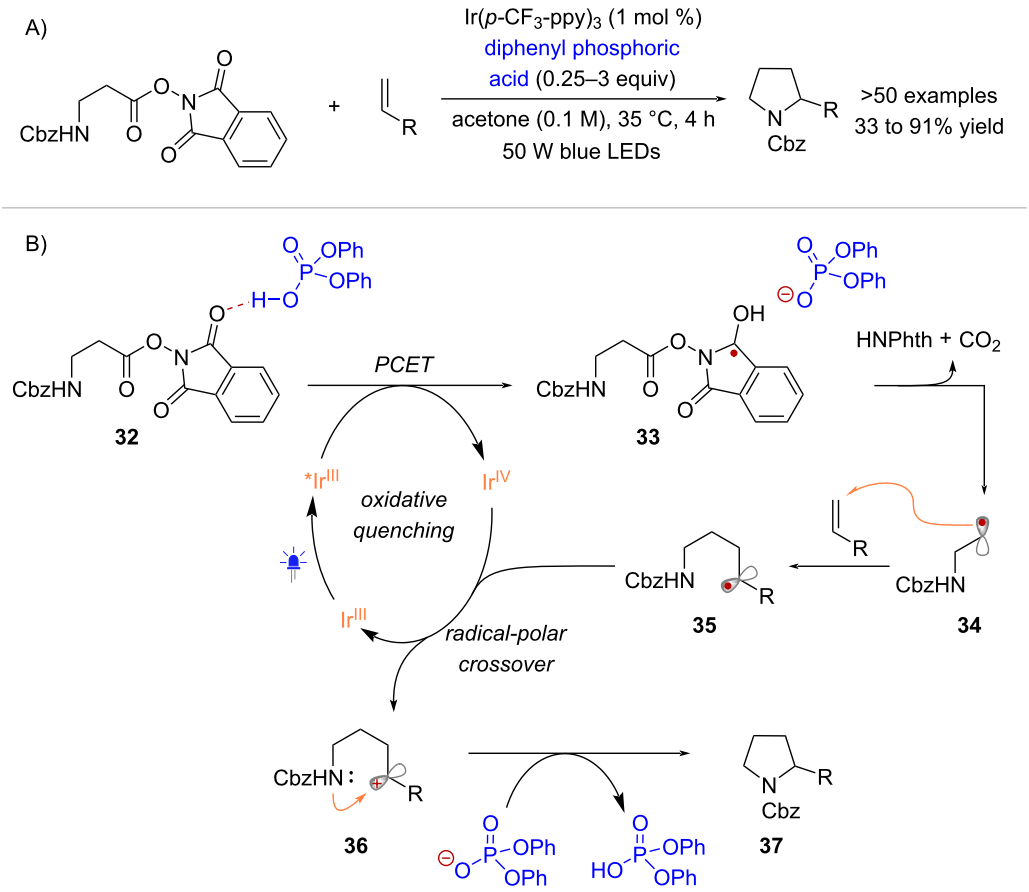

Scheme 8: PCET activation of NHPI esters in the context of a radical-redox annulation.

Lumb and co-workers recently published a study on the conversion of biaryl-derived NHPI esters into spirocyclic cyclohexadienones through a photocatalytic radical-mediated dearomatization, with H_2O serving as the nucleophile [54] (Scheme 9A). Despite the presence of H_2O in the reaction, the reduction of **38** to its corresponding radical anion **39** could occur without the need for hydrogen-bonding (Scheme 9B). Cyclic voltammetry measurements of NHPI ester **38** displayed a reduction half peak potential ($E_{p/2}$) of −1.17 V (vs SCE in MeCN) indicating that the single-electron reduction of **38** by a suitably strong reductant, such as *Ir(ppy)$_3$ ($E_{1/2}^{red}$[IrIV/*IrIII] = −1.73 V vs SCE in MeCN) would be thermodynamically favorable. Indeed, Stern–Volmer photoquenching experiments confirmed that **38** effectively quenched *Ir(ppy)$_3$ under anhydrous conditions. Consequently, the SET reduction of **38**, followed by fragmentation of **39** yielded α-oxy radical intermediate **40**. Subsequently, the spirocyclization of **40** induced the dearomatization of the methoxy-substituted aromatic ring, forming intermediate **41**, which was then oxidized to cation **42**, thereby completing the photocatalytic cycle. The reaction proceeded by regioselective nucleophilic addition of H_2O, accompanied by the loss of MeOH to deliver spirocycle **43**. Notably, the dearomative spirocyclization of biaryl-derived NHPI esters has found application in the total synthesis of natural products, including the plant metabolite denobilone A and the highly oxidized dibenzocyclooctadiene lignans heteroclitin J and kadsulignan E [55].

Activation via charge-transfer complex formation

Under conditions where oxidative quenching is not thermodynamically favorable, the single electron reduction of RAEs can proceed via an alternative mechanism. For example, in the transformation of NHPI ester **44** into spirocycle **45** catalyzed by [Ir(ppy)$_2$(dtbbpy)][PF]$_6$, Reiser and co-workers observed that the excited state of this Ir-catalyst ($E_{1/2}^{red}$[Ir^{IV}/*Ir^{III}] = −0.96 V vs SCE) would not promote the reduction of **44** (−1.25 V vs SCE) [56] (Scheme 10). Interestingly, the role of H-bonding in substrate activation was not considered. To explain the observed transformation, it was suggested that the Ir^{III}-photocatalyst acted as a photosensitizer in an energy-transfer (EnT) mechanism. This proposal was supported by fluorescence quenching measurements, as well as the direct excitation of **44** by UV irradiation, resulting in the formation of **45** in a 45% yield. According to this hypothesis, NHPI ester **44** would adopt

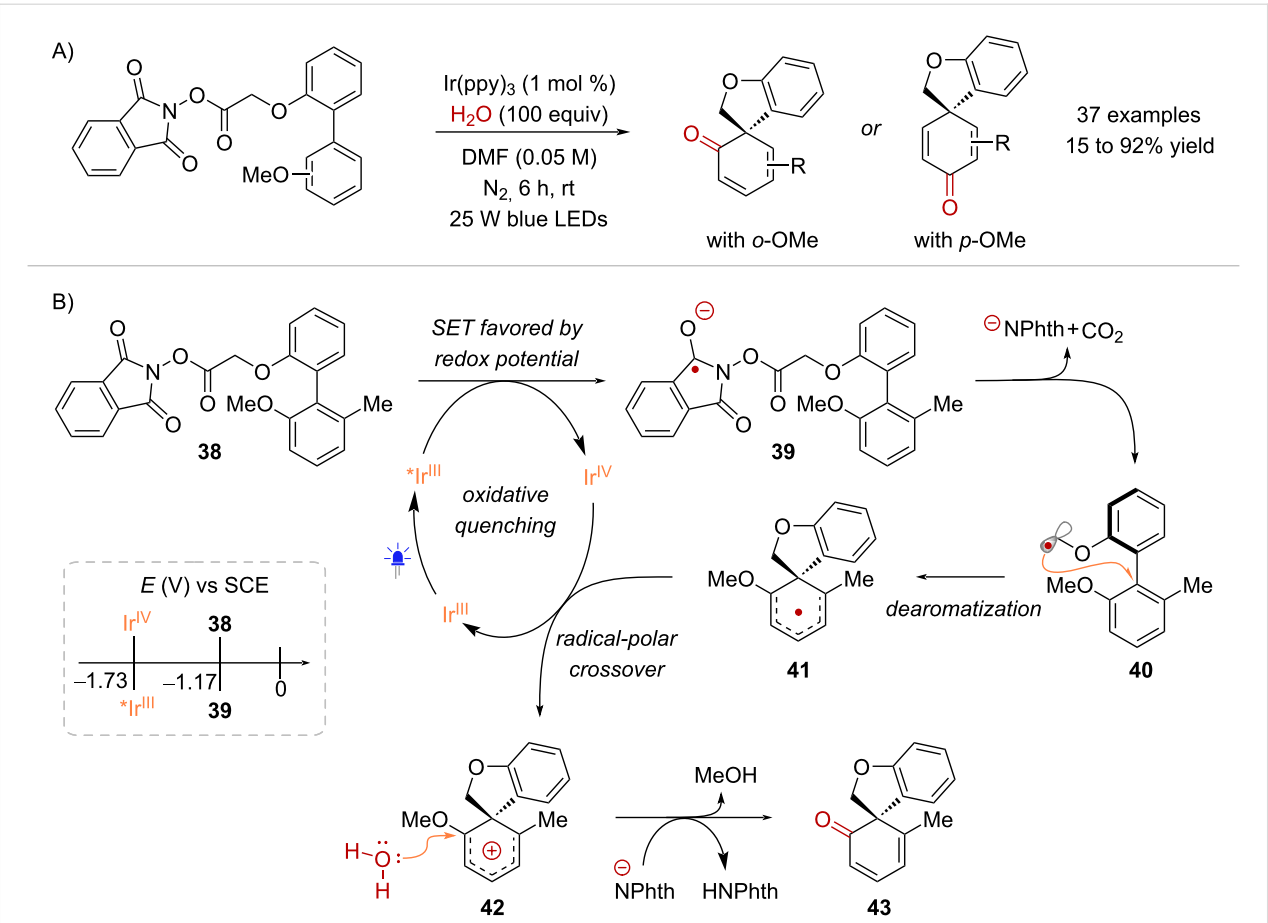

Scheme 9: Activation enabled by a strong excited-state reductant catalyst and its application in the dearomative spirocyclization of biaryls.

a favorable conformation (**46**) for π-stacking between the furan and phthalimide rings, before EnT from $*Ir^{III}$ leads to the formation of an excited charge-transfer complex **47**. This species would undergo intramolecular electron transfer (IET) giving rise to intermediate **48**, which upon fragmentation would form radical **49**. Intramolecular radical addition into the radical cation of the furan ring would then form cation **50** before nucleophilic capture by H_2O leads to product **45**.

In 2020, the Wang group reported the functionalization of enamides employing radicals derived from NHPI esters in combination with indole nucleophiles [57] (Scheme 11A). This transformation occurred under light irradiation either in the presence or absence of a Ru^{II} photoredox catalyst. It was found that the chiral lithium phosphate catalyst (*R*)-TRIP-Li played a crucial role in accelerating the reaction rate. Following an in-depth analysis of the mechanism, the authors proposed that (*R*)-TRIP-Li has the capability to engage enamide **51** through H-bonding and NHPI ester **3** through Li-promoted Lewis acid activation, acting as a pocket that facilitates the formation of charge-transfer complex **52** (Scheme 11B). This complex can be excited either by direct irradiation at 390 nm or through Ru^{II}-mediated EnT under blue light irradiation (456 nm). Following excitation, SET from the enamide to the active ester forms intermediate **53**, which undergoes fragmentation and radical recombination to afford intermediate **54**. At this stage, the indole nucleophile substitutes the phthalimidyl anion within the chiral pocket of the phosphate catalyst to form complex **55**, before enantioselective addition to the iminium ion affords product **56**.

NHPI esters can also engage in π–π interactions with electron-rich species to generate charge-transfer complexes that can absorb light in the visible region. These species are referred to in the literature as electron donor–acceptor (EDA) complexes [58,59] and undergo photoexcitation in the absence of an exogenous photoredox catalyst. When excited by visible light, an intra-complex SET from the donor substrate **D** to the NHPI ester acceptor takes place, generating radical ion pair **57**. Subsequently, this ion pair undergoes fragmentation, forming the corresponding substrate radical **9**, which can participate in diverse chemical transformations (Scheme 12).

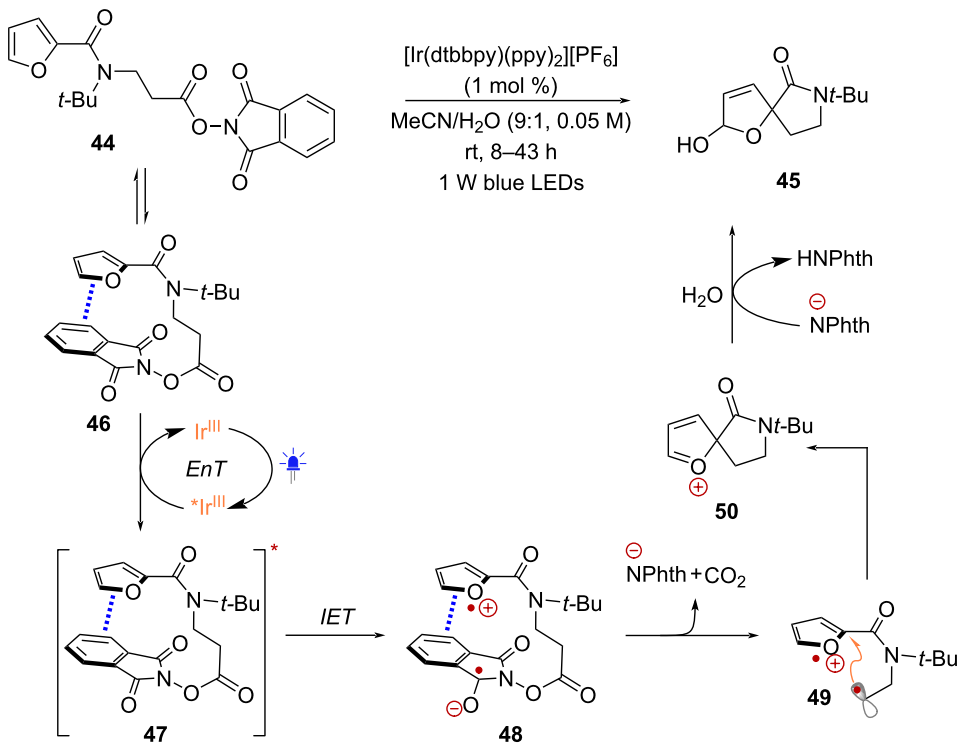

Scheme 10: Proposed formation of an intramolecular charge-transfer complex in the synthesis of (spiro)anellated furans.

Different donor molecules are known to form EDA complexes with NHPI esters. For example, the NHPI ester derived from pivalic acid **58** and Hantzsch ester **HE** form EDA complex **59** which participates in radical mediated hydroalkylation reactions [60,61] (Scheme 13A). In the presence of electron deficient olefin **60**, classic Giese-type addition takes place under photocatalyst-free conditions, affording product **61** [60]. On the other hand, reaction with 1,7-enyne **62** affords dihydroquinolinone product **63** via a cascade radical addition/cyclization process [61]. In both transformations, **HE** serves a dual role by activating the NHPI ester through EDA complex formation and providing a hydrogen atom to terminate the radical reaction. The proposed mechanism of the hydroalkylation cascade is depicted in Scheme 13B. Upon excitation of complex **59** with blue light, intra-complex SET takes place from the **HE** to the NHPI ester, leading to the formation of *tert*-butyl radical **64** and radical cation **65**. Addition of radical **64** to enyne **62** followed by *6-exo-dig* cyclization yields radical intermediate **66**. Finally, species **65** acts as a hydrogen atom donor, delivering product **63** while forming pyridine **67** as a byproduct.

A similar mechanism would in principle account for EDA-complex-mediated Giese-type additions. However, an alternative radical chain mechanism has been discussed in the literature [62] (Scheme 14). In this instance, chain initiation takes place through photoinduced SET, enabled by EDA complex formation between the reductant *N*-(*n*-butyl)-1,4-dihydronicotinamide (**BuNAH**) and an NHPI ester (complex **68**). This process delivers substrate radical **9** and nicotinyl radical **69** following proton transfer to the phthalimidyl anion. Then, addition of **9** to α,β-unsaturated ester **70** yields radical intermediate **71**. At this stage, HAT mediated by another equivalent of **BuNAH** delivers product **72**, with concomitant formation of radical **69**. Finally, aromatization of **69** via SET to NHPI ester **3**, generates pyridinium **73** as a byproduct, while propagating the radical chain reaction.

Aggarwal and co-workers discovered the photoinduced decarboxylative borylation of NHPI esters mediated by bis(catecholato)diboron (B_2cat_2) [63] (Scheme 15A). UV–vis absorption measurements showed that a mixture of a model NHPI ester with B_2cat_2 in dimethylacetamide (DMA) formed a new charge-transfer band in the visible region (>390 nm), which was attributed to the formation of EDA complex **74** (Scheme 15B). Under blue light irradiation, EDA complex **74** triggered a radical chain process initiated by B–B bond cleavage, forming boryl-NHPI ester radical **75** and boryl radical **76**. Subsequent decarboxylation of **75** yields carbon-centered radical **9** and boryl-phthalimide byproduct **77**. Meanwhile DMA-ligated B_2cat_2 **78** is formed upon dimerization of radical **76**. Reaction between radical **9** and species **78** affords boronic ester **79** while returning boryl radical **76**. Finally, chain propa-

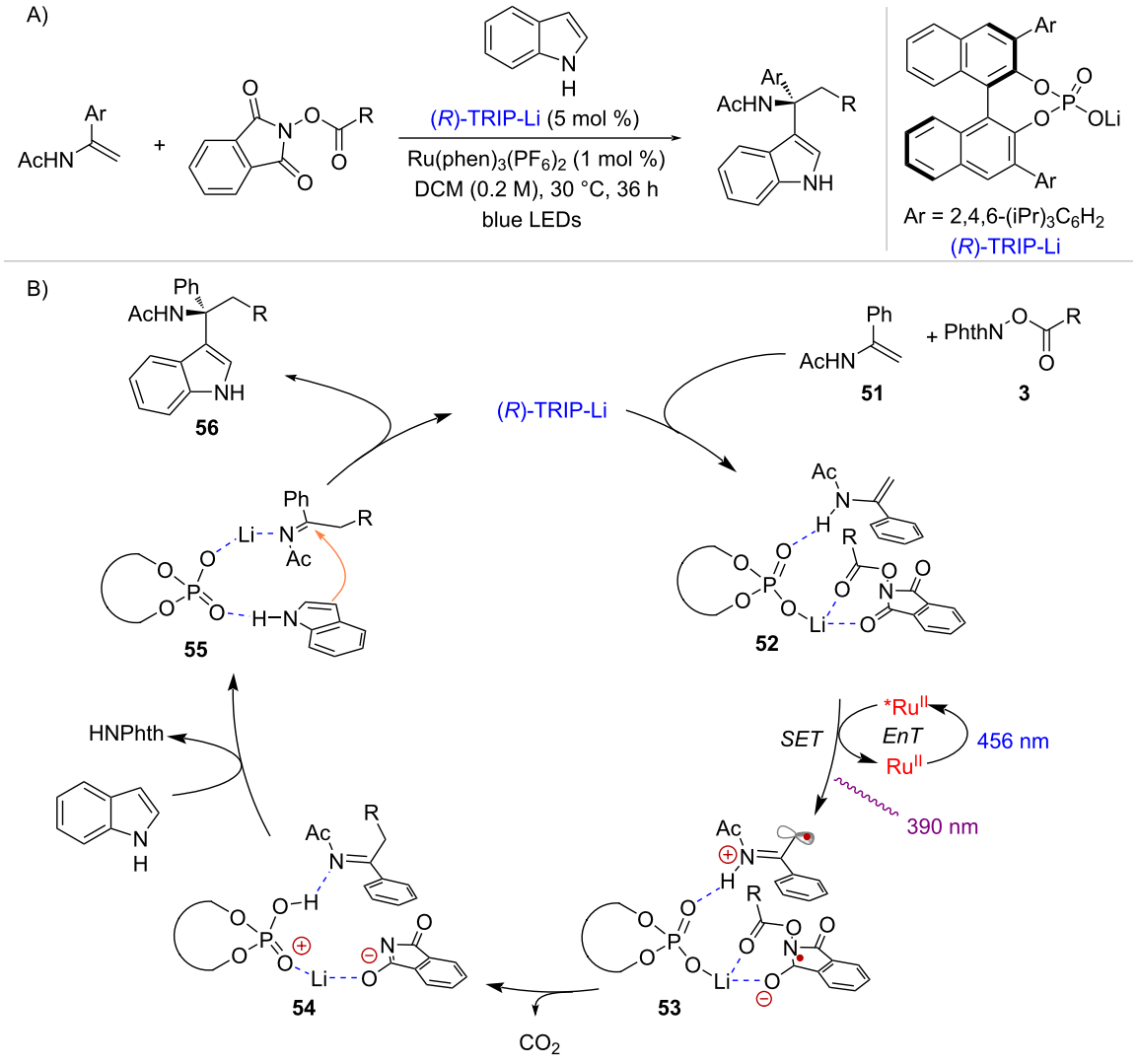

Scheme 11: Formation of a charge-transfer complex between enamides and NHPI esters enabled by a chiral phosphate catalyst.

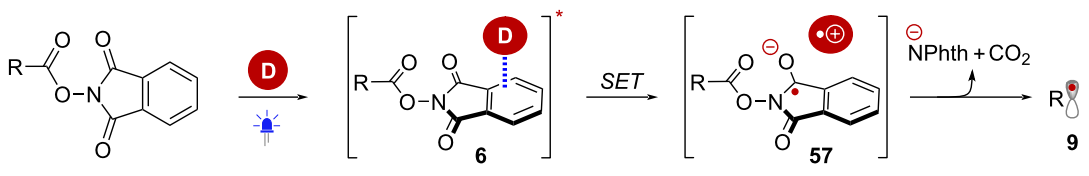

Scheme 12: Activation of NHPI ester through the formation of photoactive EDA-complexes.

gation takes place via reaction of **76** with another equivalent of the NHPI ester **3**.

The Baran lab has recently published a complementary electrochemical method, wherein the activation of complex **74** takes place through SET under constant current electrolysis [64]. The Glorius and Y. Fu groups have independently proposed the formation of analogous charge-transfer complexes involving NHPI esters, bis(pinacolato)diboron (B_2pin_2), and Lewis bases (pyridine or isonicotinate *tert*-butyl ester) in C(sp^2)-borylation methods under photochemical and thermal conditions, respectively [65,66].

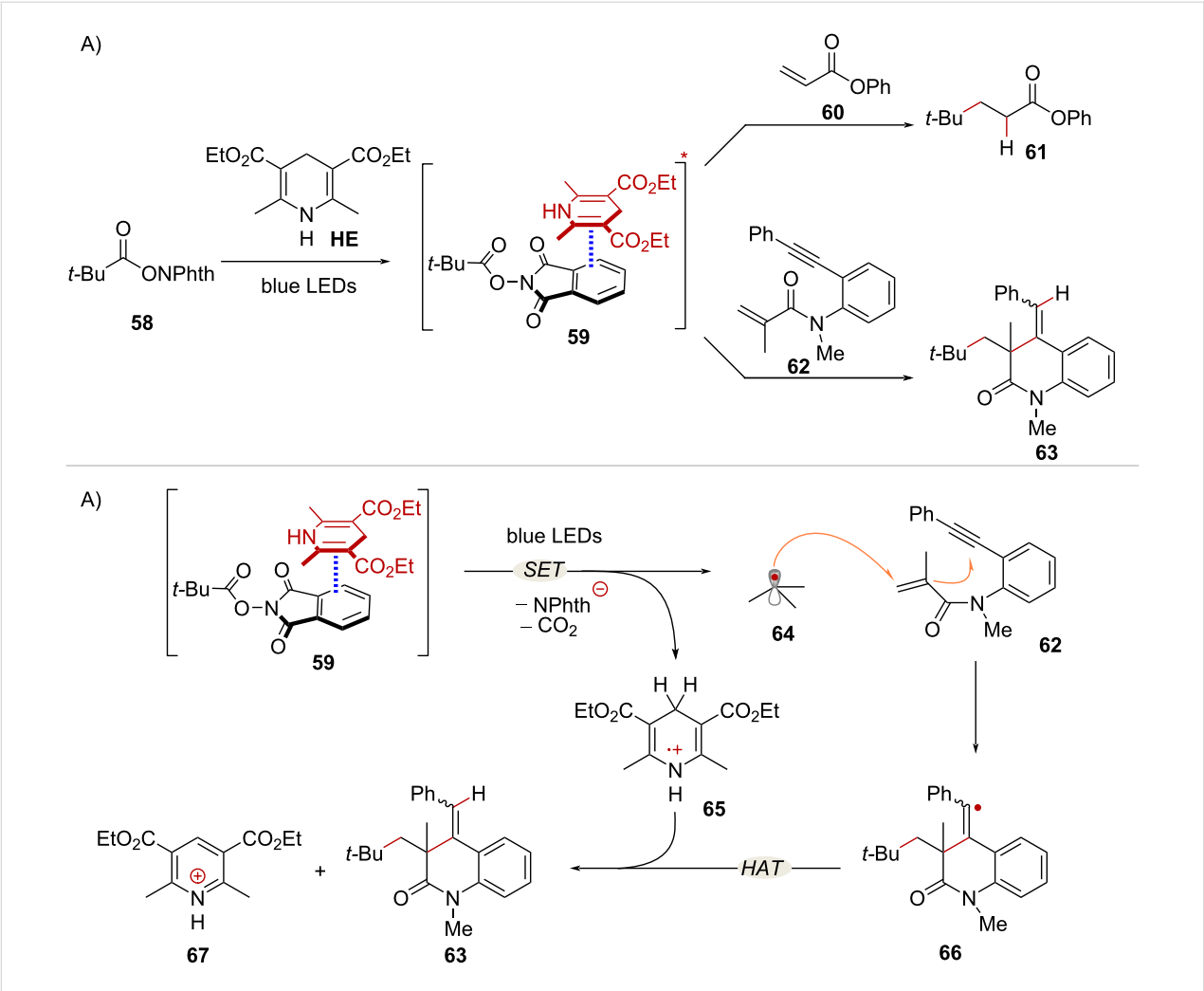

Scheme 13: A) EDA complex-mediated radical hydroalkylation reactions of NHPI esters. B) Proposed mechanism for the hydroalkylation cascade.

The activation of NHPI esters through EDA complex formation is also possible by employing a catalytic donor species, which enables a range of redox neutral transformations. In 2019, Shang and Fu initially demonstrated this approach by utilizing catalytic amounts of triphenylphosphine (PPh_3) and sodium iodide (NaI) [67]. Upon formation of EDA complex **80**, radical addition to silyl enol ether **81** was promoted under blue light irradiation, affording acetophenone product **82** (Scheme 16A). Additionally, Minisci-type additions were carried out in the presence of protonated quinoline radical acceptor **83**, affording product **84** (Scheme 16A). Mechanistically, this activation mode involves an intra-complex SET that forms the Ph_3P–NaI radical cation species **85** and the corresponding radical anion **86**. Decarboxylative fragmentation of **86** forms radical **9**, which upon radical addition to **84** and deprotonation yields radical **87**. Finally, oxidation of **87** mediated by **85** delivers the Minisci addition product **84** while regenerating PPh_3 and NaI (Scheme 16B).

The Ohmiya group has developed a series of light-mediated decarboxylative transformations of NHPI esters using a phenothiazine-based organophotoredox catalyst **PTH1**. This type of catalyst is believed to facilitate SET to NHPI esters through the formation of EDA complexes. Interestingly, upon addition of RAE **58** to a solution of **PTH1**, a noticeable red shift in the UV–vis absorption spectra of **PTH1** was observed, suggesting the formation of a charge transfer complex of the type **88** [68] (Scheme 17A). *tert*-Butyl radical (**64**), along with additional 2° and 3° alkyl radicals, resulting from these EDA complexes were harnessed in C(sp^3)-heteroatom bond forming reactions [69], and in the difunctionalization of styrenes [68] (Scheme 17B).

The catalytic cycle for the styrene difunctionalization reaction is depicted in Scheme 18. First, EDA complex **88** consisting of RAE **58** and the **PTH1** catalyst is formed. Under blue light irradiation, intra-complex SET leads to the formation of PTH

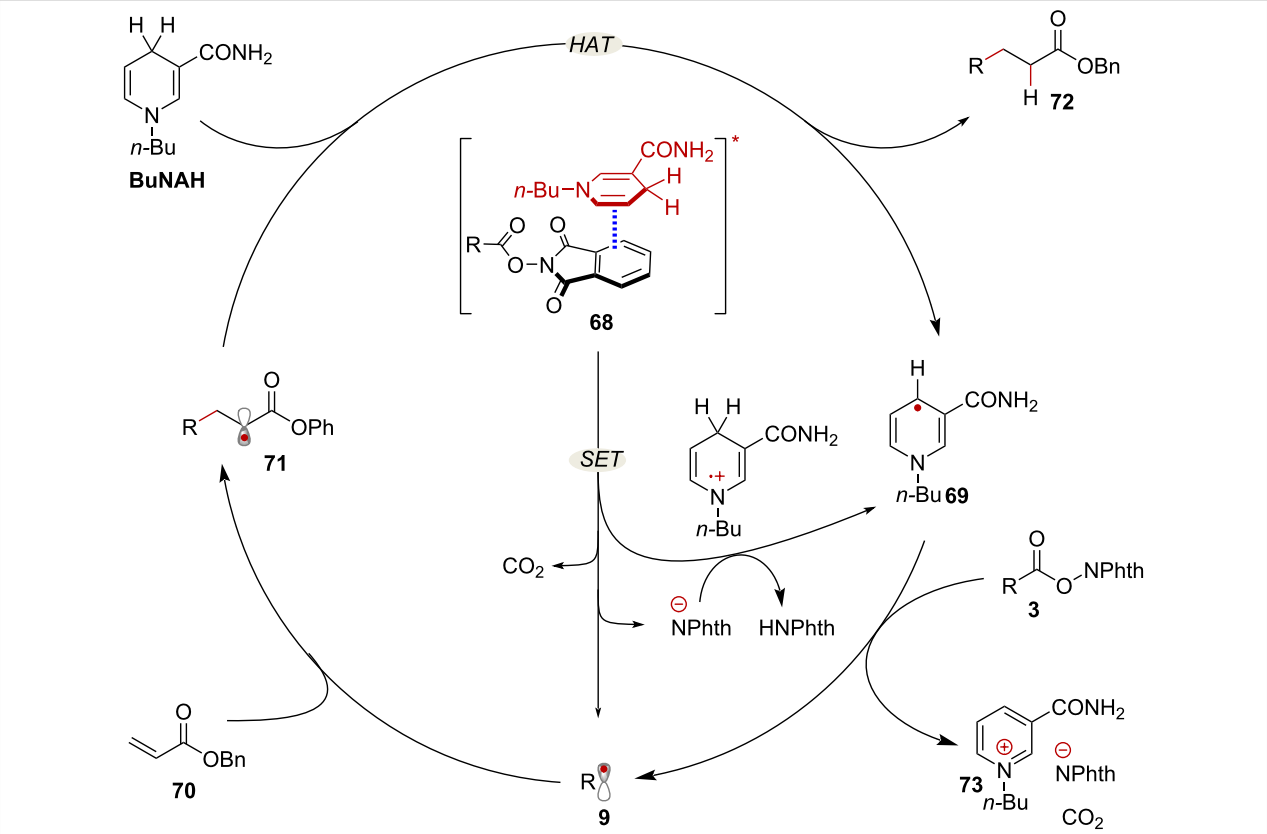

Scheme 14: Proposed radical chain mechanism initiated by EDA-complex formation.

radical cation species **89** and the radical anion **90** with the corresponding charges balanced by the $LiBF_4$ additive. Notably, it was suggested that $LiBF_4$ could also facilitate the reduction of the NHPI ester substrate, potentially by the coordination of Li cation to the phthalimide moiety. Next, fragmentation of **90** yields *tert*-butyl radical **64**, which then adds to styrene **91** affording radical intermediate **92**. At this stage, recombination of intermediates **89** and **92** may occur via SET followed by addition or through radical–radical coupling, affording benzylsulfonium intermediate **93**. Finally, nucleophilic substitution with alcohol **94** in the presence of lithium phthalimide **95** leads to product **96** and turns over the catalytic cycle. Importantly, species **93** can be detected by high resolution mass spectrometry, when the reaction is carried out without nucleophile and using stoichiometric amounts of **PTH1**.

H. Fu and co-workers reported that the combination of NHPI esters and cesium carbonate (Cs_2CO_3) gave rise to a new absorption band in the visible region, suggesting the formation of a photoactive charge-transfer complex [70]. This activation mode was initially employed in a decarboxylative coupling reaction with aryl thiols [70]. Further studies showed that 4-(trifluoromethyl)thiophenol (**97**) could act as a catalytic reductant in the aminodecarboxylation reaction of NHPI esters derived from α-amino acids [71] (Scheme 19). Accordingly, visible light irradiation of a mixture consisting of *N*-Boc-alanine NHPI ester **98** and Cs_2CO_3 in DMF resulted in the generation of the excited charge transfer complex **99**. Subsequent SET mediated by the thiol catalyst followed by fragmentation afforded α-amino radical **100**, which was then oxidized by the resulting thiol-radical species, regenerating the thiol catalyst while forming an iminium intermediate **101**. Finally, nucleophilic addition of phthalimide anion **102** afforded the amination product **103**.

Bosque and Bach reported the use of 3-acetoxyquinuclidine (**q-Ac**) as a catalytic donor for the activation of TCNHPI esters derived from α-amino acids [72] (Scheme 20). Treatment of *N*-Boc-proline-derived TCNHPI ester **104** with **q-OAc** in MeCN resulted in the formation of a yellow solution, which upon blue light irradiation provided the aminodecarboxylation product **105** in 69% yield. It was hypothesized that the reaction involved the formation of EDA complex **106** that led to the formation of α-amino radical **107** through photoinduced SET followed by fragmentation. Subsequent oxidation of **107** by radical cation **q-Ac**$^{\bullet+}$ afforded iminium ion **108** before nucleophilic addition of the in situ-generated tetrachlorophthalimyl anion ($^{-}$TCPhth) led to the formation of aminal product **105**. Of note,

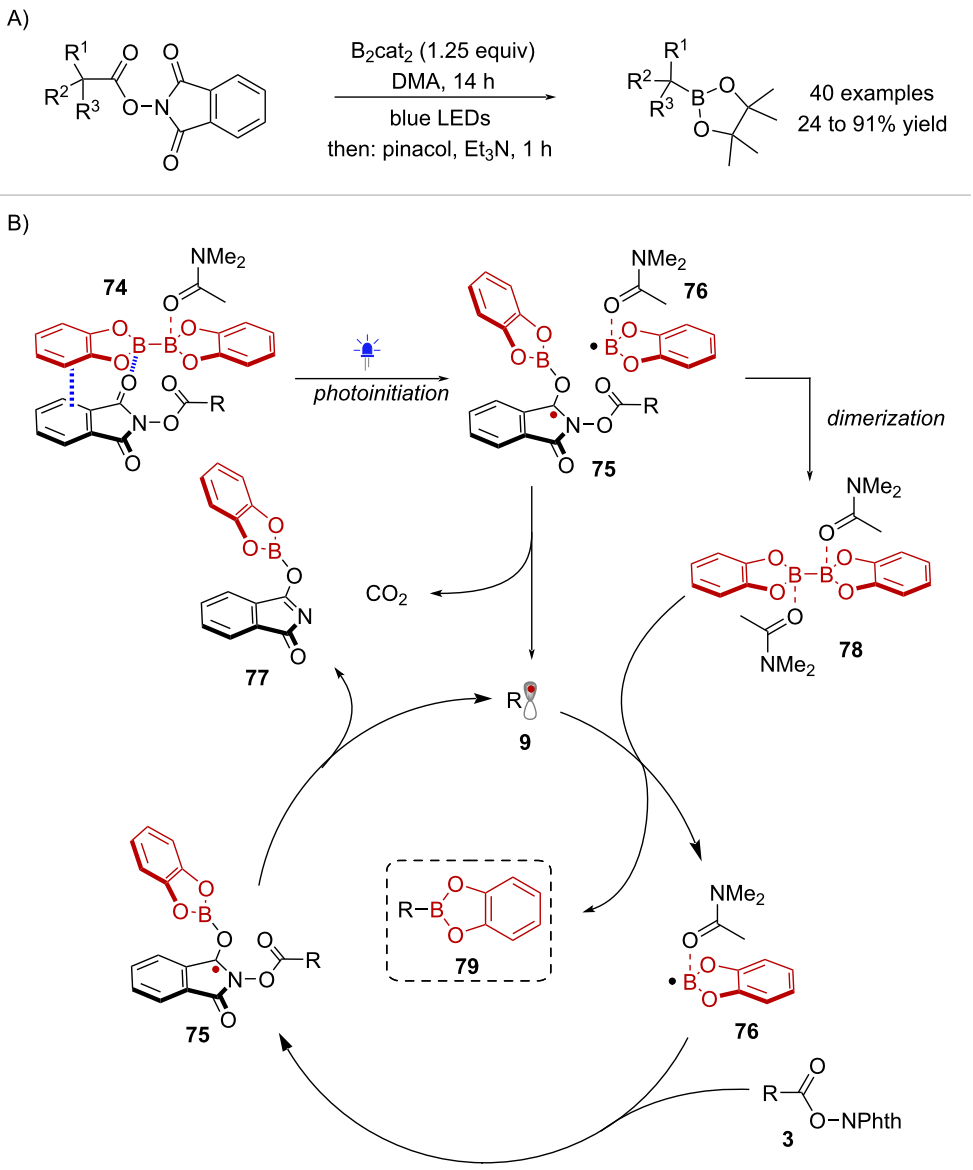

Scheme 15: A) Photoinduced decarboxylative borylation. B) Proposed radical chain mechanism.

the amino-decarboxylation reaction proved unsuccessful when employing alternative photocatalysts such as $Ru(bpy)_3Cl_2$ or eosin Y, underscoring the distinctive ability of **q-OAc** to activate TCNHPI esters via EDA complex formation.

Photoinduced transition metal-catalyzed mechanisms

The in situ formation of photoactive catalysts can be achieved by combining simple transition metal (TM) salts with suitable ligands. These TM catalysts are fundamentally distinct from traditional Ru- and Ir-based photoredox catalysts, as they play a dual role, by engaging in photoinduced electron transfer processes with the substrate and participating in the key bond-forming/breaking steps via substrate–TM interactions [73,74]. This paradigm has been employed in the activation of NHPI esters under photoinduced copper (Cu) and palladium (Pd) catalysis.

In 2017, Peters and Fu reported a Cu-catalyzed decarboxylative $C(sp^3)$–N coupling employing NHPI esters as dual reagents [75] (Scheme 21A). The combination of CuCN and the ligands xantphos and neocuproine in a 2:3:1 ratio resulted in the formation of a light absorbing species with an absorption band in the 380–460 nm range. Thus, it was hypothesized that Cu^I catalytic species **109** would give rise to photoexcited complex **110** under blue light irradiation (Scheme 21B). Complex **110** and NHPI

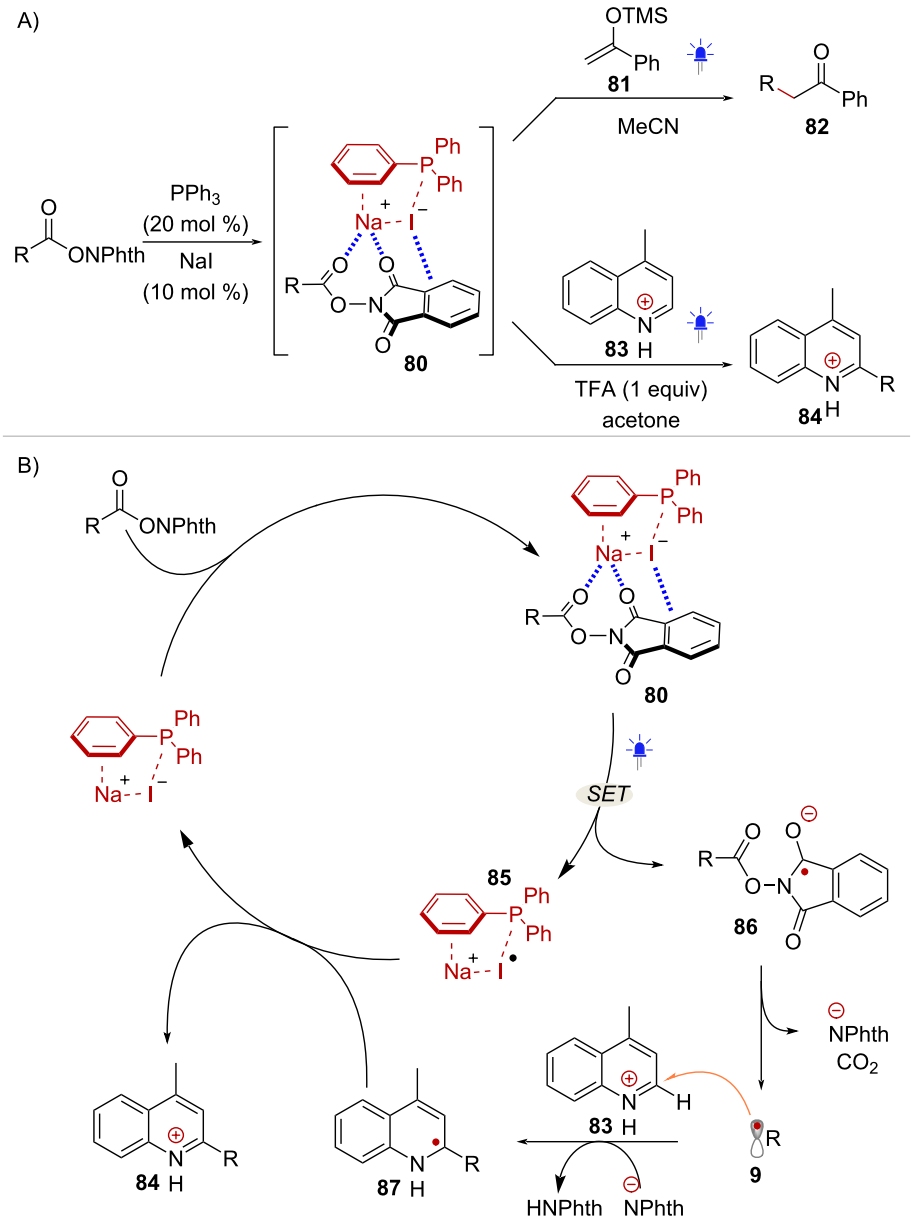

Scheme 16: A) Activation of NHPI esters mediated by PPh_3/NaI. B) Proposed catalytic cycle involving EDA-complex formation.

ester **3** would then engage in SET likely through an inner sphere mechanism, providing phthalimide ligated Cu^{II} intermediate **111** and carboxyl radical **112**. At this stage, the resulting radical species **9** would recombine with **111** to form Cu^{III} complex **113**. Alternatively, reaction of **3** with the photoexcited Cu^{I} complex through oxidative addition (OA) followed by decarboxylation could directly lead to intermediate **113** (Scheme 21B, blue arrow). However, radical clock experiments support the intermediacy of free radicals, indicating the involvement of the SET pathway (Scheme 21C). Eventually, reductive elimination of **113** afforded product **114** while regenerating the catalytic species **109**. It is worth nothing that further transformations of NHPI esters under photoinduced Cu catalysis have been reported in recent years, including decarboxylative alkynylations [76-78] and the C(sp^3)–H alkylation of α-amino acids [79].

The ability of NHPI esters to act as dual reagents was also investigated by Glorius and co-workers in the context of a photoinduced Pd-catalyzed aminoalkylation of 1,4-dienes [80] (Scheme 22A). The study showed that a photoexcited Pd^0 species formed upon blue-light irradiation of $Pd(Ph_3)_4$, was able to promote the activation of NHPI esters via SET (Scheme 22B). The photoinduced electron transfer process between the Pd-photocatalyst and RAE **58** was proposed to form a

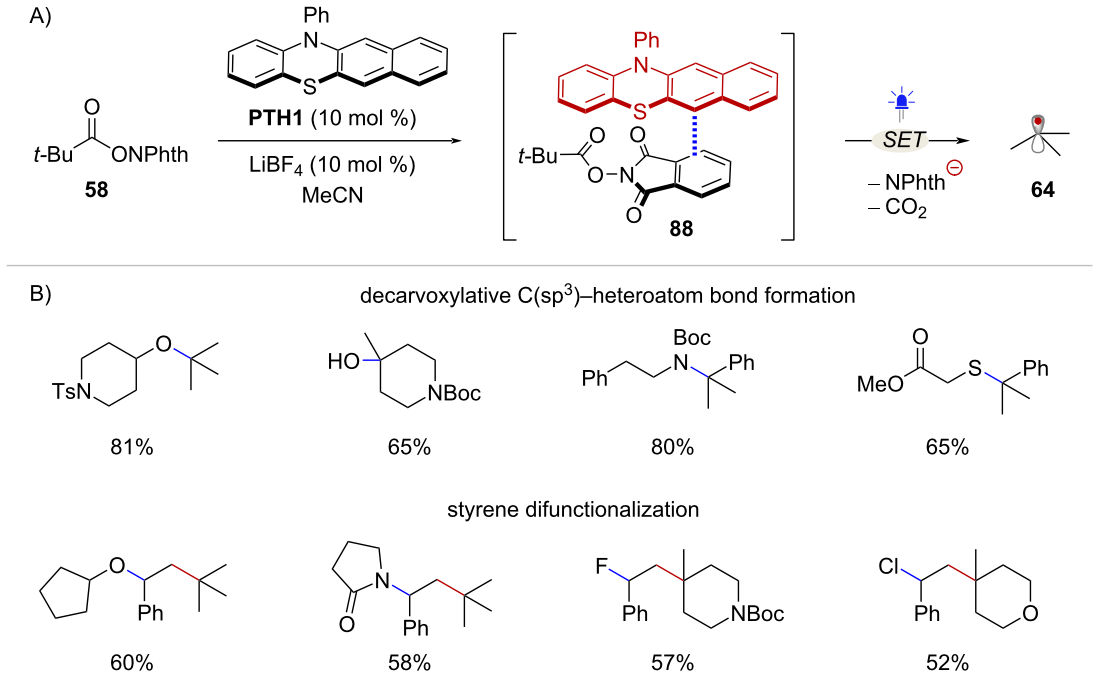

Scheme 17: A) Radical generation facilitated by EDA complex formation between **PTH1** catalyst and NHPI esters. B) Selected scope of **PTH1**-catalyzed decarboxylative transformations.

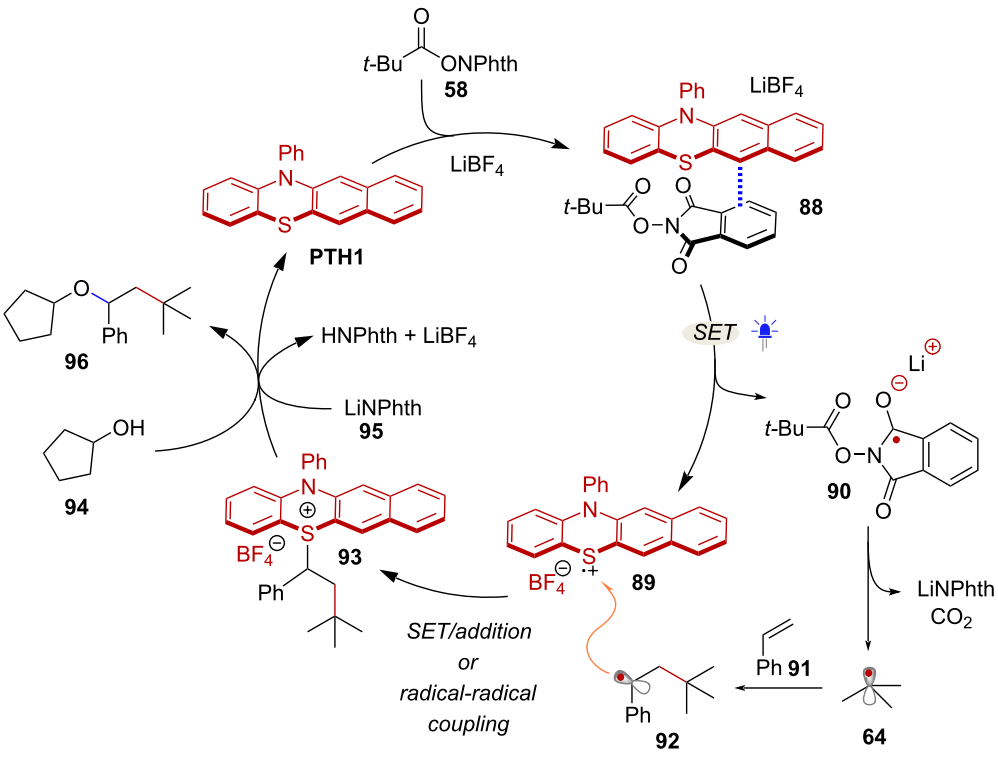

Scheme 18: Proposed catalytic cycle for the difunctionalization of styrenes.

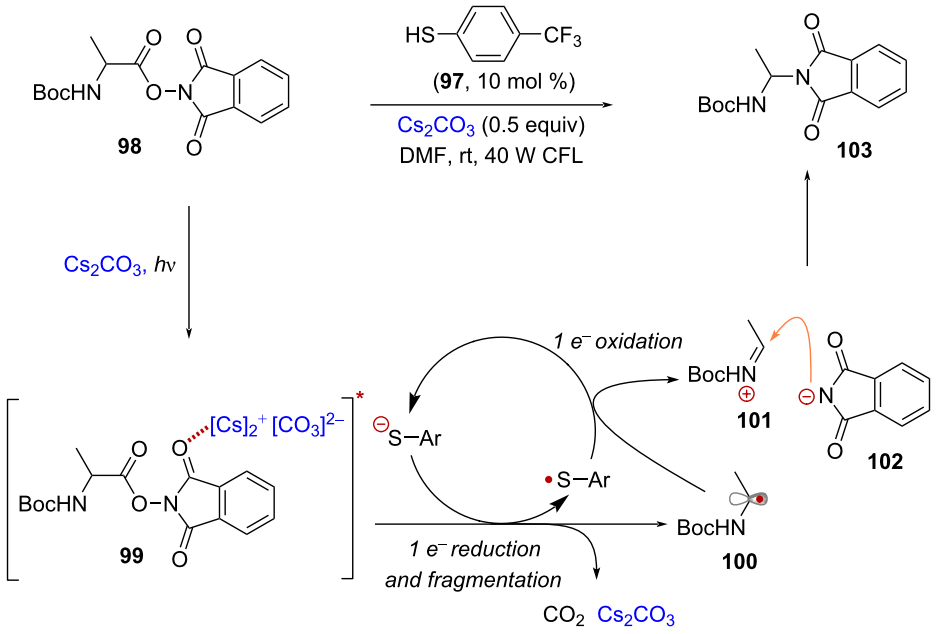

Scheme 19: Formation of a charge-transfer complex between NHPI esters and Cs_2CO_3 enables decarboxylative amination.

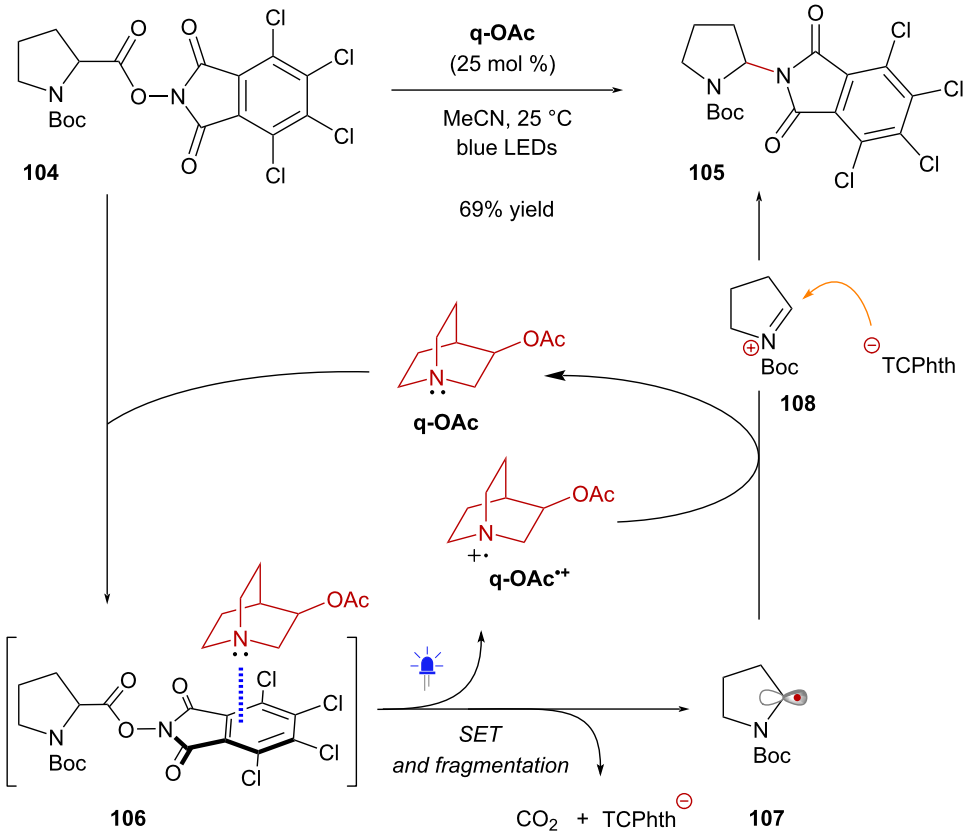

Scheme 20: 3-Acetoxyquinuclidine as catalytic donor in the activation of TCNHPI esters.

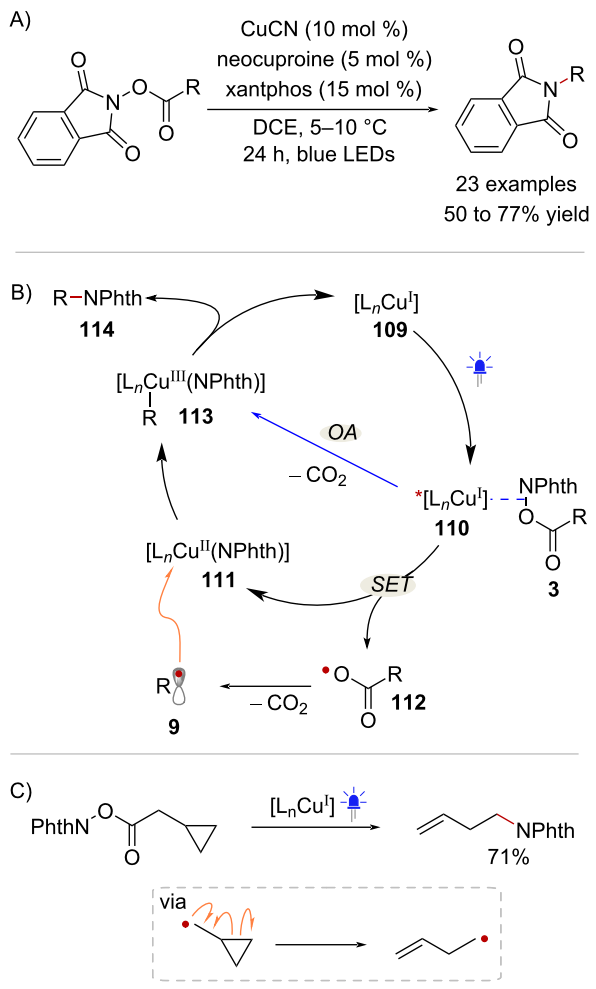

Scheme 21: A) Photoinduced Cu-catalyzed decarboxylative amination. B) Proposed catalytic cycle. C) Radical clock experiment supporting the intermediacy of radicals.

hybrid alkyl Pd^{I}-radical species **115** which could then react with 1,4-butadiene (**116**) to form hybrid allyl Pd^{I} complex **117**. Subsequently, it was suggested that the species **117** would lead to the formation of a π-allylpalladium intermediate **118** through radical recombination. Ultimately, nucleophilic attack by the phthalimidyl anion would generate the aminoalkylation product **119**, completing the catalytic cycle. In addition to this aminoalkylation method, the synthetic utility of radical intermediates derived from NHPI esters under photoinduced Pd-catalysis has been demonstrated in Heck-type couplings [81,82] and in the desaturation of aliphatic carboxylic acids [83].

Initiation by metal catalysts and stoichiometric reductants

The activation of NHPI esters under transition metal catalysis without the need of light is also feasible, and generally, two types of coupling reactions can be envisioned. On one hand, the decarboxylative cross-coupling (DCC) of NHPI esters with organometallic reagents, resembling classic Kumada, Negishi, and Suzuki couplings, has been enabled by nickel (Ni), cobalt (Co), iron (Fe), and copper (Cu) catalysts [84-91] (Scheme 23A). The typical mechanism begins by transmetallation of the organometallic coupling partner **120** to the TM catalyst (Scheme 23B). The resulting organometallic intermediate **121** can act as a reducing agent, transferring an electron to RAE **10** to form radical anion **11** and the corresponding oxidized metal complex **122**. Following fragmentation, the ensuing alkyl radical **12** is captured by intermediate **122**, resulting in the formation of complex **123**. At this point, the metal center has undergone a two-electron oxidation, making it well-suited for reductive elimination yielding the cross-coupling product **124**.

Under these catalytic conditions, various TM-catalyzed decarboxylative functionalizations employing RAEs have been established (Scheme 24). Baran and co-workers have reported arylation protocols (Scheme 24A) using arylzinc reagents [84,85], Grignard reagents [85] and arylboronic acids [86], as well as decarboxylative alkenylation [87] (Scheme 24B), alkynylation [88] (Scheme 24C) and $C(sp^3)$–$C(sp^3)$ cross-coupling [89] (Scheme 24D). Finally, similar chemistry has been extended to the decarboxylative borylation of RAEs under Ni [90] and Cu [91] catalysis (Scheme 24E). Importantly, the Wang group has independently studied the decarboxylative Negishi coupling of RAEs with organozinc reagents under Co-catalysis, effecting diverse arylation, alkenylation, and alkynylation reactions [92].

The second type of reaction is referred to as cross-electrophile coupling and involves the Ni-catalyzed reaction of NHPI esters with aryl- and vinyl halides under reducing conditions (Scheme 25A). The general catalytic cycle begins with oxidative addition of an organohalide into a Ni^0 catalyst yielding Ni^{II} complex **125** (Scheme 25B). In parallel, the initial SET activation of RAE **10**, leading to the formation of radical anion **11**, takes place in the presence of a stoichiometric reductant, which can be an organic reductant, such as tetrakis(*N*,*N*-dimethylamino)ethylene (TDAE) or Hantzsch ester (HE), or a metal such as zinc (Zn^0) or manganese (Mn^0). Upon fragmentation, radical species **12** is captured by the oxidative addition complex **125**, giving rise to Ni^{III} complex **126**. The cross-coupling product **127** is then formed via reductive elimination of **126** which gives Ni^{I} intermediate **128**. At this stage, it is proposed that the Ni^{I} complex **128** can participate in a SET event with another equivalent of substrate **10**, generating another equivalent of radical **12**, that propagates into the next catalytic cycle. Finally, the corresponding Ni^{II} complex **129** is reduced back to

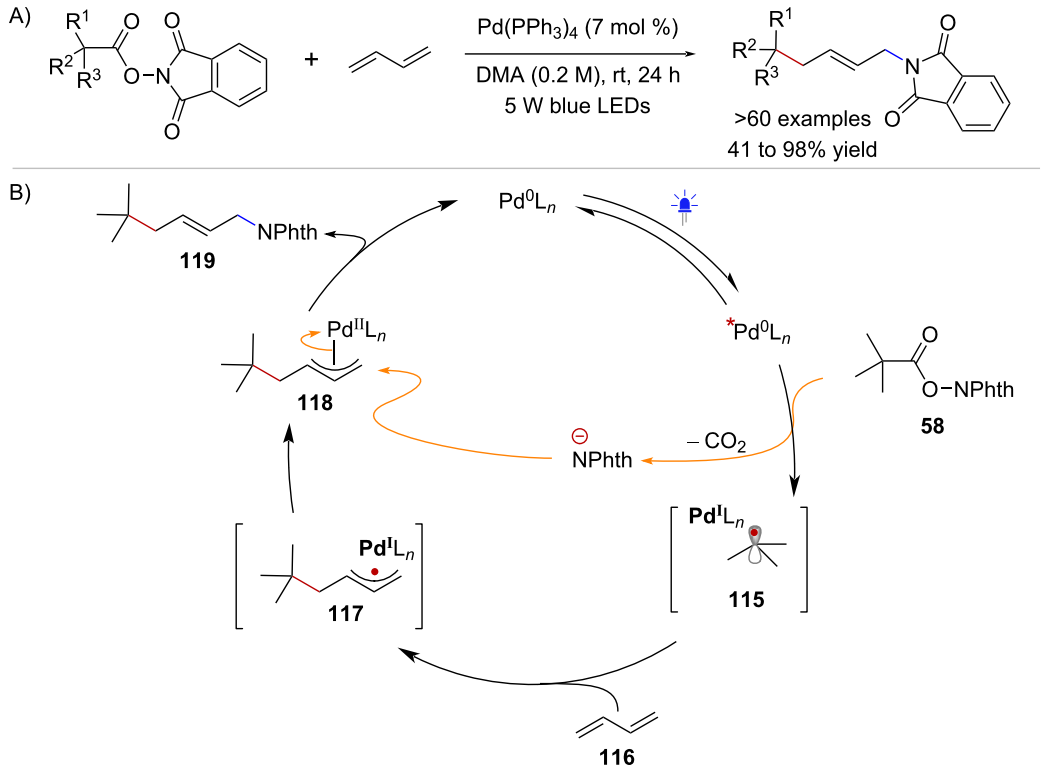

Scheme 22: A) Photoinduced Pd-catalyzed aminoalkylation of 1,4-dienes. B) Proposed catalytic cycle.

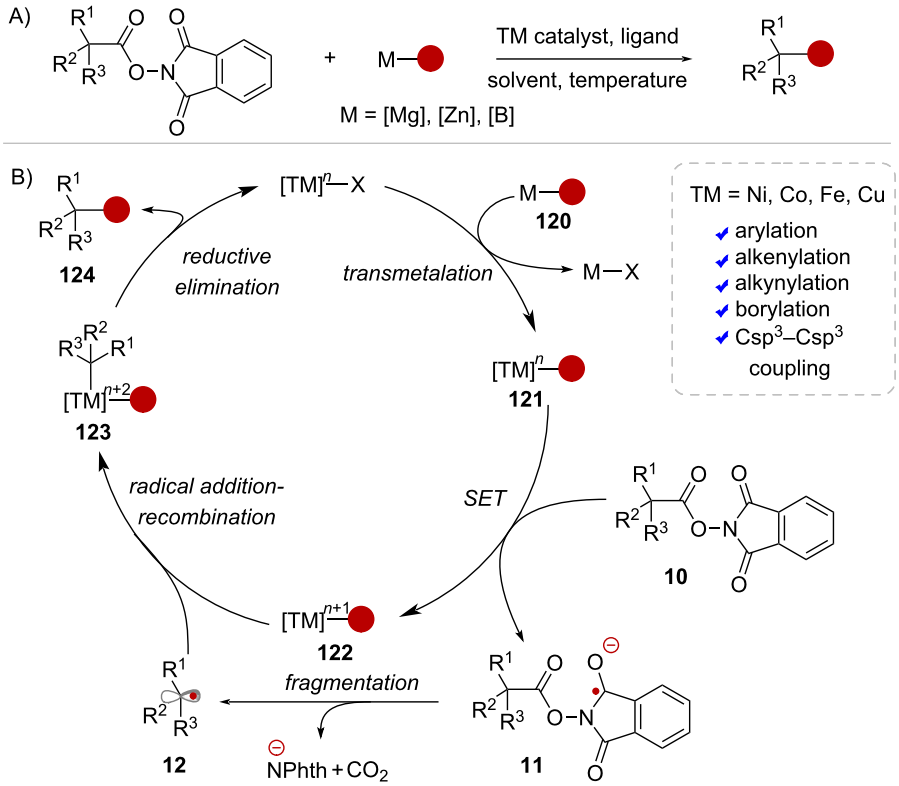

Scheme 23: A) TM-catalyzed decarboxylative coupling of NHPI esters and organometallic reagents. B) Representative catalytic cycle.

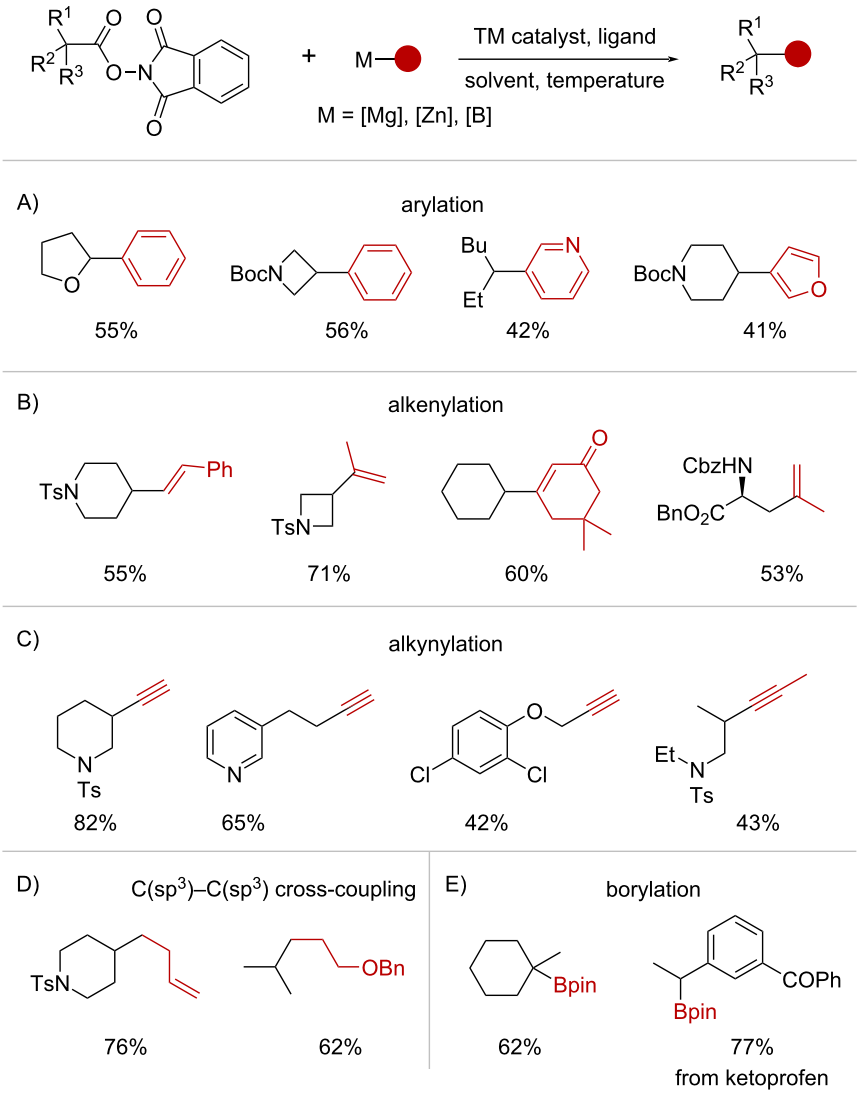

Scheme 24: Synthetic applications of the TM-catalyzed decarboxylative coupling of NHPI esters and organometallic reagents.

the corresponding Ni^0 species by the stoichiometric reductant, initiating a new catalytic cycle.

Weix and co-workers have developed a series of Ni-catalyzed couplings of NHPI esters with different electrophiles, including aryl halides [93,94], bromoalkynes [95], bromoalkanes [96], and pyridyl thioesters [97] (Scheme 26A). Likewise, the Rousseaux group has recently documented the arylation of NHPI esters obtained from cyclopropanecarboxylic acids [98] and malonic acid half amides [99], while the Reisman lab has pioneered an enantioselective cross-electrophile coupling between NHPI esters and alkenyl bromides [100] (Scheme 26A). In addition, Jolit and Molander disclosed the decarboxylative arylation of NHPI esters derived from bicyclo[1.1.1]pentanes (BCPs) by combining Ni-catalysis and photoinduced EDA complex activation [101] (Scheme 26B).

A novel approach for the activation of redox-active esters was recently reported by Cornella and co-workers [32]. In this study, low valent bismuth (Bi) complex **Bi-1** was found to exhibit redox properties similar to those of first row-transition metal catalysts, enabling the activation of tetrachlorophthalimide (TCPhth) active esters towards $C(sp^3)$–N cross-couplings with nitrogen heterocycles (Scheme 27). The catalytic reaction was proposed to begin by oxidative addition of RAE **104** to catalyst **Bi-1**, forming an in cage radical pair consisting of Bi^{II} species **130** and α-amino radical **107** (Scheme 27B). Importantly, electron paramagnetic resonance (EPR) spectroscopy at

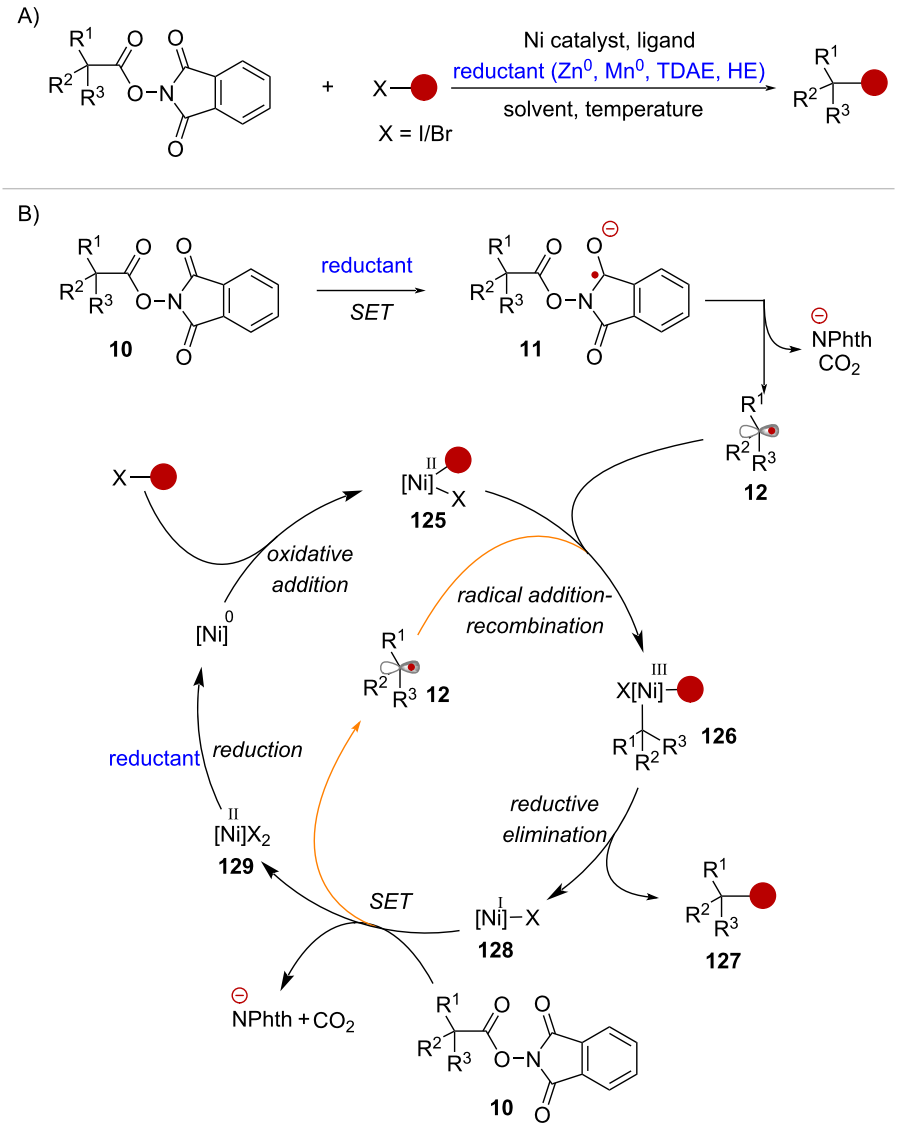

Scheme 25: A) Ni-catalyzed cross-electrophile coupling of NHPI esters. B) Representative catalytic cycle.

25 °C supported the formation of species **107**. However, NMR measurements at −40 °C showed the accumulation of Bi^{III} complex **131**, which can be prepared separately in a stoichiometric experiment. As such, two different pathways may lead to the C(sp^3)–N cross-coupling products. On one hand, in-cage electron transfer from radical **107** to Bi^{II} complex **130** can generate iminium ion **108**. Alternatively, intermediate **108** could arise from complex **131** by reductive elimination. Ultimately, the iminium ion can be trapped by the nitrogen nucleophile to form product **132** or by the in-situ-generated tetrachlorophthalimyl anion ($^{-}$TCPhth) affording product **105**.

Stoichiometric reductants can facilitate certain radical-mediated transformations that involve NHPI esters, even without the presence of metal catalysts. Larionov and Sun have independently reported notable examples of these transformations, involving the Zn^0-mediated cross-coupling of redox-active esters with chlorophosphines [102] and *gem*-difluoroalkenes [103], respectively. In the report by Sun and co-workers, it was proposed that the activation of RAE **10** occurs upon reduction with Zn powder to give radical anion **11** (Scheme 28). Following fragmentation, radical intermediate **12** would then attack *gem*-difluoroalkene **133**, affording intermediate **134**. Reduction of this radical species by another equivalent of Zn^0 would then form anionic intermediate **135**. Finally, the selective formation of *Z*-monofluoroalkene product **136** is achieved through anti-coplanar elimination of fluoride.

Shuhua Li and co-workers reported the generation of alkyl radicals from NHPI esters, mediated by a pyridine-boryl radical

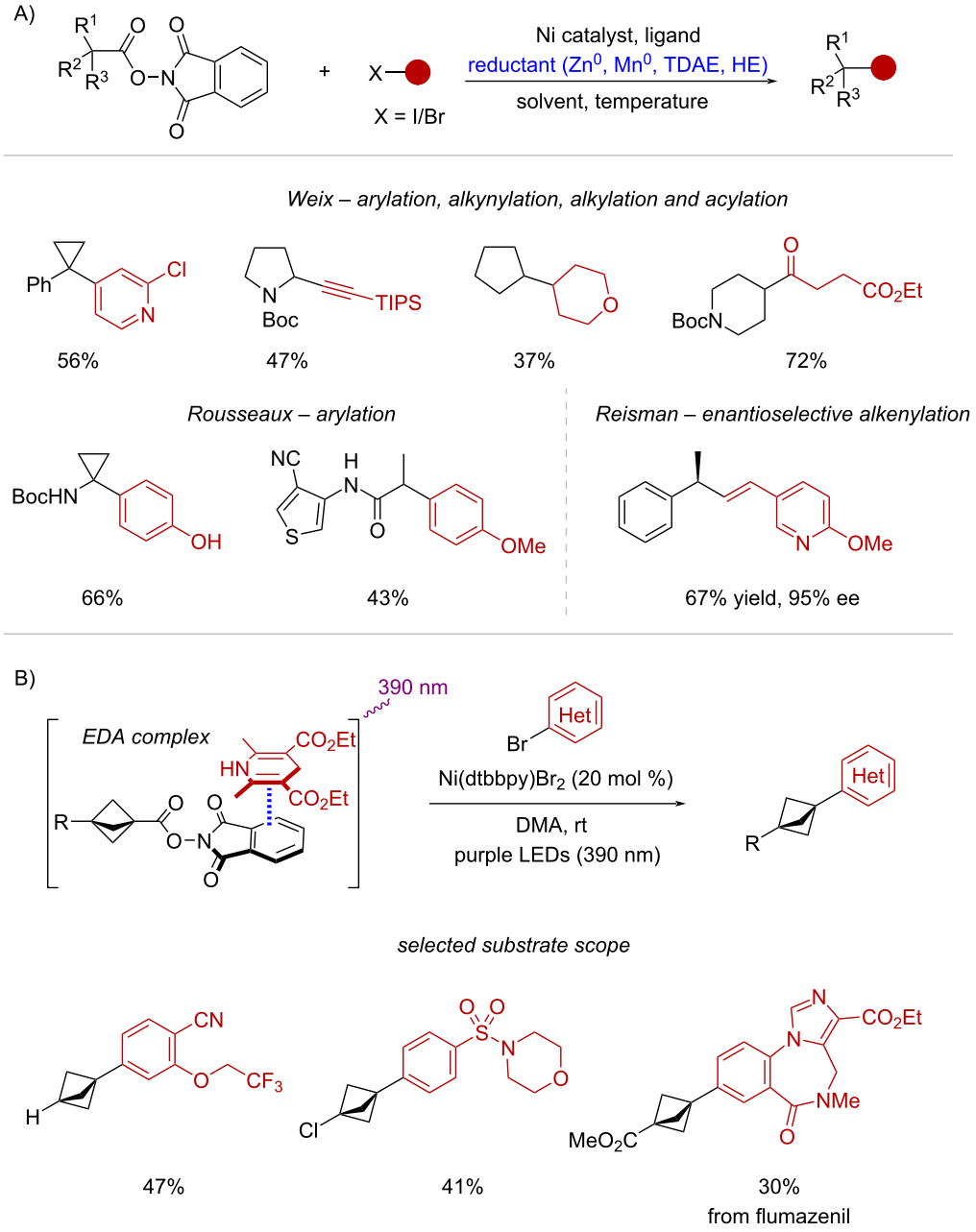

Scheme 26: A) Synthetic applications of decarboxylative cross-electrophile couplings. B) Decarboxylative arylation of BCP-redox active esters enabled by EDA complex activation and Ni catalysis.

reductant species in the context of alkene hydroalkylation [104] and cross-decarboxylative couplings with 4-cyanopyridines [105] (Scheme 29A). In the mechanism of the latter transformation, pyridine **137** also serves as a catalyst, generating the crucial pyridine-boryl radical **138** via reaction with B_2pin_2 (Scheme 29B). The proposed species **138** induces the reductive fragmentation of active ester **10**, regenerating pyridine **137** while forming alkyl radical **12**, CO_2 and phthalimide–B(pin) adduct **139**. Subsequently, radical–radical coupling between **12** and one equivalent of **138** affords dihydropyridine **140**, which upon re-aromatization, facilitated by $ZnCl_2$ acting as a Lewis acid, yields product **141**, accompanied by the formation of cyano-B(pin) **142**. Importantly, in the absence of $ZnCl_2$, intermediate **140** could be detected by HRMS and ^{11}B NMR, highlighting the pivotal role of $ZnCl_2$ in promoting rearomatization.

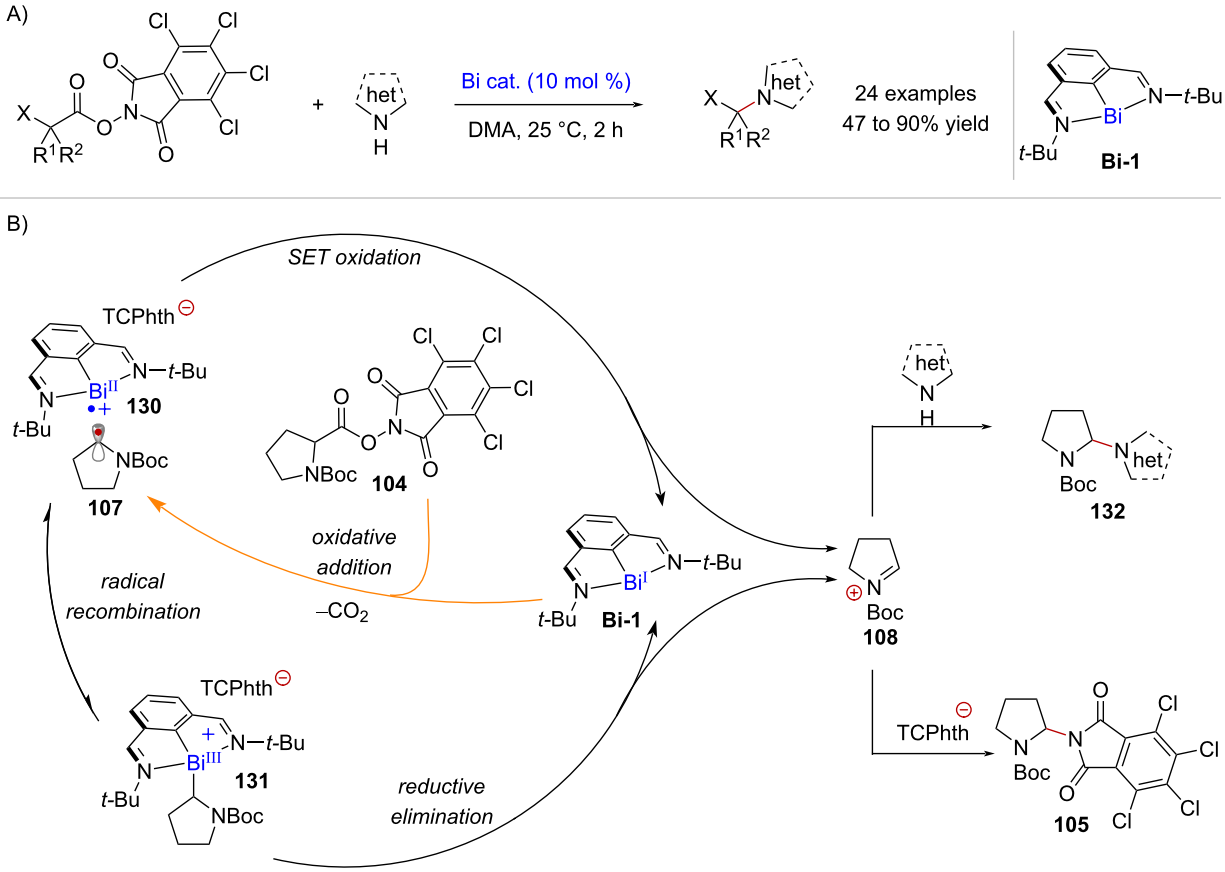

Scheme 27: A) Activation of tetrachlorophthalimide redox-active esters enabled by a low-valency Bi complex. B) Proposed mechanism involving two plausible reaction pathways.

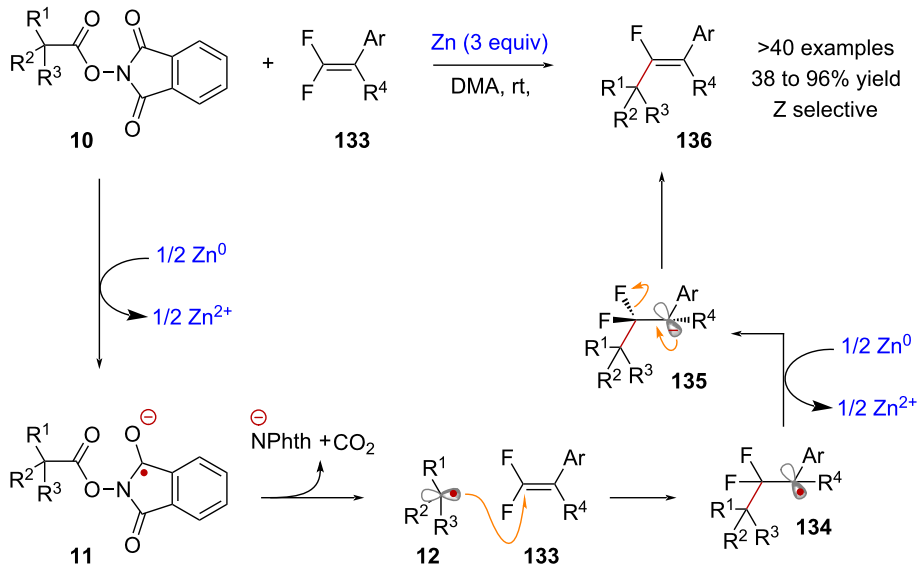

Scheme 28: Activation of NHPI esters mediated by Zn^0 applied in a *Z*-selective alkenylation reaction.

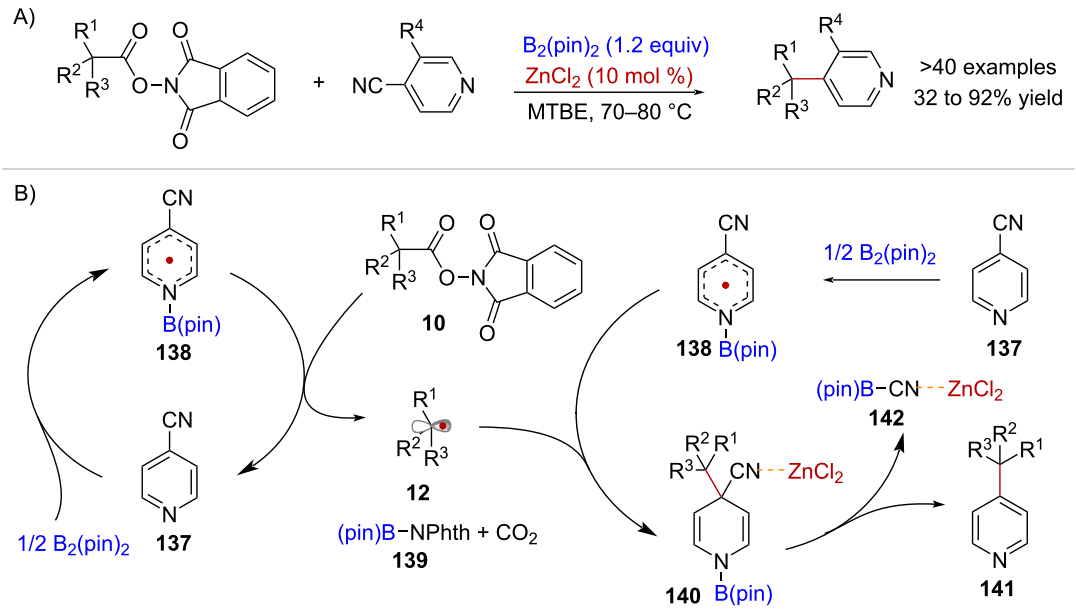

Scheme 29: A) Activation of NHPI esters enabled by a pyridine-boryl radical species applied to the decarboxylative alkylation of pyridines. B) Reaction mechanism.

N-Heterocyclic carbene (NHC) catalysis

In 2019, Nagao and Ohmiya reported the decarboxylative coupling of NHPI esters with aldehydes enabled by NHC catalysis [106]. The reaction proceeds with the catalyst **NHC-1** at 60 °C and gives rise to ketones (Scheme 30A). The proposed mechanism begins with the reaction of benzaldehyde (**143**) and the NHC-catalyst **144** to form the neutral Breslow intermediate **145** (Scheme 30B). Then, cesium carbonate deprotonates the enol OH in **145**, to provide the enolate form of Breslow's intermediate **146**, which is a suitable reducing agent to trigger the fragmentation of NHPI ester **58** ($E°_{ox}$ = −0.97 V vs SCE in MeCN). Hence, it is proposed that enolate **146** induces the single electron reduction of **58**, generating the persistent radical **147** and the transient species **148**, which fragments into *tert*-butyl radical (**64**). Notably, the reduction of NHPI ester **58** could be facilitated by interaction of a cesium cation with the oxygen lone pair of the phthalimide, in analogy to the mechanism discussed in Scheme 7B. Lastly, radical–radical coupling between **64** and **147**, accompanied by elimination of the NHC catalyst, yields ketone product **149**. In subsequent studies, this NHC-catalyzed radical relay activation mode has been extended to the alkylation of aliphatic aldehydes [107] and to the three-component alkylacylation of olefins [108].

Alternatively, NHC catalysts can mediate the generation of radical intermediates from NHPI esters via the stabilization of a photoactive EDA complex. In 2020, Wang and Chen reported a photochemical C(sp^3)-heteroatom coupling reaction of NHPI esters mediated by NaI and the catalyst **NHC-2** [109] (Scheme 31A). Initial investigations showed that the reaction proceeded in the absence of the NHC catalyst, and it was reasoned that substrate **150** and NaI formed EDA complex **151** that would undergo light-mediated decarboxylation (Scheme 31B). However, upon addition of catalyst **NHC-2** an improvement of the reaction yield from 36% to 63% was observed. The authors proposed that the addition of the NHC catalyst facilitates the formation of EDA complex **151**. In addition, it is thought that the stabilization imparted by the NHC catalyst is crucial in the subsequent radical recombination between C(sp^3) radical **152** and the corresponding iodine-centered radical which provides iodination product **153** (Scheme 31B). It is worth noting that the iodination product is formed exclusively when using acetone as the solvent (see compound **154** in scheme C) whereas in DMF a nucleophilic substitution takes place to afford products of the type **155** (Scheme 31B). Representative examples of the substrate scope are shown in Scheme 31C. The in situ-generated phthalimidyl anion (–Nphth) is a competent nucleophile and gives rise to primary protected amines such as **156**. Additionally, sodium phenolate and thiophenolate salts give rise to products **157** and **158**, respectively, while the chlorination product **159** was obtained upon the addition of tetrabutylammonium chloride (Scheme 31C).

Mechanisms under electrochemical activation

The electrochemical activation of NHPI esters provides significant advantages compared to other methods. It allows for single

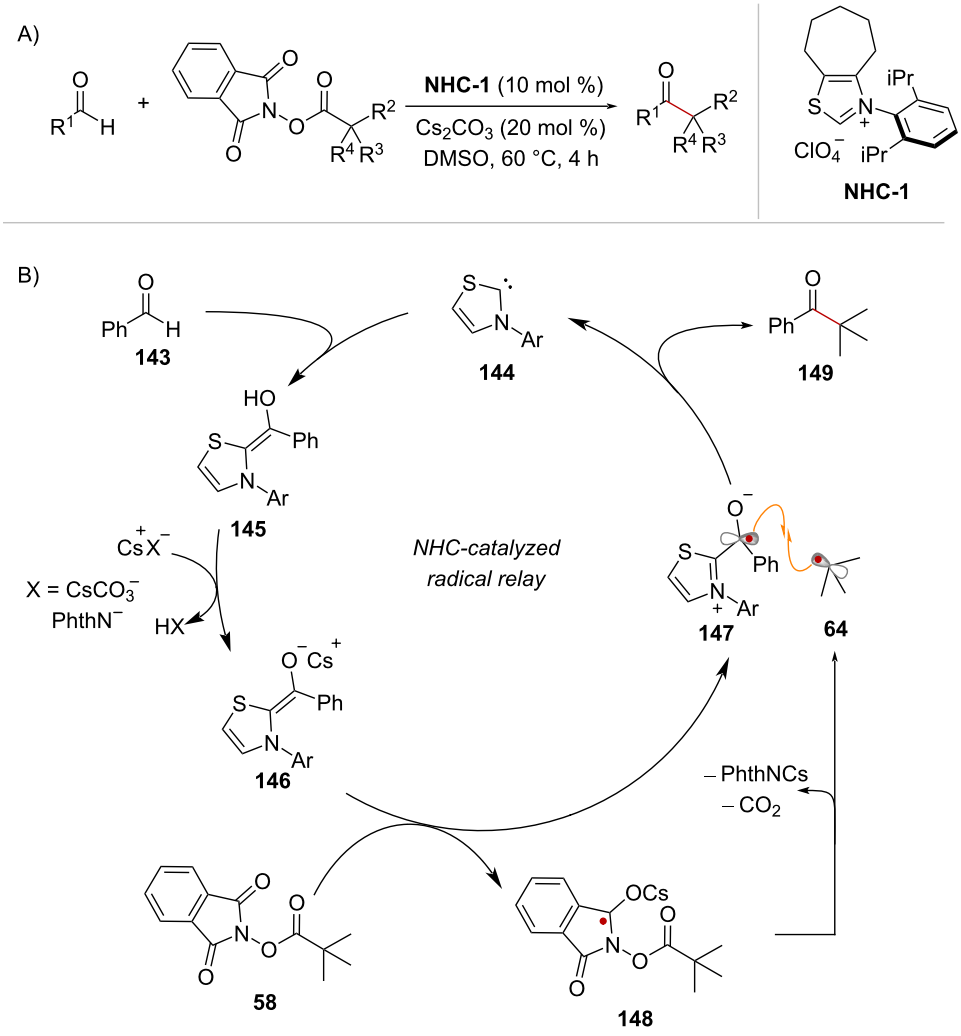

Scheme 30: A) Decarboxylative coupling of RAE and aldehydes enabled by NHC-catalyzed radical relay. B) Proposed reaction mechanism.

electron reduction to be facilitated by cost-effective carbon-based cathodes, eliminating the requirement for precious metal photocatalysts or exogeneous reductants such as Zn^0. In the final section of this perspective, we explore examples where NHPI esters have been utilized as radical precursors under electrochemical conditions.

Giese-type radical additions, which are usually performed under conditions of photoredox-catalysis (see Scheme 4), can also be achieved under constant-potential electrolysis employing graphite electrodes [110] (Scheme 32A). Under these conditions, activation of NHPI ester **160** by SET occurs at the cathode's surface affording the corresponding radical anion **161** (Scheme 32B). Subsequent fragmentation leads to the cyclohexyl radical (**162**) which then adds to the terminal carbon of radical acceptor **163**, leading to radical intermediate **164**. In the other redox half-reaction, Hantzsch ester (**HE**) undergoes anodic oxidation to form radical cation **65**, which then transfers a proton, likely to the phthalimidyl anion (⁻Nphth), resulting in the formation of radical species **165**. Finally, reaction between intermediates **164** and **165** through sequential electron transfer and proton transfer (ET/PT) leads to the hydroalkylation product **166** and the pyridine byproduct **167**.

In addition, there have been reports of Minisci-type additions where radical intermediates are electrochemically generated from NHPI esters [111-113] (Scheme 33A). The mechanism of this redox neutral reaction involves reductive fragmentation of the radical precursor **3** mediated by the cathode under constant-current electrolysis (Scheme 33B). The resulting alkyl radical **9** attacks the protonated quinoline **168**, forming radical cation intermediate **169**. Finally, single electron oxidation of **169** at the

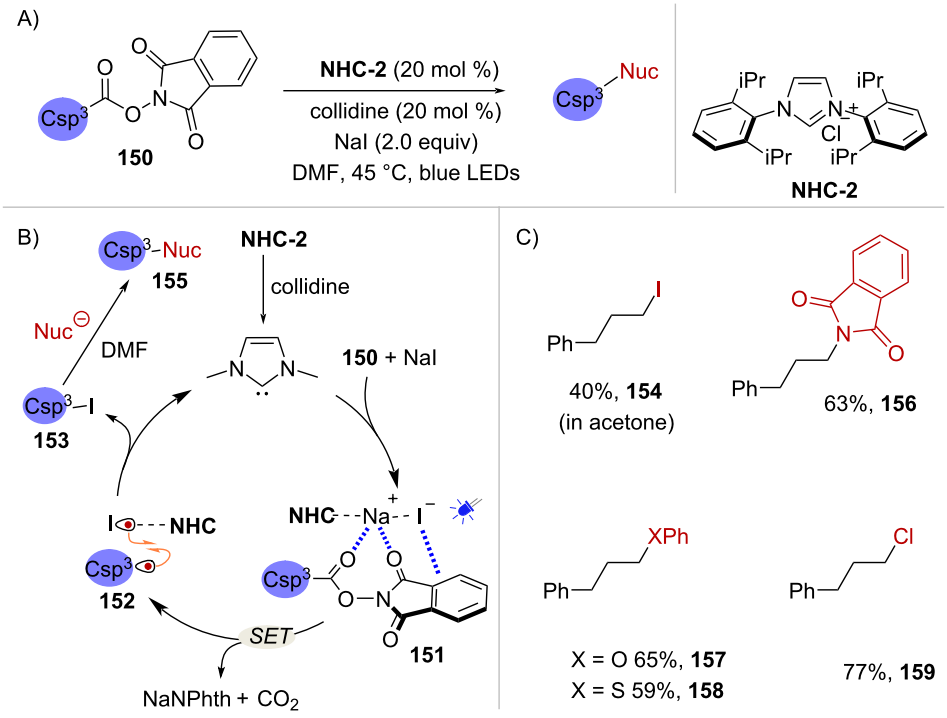

Scheme 31: A) Decarboxylative C(sp^3)–heteroatom coupling reaction of NHPI esters under NHC catalysis B) The NHC catalyst improves reaction efficiency by EDA complex stabilization. C) Examples of substrate scope.

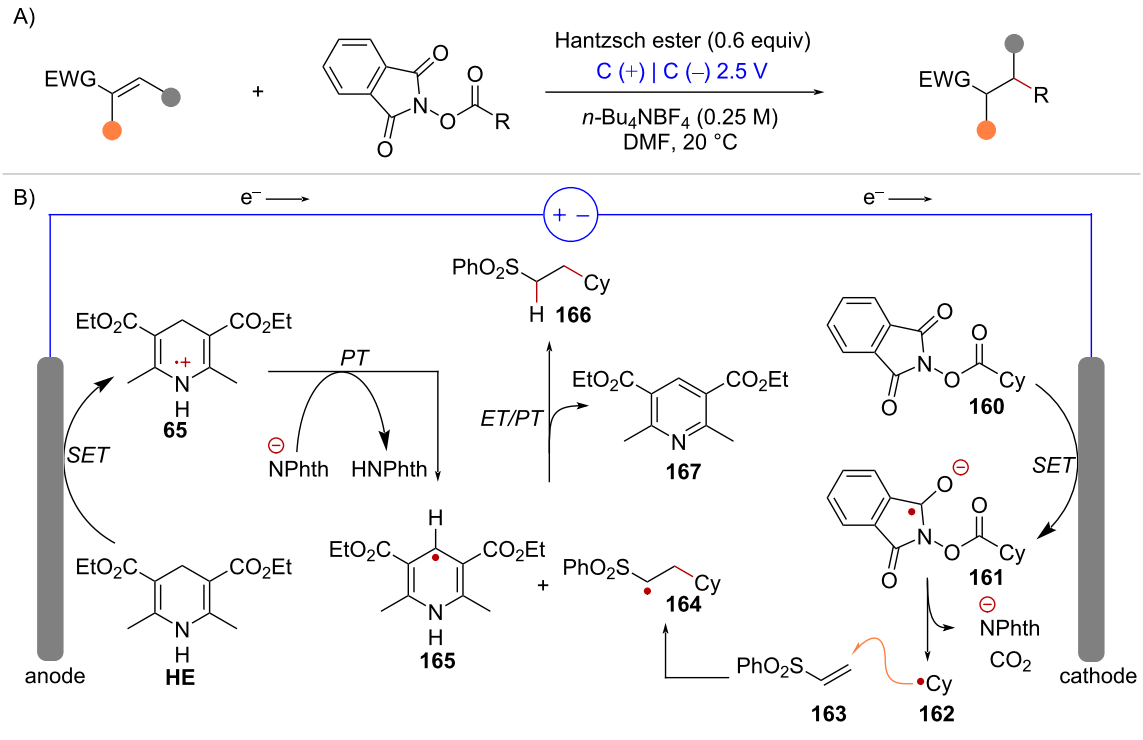

Scheme 32: A) Electrochemical Giese-type radical addition of NHPI esters. B) Reaction mechanism.

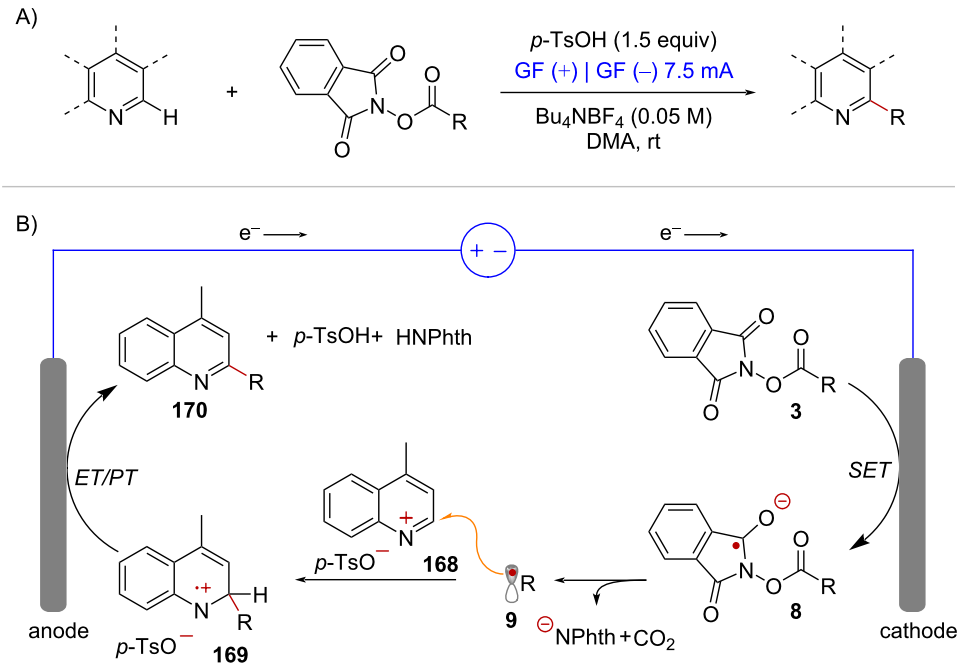

Scheme 33: Electrochemical Minisci-type radical addition of NHPI-esters.

anode, followed by rearomatization via proton-transfer forms the alkylated heterocycle **170**.

As discussed in Scheme 25, the Ni-catalyzed cross-electrophile coupling between redox-active esters and aryl halides requires the addition of a stoichiometric reductant (typically Zn^0 or Mn^0) to both activate the NHPI ester and turn-over the catalytic cycle. However, the merger of Ni-catalysis and electrochemistry allows for the implementation of more convenient conditions in which these two crucial reductive steps can be mediated by the cathode (Scheme 34). In this context, Jamison and co-workers developed an electrochemically driven decarboxylative $C(sp^3)$–$C(sp^2)$ cross-coupling protocol that proceeds in a divided electrochemical cell with reticulated vitreous carbon (RVC) electrodes and triethylamine (NEt_3) as sacrificial reductant [114] (Scheme 34A). In the proposed mechanism, radical species **9**, which is generated upon cathodic reduction of active ester **3**, is captured by complex **171** (Scheme 34B). The resulting Ni^{III} complex **172** undergoes facile reductive elimination to form cross-coupling product **173** and Ni^{I} intermediate **174**. Finally, reduction of **174** at the cathode surface restores the Ni^0 species **175** giving rise to a new catalytic cycle.

Reductive cross-electrophile couplings that incorporate redox-active esters and aryl halides have the potential to simplify the syntheses of drug-like compounds through $C(sp^3)$–$C(sp^2)$ bond formation. However, their synthetic utility is frequently restricted due to various challenges, such as RAE decomposition and a limited aryl halide scope. In recent years, the Baran lab has made progress in enhancing the practicality and applicability of electrochemically driven decarboxylative couplings involving NHPI esters and aryl-halides [115]. Their optimized reaction conditions required a Ni^{II} precursor, 2,2'-bipyridine (bpy) as ligand, silver nitrate ($AgNO_3$) as an additive and the combination of a magnesium (Mg) sacrificial anode and a RVC cathode (Scheme 35A). A crucial discovery in advancing this methodology was the in situ formation of silver nanoparticles (AgNP) on the cathode's surface [116] (Scheme 35B). The use of this Ag-doped cathode led to slower mass transport and minimized side reactions caused by rapid reduction of RAEs, thereby avoiding substrate decomposition and enhancing reaction yields (Scheme 35B). Furthermore, the presence of the AgNP layer on the cathode caused a decrease of the reaction's overpotential from –1.66 V to –1.15 V (vs Ag/AgCl), which is thought to prevent catalyst deactivation via successive reduction of the various Ni species, while also avoiding electrode passivation caused by catalyst adsorption (Scheme 35B).

Baran and co-workers have demonstrated that these overall milder reaction conditions greatly improved the functional group compatibility of decarboxylative couplings under reducing conditions. For example, the cross-coupling between NHPI esters and both electron-poor and electron-rich

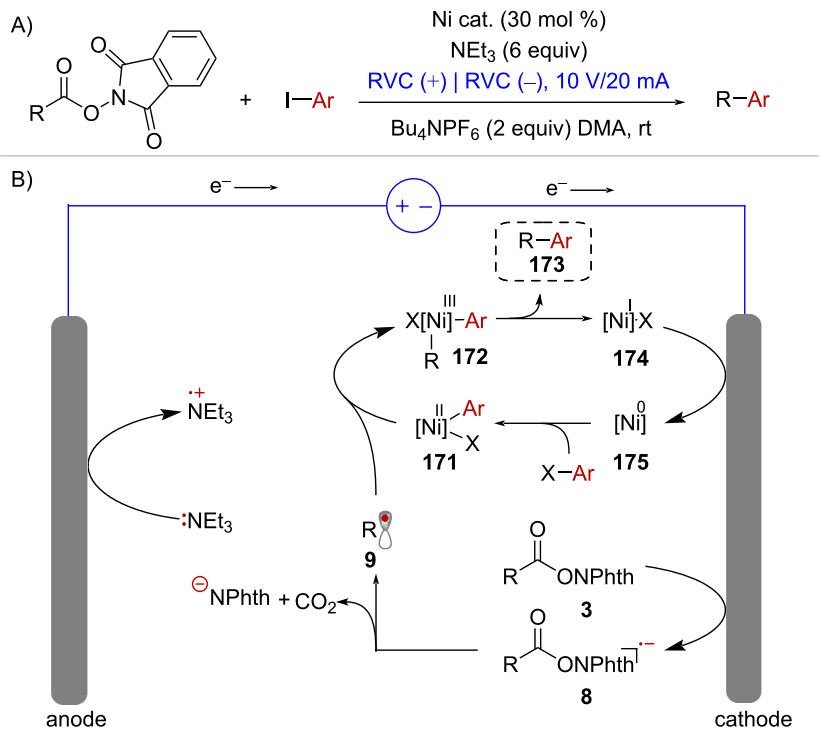

Scheme 34: Ni-electrocatalytic cross-electrophile coupling of NHPI esters with aryl iodides.

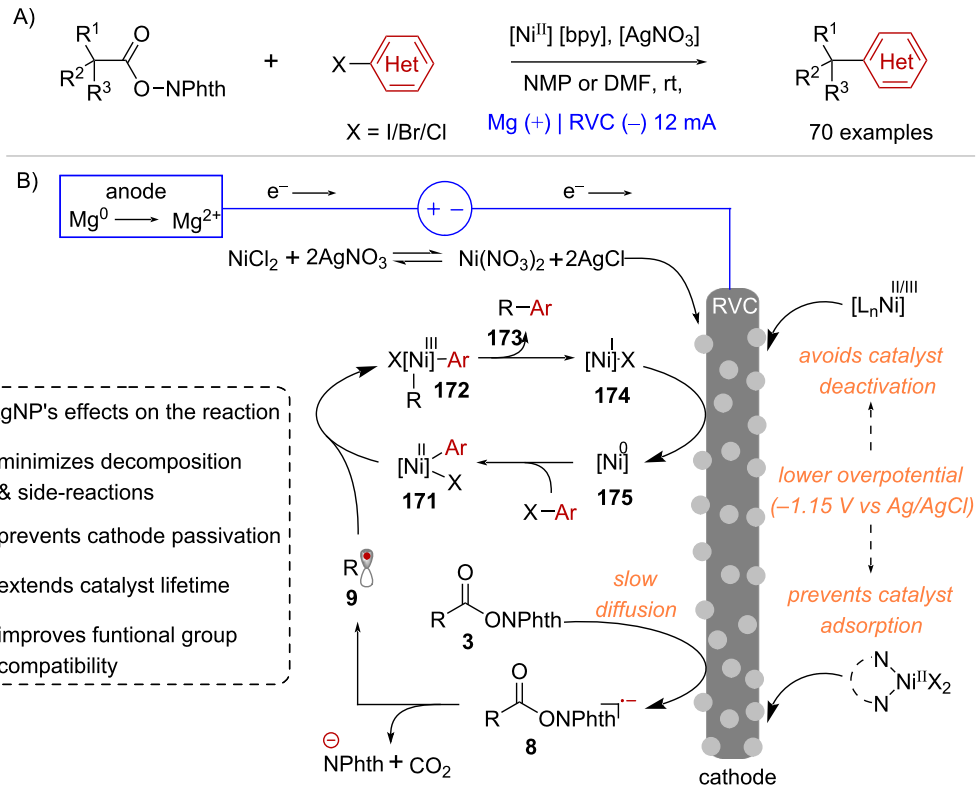

Scheme 35: A) Decarboxylative arylation of NHPI esters under Ag-Ni electrocatalysis B) Formation of AgNP on the cathode's surface and its effect on the reaction.

(hetero)aryl halides was equally effective (Scheme 36). In addition, the preparation of unnatural amino acids in multigram scale [115], along with the syntheses of complex terpenes [116] and (+)-calcipotriol [117] have showcased the vast synthetic potential and broad applicability of NHPI esters activated under these electrochemical conditions (Scheme 36).

Conclusion

Given their rich history and their continued use in diverse methodologies, *N*-hydroxyphthalimide esters have been and will remain to be important tools in synthetic organic chemistry. In this perspective, we have surveyed recent advancements in photochemistry, TM catalysis, NHC catalysis, and electrochemistry to show the generality of these RAEs in diverse mechanistic paradigms. Their application as radical progenitors continues to broaden the scope of radical-mediated reactions, especially in complex molecular settings, where issues of chemoselectivity can benefit from the multitude of mechanisms for their activation.

Particularly, the use of RAEs in natural product total synthesis enables the assembly of strategic C–C bonds through radical coupling reactions that can draw from a wide range of reaction conditions (Scheme 37). Pioneering work by Schnermann and Overman demonstrated the early potential of photocatalytic Giese-type additions, successfully coupling two complex ring fragments and creating adjacent stereocenters, which effectively solved major challenges in the synthesis of (–)-aplyviolene [38] (Scheme 37A). Brown and co-workers devised a diastereoselective Ni-catalyzed decarboxylative arylation as a crucial step in the synthesis of (–)-cajanusine [118] (Scheme 37A). Likewise, the Baran lab employed Ni-catalyzed decarboxylative couplings of RAEs to form two strategic C–C bonds in the synthesis of higginsianin A [119] (Scheme 37A). Recently, Lumb and co-workers showcased the use of NHPI esters in key radical cyclizations, allowing the synthesis of diverse dibenzocyclooctadiene lignans [55] (Scheme 37B). A Ru-catalyzed cyclization was employed to construct the quaternary stereocenter in taiwankadsurin A, whereas the corresponding spirocycle in kadsulignan E was formed under Ir photocatalysis. In addition, photoinduced Pd catalysis was applied in the key macrocyclization step to complete the synthesis of kadsuphilin N.

These applications in total synthesis serve as a testament to the synthetic versatility of radical reactions facilitated by the use of

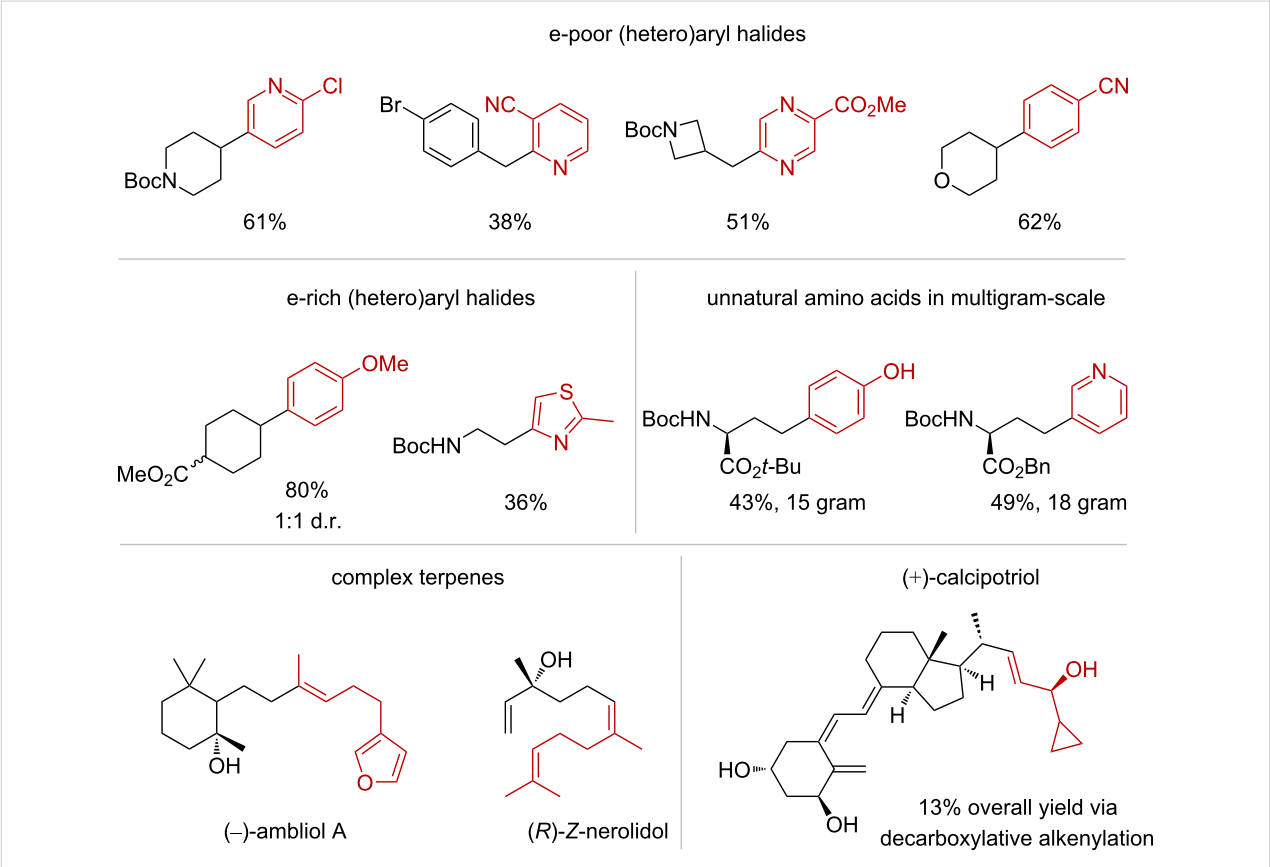

Scheme 36: Synthetic applications of decarboxylative couplings of NHPI esters under Ni-electrocatalysis.

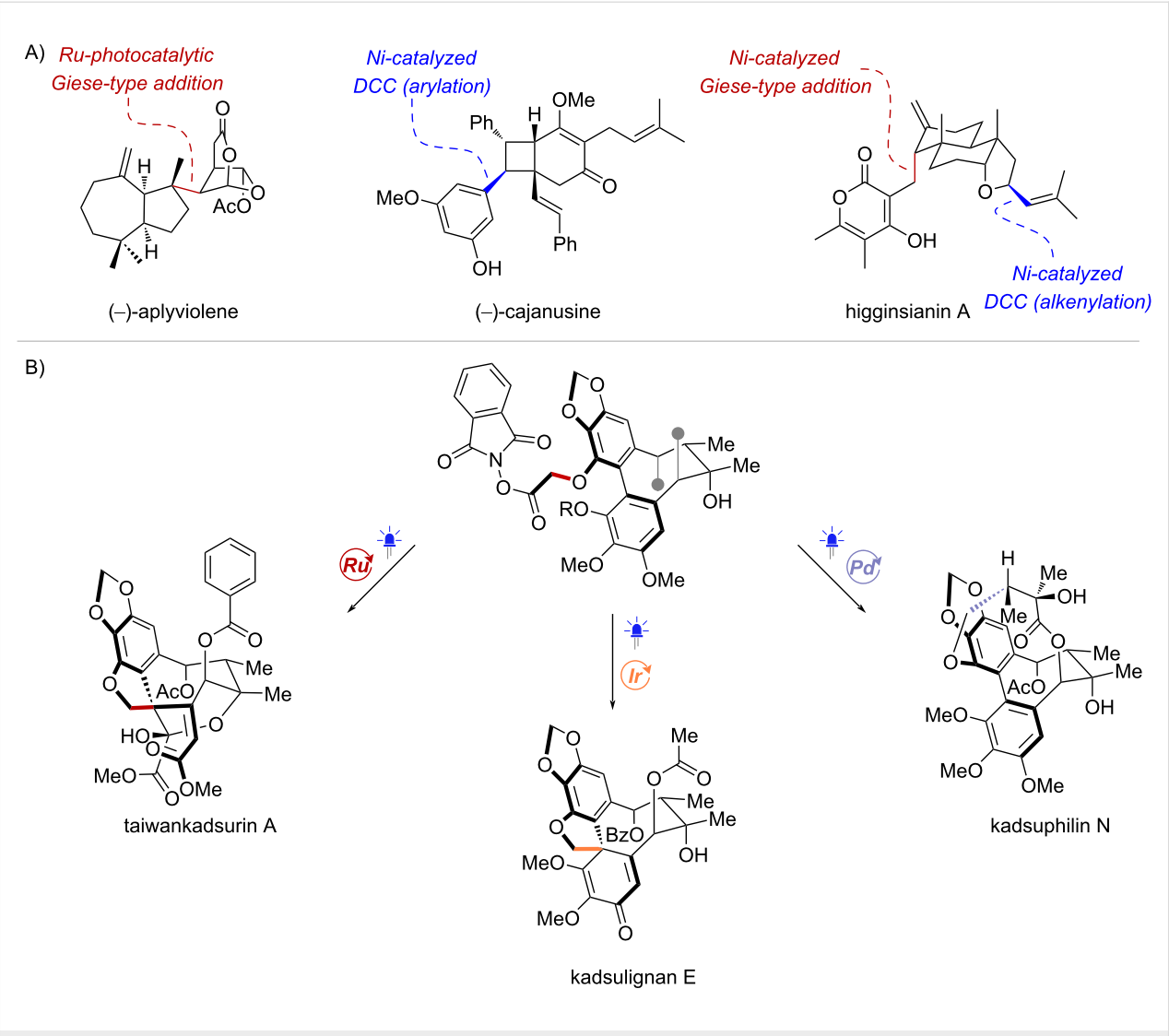

Scheme 37: Examples of natural product syntheses in which RAEs were used in key C–C bond forming reactions.

RAEs. In the years to come, we anticipate that the continued development of new catalysts and the implementation of increasingly mild reaction conditions will open new possibilities for further applications of NHPI esters in radical reactions. Expanding the mechanisms and reactivity discussed herein will continue to improve our understanding of radical chemistry toward exploring novel chemical space.

Funding

Financial support was provided by the Natural Sciences and Engineering Research Council of Canada (Discovery Grant to J.-P.L.) and the FRQNT Center for Green Chemistry and Catalysis. C.R.A.N. is grateful to Mitacs (Globalink), FRQNT (PBEEE), and CONACyT (Mexican National Council of Science and Technology) for the doctoral scholarships awarded.

ORCID® iDs

Carlos R. Azpilcueta-Nicolas - https://orcid.org/0000-0002-8839-3501
Jean-Philip Lumb - https://orcid.org/0000-0002-9283-1199

References

1. Yan, M.; Lo, J. C.; Edwards, J. T.; Baran, P. S. *J. Am. Chem. Soc.* **2016,** *138,* 12692–12714. doi:10.1021/jacs.6b08856
2. Zard, S. Z. *Org. Lett.* **2017,** *19,* 1257–1269. doi:10.1021/acs.orglett.7b00531
3. Kuivila, H. G. *Acc. Chem. Res.* **1968,** *1,* 299–305. doi:10.1021/ar50010a002
4. Galliher, M. S.; Roldan, B. J.; Stephenson, C. R. J. *Chem. Soc. Rev.* **2021,** *50,* 10044–10057. doi:10.1039/d1cs00411e
5. Kvasovs, N.; Gevorgyan, V. *Chem. Soc. Rev.* **2021,** *50,* 2244–2259. doi:10.1039/d0cs00589d
6. Crespi, S.; Fagnoni, M. *Chem. Rev.* **2020,** *120,* 9790–9833. doi:10.1021/acs.chemrev.0c00278

7. Matsui, J. K.; Lang, S. B.; Heitz, D. R.; Molander, G. A. *ACS Catal.* **2017,** *7,* 2563–2575. doi:10.1021/acscatal.7b00094
8. Prier, C. K.; Rankic, D. A.; MacMillan, D. W. C. *Chem. Rev.* **2013,** *113,* 5322–5363. doi:10.1021/cr300503r
9. Yan, M.; Kawamata, Y.; Baran, P. S. *Chem. Rev.* **2017,** *117,* 13230–13319. doi:10.1021/acs.chemrev.7b00397
10. Siu, J. C.; Fu, N.; Lin, S. *Acc. Chem. Res.* **2020,** *53,* 547–560. doi:10.1021/acs.accounts.9b00529
11. Kaga, A.; Chiba, S. *ACS Catal.* **2017,** *7,* 4697–4706. doi:10.1021/acscatal.7b01405
12. Smith, J. M.; Harwood, S. J.; Baran, P. S. *Acc. Chem. Res.* **2018,** *51,* 1807–1817. doi:10.1021/acs.accounts.8b00209
13. Gennaiou, K.; Kelesidis, A.; Kourgiantaki, M.; Zografos, A. L. *Beilstein J. Org. Chem.* **2023,** *19,* 1–26. doi:10.3762/bjoc.19.1
14. Laudadio, G.; Palkowitz, M. D.; El-Hayek Ewing, T.; Baran, P. S. *ACS Med. Chem. Lett.* **2022,** *13,* 1413–1420. doi:10.1021/acsmedchemlett.2c00286
15. Ni, S.; Padial, N. M.; Kingston, C.; Vantourout, J. C.; Schmitt, D. C.; Edwards, J. T.; Kruszyk, M. M.; Merchant, R. R.; Mykhailiuk, P. K.; Sanchez, B. B.; Yang, S.; Perry, M. A.; Gallego, G. M.; Mousseau, J. J.; Collins, M. R.; Cherney, R. J.; Lebed, P. S.; Chen, J. S.; Qin, T.; Baran, P. S. *J. Am. Chem. Soc.* **2019,** *141,* 6726–6739. doi:10.1021/jacs.9b02238
16. Wiles, R. J.; Molander, G. A. *Isr. J. Chem.* **2020,** *60,* 281–293. doi:10.1002/ijch.201900166
17. Pitzer, L.; Schwarz, J. L.; Glorius, F. *Chem. Sci.* **2019,** *10,* 8285–8291. doi:10.1039/c9sc03359a
18. Gooßen, L. J.; Rodríguez, N.; Gooßen, K. *Angew. Chem., Int. Ed.* **2008,** *47,* 3100–3120. doi:10.1002/anie.200704782
19. Xuan, J.; Zhang, Z.-G.; Xiao, W.-J. *Angew. Chem., Int. Ed.* **2015,** *54,* 15632–15641. doi:10.1002/anie.201505731
20. Wang, Z.; Zhu, L.; Yin, F.; Su, Z.; Li, Z.; Li, C. *J. Am. Chem. Soc.* **2012,** *134,* 4258–4263. doi:10.1021/ja210361z
21. Concepcion, J. I.; Francisco, C. G.; Freire, R.; Hernandez, R.; Salazar, J. A.; Suarez, E. *J. Org. Chem.* **1986,** *51,* 402–404. doi:10.1021/jo00353a026
22. Li, Q. Y.; Gockel, S. N.; Lutovsky, G. A.; DeGlopper, K. S.; Baldwin, N. J.; Bundesmann, M. W.; Tucker, J. W.; Bagley, S. W.; Yoon, T. P. *Nat. Chem.* **2022,** *14,* 94–99. doi:10.1038/s41557-021-00834-8
23. Su, W.; Xu, P.; Ritter, T. *Angew. Chem., Int. Ed.* **2021,** *60,* 24012–24017. doi:10.1002/anie.202108971
24. Chen, T. Q.; Pedersen, P. S.; Dow, N. W.; Fayad, R.; Hauke, C. E.; Rosko, M. C.; Danilov, E. O.; Blakemore, D. C.; Dechert-Schmitt, A.-M.; Knauber, T.; Castellano, F. N.; MacMillan, D. W. C. *J. Am. Chem. Soc.* **2022,** *144,* 8296–8305. doi:10.1021/jacs.2c02392
25. Barton, D. H. R.; Crich, D.; Motherwell, W. B. *J. Chem. Soc., Chem. Commun.* **1983,** 939–941. doi:10.1039/c39830000939
26. Barton, D. H. R.; Crich, D.; Motherwell, W. B. *Tetrahedron* **1985,** *41,* 3901–3924. doi:10.1016/s0040-4020(01)97173-x
27. Saraiva, M. F.; Couri, M. R. C.; Le Hyaric, M.; de Almeida, M. V. *Tetrahedron* **2009,** *65,* 3563–3572. doi:10.1016/j.tet.2009.01.103
28. St. John, P. C.; Guan, Y.; Kim, Y.; Kim, S.; Paton, R. S. *Nat. Commun.* **2020,** *11,* 2328. doi:10.1038/s41467-020-16201-z
    BDE values were predicted using the ALFABET web server: https://bde.ml.nrel.gov/. More details can be found in this referenced article.
29. Okada, K.; Okamoto, K.; Oda, M. *J. Am. Chem. Soc.* **1988,** *110,* 8736–8738. doi:10.1021/ja00234a047
30. Parida, S. K.; Mandal, T.; Das, S.; Hota, S. K.; De Sarkar, S.; Murarka, S. *ACS Catal.* **2021,** *11,* 1640–1683. doi:10.1021/acscatal.0c04756
31. Murarka, S. *Adv. Synth. Catal.* **2018,** *360,* 1735–1753. doi:10.1002/adsc.201701615
32. Mato, M.; Spinnato, D.; Leutzsch, M.; Moon, H. W.; Reijerse, E. J.; Cornella, J. *Nat. Chem.* **2023,** *15,* 1138–1145. doi:10.1038/s41557-023-01229-7
33. Bach, R. D.; Schlegel, H. B. *J. Phys. Chem. A* **2021,** *125,* 5014–5021. doi:10.1021/acs.jpca.1c02741
34. Sayre, H.; Ripberger, H. H.; Odella, E.; Zieleniewska, A.; Heredia, D. A.; Rumbles, G.; Scholes, G. D.; Moore, T. A.; Moore, A. L.; Knowles, R. R. *J. Am. Chem. Soc.* **2021,** *143,* 13034–13043. doi:10.1021/jacs.1c01701
35. Tucker, J. W.; Stephenson, C. R. J. *J. Org. Chem.* **2012,** *77,* 1617–1622. doi:10.1021/jo202538x
    The cyclic voltammetry and spectroscopic data reported by Knowles was used to approximate the $E_{1/2}^{red}[Ir^{IV}/^*Ir^{III}]$ value, following the procedure reported by Tucker and Stephenson.
36. Schultz, D. M.; Yoon, T. P. *Science* **2014,** *343,* 1239176. doi:10.1126/science.1239176
37. Okada, K.; Okamoto, K.; Morita, N.; Okubo, K.; Oda, M. *J. Am. Chem. Soc.* **1991,** *113,* 9401–9402. doi:10.1021/ja00024a074
38. Schnermann, M. J.; Overman, L. E. *Angew. Chem., Int. Ed.* **2012,** *51,* 9576–9580. doi:10.1002/anie.201204977
39. Müller, D. S.; Untiedt, N. L.; Dieskau, A. P.; Lackner, G. L.; Overman, L. E. *J. Am. Chem. Soc.* **2015,** *137,* 660–663. doi:10.1021/ja512527s
40. Pratsch, G.; Lackner, G. L.; Overman, L. E. *J. Org. Chem.* **2015,** *80,* 6025–6036. doi:10.1021/acs.joc.5b00795
41. Schwarz, J.; König, B. *Green Chem.* **2016,** *18,* 4743–4749. doi:10.1039/c6gc01101b
42. Xu, R.; Xu, T.; Yang, M.; Cao, T.; Liao, S. *Nat. Commun.* **2019,** *10,* 3752. doi:10.1038/s41467-019-11805-6
43. Shu, X.; Xu, R.; Ma, Q.; Liao, S. *Org. Chem. Front.* **2020,** *7,* 2003–2007. doi:10.1039/d0qo00440e
44. Proctor, R. S. J.; Davis, H. J.; Phipps, R. J. *Science* **2018,** *360,* 419–422. doi:10.1126/science.aar6376
45. Ermanis, K.; Colgan, A. C.; Proctor, R. S. J.; Hadrys, B. W.; Phipps, R. J.; Goodman, J. M. *J. Am. Chem. Soc.* **2020,** *142,* 21091–21101. doi:10.1021/jacs.0c09668
46. Tlahuext-Aca, A.; Garza-Sanchez, R. A.; Glorius, F. *Angew. Chem., Int. Ed.* **2017,** *56,* 3708–3711. doi:10.1002/anie.201700049
47. Wang, X.; Han, Y.-F.; Ouyang, X.-H.; Song, R.-J.; Li, J.-H. *Chem. Commun.* **2019,** *55,* 14637–14640. doi:10.1039/c9cc07494e
48. Murray, P. R. D.; Leibler, I. N.-M.; Hell, S. M.; Villalona, E.; Doyle, A. G.; Knowles, R. R. *ACS Catal.* **2022,** *12,* 13732–13740. doi:10.1021/acscatal.2c04316
49. Sherwood, T. C.; Xiao, H.-Y.; Bhaskar, R. G.; Simmons, E. M.; Zaretsky, S.; Rauch, M. P.; Knowles, R. R.; Dhar, T. G. M. *J. Org. Chem.* **2019,** *84,* 8360–8379. doi:10.1021/acs.joc.9b00432
50. Sherwood, T. C.; Li, N.; Yazdani, A. N.; Dhar, T. G. M. *J. Org. Chem.* **2018,** *83,* 3000–3012. doi:10.1021/acs.joc.8b00205
51. He, J.; Chen, G.; Zhang, B.; Li, Y.; Chen, J.-R.; Xiao, W.-J.; Liu, F.; Li, C. *Chem* **2020,** *6,* 1149–1159. doi:10.1016/j.chempr.2020.02.003
52. Reich, D.; Noble, A.; Aggarwal, V. K. *Angew. Chem., Int. Ed.* **2022,** *61,* e202207063. doi:10.1002/anie.202207063

53. Williams, O. P.; Chmiel, A. F.; Mikhael, M.; Bates, D. M.; Yeung, C. S.; Wickens, Z. K. *Angew. Chem., Int. Ed.* **2023,** *62,* e202300178. doi:10.1002/anie.202300178
54. Azpilcueta-Nicolas, C. R.; Meng, D.; Edelmann, S.; Lumb, J.-P. *Angew. Chem., Int. Ed.* **2023,** *62,* e202215422. doi:10.1002/anie.202215422
55. Huang, Z.; Lumb, J.-P. *Nat. Chem.* **2021,** *13,* 24–32. doi:10.1038/s41557-020-00603-z
56. Kachkovskyi, G.; Faderl, C.; Reiser, O. *Adv. Synth. Catal.* **2013,** *355,* 2240–2248. doi:10.1002/adsc.201300221
57. Shen, Y.; Shen, M.-L.; Wang, P.-S. *ACS Catal.* **2020,** *10,* 8247–8253. doi:10.1021/acscatal.0c02660
58. Crisenza, G. E. M.; Mazzarella, D.; Melchiorre, P. *J. Am. Chem. Soc.* **2020,** *142,* 5461–5476. doi:10.1021/jacs.0c01416
59. Lima, C. G. S.; de M. Lima, T.; Duarte, M.; Jurberg, I. D.; Paixão, M. W. *ACS Catal.* **2016,** *6,* 1389–1407. doi:10.1021/acscatal.5b02386
60. Zheng, C.; Wang, G.-Z.; Shang, R. *Adv. Synth. Catal.* **2019,** *361,* 4500–4505. doi:10.1002/adsc.201900803
61. Correia, J. T. M.; Piva da Silva, G.; Kisukuri, C. M.; André, E.; Pires, B.; Carneiro, P. S.; Paixão, M. W. *J. Org. Chem.* **2020,** *85,* 9820–9834. doi:10.1021/acs.joc.0c01130
62. Chowdhury, R.; Yu, Z.; Tong, M. L.; Kohlhepp, S. V.; Yin, X.; Mendoza, A. *J. Am. Chem. Soc.* **2020,** *142,* 20143–20151. doi:10.1021/jacs.0c09678
63. Fawcett, A.; Pradeilles, J.; Wang, Y.; Mutsuga, T.; Myers, E. L.; Aggarwal, V. K. *Science* **2017,** *357,* 283–286. doi:10.1126/science.aan3679
64. Barton, L. M.; Chen, L.; Blackmond, D. G.; Baran, P. S. *Proc. Natl. Acad. Sci. U. S. A.* **2021,** *118,* e2109408118. doi:10.1073/pnas.2109408118
65. Candish, L.; Teders, M.; Glorius, F. *J. Am. Chem. Soc.* **2017,** *139,* 7440–7443. doi:10.1021/jacs.7b03127
66. Cheng, W.-M.; Shang, R.; Zhao, B.; Xing, W.-L.; Fu, Y. *Org. Lett.* **2017,** *19,* 4291–4294. doi:10.1021/acs.orglett.7b01950
67. Fu, M.-C.; Shang, R.; Zhao, B.; Wang, B.; Fu, Y. *Science* **2019,** *363,* 1429–1434. doi:10.1126/science.aav3200
68. Shibutani, S.; Nagao, K.; Ohmiya, H. *Org. Lett.* **2021,** *23,* 1798–1803. doi:10.1021/acs.orglett.1c00211
69. Shibutani, S.; Kodo, T.; Takeda, M.; Nagao, K.; Tokunaga, N.; Sasaki, Y.; Ohmiya, H. *J. Am. Chem. Soc.* **2020,** *142,* 1211–1216. doi:10.1021/jacs.9b12335
70. Jin, Y.; Yang, H.; Fu, H. *Chem. Commun.* **2016,** *52,* 12909–12912. doi:10.1039/c6cc06994k
71. Jin, Y.; Yang, H.; Fu, H. *Org. Lett.* **2016,** *18,* 6400–6403. doi:10.1021/acs.orglett.6b03300
72. Bosque, I.; Bach, T. *ACS Catal.* **2019,** *9,* 9103–9109. doi:10.1021/acscatal.9b01039
73. Parasram, M.; Gevorgyan, V. *Chem. Soc. Rev.* **2017,** *46,* 6227–6240. doi:10.1039/c7cs00226b
74. Cheung, K. P. S.; Sarkar, S.; Gevorgyan, V. *Chem. Rev.* **2022,** *122,* 1543–1625. doi:10.1021/acs.chemrev.1c00403
75. Zhao, W.; Wurz, R. P.; Peters, J. C.; Fu, G. C. *J. Am. Chem. Soc.* **2017,** *139,* 12153–12156. doi:10.1021/jacs.7b07546
76. Xia, H.-D.; Li, Z.-L.; Gu, Q.-S.; Dong, X.-Y.; Fang, J.-H.; Du, X.-Y.; Wang, L.-L.; Liu, X.-Y. *Angew. Chem., Int. Ed.* **2020,** *59,* 16926–16932. doi:10.1002/anie.202006317
77. Mao, Y.; Zhao, W.; Lu, S.; Yu, L.; Wang, Y.; Liang, Y.; Ni, S.; Pan, Y. *Chem. Sci.* **2020,** *11,* 4939–4947. doi:10.1039/d0sc02213f
78. Zhang, Y.; Zhang, D. *Org. Biomol. Chem.* **2020,** *18,* 4479–4483. doi:10.1039/d0ob00835d
79. Wang, C.; Guo, M.; Qi, R.; Shang, Q.; Liu, Q.; Wang, S.; Zhao, L.; Wang, R.; Xu, Z. *Angew. Chem., Int. Ed.* **2018,** *57,* 15841–15846. doi:10.1002/anie.201809400
80. Huang, H.-M.; Koy, M.; Serrano, E.; Pflüger, P. M.; Schwarz, J. L.; Glorius, F. *Nat. Catal.* **2020,** *3,* 393–400. doi:10.1038/s41929-020-0434-0
81. Wang, G.-Z.; Shang, R.; Fu, Y. *Org. Lett.* **2018,** *20,* 888–891. doi:10.1021/acs.orglett.8b00023
82. Koy, M.; Sandfort, F.; Tlahuext-Aca, A.; Quach, L.; Daniliuc, C. G.; Glorius, F. *Chem. – Eur. J.* **2018,** *24,* 4552–4555. doi:10.1002/chem.201800813
83. Cheng, W.-M.; Shang, R.; Fu, Y. *Nat. Commun.* **2018,** *9,* 5215. doi:10.1038/s41467-018-07694-w
84. Cornella, J.; Edwards, J. T.; Qin, T.; Kawamura, S.; Wang, J.; Pan, C.-M.; Gianatassio, R.; Schmidt, M.; Eastgate, M. D.; Baran, P. S. *J. Am. Chem. Soc.* **2016,** *138,* 2174–2177. doi:10.1021/jacs.6b00250
85. Toriyama, F.; Cornella, J.; Wimmer, L.; Chen, T.-G.; Dixon, D. D.; Creech, G.; Baran, P. S. *J. Am. Chem. Soc.* **2016,** *138,* 11132–11135. doi:10.1021/jacs.6b07172
86. Wang, J.; Qin, T.; Chen, T.-G.; Wimmer, L.; Edwards, J. T.; Cornella, J.; Vokits, B.; Shaw, S. A.; Baran, P. S. *Angew. Chem., Int. Ed.* **2016,** *55,* 9676–9679. doi:10.1002/anie.201605463
87. Edwards, J. T.; Merchant, R. R.; McClymont, K. S.; Knouse, K. W.; Qin, T.; Malins, L. R.; Vokits, B.; Shaw, S. A.; Bao, D.-H.; Wei, F.-L.; Zhou, T.; Eastgate, M. D.; Baran, P. S. *Nature* **2017,** *545,* 213–218. doi:10.1038/nature22307
88. Smith, J. M.; Qin, T.; Merchant, R. R.; Edwards, J. T.; Malins, L. R.; Liu, Z.; Che, G.; Shen, Z.; Shaw, S. A.; Eastgate, M. D.; Baran, P. S. *Angew. Chem., Int. Ed.* **2017,** *56,* 11906–11910. doi:10.1002/anie.201705107
89. Qin, T.; Cornella, J.; Li, C.; Malins, L. R.; Edwards, J. T.; Kawamura, S.; Maxwell, B. D.; Eastgate, M. D.; Baran, P. S. *Science* **2016,** *352,* 801–805. doi:10.1126/science.aaf6123
90. Li, C.; Wang, J.; Barton, L. M.; Yu, S.; Tian, M.; Peters, D. S.; Kumar, M.; Yu, A. W.; Johnson, K. A.; Chatterjee, A. K.; Yan, M.; Baran, P. S. *Science* **2017,** *356,* eaam7355. doi:10.1126/science.aam7355
91. Wang, J.; Shang, M.; Lundberg, H.; Feu, K. S.; Hecker, S. J.; Qin, T.; Blackmond, D. G.; Baran, P. S. *ACS Catal.* **2018,** *8,* 9537–9542. doi:10.1021/acscatal.8b02928
92. Liu, X.-G.; Zhou, C.-J.; Lin, E.; Han, X.-L.; Zhang, S.-S.; Li, Q.; Wang, H. *Angew. Chem., Int. Ed.* **2018,** *57,* 13096–13100. doi:10.1002/anie.201806799
93. Huihui, K. M. M.; Caputo, J. A.; Melchor, Z.; Olivares, A. M.; Spiewak, A. M.; Johnson, K. A.; DiBenedetto, T. A.; Kim, S.; Ackerman, L. K. G.; Weix, D. J. *J. Am. Chem. Soc.* **2016,** *138,* 5016–5019. doi:10.1021/jacs.6b01533
94. Salgueiro, D. C.; Chi, B. K.; Guzei, I. A.; García-Reynaga, P.; Weix, D. J. *Angew. Chem., Int. Ed.* **2022,** *61,* e202205673. doi:10.1002/anie.202205673
95. Huang, L.; Olivares, A. M.; Weix, D. J. *Angew. Chem., Int. Ed.* **2017,** *56,* 11901–11905. doi:10.1002/anie.201706781
96. Kang, K.; Weix, D. J. *Org. Lett.* **2022,** *24,* 2853–2857. doi:10.1021/acs.orglett.2c00805

97. Wang, J.; Cary, B. P.; Beyer, P. D.; Gellman, S. H.; Weix, D. J. *Angew. Chem., Int. Ed.* **2019,** *58,* 12081–12085. doi:10.1002/anie.201906000
98. West, M. S.; Gabbey, A. L.; Huestis, M. P.; Rousseaux, S. A. L. *Org. Lett.* **2022,** *24,* 8441–8446. doi:10.1021/acs.orglett.2c03570
99. Gabbey, A. L.; Michel, N. W. M.; Hughes, J. M. E.; Campeau, L.-C.; Rousseaux, S. A. L. *Org. Lett.* **2022,** *24,* 3173–3178. doi:10.1021/acs.orglett.2c00918
100. Suzuki, N.; Hofstra, J. L.; Poremba, K. E.; Reisman, S. E. *Org. Lett.* **2017,** *19,* 2150–2153. doi:10.1021/acs.orglett.7b00793
101. Polites, V. C.; Badir, S. O.; Keess, S.; Jolit, A.; Molander, G. A. *Org. Lett.* **2021,** *23,* 4828–4833. doi:10.1021/acs.orglett.1c01558
102. Jin, S.; Haug, G. C.; Nguyen, V. T.; Flores-Hansen, C.; Arman, H. D.; Larionov, O. V. *ACS Catal.* **2019,** *9,* 9764–9774. doi:10.1021/acscatal.9b03366
103. Yu, L.; Tang, M.-L.; Si, C.-M.; Meng, Z.; Liang, Y.; Han, J.; Sun, X. *Org. Lett.* **2018,** *20,* 4579–4583. doi:10.1021/acs.orglett.8b01866
104. Gao, L.; Wang, G.; Cao, J.; Yuan, D.; Xu, C.; Guo, X.; Li, S. *Chem. Commun.* **2018,** *54,* 11534–11537. doi:10.1039/c8cc06152a
105. Gao, L.; Wang, G.; Cao, J.; Chen, H.; Gu, Y.; Liu, X.; Cheng, X.; Ma, J.; Li, S. *ACS Catal.* **2019,** *9,* 10142–10151. doi:10.1021/acscatal.9b03798
106. Ishii, T.; Kakeno, Y.; Nagao, K.; Ohmiya, H. *J. Am. Chem. Soc.* **2019,** *141,* 3854–3858. doi:10.1021/jacs.9b00880
107. Kakeno, Y.; Kusakabe, M.; Nagao, K.; Ohmiya, H. *ACS Catal.* **2020,** *10,* 8524–8529. doi:10.1021/acscatal.0c02849
108. Ishii, T.; Ota, K.; Nagao, K.; Ohmiya, H. *J. Am. Chem. Soc.* **2019,** *141,* 14073–14077. doi:10.1021/jacs.9b07194
109. Chen, K.-Q.; Wang, Z.-X.; Chen, X.-Y. *Org. Lett.* **2020,** *22,* 8059–8064. doi:10.1021/acs.orglett.0c03006
110. Chen, X.; Luo, X.; Peng, X.; Guo, J.; Zai, J.; Wang, P. *Chem. – Eur. J.* **2020,** *26,* 3226–3230. doi:10.1002/chem.201905224
111. Mo, Y.; Lu, Z.; Rughoobur, G.; Patil, P.; Gershenfeld, N.; Akinwande, A. I.; Buchwald, S. L.; Jensen, K. F. *Science* **2020,** *368,* 1352–1357. doi:10.1126/science.aba3823
112. Niu, K.; Song, L.; Hao, Y.; Liu, Y.; Wang, Q. *Chem. Commun.* **2020,** *56,* 11673–11676. doi:10.1039/d0cc05391k
113. Liu, Y.; Xue, L.; Shi, B.; Bu, F.; Wang, D.; Lu, L.; Shi, R.; Lei, A. *Chem. Commun.* **2019,** *55,* 14922–14925. doi:10.1039/c9cc08528a
114. Li, H.; Breen, C. P.; Seo, H.; Jamison, T. F.; Fang, Y.-Q.; Bio, M. M. *Org. Lett.* **2018,** *20,* 1338–1341. doi:10.1021/acs.orglett.8b00070
115. Palkowitz, M. D.; Laudadio, G.; Kolb, S.; Choi, J.; Oderinde, M. S.; Ewing, T. E.-H.; Bolduc, P. N.; Chen, T.; Zhang, H.; Cheng, P. T. W.; Zhang, B.; Mandler, M. D.; Blasczak, V. D.; Richter, J. M.; Collins, M. R.; Schioldager, R. L.; Bravo, M.; Dhar, T. G. M.; Vokits, B.; Zhu, Y.; Echeverria, P.-G.; Poss, M. A.; Shaw, S. A.; Clementson, S.; Petersen, N. N.; Mykhailiuk, P. K.; Baran, P. S. *J. Am. Chem. Soc.* **2022,** *144,* 17709–17720. doi:10.1021/jacs.2c08006
116. Harwood, S. J.; Palkowitz, M. D.; Gannett, C. N.; Perez, P.; Yao, Z.; Sun, L.; Abruña, H. D.; Anderson, S. L.; Baran, P. S. *Science* **2022,** *375,* 745–752. doi:10.1126/science.abn1395
117. Gu, J.; Rodriguez, K. X.; Kanda, Y.; Yang, S.; Ociepa, M.; Wilke, H.; Abrishami, A. V.; Jørgensen, L.; Skak-Nielsen, T.; Chen, J. S.; Baran, P. S. *Proc. Natl. Acad. Sci. U. S. A.* **2022,** *119,* e2200814119. doi:10.1073/pnas.2200814119
118. Guo, R.; Witherspoon, B. P.; Brown, M. K. *J. Am. Chem. Soc.* **2020,** *142,* 5002–5006. doi:10.1021/jacs.0c00359
119. Merchant, R. R.; Oberg, K. M.; Lin, Y.; Novak, A. J. E.; Felding, J.; Baran, P. S. *J. Am. Chem. Soc.* **2018,** *140,* 7462–7465. doi:10.1021/jacs.8b04891

License and Terms

BEILSTEIN JOURNAL OF ORGANIC CHEMISTRY

Phenotellurazine redox catalysts: elements of design for radical cross-dehydrogenative coupling reactions

Alina Paffen, Christopher Cremer and Frederic W. Patureau*

Letter

Open Access

Address:
Institute of Organic Chemistry, RWTH Aachen University, Landoltweg 1, 52074 Aachen, Germany

Email:
Frederic W. Patureau* - Frederic.patureau@rwth-aachen.de

* Corresponding author

Keywords:
cross-dehydrogenative coupling; O_2 activation; phenotellurazine; redox catalysis; Te catalysis

Beilstein J. Org. Chem. **2024,** *20,* 1292–1297.
https://doi.org/10.3762/bjoc.20.112

Received: 21 February 2024
Accepted: 06 May 2024
Published: 04 June 2024

This article is part of the thematic issue "Modern radical chemistry".

Guest Editor: H.-M. Huang

Abstract

Redox active phenotellurazine catalysts have been recently utilized in two different cross-dehydrogenative coupling reactions. In this study, we revisit the design of the phenotellurazine redox catalysts. In particular, we investigate the level of cooperativity between the Te- and N-centers, the effect of secondary versus tertiary N-centers, the effect of heterocyclic versus non-heterocyclic structures, and the effect of substitution patterns on the redox catalytic activity.

Introduction

Tellurium catalysis has become increasingly important in recent years. This is due to its unique chalcogen bonding ability, thus enabling the activation of small yet highly relevant organic substrates. For example, Huber and co-authors recently designed a Te-based catalyst in an indole Michael addition reaction [1-5]. Pale and Mamane utilized another Te-based catalyst in an electrophilic bromine-mediated cyclization reaction [6,7], and Gabbaï yet another in a different cyclization reaction [8,9], among other catalytic chalcogen bonding activation examples [10-29]. In contrast, we have reported recently some redox-active Te-based catalysts, which exploit the redox flexibility of tellurium, especially in the context of phenotellurazine scaffolds. Notably, we showed that phenotellurazine **PTeZ1** could significantly catalyze the cross-dehydrogenative phenothiazination of phenols bearing challenging electron-withdrawing substituents under a simple oxygen atmosphere (Scheme 1a) [30-32]. Most recently, we also showed that phenotellurazines could catalyze the oxidative dimerization of indoles, likewise under a simple oxygen atmosphere. 2-Methoxyphenotellurazine **PTeZ2** proved to be the optimal catalyst in the latter case (Scheme 1b) [33].

In the present study, we decided to revisit the design of the phenotellurazine redox catalyst, in the hope of improving it as well as enabling new catalytic reactivity. In particular, we wished to investigate and optimize the level of electronic cooperativity between the Te- and N-centers, the effect of secondary versus tertiary N-centers, the effect of heterocyclic versus non-

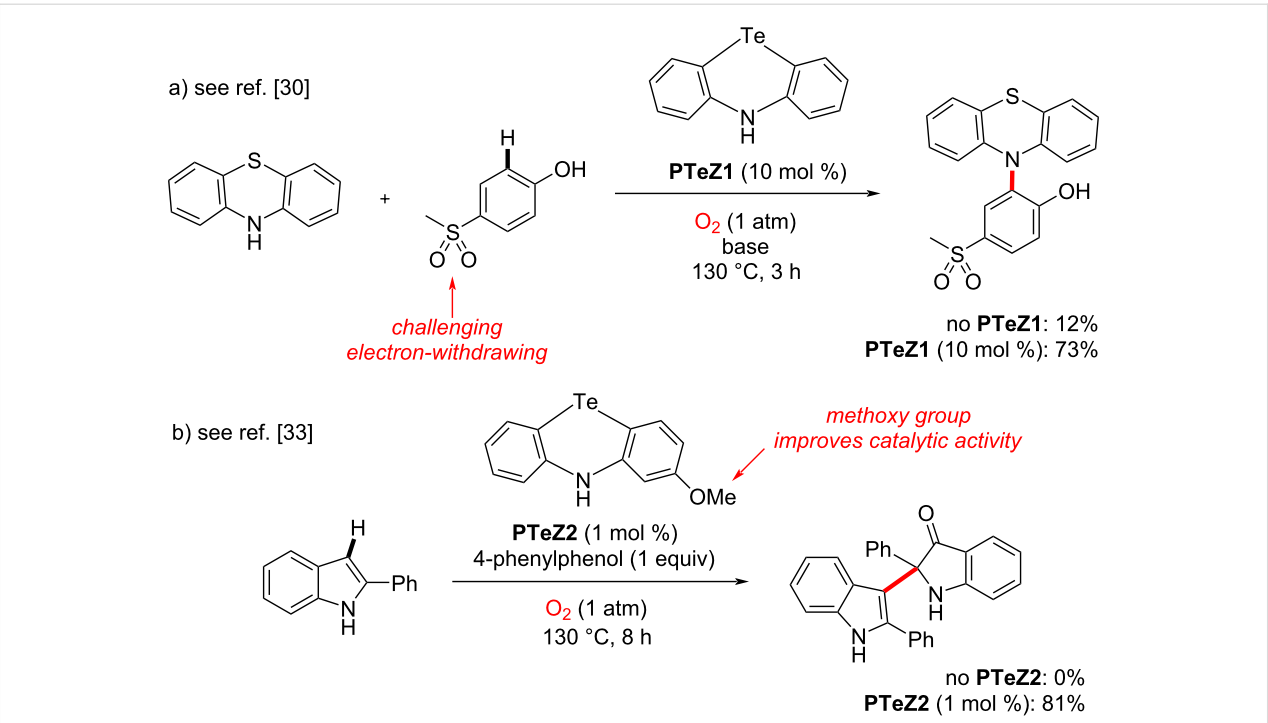

Scheme 1: Phenotellurazine-catalyzed cross-dehydrogenative couplings.

heterocyclic structures, and the effect of various substitution patterns.

Results and Discussion

With this aim in mind, we thus started investigating Te(II) redox catalyst candidates that do not necessarily carry a N-atom in the structure, or else at different positions, in order to establish how their redox catalytic reactivity might be affected. Indeed, we learned recently that amino-arenes possess some level of redox catalytic activity by themselves, in the absence of a Te-center [34], and therefore wished to investigate and optimize their redox contribution within the Te(II) catalysts.

Multiple synthetic efforts were therefore deployed in order to access several key Te(II) targets, both with and without N-functional groups, in heterocyclic as well as in non-heterocyclic fashion. These were then investigated in the Te(II)-catalyzed benchmark dehydrogenative phenothiazination of phenols, a reaction that we discovered in 2015 [35-37], under analogous conditions as previously described [30-32]. The results are summarized in Scheme 2. The multistep synthesis and characterization of all Te-based catalyst candidates can be found in Supporting Information File 1. In the main article we will focus on catalysis results.

We therefore first tested various telluracycle candidates, in particular without an NH bridge (catalyst candidates **PTeZ3**, **Te4**–**Te7**, Scheme 2A). These telluracycles, bridged by very diverse electron-donating or -withdrawing functional groups all featured significantly inferior catalytic activity in the selected benchmark reaction (O_2-mediated dehydrogenative phenothiazination of 4-phenylphenol). It can therefore be deduced that the N-bridging atom is important for catalytic activity. In order to further investigate the matter, we next turned our attention to non-heterocyclic tellurethers **Te8**–**Te13**, bearing various substituents (Scheme 2B). Expectedly, simple diphenyl tellurether **Te8** featured degraded catalytic activity (**3aa**, 55% after 3 h), although this still represents a significantly superior result compared to catalyst-free conditions (**3aa**, 22% after 3 h). Electron π-donating substituents considerably improved catalytic activity, with an optimum among tested structures for **Te10** (**3aa**, 74% after 3 h), which is intriguingly similar to the previously reported best catalyst for this reaction: **PTeZ1** (**3aa**, 73% after 3 h). In other words, the cyclic phenotellurazine character of the catalyst does not seem to be essential in the context of this particular reaction, as opposed to the *ortho/para* substitution pattern of Te- and N-atoms. Nevertheless, all results considered, we elected at this point to keep the cyclic phenotellurazine structure of the catalyst in the hope of increased catalytic robustness, especially in view of further increasing substitution. Next, we therefore tested methoxy-substituted **PTeZ2**, a successful catalyst structure which we recently developed for the cross-dehydrogenative coupling of indoles [33], in the same benchmark reaction. To our satisfaction, **PTeZ2** proved to be

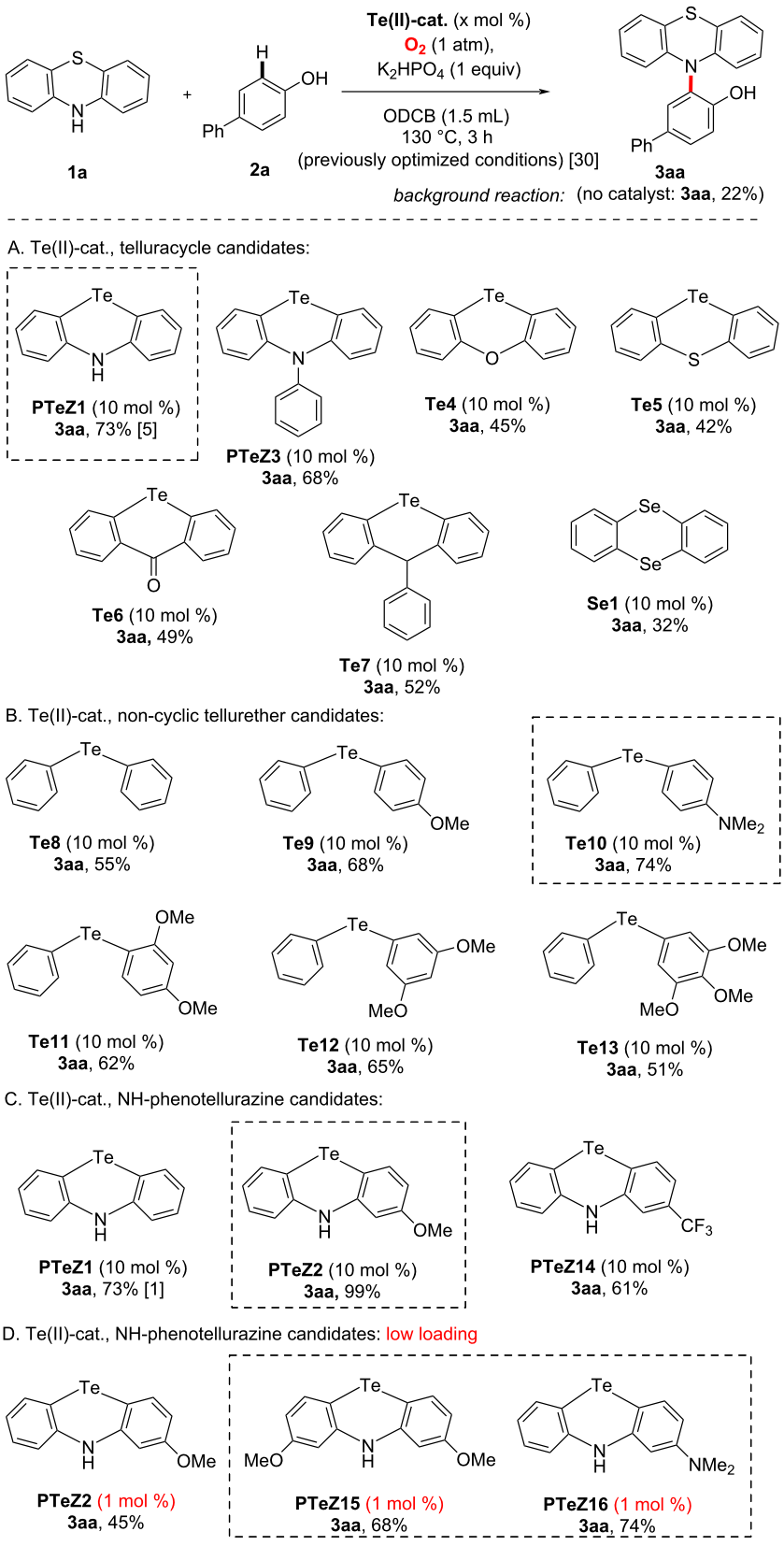

Scheme 2: Screening of new Te(II)-catalyst candidates. ODCB: *ortho*-dichlorobenzene.

the most active catalyst so far in this study (**3aa**, 99% after 3 h). In order to further optimize the catalyst structure, we then reduced the catalytic loading by one order of magnitude, from the standard 10 mol % to only 1 mol %, all other reaction parameters remaining identical. In these considerably more demanding conditions, **PTeZ2** still performed admirably well (**3aa**, 45% at 3 h), significantly better than the non-catalyzed reaction (**3aa**, 22% after 3 h). Going from 2-methoxy towards 2,8-dimethoxy substitution (**PTeZ15**) allowed to significantly increase catalytic activity (**3aa**, 68% after 3 h), still at 1 mol % loading. Encouraged by this trend, which seemed to indicate that the more π-electron-donating substituents increase catalytic activity, we continued structural optimization. Thus, 2-dimethylamino-substituted **PTeZ16** performed even better (**3aa**, 74% after 3 h and 1 mol % loading).

In order to evaluate these new Te-catalysts further, we then turned our attention to the second, arguably more challenging test reaction (Scheme 3). In particular, we hoped that the more π-electron-rich optimized **PTeZ16** (2-dimethylamino substituent) would outperform previously published **PTeZ2** (2-methoxy) in that particular reaction. Unfortunately, this was not the case. At 1 mol % catalytic loading and 8 h reaction time, **PTeZ2** considerably outperforms **PTeZ16** (indole **4a** towards product **5a**, 81 versus 41%, respectively). Intrigued by these results, we also checked yields of product **5a** at only 3 h reaction time for both catalysts. Thus, at shorter reaction time, it transpires that **PTeZ2** and **PTeZ16** perform similarly overall (**5a**, 37 versus 40%, respectively). It can therefore be concluded that while **PTeZ16** (2-dimethylamino) shows promising initial catalytic activity, it is not robust enough to survive the oxidative high temperature conditions for a prolonged period of time. In contrast, as was previously demonstrated in the literature, **PTeZ2** (2-methoxy substituent) features a far greater chemical stability, to such an extent that it could be in large part recovered at the end of the reaction (see previous study) [33]. In other words, **PTeZ2** (2-methoxy substituent) features the best compromise in terms of electronic effects, which affect both the stability and reactivity of the key catalytically active intermediate(s), possibly including chalcogen bonding activation ability of the substrates [38].

Conclusion

In conclusion, we demonstrated the importance of the phenotellurazine scaffold, bearing both a Te(II) center as well as a N-bridge, for redox catalytic activity. However, although the idea of increasing the π-electron-rich character of the phenotellurazine catalyst had seemed very promising at first, our results show that this strategy leads to overall less robust Te(II) catalysts under oxidative reaction conditions. This in turn generally leads to inferior catalytic performance. Our future research efforts in the area of Te(II) catalysis will likely focus on milder coupling reactions on the one hand, and/or on novel more robust and more active ligand designs on the other. In particular, more investigations will likely be needed regarding the optimization of the possible Te-substrate interaction.

Supporting Information

Supporting Information File 1

Experimental section and characterization of synthesized compounds.
[https://www.beilstein-journals.org/bjoc/content/supplementary/1860-5397-20-112-S1.pdf]

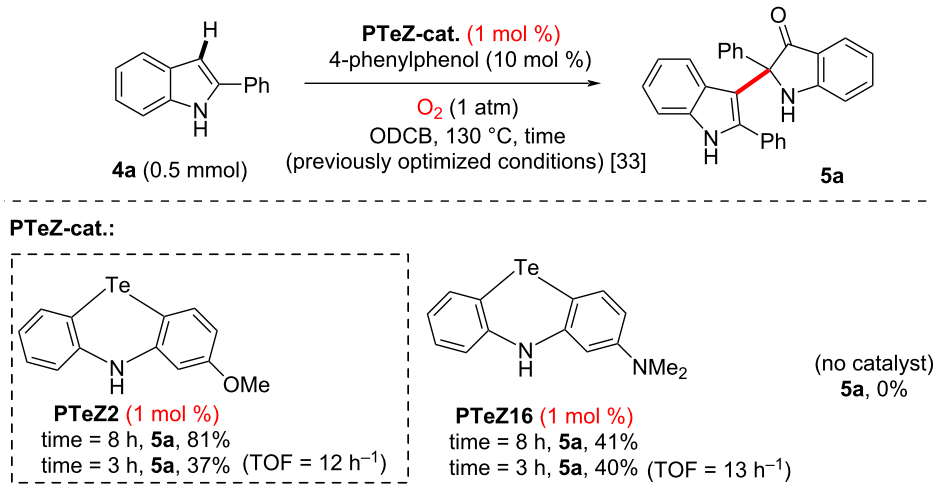

Scheme 3: Phenotellurazine-catalyzed cross-dehydrogenative indole dimerization.

Acknowledgements

Pola A. Hild and Steffen Schauerte, both students at the RWTH Aachen University, are acknowledged for short internships in the group on topics peripherally related to this research.

Funding

DFG-funded transregional collaborative research center SFB/TRR 88 ''Cooperative effects in homo and heterometallic complexes'' (http://3MET.de) is acknowledged for generous financial support.

ORCID® iDs

Alina Paffen - https://orcid.org/0000-0002-7406-1047
Christopher Cremer - https://orcid.org/0000-0002-3484-0505
Frederic W. Patureau - https://orcid.org/0000-0002-4693-7240

Data Availability Statement

All data that supports the findings of this study is available in the published article and/or the supporting information to this article.

References

1. Wonner, P.; Dreger, A.; Vogel, L.; Engelage, E.; Huber, S. M. *Angew. Chem., Int. Ed.* **2019,** *58,* 16923–16927. doi:10.1002/anie.201910639
2. Wonner, P.; Steinke, T.; Vogel, L.; Huber, S. M. *Chem. – Eur. J.* **2020,** *26,* 1258–1262. doi:10.1002/chem.201905057
3. Tarannam, N.; Voelkel, M. H. H.; Huber, S. M.; Kozuch, S. *J. Org. Chem.* **2022,** *87,* 1661–1668. doi:10.1021/acs.joc.1c00894
4. Steinke, T.; Wonner, P.; Gauld, R. M.; Heinrich, S.; Huber, S. M. *Chem. – Eur. J.* **2022,** *28,* e202200917. doi:10.1002/chem.202200917
5. Pal, D.; Steinke, T.; Vogel, L.; Engelage, E.; Heinrich, S.; Kutzinski, D.; Huber, S. M. *Adv. Synth. Catal.* **2023,** *365,* 2718–2723. doi:10.1002/adsc.202300502
6. Weiss, R.; Aubert, E.; Pale, P.; Mamane, V. *Angew. Chem., Int. Ed.* **2021,** *60,* 19281–19286. doi:10.1002/anie.202105482
7. Groslambert, L.; Padilla-Hernandez, A.; Weiss, R.; Pale, P.; Mamane, V. *Chem. – Eur. J.* **2023,** *29,* e202203372. doi:10.1002/chem.202203372
8. Zhou, B.; Gabbaï, F. P. *J. Am. Chem. Soc.* **2021,** *143,* 8625–8630. doi:10.1021/jacs.1c04482
9. Zhou, B.; Gabbaï, F. P. *Organometallics* **2021,** *40,* 2371–2374. doi:10.1021/acs.organomet.1c00279
10. Rettig, I. D.; Van, J.; Brauer, J. B.; Luo, W.; McCormick, T. M. *Dalton Trans.* **2019,** *48,* 5665–5673. doi:10.1039/c9dt00487d
11. Lutkus, L. V.; Rettig, I. D.; Davies, K. S.; Hill, J. E.; Lohman, J. E.; Eskew, M. W.; Detty, M. R.; McCormick, T. M. *Organometallics* **2017,** *36,* 2588–2596. doi:10.1021/acs.organomet.7b00166
12. Oba, M.; Tanaka, K.; Nishiyama, K.; Ando, W. *J. Org. Chem.* **2011,** *76,* 4173–4177. doi:10.1021/jo200496r
13. Okada, Y.; Oba, M.; Arai, A.; Tanaka, K.; Nishiyama, K.; Ando, W. *Inorg. Chem.* **2010,** *49,* 383–385. doi:10.1021/ic9022745
14. Oba, M.; Okada, Y.; Nishiyama, K.; Ando, W. *Org. Lett.* **2009,** *11,* 1879–1881. doi:10.1021/ol900240s
15. You, Y.; Ahsan, K.; Detty, M. R. *J. Am. Chem. Soc.* **2003,** *125,* 4918–4927. doi:10.1021/ja029590m
16. Ahsan, K.; Drake, M. D.; Higgs, D. E.; Wojciechowski, A. L.; Tse, B. N.; Bateman, M. A.; You, Y.; Detty, M. R. *Organometallics* **2003,** *22,* 2883–2890. doi:10.1021/om030232h
17. Kanda, T.; Engman, L.; Cotgreave, I. A.; Powis, G. *J. Org. Chem.* **1999,** *64,* 8161–8169. doi:10.1021/jo990842k
18. Detty, M. R.; Zhou, F.; Friedman, A. E. *J. Am. Chem. Soc.* **1996,** *118,* 313–318. doi:10.1021/ja953187g
19. Engman, L.; Stern, D.; Pelcman, M.; Andersson, C. M. *J. Org. Chem.* **1994,** *59,* 1973–1979. doi:10.1021/jo00087a008
20. Detty, M. R.; Friedman, A. E.; Oseroff, A. R. *J. Org. Chem.* **1994,** *59,* 8245–8250. doi:10.1021/jo00105a049
21. Detty, M. R.; Gibson, S. L. *Organometallics* **1992,** *11,* 2147–2156. doi:10.1021/om00042a031
22. Benz, S.; Poblador-Bahamonde, A. I.; Low-Ders, N.; Matile, S. *Angew. Chem., Int. Ed.* **2018,** *57,* 5408–5412. doi:10.1002/anie.201801452
23. Nakamura, Y.; Yamago, S. *Beilstein J. Org. Chem.* **2013,** *9,* 1607–1612. doi:10.3762/bjoc.9.183
24. Drake, M. D.; Bright, F. V.; Detty, M. R. *J. Am. Chem. Soc.* **2003,** *125,* 12558–12566. doi:10.1021/ja0367593
25. McKee, D. W. *Carbon* **1984,** *22,* 513–516. doi:10.1016/0008-6223(84)90084-8
26. Kolb, S.; Oliver, G. A.; Werz, D. B. *Angew. Chem., Int. Ed.* **2020,** *59,* 22306–22310. doi:10.1002/anie.202007314
27. Haberhauer, G.; Gleiter, R. *Angew. Chem., Int. Ed.* **2020,** *59,* 21236–21243. doi:10.1002/anie.202010309
28. Mehrparvar, S.; Wölper, C.; Gleiter, R.; Haberhauer, G. *Org. Mater.* **2022,** *4,* 43–52. doi:10.1055/a-1883-6076
29. Mehrparvar, S.; Wölper, C.; Haberhauer, G. *Angew. Chem., Int. Ed.* **2023,** *62,* e202304202. doi:10.1002/anie.202304202
30. Cremer, C.; Goswami, M.; Rank, C. K.; de Bruin, B.; Patureau, F. W. *Angew. Chem., Int. Ed.* **2021,** *60,* 6451–6456. doi:10.1002/anie.202015248
31. Cremer, C.; Eltester, M. A.; Bourakhouadar, H.; Atodiresei, I. L.; Patureau, F. W. *Org. Lett.* **2021,** *23,* 3243–3247. doi:10.1021/acs.orglett.1c00573
32. Vemuri, P. Y.; Cremer, C.; Patureau, F. W. *Org. Lett.* **2022,** *24,* 1626–1630. doi:10.1021/acs.orglett.2c00125
33. Cremer, C.; Patureau, F. W. *JACS Au* **2022,** *2,* 1318–1323. doi:10.1021/jacsau.2c00193
34. Nandi, S.; Paffen, A.; Patureau, F. W. *Synlett* **2024,** *35,* 967–972. doi:10.1055/a-2225-8736
35. Louillat-Habermeyer, M.-L.; Jin, R.; Patureau, F. W. *Angew. Chem., Int. Ed.* **2015,** *54,* 4102–4104. doi:10.1002/anie.201500089
    See for the original discovery of the dehydrogenative phenothiazination reaction.
36. Goswami, M.; Konkel, A.; Rahimi, M.; Louillat-Habermeyer, M.-L.; Kelm, H.; Jin, R.; de Bruin, B.; Patureau, F. W. *Chem. – Eur. J.* **2018,** *24,* 11936–11943. doi:10.1002/chem.201800730
    See for the mechanistic investigation of the dehydrogenative phenothiazination reaction.
37. Patureau, F. W. *ChemCatChem* **2019,** *11,* 5227–5231. doi:10.1002/cctc.201900152
    See for an early review on the dehydrogenative phenothiazination reaction.
38. Gleiter, R.; Haberhauer, G.; Werz, D. B.; Rominger, F.; Bleiholder, C. *Chem. Rev.* **2018,** *118,* 2010–2041. doi:10.1021/acs.chemrev.7b00449

BEILSTEIN JOURNAL OF ORGANIC CHEMISTRY

Efficacy of radical reactions of isocyanides with heteroatom radicals in organic synthesis

Akiya Ogawa*,‡[1] and Yuki Yamamoto‡[2]

Perspective

Open Access

Address:
[1]Organization for Research Promotion, Osaka Metropolitan University, 1-1 Gakuen-cho, Nakaku, Sakai, Osaka 599-8531, Japan and [2]Graduate Faculty of Interdisciplinary Research, University of Yamanashi, 4-4-37 Takeda, Kofu 400-8510, Japan

Email:
Akiya Ogawa* - ogawa@omu.ac.jp

* Corresponding author ‡ Equal contributors

Keywords:
aza-Bergman cyclization; heteroatom-mixed system; imidoyl radical; isocyanide; radical addition; radical cyclization

Beilstein J. Org. Chem. **2024,** *20,* 2114–2128.
https://doi.org/10.3762/bjoc.20.182

Received: 08 May 2024
Accepted: 08 August 2024
Published: 26 August 2024

This article is part of the thematic issue "Modern radical chemistry".

Guest Editor: H.-M. Huang

Abstract

Isocyanide is a promising synthetic reagent not only as a one-carbon homologation reagent but also as a nitrogen source for nitrogen-containing molecules. Because of their isoelectronic structure with carbon monoxide, isocyanides also react with nucleophiles, electrophiles, carbon radicals, and transition metal reagents, and are widely used in organic synthesis. On the other hand, the use of isocyanides in reactions with heteroatom radicals is limited. However, the reaction of isocyanides with heteroatom radicals is a promising synthetic tool for the construction of nitrogen-containing organic molecules modified with a variety of heteroatoms. In this Perspective, we review the addition and cyclization reactions of heteroatom radicals with isocyanides and discuss the synthetic prospects of the reaction of isocyanides with heteroatom radicals.

Introduction

Carbon monoxide is a very important C1 resource in both synthetic and industrial chemistry and is not only capable of reacting with a variety of active species such as carbon cations, carbon anions, and carbon radicals (Figure 1), but is also widely used in transition-metal-catalyzed carbonylation reactions [1,2]. However, carbon monoxide is a flammable gas with a wide explosive range, although colorless and odorless, and requires special care in handling due to its high toxicity. In addition, when carbon monoxide is used in a reaction, pressurization in an autoclave or other pressurization device is required to increase the CO concentration.

Isocyanides, on the other hand, have an isoelectronic structure with carbon monoxide and are expected to be not only a promising C1 resource but also an important synthetic reagent for nitrogen-containing compounds [3-7]. Furthermore, by adjusting the substituents on the nitrogen, reactivity can be controlled and solubility in various solvents can be tuned (Figure 2).

However, the use of isocyanide as a C1 resource is somewhat limited compared to that of carbon monoxide [8] because isocyanide is susceptible to multiple imidoylation [9-11],

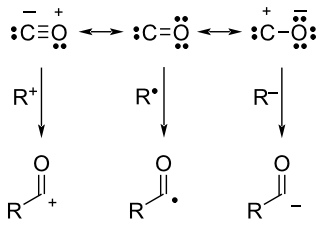

Figure 1: Resonance structures and reactivity of carbon monoxide.

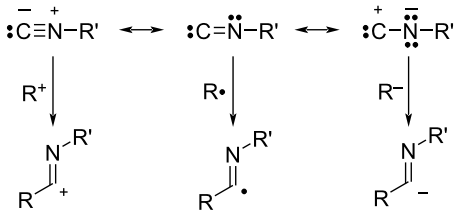

Figure 2: Resonance structures and reactivity of isocyanides.

whereas carbon monoxide is less susceptible to multiple carbonylation. Therefore, precise control of the reaction is required for selective formation of the monoimidoylation product.

Regarding the radical reaction of isocyanides, the reaction of carbon radicals with isocyanides generates imidoyl radicals as key active species [12], and addition and cyclization reactions using these radical species are useful in synthetic organic chemistry, especially multicomponent synthesis. If various functional groups can be appropriately attached to imidoyl units generated in situ by radical addition to isocyanides, innovative molecules with a variety of functions can be obtained. In other words, if functional groups can be prepared simultaneously with the formation of an imidoyl group, it would be an extremely useful method for the synthesis of nitrogen-containing functional molecules. To achieve this goal, it is expected to be effective to develop a new method to react heteroatom radicals with isocyanides to generate imidoyl radicals to which various heteroatom groups are attached and to use them as synthetic reagents. However, systematic studies of addition reactions of heteroatom radicals to isocyanides are still limited. In this perspective paper, we systematically review the addition reactions of heteroatom radicals to isocyanides and discuss prospects.

Discussion

1,1-Addition of heteroatom radicals to isocyanides

Generation of heteroatom radicals

When reacting a heteroatom radical with an isocyanide, the first thing to consider is the method of generating the heteroatom radicals [13-15]. As mentioned above, isocyanides are readily polymerizable molecules, so to suppress the polymerization of isocyanides, it is necessary to understand the conditions for the generation of heteroatom radicals. In addition, from the perspective of recent green chemistry, the development of environmentally friendly synthetic methods is strongly demanded. In other words, a new synthetic method should have excellent atom economy, produce no waste, be aware of resource recycling, and promote the use of natural energy [16].

The following three methods are generally used to generate heteroatom radicals (E•) (Scheme 1). In method 1, E• is generated by hydrogen abstraction from E–H by cyanoisopropyl radicals generated by thermal decomposition of 2,2'-azobis(isobutyronitrile) (AIBN). Then, E• adds to isocyanide **1** to form imidoyl radical **2**, which abstracts hydrogen from E–H. The addition reaction proceeds by a radical chain mechanism, producing the 1,1-addition product **3** with regeneration of E•. In method 2, E• is generated by homolysis of a heteroatom–heteroatom bonded compound (E–E) upon heating or photoirradiation.

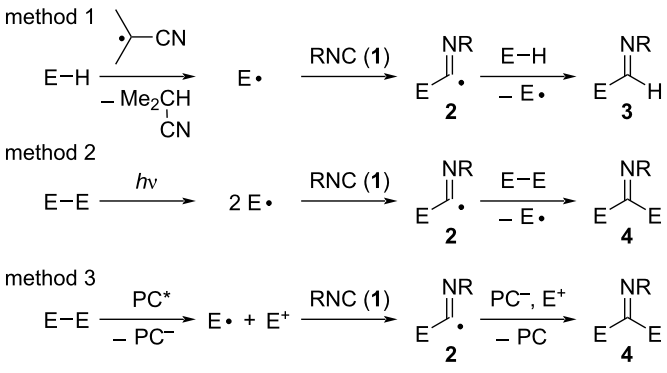

Scheme 1: Possible three pathways of the E• formation for imidoylation.

Similarly, E• adds to **1** to form **2**, which undergoes atom (or group)-transfer from E–E to give the 1,1-addition product **4** with regeneration of E• [17,18]. In method 3, the photoinduced redox reaction of a heteroatom compound takes place using metal complex or functional dye as a photocatalyst (PC) [19,20]. Recently, some important reviews summarize and discuss the use of method 3 in synthetic organic chemistry [21,22]; in contrast, there is little detailed and coherent literature on the overall research trends regarding the latest research on molecular transformations by the reactions of heteroatom radicals with isocyanides using methods 1 and 2. Thus, in this perspective, we mainly focused on the use of method 1 and method 2 for the generation of heteroatom radicals and the reactivity of them with isocyanides.

Among these three methods, methods 1 and 3 require the addition of a radical initiator and a photocatalyst, respectively. In contrast, method 2 does not require any additive, although, if the heating or photoirradiation is performed by electricity, the combustion of fossil fuels may cause environmental pollution. However, when using sunlight, which is an inexhaustible natural energy, it is expected to be the most environmentally friendly method.

The homolysis of E–E upon visible light irradiation is induced by exciting one electron of the isolated electron pair on E to the anti-bonding orbital of the E–E-bond (σ* orbital). Such an n–σ* transition usually indicates the maximum absorption in the near-UV region, and the absorption cutoff reaches the visible region, especially in the case of highly periodic E–E. Therefore, interelement compounds E–E with groups 15–17 heteroatoms have isolated electron pairs, and E• can be generated by photoirradiation. On the other hand, the photoinduced homolysis of groups 13 and 14 interelement compounds with B–B, Si–Si, Sn–Sn bonds, etc. is generally impossible, because such E–E compounds have no isolated electronic pair. Therefore, the use of a photocatalyst (method 3) or the combination with groups 15–17 interelement compounds would be considered effective for the generation of groups 13 and 14 heteroatom radicals.

Radical addition of group 17 compounds to isocyanides

If isocyanides (RNC) can undergo a radical addition of hydrogen halides (HX) and molecular halogens (X_2), 1,1-addition products RN=CH-X, **3** (E = X: F, Cl, Br, I) and RN=CX_2, **4** (E = X), respectively, could be formed. In practice, however, very few examples of such radical addition to isocyanides are known, and the 1,1-addition products **3** and **4** have usually been synthesized by ionic reactions. 1,1-Addition of molecular bromine to phenyl isocyanide was reported by E. Kühle et al. to afford the corresponding 1,1-adduct (PhN=CBr_2) [23]. Since dichloro compounds (RN=CCl_2) [24] are the imino derivatives of highly toxic phosgene (O=CCl_2), reactions using them as key intermediates are not safe synthetic methods. For these reasons, it is no exaggeration to say that radical reactions of group 17 interelement compounds with isocyanides have hardly been developed.

Upon exposure to near-UV light, perfluoroalkyl iodides (R_FI) undergo homolysis to form perfluoroalkyl radicals (R_F•) and iodine radical (I•). The perfluoroalkyl radical, as a carbon radical, rather than iodine radical can add to isocyanides to form imidoyl radicals. Then, the iodine atom of R_FI can trap the imidoyl radicals to give the corresponding 1,1-adducts (R–N=C(I)–R_F) in good yields [25,26].

Radical addition of group 16 compounds to isocyanides

In a pioneering study, Ito and Saegusa et al. reported the radical addition of thiols to isocyanides (Scheme 2) [27]. Thermal decomposition of AIBN as a radical initiator generates the 2-cyano-2-propyl radical ((NC)$(CH_3)_2$C•), which abstracts hydrogen from the thiol (R'SH) to form the thiyl radical (R'S•). The formed R'S• adds to isocyanide (RNC) to generate imidoyl radical intermediate **2** (E = R'S), which abstracts hydrogen from thiol to give the corresponding thioformimidate **3** (E = R'S) with regeneration of R'S•. Thus, the hydrothiolation of isocyanides with thiols proceeds by the radical chain mechanism. In the case of tertiary alkanethiols and arylmethanethiols, the corresponding imidoyl radicals **2** decompose to give tertiary alkyl and benzylic radicals, respectively, to form isothiocyanates **5**.

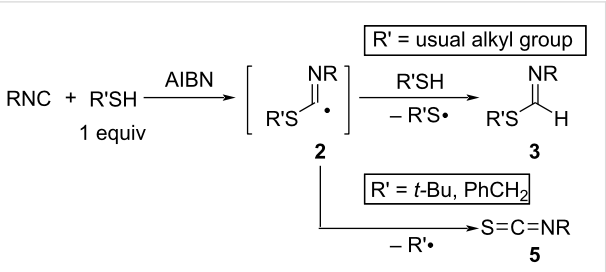

Scheme 2: Radical addition of thiols to isocyanides.

On the other hand, we have investigated the radical addition of diphenyl disulfide to isocyanides under photoirradiation. The photoinduced radical addition of the disulfide to aliphatic isocyanides hardly proceeds, whereas the radical addition to aromatic isocyanides proceeds under high concentration conditions using excess amounts of $(PhS)_2$, selectively yielding 1,1-addition product **4** (R = 2,6-xylyl, E = PhS) [28]. In the case of aromatic isocyanides, the 1,1-addition reaction is probably more

likely to proceed because the C–N double bond of the 1,1-addition product **4** (R = Ar, E = PhS) is conjugated to the aromatic ring, which stabilizes it compared to the corresponding adduct with aliphatic isocyanides. Because of this conjugation, the aromatic ring at the N of the 1,1-addition product **4** (R = Ar, E = PhS) geometrically isomerizes faster than the NMR timescale, so that the two thio groups of **4** are observed to be equivalent in NMR spectroscopy.

In the case of diphenyl diselenide as a representative organic diselenide, the addition of PhSe• to alkenes proceeds 10 to 50 times slower than PhS• [29]. For this reason, the addition of $(PhSe)_2$ to isocyanides, whether aliphatic or aromatic, rarely proceeds. The exception is the addition to *p*-nitrophenyl isocyanides, which does proceed, but this is because the electron-withdrawing group improves the stability of the product **4** (R = *p*-O_2N-C_6H_4, E = PhSe) and also because phase separation is caused by the product precipitation from the reaction solution. On the other hand, the addition reaction of $(PhTe)_2$ to isocyanides does not proceed at all [30]. This is because the addition product **4** (E = PhTe) is unstable under photoirradiation conditions.

The photoinduced 1,1-dithiolation reaction of isocyanides required an excess of $(PhS)_2$ due to the low carbon radical capturing ability of $(PhS)_2$ ($k_S = 7.6 \times 10^4$ $M^{-1}s^{-1}$). In contrast, the carbon radical capturing ability of $(PhSe)_2$ ($k_{Se} = 1.2 \times 10^7$ $M^{-1}s^{-1}$) is known to be ca. 160 times higher than that of $(PhS)_2$ [31]. Therefore, we investigated the radical addition to isocyanides using a disulfide–diselenide binary system under photoirradiation and found that the thioselenation of aromatic isocyanides proceeded efficiently to afford the corresponding thioselenation products **6** (Scheme 3a).

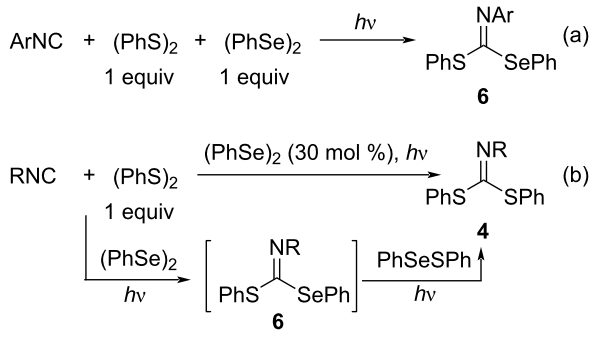

Scheme 3: Selective thioselenation and catalytic dithiolation of isocyanides.

More interestingly, it was found that the thioselenation of aliphatic isocyanides also proceeds in the initial stage of the reaction, but the formed thioselenation products **6** were gradually converted to the dithiolation products **4** under photoirradiation conditions (Scheme 3b). Thus, it was shown that the photoirradiated dithiolation of aliphatic isocyanides with $(PhS)_2$ proceeded as a catalytic reaction of $(PhSe)_2$ (30 mol %). In the dithiolation products **4** from aliphatic isocyanides, two PhS-groups were observed non-equivalently, suggesting the lack of geometrical isomerization of the C–N double bond of the dithiolation products [32].

The thioselenation product **6'**, an imine derivative, can be converted to a β-lactam derivative by [2 + 2] cycloaddition with ketene generated in situ. For example, thioselenation of RNC (R = $(EtO)_2P(O)$–CH_2) gave imine **6'** (96%), which underwent [2 + 2] cycloaddition with methoxyketene to afford β-lactam derivative **7** (79%) (Scheme 4). Selective replacement of the PhSe group of **7** with a 3-butanonyl group (34%) and the subsequent intramolecular Horner–Emmons reaction successfully led to carbacephem skeleton **8** (96%).

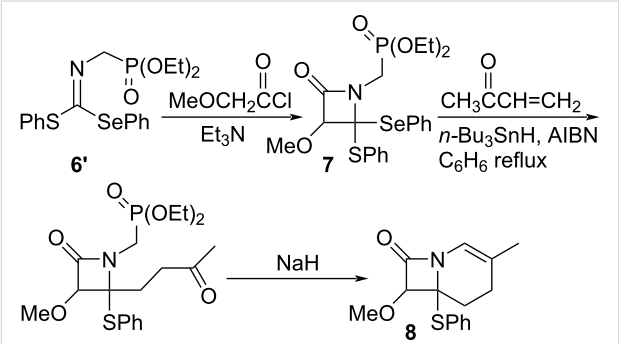

Scheme 4: Synthesis of carbacephem framework.

Since it is known that the carbon radical capturing ability of $(PhTe)_2$ is even four times higher than that of $(PhSe)_2$ [31], we investigated the radical addition to isocyanides using a disulfide–ditelluride binary system under photoirradiation. The visible-light-irradiated thiotelluration reaction did not proceed at all for normal isocyanides, but for aromatic isocyanides with electron-withdrawing groups (EWG) such as *p*-NO_2, *p*-CF_3, *p*-CN, *p*-Cl, and *m*-MeO, the desired thiotelluration reaction proceeded under visible light irradiation to successfully afford the corresponding thiotelluration products **4** (R = EWG-C_6H_4, E = PhS and PhTe) in moderate to high yields [30].

Very few examples of intermolecular cascade reactions with imidoyl radicals as key intermediates have been reported. The intermolecular cascade reaction of diselenide, electron-deficient acetylene, and isocyanide under photoirradiation yields the sequential addition products **9** in moderate to excellent yields (Scheme 5) [33]. The product can be used as a precursor for the carbapenem scaffold, one of the basic scaffolds of antibiotics.

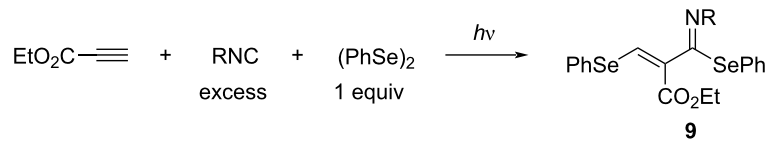

Scheme 5: Sequential addition of $(PhSe)_2$ to ethyl propiolate and isocyanide.

Thermal or photoirradiated decomposition of organotellurium compounds generates carbon radicals that can add to isocyanides to form the imidoyl radicals. In this reaction, telluro radicals (ArTe•) also forms in situ, but the relative reactivity of them toward isocyanides might be very low. In addition, dimerization of ArTe• to $(ArTe)_2$ is very fast, and therefore, the ArTe-substituted imidoyl radical (ArTe-C•(=NR')) could not be observed. However, the tellurium group of RTeAr can successfully trap the imidoyl radicals to yield the corresponding isocyanide-inserted organotellurium compounds (Scheme 6) [34-36].

Radical addition of group 15 compounds to isocyanides

Tetrakis(trimethylsilyl)hydrazine ($(Me_3Si)_2N–N(SiMe_3)_2$, **10**) undergoes ultraviolet light-induced homolysis of the N–N single bond of **10** to form bis(trimethylsilyl)aminyl radical ($(Me_3Si)_2N•$, **11**). The aminyl radical **11** adds to *tert*-butyl isocyanide to form the corresponding imidoyl radical **2** (R = *t*-Bu, E = $(Me_3Si)_2N$), as confirmed by ESR measurement [37].

Similar to the thiol addition to isocyanides, disubstituted phosphines (R'_2PH) induce radical addition to isocyanides in the presence of AIBN as a radical initiator yielding the corresponding iminoformyl phosphines, $R'_2P–CH=NR$, (**12**, R = c-C_6H_{11} or *n*-C_6H_{11}, E = Et_2P) in good yields. In the case of *tert*-butyl and benzyl isocyanides, the substituents on the nitrogen of imidoyl radical **2** (R = *t*-Bu or $PhCH_2$, E = Et_2P or Ph_2P) were eliminated to give cyanophosphines ($R'_2P–CN$, Scheme 7) [38].

On the other hand, we attempted a photoinduced addition of phosphorus–phosphorus interelement compounds such as $Ph_2P–PPh_2$ and $Ph_2P(S)–PPh_2$ to phenyl isocyanide, but the addition did not proceed at all. This is most likely due to the bulkiness of the Ph_2P and $Ph_2P(S)$ groups (Scheme 8) [39].

In sharp contrast, the addition of a germyl phosphine ($Et_2P–GeEt_3$) to phenyl isocyanide was reported to give the corresponding 1,1-adduct ($Et_2P–C(=NPh)–GeEt_3$, **13**) in 46% yield [40]. Similarly, $Me_2N-SnMe_3$ was known to add to *p*-tolyl isocyanide to give $Me_2N–C(=N–C_6H_4–p\text{-}Me)–SnMe_3$ (**14**) in good yield [41]. However, the authors did not specify whether the addition reactions proceeded by a radical or ionic mechanism.

Radical addition of group 14 compounds to isocyanides

Group 14 compounds with an E–H or E–E bond (E = Si, Ge, Sn) have no lone-pair electrons and therefore cannot generate group 14 heteroatom radicals by homolysis via the n–σ* transition. To generate group 14 heteroatom radicals, the hydrogen abstraction reaction from tin hydride or hydrosilane by radical initiators such as AIBN has effectively been used. When tin and silyl radicals generated in this way are reacted with isocyanides, they are more susceptible to steric hindrance than group 16 or

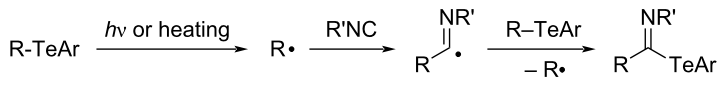

Scheme 6: Isocyanide insertion reaction into carbon-tellurium bonds.

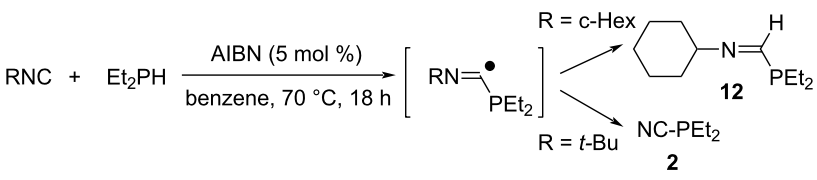

Scheme 7: Radical addition to isocyanides with disubstituted phosphines.

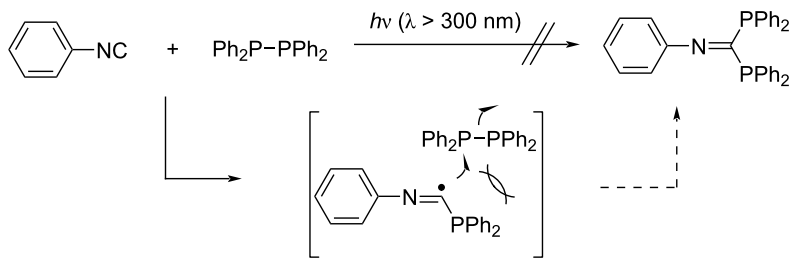

Scheme 8: Radical addition to phenyl isocyanides with diphosphines.

15 heteroatom radicals due to the greater number of substituents on the heteroatom. For this reason, the 1,1-addition is less likely to proceed as with group 16 or 15 heteroatom radicals. In the case of stannyl and silyl radicals, the alkyl group of the isocyanide is eliminated as an alkyl radical from the imidoyl radical intermediate **2** [42]. The formed alkyl radicals abstract hydrogen from the tin hydride or hydrosilane, and the reduction reaction proceeds with the concomitant formation of stannyl or silyl cyanide **15** as byproducts (Scheme 9a) [38,43].

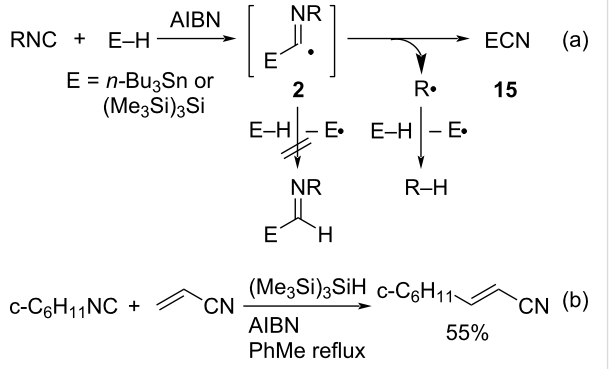

Scheme 9: Radical reaction of tin hydride and hydrosilane toward isocyanide.

In the presence of acrylonitrile, the formed alkyl radical can add to acrylonitrile, affording the addition product (c-$C_6H_{11}CH_2CH_2CN$) after hydrogen abstraction from tris(trimethylsilyl)silane (TTMSS, $(Me_3Si)_3SiH$) (Scheme 9b) [44]. Triethylsilane (Et_3SiH), one of the most popular hydrosilanes, has a strong Si–H bond (90 kcal/mol), and therefore the radical-chain reaction using Et_3SiH is often difficult to perform. In contrast, tris(trimethylsilyl)silane, $(Me_3Si)_3SiH$, has a bond dissociation energy similar to that of *n*-Bu_3SnH (74 kcal/mol) and can be used as an efficient reducing agent/mediator.

Radical addition of group 13 compounds to isocyanides

Boron, a group 13 typical element, also lacks a non-covalent electron pair, making it impossible to generate boron radicals by homolysis via the n–σ* transition. In addition, since boron has an empty orbital, it forms ate complexes when Lewis base compounds coexist. As the result, the boryl groups of the ate complexes are bulky and often cause steric hindrance. However, several examples of isocyanide insertion reactions into B–H and B–B bonds are known. For example, isocyanides coordinate to diborane (B_2H_6) or trialkylboranes (BR'_3) to form Lewis acid–base complexes (RNC→BH_3 or RNC→BR'_3), but these complexes are thermally labile, and hydrogen or alkyl groups on boron are 1,2-shifted to the isocyanide carbon, yielding the compounds (H_2B-C(=NR)-H or R'_2B-C(=NR)-R') with the isocyanide inserted between the B–H or B–alkyl bond [45,46]. The insertion products easily underwent dimerization to afford 2,5-diboradihydropyrazine derivatives **16** (Scheme 10a). Since this 1,2-shift reaction proceeds under mild conditions and in the absence of a radical initiator, it is thought to proceed by an ionic rather than a radical mechanism.

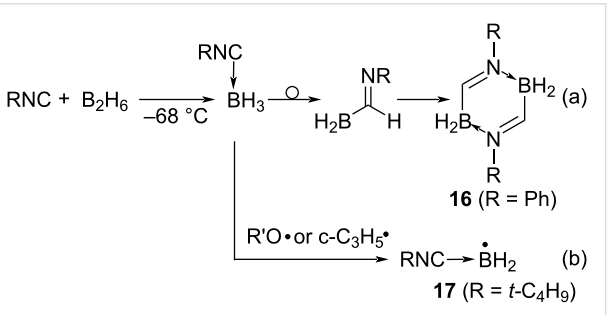

Scheme 10: Isocyanide insertion into boron compounds.

Alkoxy and cyclopropyl radicals, which are more reactive than the usual alkyl radicals, are capable of abstracting hydrogen from Lewis acid–base complexes (*t*-BuNC→BH_3) to generate the corresponding isocyanide–boryl radicals **17** (*t*-BuNC→BH_2•), which can be observed by ESR (Scheme 10b) [47]. However, the synthetic application of this boryl radical has not been investigated.

Among the cyclic diboron compounds, a series of five-membered cyclic diboron compounds **18** undergo an insertion reac-

tion of isocyanides into the boron–boron single bond of **18** under mild conditions without the addition of any additives (Scheme 11a) [48]. The reaction is thought to proceed by an ionic mechanism.

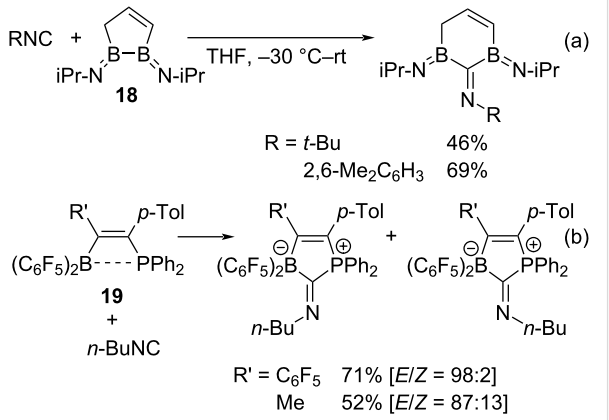

Scheme 11: Isocyanide insertion into cyclic compounds containing boron units.

Recently, several insertion-type reactions of isocyanides into diboron compounds have been reported to proceed by an ionic mechanism [49,50]. As an interesting example, a frustrated Lewis ion pair **19** consisting of a boryl and a phosphinyl group undergoes an isocyanide insertion reaction (Scheme 11b) [51,52]. As described above, the isocyanide insertion reaction into B–H or B–B bonds has been reported, but the reactions by a radical mechanism are largely unknown.

Very recently, Turlik and Schuppe reported a novel generation of nucleophilic boryl radicals using hydrogen atom transfer (HAT) and photoredox catalysis. Furthermore, its reaction with isocyanides forms boron-substituted imidoyl radical intermediates and rapid β-scission then causes elimination of the substituents on the nitrogen (Scheme 12) [53].

Radical cyclization via formation of imidoyl radical species

In the former chapter, we discussed 1,1-addition reactions of typical element compounds to isocyanides using imidoyl radicals as key intermediates. However, as the number of substituents on typical elements increases, intermolecular 1,1-addition reactions become more difficult due to the increase in steric hindrance. Therefore, it is expected that intramolecular cyclization of imidoyl radicals will be possible by introducing an unsaturated group at an appropriate position in the isocyanide molecule, since intramolecular reactions are generally 10^3 times faster than intermolecular reactions. This chapter discusses the intramolecular radical cyclization reactions of isocyanides with alkenyl, alkynyl, aryl, and isocyano groups as unsaturated groups.

Intramolecular cyclization of *ortho*-alkynylaryl- or *ortho*-alkenylaryl isocyanides

Fukuyama et al. reported that the reaction of an aryl isocyanide with an alkenyl group at the *ortho*-position with tin hydride in the presence of AIBN generates a stannylated imidoyl radical **20**. The subsequent 5-*exo* cyclization, hydrogen abstraction

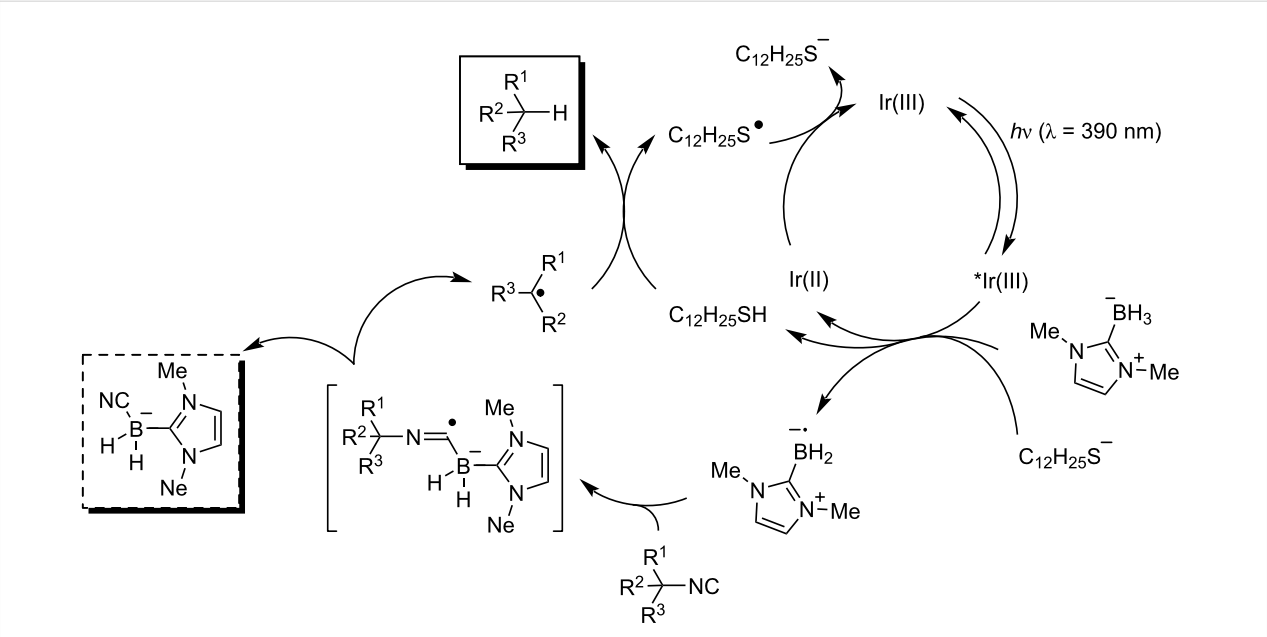

Scheme 12: Photoinduced hydrodefunctionalization of isocyanides.

from *n*-Bu_3SnH, and aromatization successfully afforded the stannylated indole derivative **21** (Scheme 13) [8,54-56]. The stannyl group of **21** could be transferred to aryl or vinyl group by cross-coupling reaction.

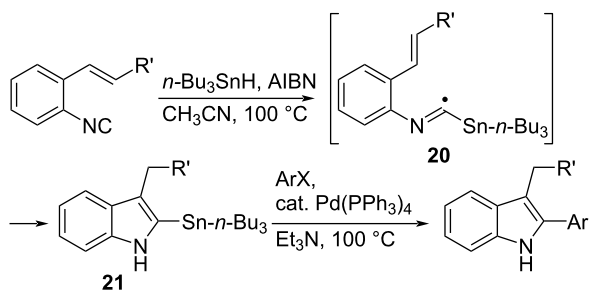

Scheme 13: Tin hydride-mediated indole synthesis and cross-coupling.

At the same time, Bachi et al. succeeded in synthesizing a 5-membered nitrogen-containing heterocycle based on the 5-*exo* cyclization of isocyanides with alkenyl or alkynyl groups using thiols as mediators (Scheme 14) [57].

The generated thiyl radical attacks the isocyano group and forms imidoyl radical, which induces *5-exo* cyclization. The following hydrogen abstraction, intramolecular ionic cyclization, and hydrolysis during chromatography on silica gel affords the cyclic amide in good yield. They further applied this radical cyclization reaction as a key step in the synthesis of (±)-α-kainic acid [58].

Rainier et al. reported the thiol-mediated 5-*exo* cyclization of *o*-alkynylaryl isocyanides, which successfully afforded dithiolated indoles **22** (Scheme 15) [59]. However, depending on the reaction conditions, quinoline derivatives were also produced as byproducts (vide infra).

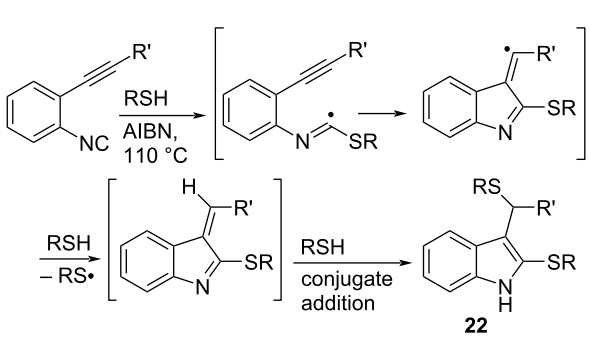

Scheme 15: Thiol-mediated radical cyclization of *o*-alkenylaryl isocyanide.

The photoinduced reaction of *o*-ethenylaryl isocyanides with disulfides in the presence of diphenyl ditelluride yields the corresponding dithiolated indole derivatives **23** (Scheme 16) [60]. Initially, the thiotelluration products via 5-*exo* cyclization are formed in situ. The subsequent aromatization followed by photoinduced displacement of the PhTe group with the PhS group afford **23**. Furthermore, the photoinduced reaction of *ortho*-ethenylaryl isocyanides with bis(2-aminophenyl) disulfides affords tetracyclic compounds **24** in a single step.

Not only alkynyl and alkenyl groups, but also heteroatom moieties such as azido and sulfide groups can intramolecularly capture imidoyl radicals generated in situ, yielding the corresponding benzoimidazoles and benzothiazoles, respectively (Scheme 17). Upon treatment with $Mn(OAc)_3{\cdot}H_2O$, diphenylphosphine oxide ($Ph_2P(O)H$) and organoboron reagents ($ArB(OH)_2$) generate $Ph_2P(O)$• and Ar•, respectively, which add to isocyanides to form the imidoyl radicals. The capture of the imidoyl radicals with the azido group proceeds with the release of N_2, and the amino radical formed abstracts hydrogen from the surroundings (Scheme 17a and 17b) [61]. The imidoyl radical formed by the addition of $Ph_2P(O)$• to isocyanide can

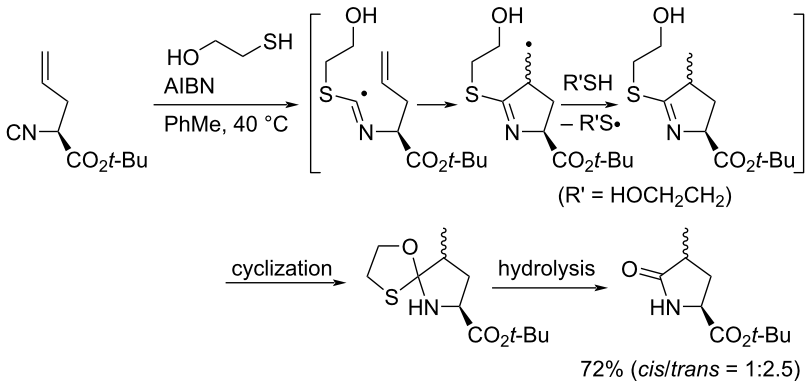

Scheme 14: 2-Thioethanol-mediated radical cyclization of alkenyl isocyanide.

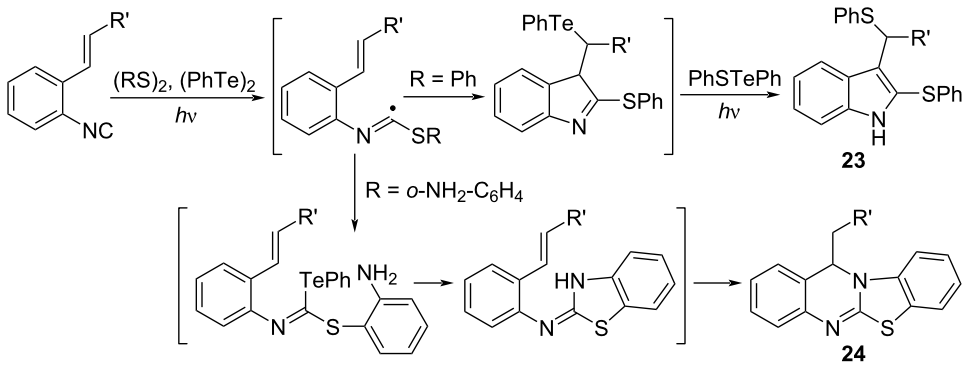

Scheme 16: $(PhTe)_2$-assisted dithiolative cyclization of *o*-alkenylaryl isocyanide.

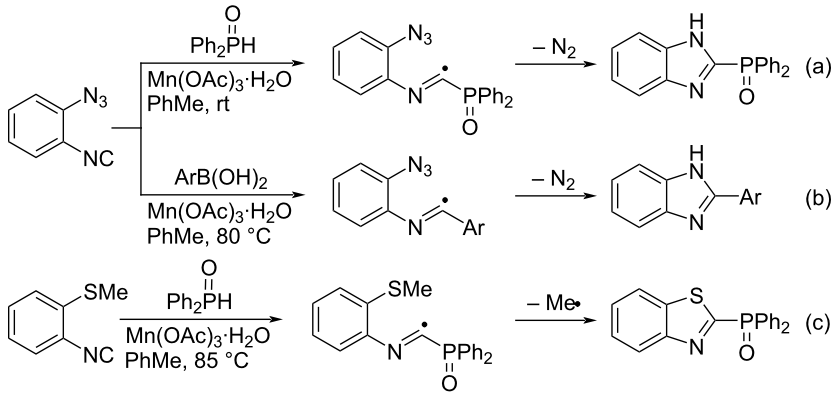

Scheme 17: Trapping imidoyl radicals with heteroatom moieties.

also be trapped intramolecularly by the methylthio group (Scheme 17c) [62].

In the case of 1,2-diisocyanoarenes, the quinoxaline synthesis can be achieved via radical cyclization of imidoyl radical species, which proceeds by intramolecular capture with the *o*-isocyano group (Scheme 18) [63-66].

The iodoperfluoroalkylation with radical cyclization of *ortho*-diisocyanoarenes proceeded efficiently by using AIBN as initiator or using a hexabutyldistannane under visible light irradiation to afford the quinoxaline derivative **25** in good yields (Scheme 18a) [63]. At the same time, a similar quinoxaline synthesis was reported to proceed by irradiation with visible light in the presence of dibenzylamine ($(PhCH_2)_2NH$, MeCN, rt, blue LED) [64]. This reaction involves a visible-light-induced single electron transfer (SET) process. An efficient radical cascade cyclization has also been reported, in which a wide-range of 2-phosphoryl-substituted quinoxalines **26** were prepared in one pot via reaction of *ortho*-diisocyanoarenes with diarylphosphine oxides in the presence of $AgNO_3$ (Scheme 18b) [65]. Chalcogen compounds such as PhSH and $(PhSe)_2$ can be used as chalcogeno radical sources for the photoinduced radical cyclization of *ortho*-diisocyanoarenes to afford the corresponding 2-thiolated and 2,3-diselenated quinoxaline derivatives (e.g., **27**), respectively (Scheme 18c) [66]. Although diphosphines such as $(Ph_2P)_2$ and $Ph_2P(S)PPh_2$ did not intermolecularly add to isocyanides under radical reaction conditions (as mentiond above), they worked well for the photoinduced radical cyclization of *o*-diisocyanoarenes (Scheme 18d) [39]. The obtained quinoxaline-2,3-diphosphines **28** are promising ligands for transition metal catalysts such as palladium catalysts.

Aza-Bergman cyclization of *o*-alkynylaryl isocyanates

In the case of *o*-alkenyl isocyanides, it has already been described that the 5-*exo* cyclization reaction proceeds selectively, yielding nitrogen-containing 5-membered cyclic products. In sharp contrast, when the photoirradiated reaction of *ortho*-alkynyl isocyanides was carried out, we found that an electrocyclization reaction, the aza-Bergmann cyclization, takes place, selectively yielding nitrogen-containing 6-membered cycliza-

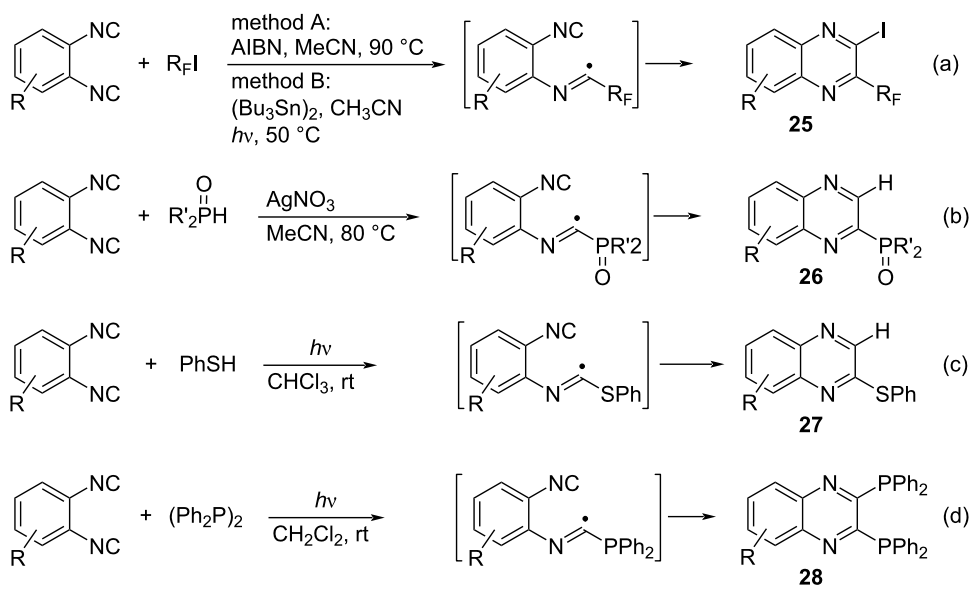

Scheme 18: Trapping imidoyl radicals with isocyano group.

tion products (Scheme 19) [67]. The aza-Bergmann cyclization of *ortho*-alkynyl isocyanides proceeds under milder conditions than the Bergmann cyclization of endiynes, forming quinoline-2,4-biradical intermediates. When diselenide, ditelluride, and diiodide are used as radical mediators, seleno, telluro, and iodo groups are introduced at the 2,4-positions of the quinoline, respectively [68-70].

On the other hand, in the case of germyl hydride, hydrosilane (TTMSS), selenol, and aliphatic thiols, hydrogen abstraction reaction by quinoline-2,4-biradical intermediates occurred to give 2,4-hydrogenated quinolines [69]. In the case of aromatic thiols, the ionic cycloaddition reaction proceeds to give 2-thiolated quinoline derivatives. In addition, the aza-Bergman cyclization can be thermally induced [71].

Radical cyclization of 2-isocyanobiarenes

The cycloaddition reaction with 2-isocyanobiaryls **29** under radical conditions is an excellent synthetic method for nitrogen-containing fused heterocycles such as phenanthridine derivatives **31** (Scheme 20) [72,73]. The reaction proceeds by addition of radical species to the isocyano group of **29** to form

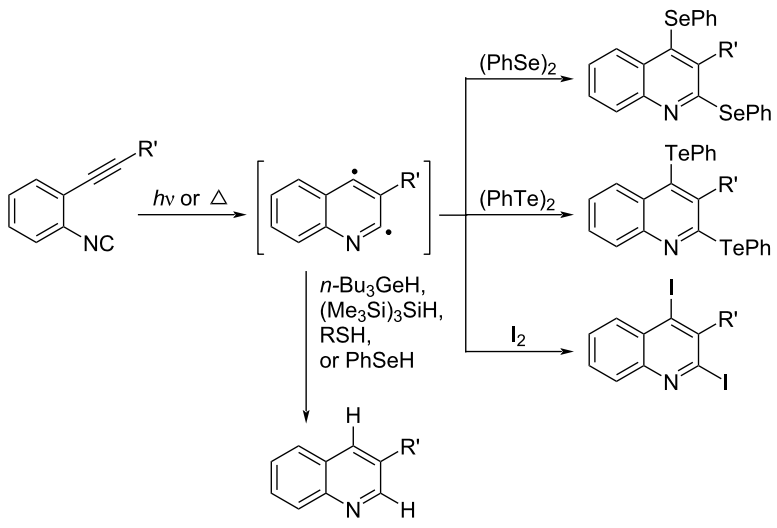

Scheme 19: Quinoline synthesis via aza-Bergman cyclization.

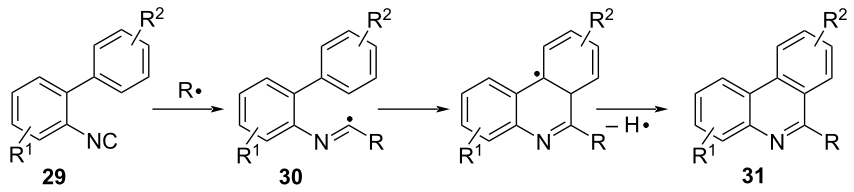

Scheme 20: Phenanthridine synthesis via radical cyclization of 2-isocyanobiaryls.

the imidoyl radical **30** as a key intermediate, which adds intramolecularly to the *ortho*-aryl group. The subsequent aromatization with the release of hydrogen (or proton) affords **31** in good yields.

Nanni et al. reported the reaction of 2-isocyanobiphenyl with AIBN or dibenzoyl peroxide (DBP) affords 6-cyanoisopropyl- or 6-phenyl-substituted phenanthridine derivatives. When the reaction was performed in the presence of TTMSS and AIBN, 6-tris(trimethylsilyl)-substituted phenanthridine derivatives were mainly obtained (Scheme 21) [74].

Tobisu and Chatani et al. reported that a carbon radical generated by the reaction of $RB(OH)_2$ with $Mn(acac)_3$, added to isocyano groups, is leading to intramolecular cyclization with an *ortho*-aryl group. The formed aryl radical is oxidized by $Mn(acac)_3$ to convert into an aryl cation, which can be deprotonated to synthesize tricyclic pyridine derivatives in a single step (Scheme 22) [75].

Zhang and Yu et al. also developed a cyclization of 2-isocyanobiaryls using a photoredox system [76-80] in which carbon radicals were generated by a photoredox reaction of α-bromopropanoates under visible light irradiation (Scheme 23) [81].

After these pioneering reports mentioned above, many examples of cyclization of 2-isocyanobiaryls using a metal-assisted

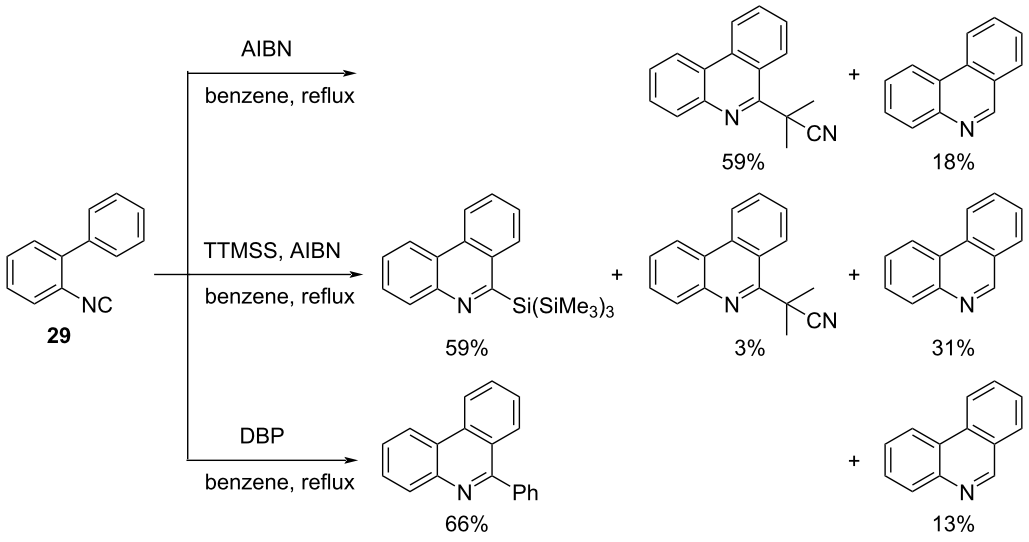

Scheme 21: Phenanthridine synthesis by radical reactions with AIBN, DBP and TTMSS.

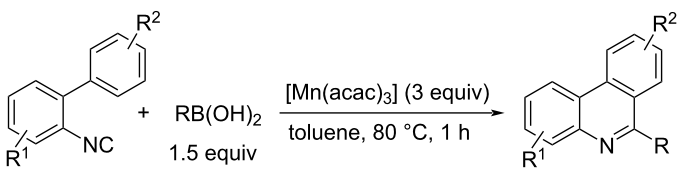

Scheme 22: Phenanthridine synthesis by oxidative cyclization of 2-isocyanobiaryls.

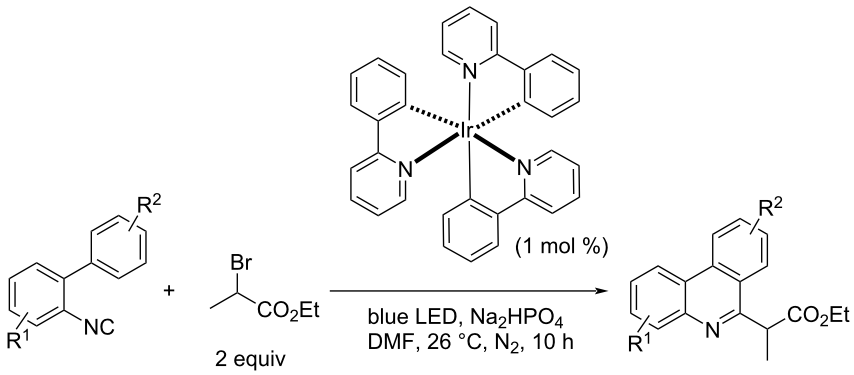

Scheme 23: Phenanthridine synthesis using a photoredox system.

system [82-86], photoredox system [21,87-90], or some other oxidation systems [91-93] were developed as excellent synthetic methods for nitrogen-containing fused heterocycles.

On the other hand, there are not as many examples of reactions in which the addition of a heteroatom radical to 2-isocyanobiaryls generates an imidoyl radical intermediate to yield nitrogen-containing fused ring compounds. A few examples have been reported in which phosphorus-centered radicals generated from diarylphosphine oxides by $Mn(OAc)_3$-assisted oxidation [94] or the photoredox system [95-97] were used in the radical cyclization reaction of 2-isocyanobiaryls (Scheme 24).

Yadav and Sigh et al. reported the direct synthesis of 6-sulfonylated phenanthridines via silver-catalyzed radical sulfonylation–cyclization of 2-isocyanobiphenyls (Scheme 25) [98].

Wang et al. reported a radical borylative cyclization of 2-isocyanobiaryls with *N*-heterocyclic carbene borane (Scheme 26) [99]. The boryl radical generated via hydrogen abstraction in the presence of di-(*tert*-butylperoxy)-2-methylpropane (DTBP) as the radical initiator attacks isocyanide units, and the subsequent radical cyclization successfully proceeds to form a variety of borylated phenanthridines in moderate to good yields.

Although the previous examples described the synthesis of phenanthridines via the radical addition of hetroatom radicals to 2-isocyanobiphenyl, another pathway to form phenanthridine scaffolds is the radical reaction of 2-aminobiaryls with free isocyanides. For example, oxidative generation of amino radicals from 2-aminobiaryls followed by intermolecular addition to isocyanides forms the imidoyl radicals, which undergo intramolecular cyclization and oxidative dehydrogenation to give phenanthridines (Scheme 27) [100].

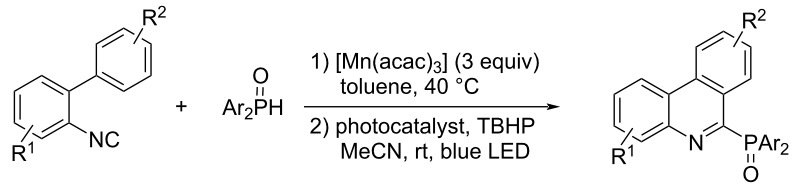

Scheme 24: Phenanthridine synthesis induced by phosphorus-centered radicals.

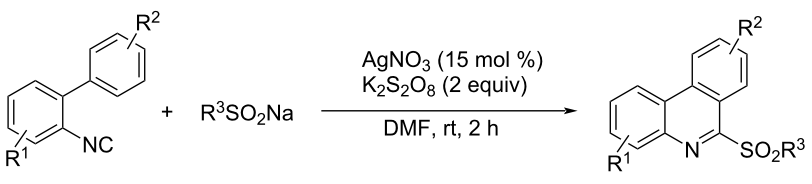

Scheme 25: Phenanthridine synthesis induced by sulfur-centered radicals.

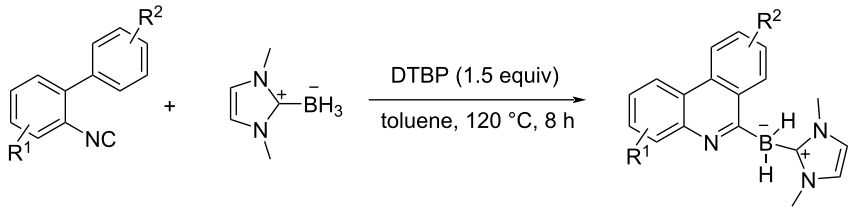

Scheme 26: Phenanthridine synthesis induced by boron-centered radicals.

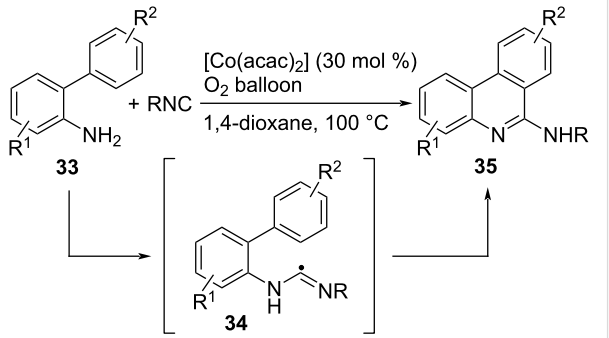

Scheme 27: Phenanthridine synthesis by oxidative cyclization of 2-aminobiaryls.

Conclusion

In this Perspective, the addition and cycloaddition reactions of heteroatom radicals with isocyanides have been described in detail and their synthetic application has been discussed. A number of useful synthetic reactions have been developed from the reactions of group 15 and 16 heteroatom radicals with isocyanides. On the other hand, the use of other heteroatoms in radical reactions with isocyanides has been limited due to the limitations of methods for generating these heteroatom radicals. It is highly expected that the radical reaction with isocyanides will be extended to many heteroatom radicals in the future, leading to the development of nitrogen-containing functional molecules modified with a variety of heteroatom functional groups. We hope that this Perspective will help in the development of such new reactions.

Acknowledgements

The authors would like to express their sincere gratitude to Professor Dr. Ilhyong Ryu (Osaka Metropolitan University) for his assistance in writing this Perspective Review.

Funding

This work was supported by Grant-in-Aid for Scientific Research (23K23392, 24K22366), from The Japan Society for the Promotion of Science (JSPS) and Grant-in-Aid for Exploratory Research from University of Yamanashi.

ORCID® iDs

Akiya Ogawa - https://orcid.org/0000-0002-8543-2560
Yuki Yamamoto - https://orcid.org/0000-0003-1166-7559

Data Availability Statement

Data sharing is not applicable as no new data was generated or analyzed in this study.

References

1. Gabrielu, B. *Carbon Monoxide in Organic Synthesis: Carbonylation Chemistry;* Wiley-VCH: Weinheim, Germany, 2021. doi:10.1002/9783527829354
2. Singh, J.; Sharma, S.; Sharma, A. *J. Org. Chem.* **2021,** *86,* 24–48. doi:10.1021/acs.joc.0c02205
3. Collet, J. W.; Roose, T. R.; Ruijter, E.; Maes, B. U. W.; Orru, R. V. A. *Angew. Chem., Int. Ed.* **2020,** *59,* 540–558. doi:10.1002/anie.201905838
4. Song, B.; Xu, B. *Chem. Soc. Rev.* **2017,** *46,* 1103–1123. doi:10.1039/c6cs00384b
5. Sadjadi, S.; Heravi, M. M.; Nazari, N. *RSC Adv.* **2016,** *6,* 53203–53272. doi:10.1039/c6ra02143c
6. Neo, A. G.; Ramiro, J. L.; García-Valverde, M.; Díaz, J.; Marcos, C. F. *Mol. Diversity* **2024,** *28,* 335–418. doi:10.1007/s11030-023-10641-7
7. Qiu, G.; Ding, Q.; Wu, J. *Chem. Soc. Rev.* **2013,** *42,* 5257–5269. doi:10.1039/c3cs35507a
8. Ryu, I.; Sonoda, N.; Curran, D. P. *Chem. Rev.* **1996,** *96,* 177–194. doi:10.1021/cr9400626
9. Zhang, S.; Wang, Y.; Huang, H.; Cao, D. *Angew. Chem., Int. Ed.* **2023,** *62,* e202308524. doi:10.1002/anie.202308524
10. Čamdžić, L.; Stache, E. E. *J. Am. Chem. Soc.* **2023,** *145,* 20311–20318. doi:10.1021/jacs.3c04595
11. Liu, N.; Zhou, L.; Wu, Z.-Q. *Acc. Chem. Res.* **2021,** *54,* 3953–3967. doi:10.1021/acs.accounts.1c00489
12. Gomes, G. d. P.; Loginova, Y.; Vatsadze, S. Z.; Alabugin, I. V. *J. Am. Chem. Soc.* **2018,** *140,* 14272–14288. doi:10.1021/jacs.8b08513
13. Taniguchi, T. *Synthesis* **2017,** *49,* 3511–3534. doi:10.1055/s-0036-1588481
14. Dénès, F. Heteroatom-Centred Radicals for the Synthesis of Heterocyclic Compounds. In *Free-Radical Synthesis and Functionaization of Heterocycles;* Landais, Y., Ed.; Springer International Publishing: Cham, Switzerland, 2018; Vol. 54, pp 151–230. doi:10.1007/7081_2018_19
15. Linker, T. *Chemistry (Basel, Switz.)* **2020,** *2,* 80–92. doi:10.3390/chemistry2010008

16. Sheldon, R. A. *Green Chem.* **2023,** *25,* 1704–1728. doi:10.1039/d2gc04747k
17. Yamamoto, Y.; Ogawa, A. *Molecules* **2023,** *28,* 787. doi:10.3390/molecules28020787
18. Ogawa, A.; Yamamoto, Y. *Molecules* **2023,** *28,* 6356. doi:10.3390/molecules28176356
19. Skubi, K. L.; Blum, T. R.; Yoon, T. P. *Chem. Rev.* **2016,** *116,* 10035–10074. doi:10.1021/acs.chemrev.6b00018
20. Romero, N. A.; Nicewicz, D. A. *Chem. Rev.* **2016,** *116,* 10075–10166. doi:10.1021/acs.chemrev.6b00057
21. Russo, C.; Brunelli, F.; Tron, G. C.; Giustiniano, M. *Chem. – Eur. J.* **2023,** *29,* e202203150. doi:10.1002/chem.202203150
22. Russo, C.; Brunelli, F.; Tron, G. C.; Giustiniano, M. *Eur. J. Org. Chem.* **2023,** *26,* e202300743. doi:10.1002/ejoc.202300743
23. Kühle, E.; Anders, B.; Zumach, G. *Angew. Chem.* **1967,** *79,* 663–680. doi:10.1002/ange.19670791504
24. Tanaka, S.; Okano, M.; Tanimoto, S. *Bull. Chem. Soc. Jpn.* **1975,** *48,* 1862–1864. doi:10.1246/bcsj.48.1862
25. Tsuchii, K.; Imura, M.; Kamada, N.; Hirao, T.; Ogawa, A. *J. Org. Chem.* **2004,** *69,* 6658–6665. doi:10.1021/jo0495889
26. Lei, J.; Wu, X.; Zhu, Q. *Org. Lett.* **2015,** *17,* 2322–2325. doi:10.1021/acs.orglett.5b00730
27. Saegusa, T.; Kobayashi, S.; Ito, Y. *J. Org. Chem.* **1970,** *35,* 2118–2121. doi:10.1021/jo00832a003
28. Tsuchii, K.; Tsuboi, Y.; Kawaguchi, S.-i.; Takahashi, J.; Sonoda, N.; Nomoto, A.; Ogawa, A. *J. Org. Chem.* **2007,** *72,* 415–423. doi:10.1021/jo061704f
29. Ito, O. *J. Am. Chem. Soc.* **1983,** *105,* 850–853. doi:10.1021/ja00342a034
30. Mitamura, T.; Tsuboi, Y.; Iwata, K.; Tsuchii, K.; Nomoto, A.; Sonoda, M.; Ogawa, A. *Tetrahedron Lett.* **2007,** *48,* 5953–5957. doi:10.1016/j.tetlet.2007.06.126
31. Russell, G. A.; Tashtoush, H. *J. Am. Chem. Soc.* **1983,** *105,* 1398–1399. doi:10.1021/ja00343a069
32. Yamamoto, Y.; Chen, Q.; Ogawa, A. *Molecules* **2023,** *28,* 2450. doi:10.3390/molecules28062450
33. Ogawa, A.; Doi, M.; Tsuchii, K.; Hirao, T. *Tetrahedron Lett.* **2001,** *42,* 2317–2319. doi:10.1016/s0040-4039(01)00123-x
34. Miyazoe, H.; Yamago, S.; Yoshida, J.-i. *Angew. Chem., Int. Ed.* **2000,** *39,* 3669–3671. doi:10.1002/1521-3773(20001016)39:20<3669::aid-anie3669>3.0.co;2-4
35. Yamago, S.; Miyazoe, H.; Goto, R.; Hashidume, M.; Sawazaki, T.; Yoshida, J.-i. *J. Am. Chem. Soc.* **2001,** *123,* 3697–3705. doi:10.1021/ja003879r
36. Yamago, S. *Synlett* **2004,** 1875–1890. doi:10.1055/s-2004-830883
37. Roberts, B. P.; Winter, J. N. *J. Chem. Soc., Chem. Commun.* **1978,** 545–546. doi:10.1039/c39780000545
38. Saegusa, T.; Ito, Y.; Yasuda, N.; Hotaka, T. *J. Org. Chem.* **1970,** *35,* 4238–4240. doi:10.1021/jo00837a625
39. Yamamoto, Y.; Ogawa, A. *Chem. – Asian J.* **2023,** *18,* e202201269. doi:10.1002/asia.202201269
40. Satgé, J.; Couret, C.; Escudié, J. *J. Organomet. Chem.* **1972,** *34,* 83–92. doi:10.1016/s0022-328x(00)88673-8
41. George, T. A.; Lappert, M. F. *J. Organomet. Chem.* **1968,** *14,* 327–337. doi:10.1016/s0022-328x(00)87672-x
42. Chatgilialoglu, C.; Ingold, K. U.; Scaiano, J. C. *J. Am. Chem. Soc.* **1983,** *105,* 3292–3296. doi:10.1021/ja00348a055
43. Saegusa, T.; Kobayashi, S.; Ito, Y.; Yasuda, N. *J. Am. Chem. Soc.* **1968,** *90,* 4182. doi:10.1021/ja01017a061
44. Ballestri, M.; Chatgilialoglu, C.; Clark, K. B.; Griller, D.; Giese, B.; Kopping, B. *J. Org. Chem.* **1991,** *56,* 678–683. doi:10.1021/jo00002a035
45. Bresadola, S.; Rossetto, F.; Puosi, G. *Tetrahedron Lett.* **1965,** *6,* 4775–4778. doi:10.1016/s0040-4039(01)89033-x
46. Bresadola, S.; Carraro, G.; Pecile, C.; Turco, A. *Tetrahedron Lett.* **1964,** *5,* 3185–3188. doi:10.1016/0040-4039(64)83131-2
47. Green, I. G.; Hudson, R. L.; Roberts, B. P. *J. Chem. Soc., Perkin Trans. 2* **1987,** 1773–1779. doi:10.1039/p29870001773
48. Teichmann, J.; Stock, H.; Pritzkow, H.; Siebert, W. *Eur. J. Inorg. Chem.* **1998,** 459–463. doi:10.1002/(sici)1099-0682(199804)1998:4<459::aid-ejic459>3.0.co;2-u
49. Katsuma, Y.; Tsukahara, N.; Wu, L.; Lin, Z.; Yamashita, M. *Angew. Chem., Int. Ed.* **2018,** *57,* 6109–6114. doi:10.1002/anie.201800878
50. Yamashita, M. *J. Synth. Org. Chem., Jpn.* **2018,** *76,* 1223–1231. doi:10.5059/yukigoseikyokaishi.76.1223
51. Ekkert, O.; Miera, G. G.; Wiegand, T.; Eckert, H.; Schirmer, B.; Petersen, J. L.; Daniliuc, C. G.; Fröhlich, R.; Grimme, S.; Kehr, G.; Erker, G. *Chem. Sci.* **2013,** *4,* 2657–2664. doi:10.1039/c3sc00082f
52. Cardenas, A. J. P.; Hasegawa, Y.; Kehr, G.; Warren, T. H.; Erker, G. *Coord. Chem. Rev.* **2016,** *306,* 468–482. doi:10.1016/j.ccr.2015.01.006
53. Jiao, Z.; Jaunich, K. T.; Tao, T.; Gottschall, O.; Hughes, M. M.; Turlik, A.; Schuppe, A. W. *Angew. Chem., Int. Ed.* **2024,** *63,* e202405779. doi:10.1002/anie.202405779
54. Fukuyama, T.; Chen, X.; Peng, G. *J. Am. Chem. Soc.* **1994,** *116,* 3127–3128. doi:10.1021/ja00086a054
55. Stork, G.; Sher, P. M. *J. Am. Chem. Soc.* **1983,** *105,* 6765–6766. doi:10.1021/ja00360a062
56. Curran, D. P.; Liu, H. *J. Am. Chem. Soc.* **1991,** *113,* 2127–2132. doi:10.1021/ja00006a033
57. Bachi, M. D.; Balanov, A.; Bar-Ner, N. *J. Org. Chem.* **1994,** *59,* 7752–7758. doi:10.1021/jo00104a035
58. Bachi, M. D.; Bar-Ner, N.; Melman, A. *J. Org. Chem.* **1996,** *61,* 7116–7124. doi:10.1021/jo9607875
59. Rainier, J. D.; Kennedy, A. R. *J. Org. Chem.* **2000,** *65,* 6213–6216. doi:10.1021/jo000831n
60. Mitamura, T.; Iwata, K.; Ogawa, A. *J. Org. Chem.* **2011,** *76,* 3880–3887. doi:10.1021/jo200299d
61. Li, D.; Mao, T.; Huang, J.; Zhu, Q. *Org. Lett.* **2017,** *19,* 3223–3226. doi:10.1021/acs.orglett.7b01339
62. Yang, W.-C.; Wei, K.; Sun, X.; Zhu, J.; Wu, L. *Org. Lett.* **2018,** *20,* 3144–3147. doi:10.1021/acs.orglett.8b01278
63. Leifert, D.; Studer, A. *Angew. Chem., Int. Ed.* **2016,** *55,* 11660–11663. doi:10.1002/anie.201606023
64. Sun, X.; Wang, W.; Li, Y.; Ma, J.; Yu, S. *Org. Lett.* **2016,** *18,* 4638–4641. doi:10.1021/acs.orglett.6b02271
65. Liu, Y.; Chen, X.-L.; Zeng, F.-L.; Sun, K.; Qu, C.; Fan, L.-L.; An, Z.-L.; Li, R.; Jing, C.-F.; Wei, S.-K.; Qu, L.-B.; Yu, B.; Sun, Y.-Q.; Zhao, Y.-F. *J. Org. Chem.* **2018,** *83,* 11727–11735. doi:10.1021/acs.joc.8b01657
66. Tran, C. C.; Kawaguchi, S.-i.; Sato, F.; Nomoto, A.; Ogawa, A. *J. Org. Chem.* **2020,** *85,* 7258–7266. doi:10.1021/acs.joc.0c00647
67. Ogawa, A.; Tamai, T.; Mitamura, T.; Nomoto, A. *Pure Appl. Chem.* **2013,** *85,* 785–799. doi:10.1351/pac-con-12-07-01
68. Mitamura, T.; Iwata, K.; Ogawa, A. *Org. Lett.* **2009,** *11,* 3422–3424. doi:10.1021/ol901267h

69. Mitamura, T.; Iwata, K.; Nomoto, A.; Ogawa, A. *Org. Biomol. Chem.* **2011,** *9,* 3768–3775. doi:10.1039/c0ob01168a
70. Mitamura, T.; Ogawa, A. *J. Org. Chem.* **2011,** *76,* 1163–1166. doi:10.1021/jo1021772
71. Mitamura, T.; Ogawa, A. *Bull. Chem. Soc. Jpn.* **2011,** *84,* 791–793. doi:10.1246/bcsj.20110041
72. Zhang, B.; Studer, A. *Chem. Soc. Rev.* **2015,** *44,* 3505–3521. doi:10.1039/c5cs00083a
73. Doraghi, F.; Amini, A.; Ghanbarlou, M.; Larijani, B.; Mahdavi, M. *Mol. Diversity* **2024,** *28,* 419–435. doi:10.1007/s11030-023-10743-2
74. Nanni, D.; Pareschi, P.; Rizzoli, C.; Sgarabotto, P.; Tundo, A. *Tetrahedron* **1995,** *51,* 9045–9062. doi:10.1016/0040-4020(95)00348-c
75. Tobisu, M.; Koh, K.; Furukawa, T.; Chatani, N. *Angew. Chem., Int. Ed.* **2012,** *51,* 11363–11366. doi:10.1002/anie.201206115
76. Nicewicz, D. A.; MacMillan, D. W. C. *Science* **2008,** *322,* 77–80. doi:10.1126/science.1161976
77. Ischay, M. A.; Anzovino, M. E.; Du, J.; Yoon, T. P. *J. Am. Chem. Soc.* **2008,** *130,* 12886–12887. doi:10.1021/ja805387f
78. Narayanam, J. M. R.; Tucker, J. W.; Stephenson, C. R. J. *J. Am. Chem. Soc.* **2009,** *131,* 8756–8757. doi:10.1021/ja9033582
79. Bellotti, P.; Huang, H.-M.; Faber, T.; Glorius, F. *Chem. Rev.* **2023,** *123,* 4237–4352. doi:10.1021/acs.chemrev.2c00478
80. Plesniak, M. P.; Huang, H.-M.; Procter, D. J. *Nat. Rev. Chem.* **2017,** *1,* 0077. doi:10.1038/s41570-017-0077
81. Jiang, H.; Cheng, Y.; Wang, R.; Zheng, M.; Zhang, Y.; Yu, S. *Angew. Chem., Int. Ed.* **2013,** *52,* 13289–13292. doi:10.1002/anie.201308376
82. Teng, F.; Hu, W.; Hu, H.; Luo, S.; Zhu, Q. *Adv. Synth. Catal.* **2019,** *361,* 1414–1418. doi:10.1002/adsc.201801623
83. Liu, S.; Fan, F.; Wang, N.; Yuan, D.; Wang, Y.; Luo, Z.; Liu, Z.-Q. *Adv. Synth. Catal.* **2019,** *361,* 3086–3093. doi:10.1002/adsc.201900221
84. Luo, Z.; Li, R.; Zhu, T.; Liu, C.-F.; Feng, H.; Aboagye Nartey, K.; Liu, Q.; Xu, X. *Asian J. Org. Chem.* **2021,** *10,* 926–930. doi:10.1002/ajoc.202100112
85. Yuan, S.; Liu, Y.; Ni, M.; Hao, T.; Peng, Y.; Ding, Q. *Chem. Commun.* **2022,** *58,* 10985–10988. doi:10.1039/d2cc04348c
86. Xiang, H.; Yu, Z.; Xie, T.; Ye, X.-Y.; Ye, Y. *Eur. J. Org. Chem.* **2022,** e202200937. doi:10.1002/ejoc.202200937
87. Wang, S.; Jia, W.-L.; Wang, L.; Liu, Q. *Eur. J. Org. Chem.* **2015,** 6817–6821. doi:10.1002/ejoc.201500988
88. Tong, K.; Zheng, T.; Zhang, Y.; Yu, S. *Adv. Synth. Catal.* **2015,** *357,* 3681–3686. doi:10.1002/adsc.201500674
89. Qin, W.-B.; Xiong, W.; Li, X.; Chen, J.-Y.; Lin, L.-T.; Wong, H. N. C.; Liu, G.-K. *J. Org. Chem.* **2020,** *85,* 10479–10487. doi:10.1021/acs.joc.0c00816
90. Zhang, J.; Xu, W.; Qu, Y.; Liu, Y.; Li, Y.; Song, H.; Wang, Q. *Chem. Commun.* **2020,** *56,* 15212–15215. doi:10.1039/d0cc06645a
91. Wang, L.; Sha, W.; Dai, Q.; Feng, X.; Wu, W.; Peng, H.; Chen, B.; Cheng, J. *Org. Lett.* **2014,** *16,* 2088–2091. doi:10.1021/ol500277u
92. He, Z.; Bae, M.; Wu, J.; Jamison, T. F. *Angew. Chem., Int. Ed.* **2014,** *53,* 14451–14455. doi:10.1002/anie.201408522
93. Wan, W.; Xu, X.; Chen, Y.; Jiang, H.; Wang, Y.; Deng, H.; Hao, J. *Eur. J. Org. Chem.* **2017,** 3145–3151. doi:10.1002/ejoc.201700470
94. Li, Y.; Qiu, G.; Ding, Q.; Wu, J. *Tetrahedron* **2014,** *70,* 4652–4656. doi:10.1016/j.tet.2014.05.039
95. Liu, Y.; Chen, X.-L.; Li, X.-Y.; Zhu, S.-S.; Li, S.-J.; Song, Y.; Qu, L.-B.; Yu, B. *J. Am. Chem. Soc.* **2021,** *143,* 964–972. doi:10.1021/jacs.0c11138
96. Wu, H.-Y.; Cao, Z.; Li, S.-Q.; Fu, Y.-W.; Li, J.-M.; Li, X.-H.; He, C.-M.; Chen, J.-Y. *J. Org. Chem.* **2023,** *88,* 17322–17329. doi:10.1021/acs.joc.3c02152
97. Liu, S.; Huang, Y.; Wang, J.; Qing, F.-L.; Xu, X.-H. *J. Am. Chem. Soc.* **2022,** *144,* 1962–1970. doi:10.1021/jacs.1c12467
98. Singh, M.; Yadav, A. K.; Yadav, L. D. S.; Singh, R. K. P. *Tetrahedron Lett.* **2018,** *59,* 3198–3201. doi:10.1016/j.tetlet.2018.07.024
99. Liu, Y.; Li, J.-L.; Liu, X.-G.; Wu, J.-Q.; Huang, Z.-S.; Li, Q.; Wang, H. *Org. Lett.* **2021,** *23,* 1891–1897. doi:10.1021/acs.orglett.1c00309
100. Zhu, T.-H.; Wang, S.-Y.; Tao, Y.-Q.; Wei, T.-Q.; Ji, S.-J. *Org. Lett.* **2014,** *16,* 1260–1263. doi:10.1021/ol500286x

License and Terms

BEILSTEIN JOURNAL OF ORGANIC CHEMISTRY

Transition-metal-free synthesis of arylboronates via thermal generation of aryl radicals from triarylbismuthines in air

Yuki Yamamoto*[1], Yuki Konakazawa[1], Kohsuke Fujiwara[2] and Akiya Ogawa*[3]

Full Research Paper

Open Access

Address:
[1]Graduate Faculty of Interdisciplinary Research, University of Yamanashi, 4-4-37 Takeda, Kofu, Yamanashi 400-8510, Japan, [2]Department of Applied Chemistry, Graduate School of Engineering, Osaka Metropolitan University, 1-1 Gakuen-cho, Nakaku, Sakai, Osaka 599-8531, Japan and [3]Organization for Research Promotion, Osaka Metropolitan University, 1-1 Gakuen-cho, Nakaku, Sakai, Osaka 599-8531, Japan

Email:
Yuki Yamamoto* - y.yamamoto@yamanashi.ac.jp; Akiya Ogawa* - ogawa@omu.ac.jp

* Corresponding author

Keywords:
arylboronates; bis(pinacolato)diboron; radical reactions; transition-metal-free synthesis; triarylbismuthines

Beilstein J. Org. Chem. **2024,** *20,* 2577–2584.
https://doi.org/10.3762/bjoc.20.216

Received: 03 June 2024
Accepted: 23 September 2024
Published: 11 October 2024

This article is part of the thematic issue "Modern radical chemistry".

Guest Editor: H.-M. Huang

Abstract

A simple and versatile synthesis of arylboronates has been achieved by using triarylbismuthines as aryl radical sources under transition-metal-free and open-air conditions. Conventional methods required photoirradiation or electrolysis to generate aryl radicals from triarylbismuthines. In this study, it was found that simply heating the solution of triarylbismuthines in benzotrifluoride (BTF) in air successfully led to the generation of aryl radicals, and the subsequent reaction with bis(pinacolato)diboron afforded a variety of arylboronates in moderate to good yields.

Introduction

Arylboronates are one of the fundamental aryl compounds in organic synthesis, especially in cross-coupling reactions [1-9], and their applications are widespread, including dye synthesis, pharmaceutical and agrochemical synthesis, and industrial manufacturing [10,11]. In recent years, a variety of transition-metal-catalyzed reactions and photoredox reactions using arylboronates as aryl sources have been energetically investigated for the construction of carbon–carbon or carbon–heteroatom bonds [12-15].

The preparation of arylboronates often requires pre-functionalized substrates with halogen or triflate groups. Recently, transition-metal-catalyzed direct borylation of arenes via C–H bond activation has been reported, although the design of the substrate and ligands is somewhat complicated [16-22]. Since the complete removal of catalyst-derived metal residues from the final products is generally difficult, there is concern about side effects or adverse effects on functional expression when used in pharmaceutical and material synthesis. In addition, many transi-

tion metal catalysts are very expensive, unstable, and difficult to handle. For these reasons, the development of new synthetic methods of arylboronates using stable and versatile reagents under transition-metal-free conditions has recently attracted much attention [23-27]. In particular, the use of radical reactions has been considered as one of the effective methods, since diborons can capture the in situ-generated carbon-centered radicals [28-36].

Among the aryl sources in organic synthesis, triarylbismuthines are shelf-stable and easy-to-handle reagents with appropriate reactivities in transition-metal-catalyzed reactions and radical reactions, and their derivatives can be easily synthesized by common Grignard reactions [37-44]. Three activation methods have been reported for their use as aryl radical sources. It has been reported that the homolysis of Ar–Bi bonds could be achieved by photoirradiation in the presence of photocatalysts or UV light irradiation without metal catalysts [45-48]. Similar homolysis by electrolysis has also been reported [49]. These two activation methods required special equipment (i.e., light sources or electronic devices). To achieve thermal homolysis of the Ar–Bi bonds, the reaction conditions were harsh, requiring heating at 260 °C for several days [50]. Thus, only two examples of the use of triarylbismuthines as aryl radical sources have been reported for the synthesis of arylboronates, which proceeds under light irradiation conditions (Scheme 1a) [47,48].

Our group has investigated various transition-metal-free methods for the generation of aryl radicals from shelf-stable aryl compounds (Scheme 1b). For example, the heating of arylhydrazine hydrochlorides ($ArNHNH_2$·HCl) in the presence of base under open-air conditions successfully led to the generation of aryl radicals and the subsequent trapping with E–E compounds (E = S, Se, Te, Br, and I) successfully formed new C–E

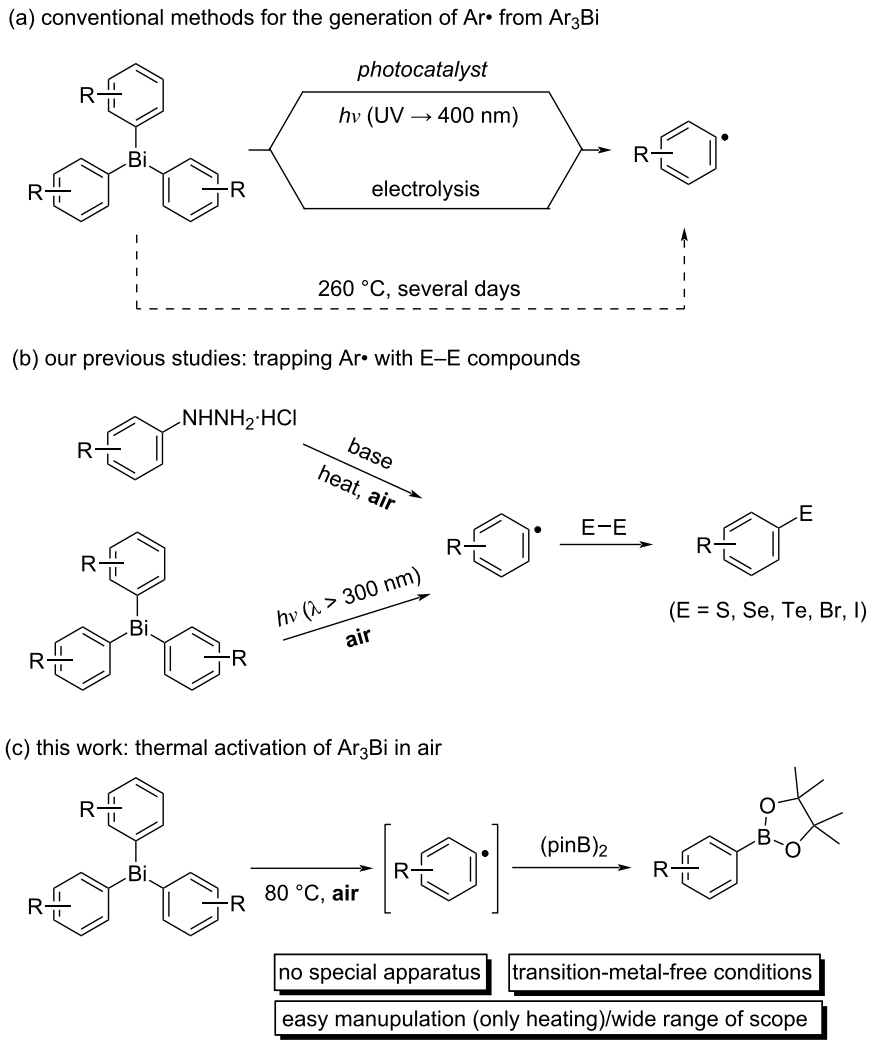

Scheme 1: (a) Conventional methods for the generation of Ar• from Ar_3Bi, (b) our previous studies, and (c) this work.

bonds (Scheme 1b) [51-58]. We also demonstrated that the photoirradiation (λ > 300 nm) of the triarylbismuthines in air successfully allowed the generation of the corresponding aryl radicals without photocatalysts, and the trapping with diselenides afforded a variety of diaryl selenides [59]. Based on these backgrounds of our studies and the fundamental property, i.e., the weak bond dissociation energy of the Ph–Bi bond (46 kcal/mol) [60], we hypothesized that aryl radicals generated from triarylbismuthines by our developed methods would be successfully trapped by diboron to form a new C–B bond.

In this study, we report a facile and versatile synthesis of arylboronates using triarylbismuthines as aryl radical sources under transition-metal-free and open-air conditions (Scheme 1c). This method could be carried out without any special apparatus, and the mild conditions led to the wide range of applications.

Results and Discussion

Initially, we used triphenylbismuthine (**1a**) and bis(pinacolato)diboron (**2**) as the model substrates to optimize the reaction conditions (Table 1). We first investigated the solubility of **1** and **2** in various solvents. It was found that both **1** and **2** showed excellent solubility towards benzotrifluoride (BTF) [61] (for diboron **2**: 637 mg/mL (BTF); 567 mg/mL (AcOEt)). Therefore, BTF is chosen as the solvent.

Surprisingly, heating the mixture of **1** and **2** in BTF (0.4 mL) at 80 °C in air successfully afforded phenylboronic acid pinacol ester **3a** in 68% yield (Table 1, entry 1). In the presence of NaOMe as a base, the reaction did not proceed (Table 1, entry 2). Increasing or decreasing the amount of diboron **2** did not improve the yield of **3a** (Table 1, entry 2 vs entries 3 and 4). Under atmospheric oxygen, the yield of **3a** decreased slightly (Table 1, entry 5). The reaction was investigated at 60 °C and 100 °C, and it was found that the reaction was most efficient at 80 °C (Table 1, entry 2 vs entries 6 and 7). We have previously succeeded in generating a boron radical (pinB$^{\bullet}$) by photoirradiation of $(Bpin)_2$ and found that the addition of $(PhS)_2$ was effective in generating the boron radical [30]. We therefore investigated this reaction by adding $(PhS)_2$ as a Lewis base, but the yield of **3a** was not improved and $(PhS)_2$ was recovered almost quantitatively (Table 1, entry 8). Furthermore, instead of BTF, the reaction was carried out with similarly polar $CHCl_3$, polar and aprotic CH_3CN, DMF, DMSO, and protic EtOH, and it was found that BTF was the optimal solvent for the synthesis of **3a** (Table 1, entry 2 vs entries 9–13).

Table 1: Optimization of the reaction conditions for synthesis of **3a** from $BiPh_3$ (**1a**) and $(pinB)_2$ (**2**).

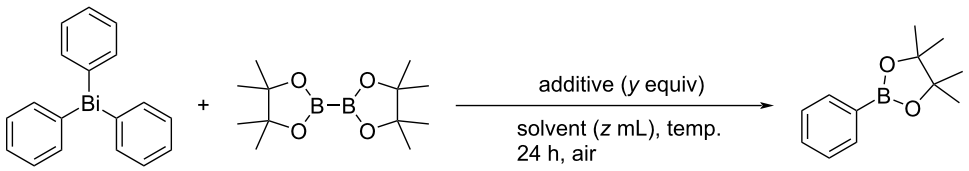

1a (0.07 mmol) **2** (*x* mmol) **3a**

Entry	**2** (mmol)	Additive (equiv)	Solvent (mL)	Temp (°C)	Yield **3a** (%)[a]	Recovery **1a** (%)[a]
1	**2.0**	**–**	**BTF (0.4)**	**80**	**68 (53)**	**trace**
2	0.5	NaOMe (1.2)	BTF (0.2)	80	N. D.	62
3	3.0	–	BTF (0.4)	80	62	trace
4	0.5	–	BTF (0.4)	80	36	30
5[b]	2.0	–	BTF (0.4)	80	58	trace
6	2.0	–	BTF (0.4)	60	59	trace
7	2.0	–	BTF (0.4)	100	61	trace
8	2.0	$(PhS)_2$ (0.01)	BTF (0.4)	80	63	trace
9	2.0	–	$CHCl_3$ (0.4)	80	36	17
10	2.0	–	CH_3CN (0.4)	80	51	17
11	2.0	–	DMF (0.4)	80	38	48
12	2.0	–	DMSO (0.4)	80	18	80
13	2.0	–	EtOH (0.4)	80	45	16

[a]Yields were determined by ^{1}H NMR spectroscopy based on **1a** as three transferable aryl groups (internal standard: 1,3,5-trioxane). Isolated yield was shown in parentheses. [b]Under O_2 (0.1 MPa).

Based on the optimized conditions (entry 2 in Table 1), we next investigated the scope and limitations of the transition-metal-free synthesis of arylboronates **3** using functionalized triarylbismuthines **1** (Scheme 2). As shown in Scheme 2, a variety of triarylbismuthines could be used for the transition-metal-free synthesis of arylboronates. For example, the use of triarylbismuthines with *o*-methyl, *m*-methyl, *p*-methyl, *p*-methoxy, and *p*-chloro groups successfully afforded the corresponding arylboronates **3a**–**e** and **3g** in 62–73% yields, respectively. The low solubility of tri(*p*-fluorophenyl) and tri(1-naphthyl)bismuthines **1h** and **1k** in BTF resulted in the low conversion. This system could be applied to the unstable dimethyl acetal-substituted triphenylbismuthine **1f**, and **3f** was obtained in 51% yield. Interestingly, the use of triarylbismuthines **1i** and **1j** with strong electron-withdrawing groups such as trifluoromethyl and formyl groups was also tolerable, and the corresponding products **3i** and **3j** were selectively obtained in moderate yields. Notably, the bulky 2,4,6-trimethylphenyl group of bisumuthine **1l** did not inhibit the transformation, and the boronate **3l** was obtained in 78% yield. The isolation of arylboronates **3c**, **3i**, and **3j** was somewhat difficult due to strong adsorption or decomposition on silica gel. Since some arylboronates are somewhat unstable, it is desirable to synthesize such compounds and then use them in a one-pot manner for the following reactions without isolation.

To gain insight into the reaction pathways, several control experiments were investigated. When the reaction was carried out in an argon atmosphere using the strict Schlenk technique, the desired product **3a** was not obtained at all and 93% of **1a** was recovered (Scheme 3).

Figure 1 shows the comparison of the crude mixture of the reactions under argon atmosphere and in the open-air. In the absence of oxygen, the color of the reaction mixture changed only slightly. In contrast, the reaction in air resulted in the for-

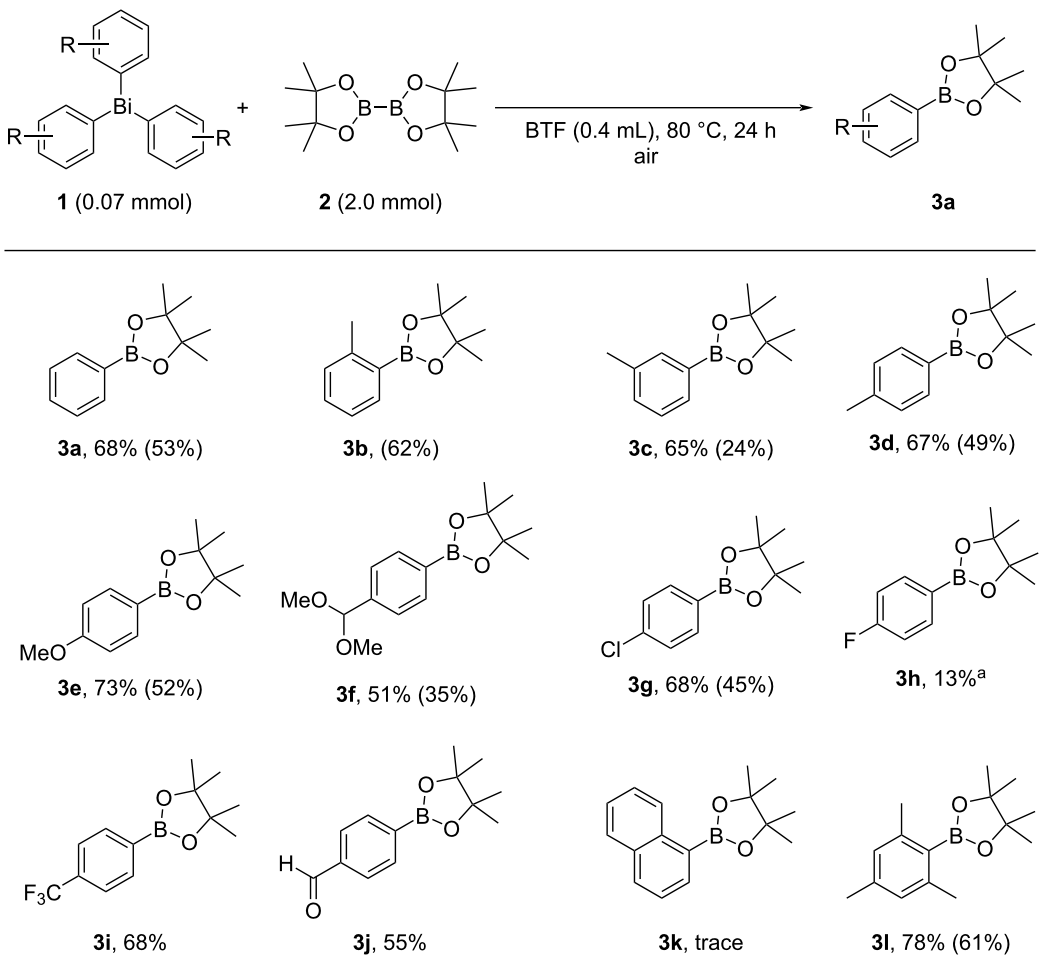

Scheme 2: Scope for transition-metal-free synthesis of arylboronates **3** using triaylbismuthines **1** and diboron **2**. Yields were determined by ^{1}H NMR spectroscopy based on **1** as three transferable aryl groups (internal standard: 1,3,5-trioxane). Isolated yield was shown in parentheses. [a]$CHCl_3$ (0.4 mL) was used as the solvent.

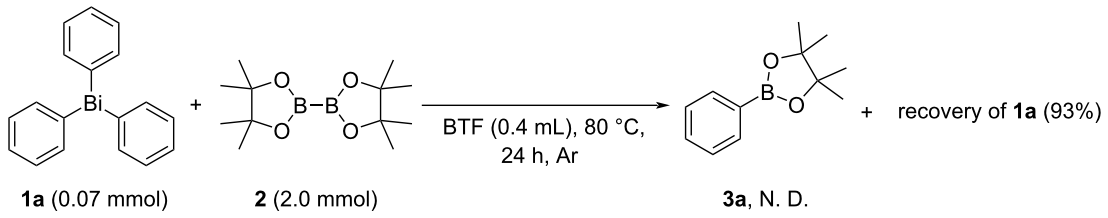

Scheme 3: Control experiment of the metal-free borylation under an argon atmosphere.

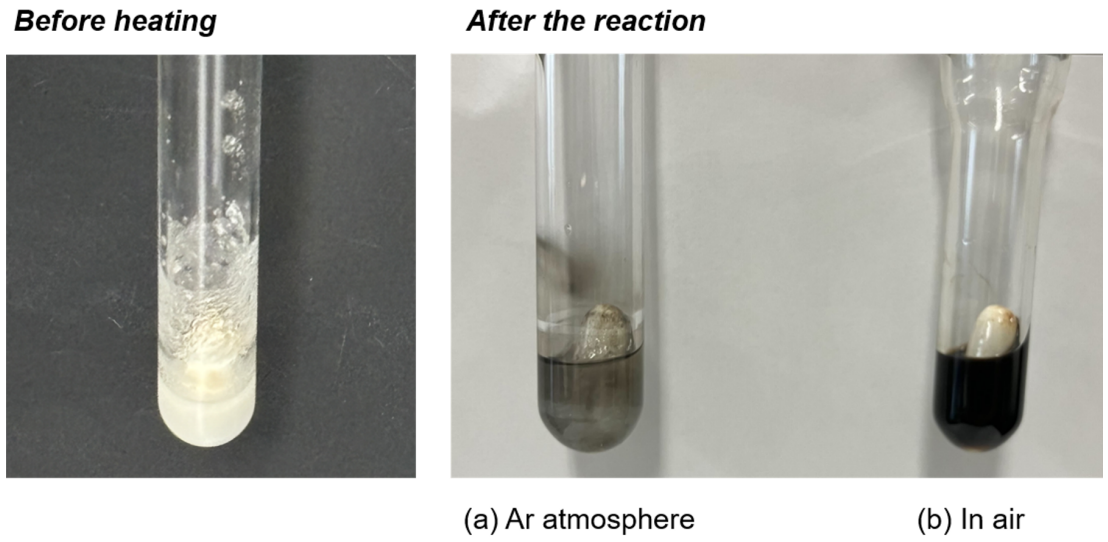

Figure 1: Comparison of the crude mixture of the reactions under (a) argon atmosphere or (b) open-air.

mation of black and a small amount of white insoluble solid (probably metallic bismuth or bismuth oxide) [55], and **3a** was successfully obtained with almost complete consumption of **1a**. The results clearly indicate that air can play an important role in the thermal activation of triarylbismuthines to generate aryl radicals.

Furthermore, the yield of **3a** was dramatically reduced in the presence of 2,2,6,6-tetramethylpiperidine 1-oxyl free radical (TEMPO) as a radical scavenger, strongly suggesting that a radical pathway is involved in the key step of the arylboronate synthesis (Scheme 4a). In addition, the reaction of triphenylbismuthine **1a** (0.07 mmol) and TEMPO (0.4 mmol) under air

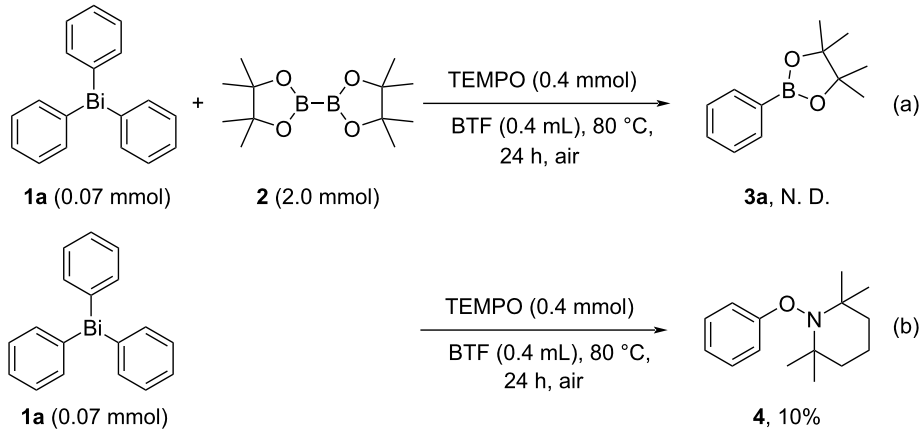

Scheme 4: Radical-trapping experiments using TEMPO as a radical scavenger.

resulted in the formation of **4** in 10% yield, which was confirmed and characterized by the ^{1}H NMR measurement of the crude reaction mixture (Scheme 4b) [48]. These results clearly showed that the thermal generation of aryl radicals from triarylbismuthines is one of the key factors for the transition-metal-free synthesis of arylboronates, and oxygen (air) would play a role as a radical initiator for the thermal activation of triarylbismuthines.

In this system, an excess amount of diboron **2** was required for the reaction to proceed efficiently. To clarify the transformation of diboron **2** under the reaction conditions, the crude reaction mixture (entry 2 in Table 1) was analyzed by ^{11}B NMR measurement. It was noteworthy that diboron **2** was reactive with air under the reaction conditions, and the decomposition of **2** to form pinB–O–Bpin and pinB–OH was confirmed. The decomposition was also occurred by heating the solution of diboron **2** in BTF in air; however, in the presence of TEMPO, the decomposition of **2** was sightly occurred, and almost all of **2** was recovered (see Supporting Information File 1). Based on the results, diboron **2** could also be activated via the thermal homolysis of the B–B bond in the presence of oxygen (air).

Based on the results of the control experiments and our previous studies, a proposed reaction pathway is shown in Scheme 5. First, thermal activation of triarylbismuthines in air forms aryl radicals together with the bismuth residues (i.e., metal bismuth and bismuth oxide). Alternatively, oxygen in air and/or boron-centered radicals thermally generated from $(pinB)_2$ in air would react with triarylbismuthines to form the aryl radicals. The generated aryl radicals were then captured with $(pinB)_2$ and the corresponding arylboronates were formed. Recombination of simultaneously formed pinB$^\bullet$ could regenerate $(pinB)_2$, and some of the pinB$^\bullet$ would react with air to form pinB–O–Bpin and pinB–OH (path A). The corresponding arylboronates could also be formed via aryl radical trapping with pinB$^\bullet$ generated by heating $(pinB)_2$ in air (path B).

Conclusion

In this study, we have developed a novel method for the transition-metal-free synthesis of arylboronates using triarylbismuthines. Most of the previous methods to generate aryl radical species from triarylbismuthines required a special apparatus. In contrast, our method was very simple, and the corresponding aryl radicals were easily accessible by simply heating the solution of triarylbismuthines in air under mild conditions. Therefore, many triarylbismuthines could be used to form a variety of useful arylboronates in moderate to good yields with excellent product selectivity. We hope that this new approach to the generation of aryl radicals from triarylbismuthines will lead to an increased use of organobismuth compounds in synthetic organic chemistry. Further applications of organobismuth compounds as aryl radical precursors are currently under investigation.

Experimental

General comments: Unless otherwise stated, all starting materials were purchased from commercial sources and used without further purification. All solvents were used without distillation. Triarylbismuthines **1** were synthesized according to the previously reported procedures [62]. ^{1}H, ^{13}C{^{1}H}, and ^{11}B NMR spectra were recorded in $CDCl_3$ using a Bruker AVANCE III HD 500 spectrometer at 500, 126, and 160 MHz, respectively. ^{1}H chemical shifts are reported in ppm relative to Me_4Si using the solvent residual as the internal standard (δ = 7.26 ppm for chloroform). ^{13}C chemical shifts are reported in ppm relative to Me_4Si, referenced to the resonances of $CDCl_3$ (δ = 77.2 ppm). ^{11}B chemical shifts are reported in ppm recorded in $CDCl_3$ using $BF_3{\cdot}Et_2O$ (δ = 0.0 ppm) as the internal standard.

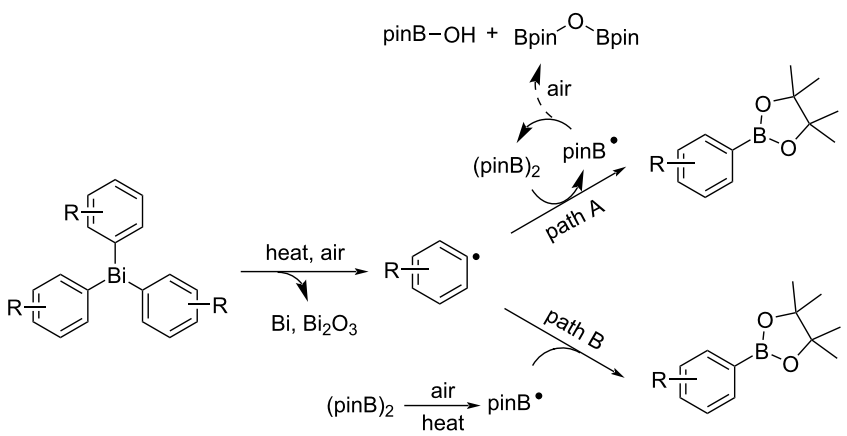

Scheme 5: A proposed reaction pathway for the synthesis of arylboronates.

General procedure for transition-metal-free synthesis of arylboronates with triarylbismuthines 1 and diboron 2 (Scheme 2)**:** To a 10 mL two-neck flask were added triarylbismuthine **1** (0.07 mmol), bis(pinacolato)diboron **2** (2.0 mmol), and benzotrifluoride (BTF, 0.4 mL). The mixture was heated at 80 °C for 24 h in air. After the reaction was completed, the mixture was filtered through a short Celite pad with AcOEt (20 mL). The filtrate was concentrated under reduced pressure. Finally, the residue was purified by preparative thin-layer chromatography (eluent: AcOEt/hexane) to give the pure product **3**. Assuming that three aryl radicals are formed from triarylbismuthine **1**, the yield of **3** was determined from the weight of the isolated product based on three times the moles of triarylbismuthine **1**. Further details of the experimental procedures and characterization data are provided in Supporting Information File 1.

Supporting Information

Supporting Information File 1

Investigation of the boron residue in the crude mixture by ^{11}B NMR measurement, characterization data of the compounds, and copies of ^{1}H NMR and $^{13}C\{^{1}H\}$ NMR spectra.
[https://www.beilstein-journals.org/bjoc/content/supplementary/1860-5397-20-216-S1.pdf]

Acknowledgements

We acknowledged Dr. Tran Dat Phuc and Mr. Soichiro Mita (Osaka Prefecture University) for their initial contribution of this work. We acknowledged Mr. Reiya Kani (University of Yamanashi) for his experimental support. Y.Y. would like to express his deepest gratitude to Prof. Dr. Tetsuo Kuwabara (University of Yamanashi) for his insightful feedback and continuous mentorship that significantly contributed to the success of this work.

Funding

This work was supported by Grant-in-Aid for Exploratory Research from University of Yamanashi and Grant-in-Aid for Scientific Research (22H02124, 24K22366) from The Japan Society for the Promotion of Science (JSPS).

ORCID® iDs

Yuki Yamamoto - https://orcid.org/0000-0003-1166-7559

Data Availability Statement

All data that supports the findings of this study is available in the published article and/or the supporting information to this article.

References

1. Ishiyama, T.; Itoh, Y.; Kitano, T.; Miyaura, N. *Tetrahedron Lett.* **1997,** *38,* 3447–3450. doi:10.1016/s0040-4039(97)00642-4
2. Murata, M.; Watanabe, S.; Masuda, Y. *J. Org. Chem.* **1997,** *62,* 6458–6459. doi:10.1021/jo970963p
3. Murata, M.; Oyama, T.; Watanabe, S.; Masuda, Y. *J. Org. Chem.* **2000,** *65,* 164–168. doi:10.1021/jo991337q
4. Ishiyama, T.; Ishida, K.; Miyaura, N. *Tetrahedron* **2001,** *57,* 9813–9816. doi:10.1016/s0040-4020(01)00998-x
5. Ishiyama, T.; Isou, H.; Kikuchi, T.; Miyaura, N. *Chem. Commun.* **2010,** *46,* 159–161. doi:10.1039/b910298a
6. Kawamorita, S.; Ohmiya, H.; Iwai, T.; Sawamura, M. *Angew. Chem., Int. Ed.* **2011,** *50,* 8363–8366. doi:10.1002/anie.201103224
7. Yoshida, T.; Ilies, L.; Nakamura, E. *ACS Catal.* **2017,** *7,* 3199–3203. doi:10.1021/acscatal.7b00310
8. Alam, S.; Karim, R.; Khan, A.; Pal, A. K.; Maruani, A. *Eur. J. Org. Chem.* **2021,** 6115–6160. doi:10.1002/ejoc.202100817
9. Zeng, J.; Naito, M.; Torigoe, T.; Yamanaka, M.; Kuninobu, Y. *Org. Lett.* **2020,** *22,* 3485–3489. doi:10.1021/acs.orglett.0c00946
10. Miyaura, N.; Yamada, K.; Suzuki, A. *Tetrahedron Lett.* **1979,** *20,* 3437–3440. doi:10.1016/s0040-4039(01)95429-2
11. Lennox, A. J. J.; Lloyd-Jones, G. C. *Chem. Soc. Rev.* **2014,** *43,* 412–443. doi:10.1039/c3cs60197h
12. Kakiuchi, F.; Kan, S.; Igi, K.; Chatani, N.; Murai, S. *J. Am. Chem. Soc.* **2003,** *125,* 1698–1699. doi:10.1021/ja029273f
13. Kakiuchi, F.; Matsuura, Y.; Kan, S.; Chatani, N. *J. Am. Chem. Soc.* **2005,** *127,* 5936–5945. doi:10.1021/ja043334n
14. Matsuda, N.; Hirano, K.; Satoh, T.; Miura, M. *Angew. Chem., Int. Ed.* **2012,** *51,* 3642–3645. doi:10.1002/anie.201108773
15. Dastbaravardeh, N.; Schnürch, M.; Mihovilovic, M. D. *Org. Lett.* **2012,** *14,* 1930–1933. doi:10.1021/ol300627p
16. Kakiuchi, F.; Chatani, N. *Adv. Synth. Catal.* **2003,** *345,* 1077–1101. doi:10.1002/adsc.200303094
17. Mkhalid, I. A. I.; Barnard, J. H.; Marder, T. B.; Murphy, J. M.; Hartwig, J. F. *Chem. Rev.* **2010,** *110,* 890–931. doi:10.1021/cr900206p
18. Hartwig, J. F. *Acc. Chem. Res.* **2012,** *45,* 864–873. doi:10.1021/ar200206a
19. Xu, L.; Wang, G.; Zhang, S.; Wang, H.; Wang, L.; Liu, L.; Jiao, J.; Li, P. *Tetrahedron* **2017,** *73,* 7123–7157. doi:10.1016/j.tet.2017.11.005
20. Kuleshova, O.; Asako, S.; Ilies, L. *ACS Catal.* **2021,** *11,* 5968–5973. doi:10.1021/acscatal.1c01206
21. Ramadoss, B.; Jin, Y.; Asako, S.; Ilies, L. *Science* **2022,** *375,* 658–663. doi:10.1126/science.abm7599
22. Jin, Y.; Ramadoss, B.; Asako, S.; Ilies, L. *Nat. Commun.* **2024,** *15,* 2886. doi:10.1038/s41467-024-46893-6
23. Légaré, M.-A.; Courtemanche, M.-A.; Rochette, É.; Fontaine, F.-G. *Science* **2015,** *349,* 513–516. doi:10.1126/science.aab3591
24. Mfuh, A. M.; Doyle, J. D.; Chhetri, B.; Arman, H. D.; Larionov, O. V. *J. Am. Chem. Soc.* **2016,** *138,* 2985–2988. doi:10.1021/jacs.6b01376
25. Candish, L.; Teders, M.; Glorius, F. *J. Am. Chem. Soc.* **2017,** *139,* 7440–7443. doi:10.1021/jacs.7b03127
26. Cuenca, A. B.; Shishido, R.; Ito, H.; Fernández, E. *Chem. Soc. Rev.* **2017,** *46,* 415–430. doi:10.1039/c6cs00692b
27. Mo, F.; Jiang, Y.; Qiu, D.; Zhang, Y.; Wang, J. *Angew. Chem., Int. Ed.* **2010,** *49,* 1846–1849. doi:10.1002/anie.200905824
28. Yu, J.; Zhang, L.; Yan, G. *Adv. Synth. Catal.* **2012,** *354,* 2625–2628. doi:10.1002/adsc.201200416

29. Qiu, D.; Jin, L.; Zheng, Z.; Meng, H.; Mo, F.; Wang, X.; Zhang, Y.; Wang, J. *J. Org. Chem.* **2013,** *78,* 1923–1933. doi:10.1021/jo3018878
30. Yoshimura, A.; Takamachi, Y.; Han, L.-B.; Ogawa, A. *Chem. – Eur. J.* **2015,** *21,* 13930–13933. doi:10.1002/chem.201502425
31. Yoshimura, A.; Takamachi, Y.; Mihara, K.; Saeki, T.; Kawaguchi, S.-i.; Han, L.-B.; Nomoto, A.; Ogawa, A. *Tetrahedron* **2016,** *72,* 7832–7838. doi:10.1016/j.tet.2016.06.040
32. Zhang, L.; Jiao, L. *J. Am. Chem. Soc.* **2017,** *139,* 607–610. doi:10.1021/jacs.6b11813
33. Yan, G.; Huang, D.; Wu, X. *Adv. Synth. Catal.* **2018,** *360,* 1040–1053. doi:10.1002/adsc.201701030
34. Zhang, L.; Jiao, L. *J. Am. Chem. Soc.* **2019,** *141,* 9124–9128. doi:10.1021/jacs.9b00917
35. Shiozuka, A.; Sekine, K.; Toki, T.; Kawashima, K.; Mori, T.; Kuninobu, Y. *Org. Lett.* **2022,** *24,* 4281–4285. doi:10.1021/acs.orglett.2c01663
36. He, T.; Wei, H.; Zhou, Y.; Jiang, L.-y.; Baell, J. B.; Yu, Y.; Huang, F. *Org. Chem. Front.* **2023,** *10,* 2918–2926. doi:10.1039/d3qo00458a
37. Suzuki, H.; Ikegami, T.; Matano, Y. *Synthesis* **1997,** 249–267. doi:10.1055/s-1997-1194
38. Matano, Y.; Miyamatsu, T.; Suzuki, H. *Organometallics* **1996,** *15,* 1951–1953. doi:10.1021/om9509709
39. Yamago, S.; Kayahara, E.; Kotani, M.; Ray, B.; Kwak, Y.; Goto, A.; Fukuda, T. *Angew. Chem., Int. Ed.* **2007,** *46,* 1304–1306. doi:10.1002/anie.200604473
40. Kayahara, E.; Yamada, H.; Yamago, S. *Chem. – Eur. J.* **2011,** *17,* 5272–5280. doi:10.1002/chem.201100265
41. Kobiki, Y.; Kawaguchi, S.-i.; Ogawa, A. *Org. Lett.* **2015,** *17,* 3490–3493. doi:10.1021/acs.orglett.5b01566
42. Kodama, S.; Yamamoto, Y.; Kobiki, Y.; Matsubara, H.; Tran, C. C.; Kawaguchi, S.-i.; Nomoto, A.; Ogawa, A. *Materials* **2021,** *14,* 4271. doi:10.3390/ma14154271
43. Birnthaler, D.; Narobe, R.; Lopez-Berguno, E.; Haag, C.; König, B. *ACS Catal.* **2023,** *13,* 1125–1132. doi:10.1021/acscatal.2c05631
44. Mato, M.; Cornella, J. *Angew. Chem., Int. Ed.* **2024,** *63,* e202315046. doi:10.1002/anie.202315046
45. Hey, D. H.; Shingleton, D. A.; Williams, G. H. *J. Chem. Soc.* **1963,** 5612–5619. doi:10.1039/jr9630005612
46. Yablokov, V. A.; Zelyaev, I. A.; Makarov, E. I.; Lokhov, N. S. *Zh. Obshch. Khim.* **1987,** *57,* 2034–2037.
47. Nakajima, M.; Nagasawa, S.; Matsumoto, K.; Kuribara, T.; Muranaka, A.; Uchiyama, M.; Nemoto, T. *Angew. Chem., Int. Ed.* **2020,** *59,* 6847–6852. doi:10.1002/anie.201915181
48. Chiappini, N. D.; Geunes, E. P.; Bodak, E. T.; Knowles, R. R. *ACS Catal.* **2024,** *14,* 2664–2670. doi:10.1021/acscatal.3c05598
49. Fuchigami, T.; Miyazaki, M. *Electrochim. Acta* **1997,** *42,* 1979–1984. doi:10.1016/s0013-4686(97)85470-9
50. Razuvaev, G. A.; Petukhov, G. G.; Titov, V. A.; Druzhkov, O. N. *Zh. Org. Khim.* **1965,** *35,* 481–485.
51. Taniguchi, T.; Imoto, M.; Takeda, M.; Matsumoto, F.; Nakai, T.; Mihara, M.; Mizuno, T.; Nomoto, A.; Ogawa, A. *Tetrahedron* **2016,** *72,* 4132–4140. doi:10.1016/j.tet.2016.05.056
52. Taniguchi, T.; Naka, T.; Imoto, M.; Takeda, M.; Nakai, T.; Mihara, M.; Mizuno, T.; Nomoto, A.; Ogawa, A. *J. Org. Chem.* **2017,** *82,* 6647–6655. doi:10.1021/acs.joc.7b00767
53. Taniguchi, T.; Murata, A.; Takeda, M.; Mizuno, T.; Nomoto, A.; Ogawa, A. *Eur. J. Org. Chem.* **2017,** 4928–4934. doi:10.1002/ejoc.201700938
54. Dong, C.-p.; Nakamura, K.; Taniguchi, T.; Mita, S.; Kodama, S.; Kawaguchi, S.-i.; Nomoto, A.; Ogawa, A.; Mizuno, T. *ACS Omega* **2018,** *3,* 9814–9821. doi:10.1021/acsomega.8b01559
55. Yamamoto, Y.; Sato, F.; Kodama, S.; Nomoto, A.; Ogawa, A. *Heteroat. Chem.* **2018,** *29,* e21471. doi:10.1002/hc.21471
56. Phuc Tran, D.; Nomoto, A.; Mita, S.; Dong, C.-p.; Kodama, S.; Mizuno, T.; Ogawa, A. *Tetrahedron Lett.* **2020,** *61,* 151959. doi:10.1016/j.tetlet.2020.151959
57. Yamamoto, Y.; Sato, F.; Chen, Q.; Kodama, S.; Nomoto, A.; Ogawa, A. *Molecules* **2022,** *27,* 809. doi:10.3390/molecules27030809
58. Yamamoto, Y.; Ogawa, A. *Molecules* **2023,** *28,* 787. doi:10.3390/molecules28020787
59. Kobiki, Y.; Kawaguchi, S.-i.; Ohe, T.; Ogawa, A. *Beilstein J. Org. Chem.* **2013,** *9,* 1141–1147. doi:10.3762/bjoc.9.127
60. Steele, W. V. *J. Chem. Thermodyn.* **1979,** *11,* 187–192. doi:10.1016/0021-9614(79)90170-8
61. Ogawa, A.; Curran, D. P. *J. Org. Chem.* **1997,** *62,* 450–451. doi:10.1021/jo9620324
62. Hébert, M.; Petiot, P.; Benoit, E.; Dansereau, J.; Ahmad, T.; Le Roch, A.; Ottenwaelder, X.; Gagnon, A. *J. Org. Chem.* **2016,** *81,* 5401–5416. doi:10.1021/acs.joc.6b00767

License and Terms

BEILSTEIN JOURNAL OF ORGANIC CHEMISTRY

Photochemical reduction of acylimidazolium salts

Michael Jakob[1], Nick Bechler[1], Hassan Abdelwahab[2], Fabian Weber[2], Janos Wasternack[1], Leonardo Kleebauer[1], Jan P. Götze[2] and Matthew N. Hopkinson[*1,3]

Letter

Open Access

Address:
[1]Institut für Chemie und Biochemie, Freie Universität Berlin, Arnimallee 20, 14195 Berlin, Germany, [2]Institut für Chemie und Biochemie, Freie Universität Berlin, Arnimallee 22, 14195 Berlin, Germany and [3]School of Natural and Environmental Sciences, Newcastle University, Bedson Building, Newcastle upon Tyne, NE1 7RU, UK

Email:
Matthew N. Hopkinson[*] - matthew.hopkinson@newcastle.ac.uk

* Corresponding author

Keywords:
carbenes; carbonyls; NHCs; photochemistry; reduction

Beilstein J. Org. Chem. **2025,** *21,* 1973–1983.
https://doi.org/10.3762/bjoc.21.153

Received: 11 June 2025
Accepted: 11 September 2025
Published: 25 September 2025

This article is part of the thematic issue "Modern radical chemistry".

Guest Editor: H.-M. Huang

Abstract

Light-mediated methodologies for the reduction of acylazolium species generated during *N*-heterocyclic carbene (NHC)-catalyzed reactions have been developed. Employing the simple amine, DIPEA, as the terminal reductant, products resulting from overall 2-electron or 4-electron-reduction processes could be obtained using either a photocatalytic approach under blue light irradiation or directly under UV-A light irradiation without an additional photocatalyst. Moreover, under the same photocatalyst-free conditions, UV-A-light-mediated reduction could be achieved using triethylsilane as the only reductant with subsequent desilylation and NHC elimination with fluoride delivering the corresponding aldehyde product.

Introduction

The introduction and exploration of *N*-heterocyclic carbenes (NHCs) ranks among the most important developments in chemistry research of the last 30 years [1-3]. In addition to their numerous valuable roles as ligands, including for important transition-metal complexes such as the Grubbs' second-generation metathesis catalyst, NHCs are now also well-established as organocatalysts. With the first application pre-dating the unambiguous characterization of a free NHC by nearly 50 years, NHCs can facilitate numerous synthetically attractive transformations of carbonyl substrates with umpolung processes of aldehydes such as the benzoin condensation and Stetter reaction being particularly well studied [4-11]. In these processes, addition of the NHC to the aldehyde followed by proton transfer generates the enamine-like Breslow intermediate **A** (Figure 1a), in which the formerly electrophilic carbonyl carbon reacts as a nucleophilic center. In this way, the traditional reactivity profile of the carbonyl group is transiently inverted, and unconventional product classes are generated. Alternatively, addition/elimination of the NHC to a suitably electrophilic substrate at the carboxylic acid oxidation level provides an acylazolium species **B**, which typically reacts directly with nucleophiles or may first be transformed into the corresponding enolate deriva-

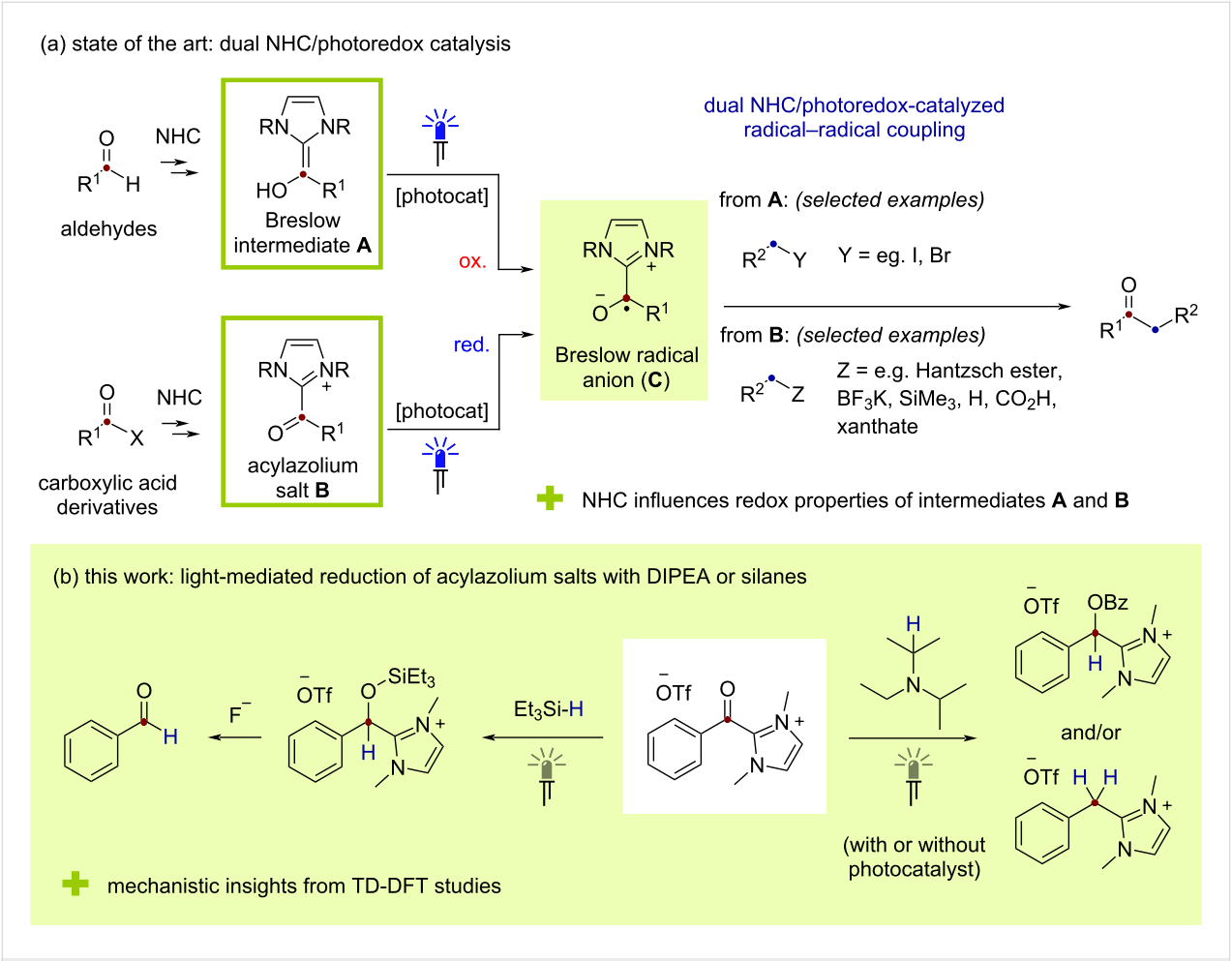

Figure 1: (a) Combining *N*-heterocyclic carbene (NHC) organocatalysis with photoredox catalysis for radical–radical coupling reactions. (b) This work: light-mediated reduction of acylimidazolium species **1** with the tertiary amine DIPEA or the simple silane $HSiEt_3$.

tive. Regardless of the individual pathway, NHC-catalyzed reactions of this type offer many synthetic advantages while the wide availability of chiral NHCs can also allow for high levels of enantioselectivity.

As effective enamine and active ester derivatives, Breslow and acylazolium intermediates **A** and **B** typically react via classical two-electron polar mechanisms, however, recent research has demonstrated that NHCs are also capable of stabilizing radical or excited-state species [12,13]. In 2020, our group reported the concept of photo-NHC catalysis where direct excitation of acylazolium intermediates generated from *o*-toluoyl fluoride substrates with UV-A light resulted in a novel catalytic photoenolization/Diels–Alder (PEDA) reaction [14,15]. In this process, the NHC fragment present in the acylazolium species influences the absorption wavelength and fundamental photochemical reactivity of the C=O bond, enabling a "ketone-like" photoreaction from otherwise unsuitable carboxylic acid derivative substrates [16]. Over the last few years, a wide range of valuable NHC-catalyzed transformations have also been developed that incorporate redox steps. As an enamine species, single-electron oxidation of a Breslow intermediate is comparatively favored with the resulting open shell species **C** benefitting from additional stabilization by virtue of electron delocalization onto the NHC-derived azolium ring [17-20]. Similarly, the cationic azolium fragment in acylazolium salts can effectively lower the carbonyl reduction potential relative to the starting material with single-electron reduction delivering the same stabilized radical **C**. Beginning with a seminal report by di Rocco and Rovis in 2012 [21], the combination of NHC and photoredox catalysis has recently been the subject of intense research activity [22-30]. Employing the latter reductive manifold with carboxylic acid derivatives, numerous coupling processes affording ketone products have been developed. Since the initial report from Scheidt and co-workers using 4-alkyl-substituted Hantzsch esters as coupling partners [31-36], several alkyl radical sources have been employed including carboxylic acids [37], xanthates [38], electron-rich toluene or heteroatom-substi-

tuted species [39-42], organoboron compounds [43,44] and organosilanes [43,45]. Moreover, three-component radical relay processes employing styrene derivatives have also been widely studied. In contrast to these numerous reports with carbon-based alkyl radicals, dual NHC/photoredox-mediated coupling processes between carboxylic acid derivatives and other classes of radical are lacking [22-30]. In particular, to the best of our knowledge, formal reduction reactions of carboxylic acid derivatives involving hydrogen-atom transfer have not been reported despite the fundamental importance of carbonyl reduction processes in organic synthesis [46]. Here, we report the results of our investigation into such reactions using an acylazolium salt derived from benzoic acid as a model substrate (Figure 1b). This led to the successful development of a novel dual NHC/light-mediated reduction process using either the simple tertiary amine, $NEt(iPr)_2$ (DIPEA) or the widely available silane $HSiEt_3$, as the only reductant. Moreover, interesting insights into the reaction mechanism supported by density functional theory (DFT) calculations were obtained.

Results and Discussion

Photoreduction of 2-benzoylimidazolium triflate with diisopropylethylamine

Initial investigations

To investigate the potential for the light-mediated reduction of acylazolium salts, compound **1** was prepared as a representative substrate in two steps from benzoyl chloride, imidazole and methyl trifluoromethanesulfonate. In an initial reaction, this species was reacted under photoredox conditions in the presence of $[Ir(dF(CF_3)ppy)_2(dtbpy)]PF_6$ (2 mol %, $dF(CF_3)ppy$ = 3,5-difluoro-2-[5-(trifluoromethyl)-2-pyridine, dtbpy = 4,4′-di-*tert*-butyl-2,2′-dipyridine) as a photocatalyst and the simple tertiary amine diisopropylethylamine (DIPEA, 5 equiv) in MeCN (0.05 M). After 24 h under irradiation with light from blue LEDs (λ_{max} = 440 nm), the crude mixture was concentrated under reduced pressure and analyzed by ^{1}H NMR spectroscopy. As shown in Figure 2, complete consumption of **1** was observed under these conditions with concomitant formation of a major new species with a characteristic ^{1}H NMR signal at δ = 4.42 ppm (in $CDCl_3$, Table 1, entry 1). Comparison of the spectrum with that of an authentic sample (see Supporting Information File 1) allowed for the unambiguous identification of this product as the 2-benzylimidazolium compound **2**. The formation of this species results from an overall 4-electron-reduction process, indicating that the photocatalytic system with DIPEA as the terminal reductant is capable of facilitating two reduction steps with an initial reaction with the acylazolium starting material being followed by a presumably more challenging second reduction of a less-activated intermediate species. Using CH_2Br_2 as an internal reference, a ^{1}H NMR yield of 39% was calculated with further analysis of the crude spectrum also indicating the presence of significant amounts of the imidazolium salt **IMeH$^+$** (characteristic C2–H signal at δ = 8.94 ppm; 28%) and benzoate species (**BzO$^-$**, *ortho*-C–H signals at δ = 7.98 ppm; 50%).

To confirm the photocatalytic nature of the novel carbonyl reduction process, a series of control reactions were carried out. As expected, conducting the reaction in the absence of the terminal reductant, DIPEA, led to a complex reaction mixture (Table 1, entry 2), while performing the reaction in the dark resulted only in recovered starting material (Table 1, entry 3). To our surprise, however, irradiation of **1** and DIPEA (5 equiv) in the absence of the photocatalyst (λ_{max} = 440 nm) did result in significant consumption of the acylazolium species (11% remaining by ^{1}H NMR) with the fully reduced species **2** being observed in trace amounts (^{1}H NMR yield = 2%). In addition to these compounds, **IMeH$^+$** (45%) and **BzO$^-$** (43%), additional signals consistent with the *O*-benzoylated species **3** were identified. This compound was synthesized independently from benzoyl chloride and 1-methylimidazole (see Supporting Information File 1) with spiking of the crude ^{1}H NMR spectrum with the authentic sample confirming the presence of this intermediate reduction product in the reaction mixture. Compound **3** is likely formed in a two-stage process involving initial reduction

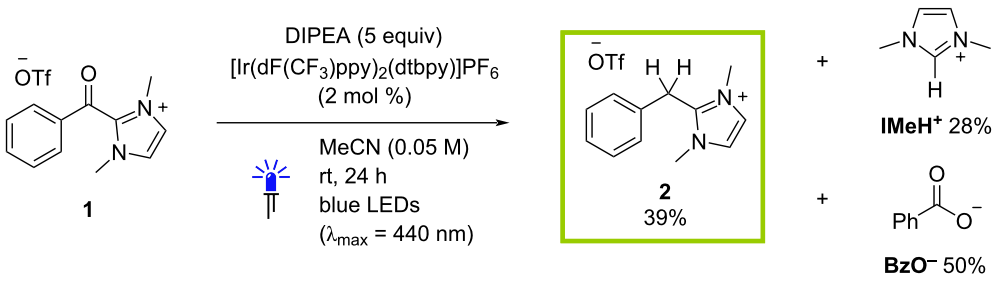

Figure 2: Initial test reaction employing $[Ir(dF(CF_3)ppy)_2(dtbpy)]PF_6$ as a photocatalyst in the presence of DIPEA (5 equiv). ^{1}H NMR yields shown using CH_2Br_2 as an internal standard and assuming a one-to-one molar ratio of starting material **1** to products.

Table 1: Survey of reaction conditions for the light-mediated reduction of 2-benzoylimidazolium salt **1** using DIPEA as the terminal reductant.

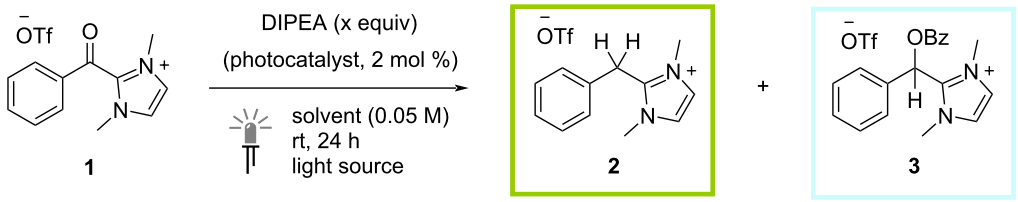

Entry[a]	Photocatalyst	Equiv of DIPEA	Solvent	Light source (λ_{max})	Yield of **2**[b]	Yield of **3**[b]
1	$[Ir(dF(CF_3)ppy)_2(dtbpy)]PF_6$	5	MeCN	440 nm	39%	–
2	$[Ir(dF(CF_3)ppy)_2(dtbpy)]PF_6$	–	MeCN	440 nm	n.d.[c]	n.d.[c]
3[d]	$[Ir(dF(CF_3)ppy)_2(dtbpy)]PF_6$	5	MeCN	440 nm	–	–
4	–	5	MeCN	440 nm	2%	15%
5	–	5	MeCN	370 nm	38%	9%
6	–	4	MeCN	370 nm	29%	21%
7	–	3	MeCN	370 nm	21%	21%
8	–	2	MeCN	370 nm	24%	17%
9	–	1	MeCN	370 nm	30%	9%
10	–	1	DCM	370 nm	6%	38%
11	–	1	DCE	370 nm	6%	35%
12	–	1	PhCl	370 nm	8%	38%
13	–	1	$PhCF_3$	370 nm	11%	24%
14	–	1	acetone	370 nm	14%	24%
15	–	1	THF	370 nm	4%	7%
16	–	1	DMF	370 nm	n.d.[c]	n.d.[c]
17	$[Ir(dF(CF_3)ppy)_2(dtbpy)]PF_6$	1	MeCN	440 nm	48%	–
18	$[Ir(ppy)_2(dtbpy)]PF_6$	1	MeCN	440 nm	46%	traces
19	4CzIPN	1	MeCN	440 nm	50%	–

[a]Reactions conducted on a 0.1 mmol scale in a dry Schlenk flask. [b]^{1}H NMR yields using CH_2Br_2 as an internal standard and assuming a one-to-one molar ratio of starting material **1** to products. [c]Complex reaction mixture. [d]Reaction conducted in the dark.

of the carbonyl group followed by addition/elimination of the resulting alkoxide into a second equivalent of the acylazolium salt **1**; a sequence which also partially explains the generation of the free **IMeH$^+$** observed in the crude reaction mixture. Integration of the signals indicated a ^{1}H NMR yield of 15% on a one-to-one molar basis relative to the acylazolium species **1**, however, given that two molecules of **1** are required to form one molecule of **3**, this represents an actual chemical yield of 30%. While seemingly less efficient than the photoredox process, the successful generation of reduced species in the absence of the catalyst is a remarkable result that highlights the unique influence of the NHC fragment on the reduction potentials and photoreactivity of acylazolium salts.

Survey of reaction conditions

To gain further insight into the photocatalyst-free reduction process, a survey of reaction conditions was conducted. In each case, the ^{1}H NMR yields of the reduced species were calculated using CH_2Br_2 as an internal standard with results displayed in Table 1. To avoid confusion and facilitate comparisons between different conditions, percentage yields are stated on a one-to-one molar basis with respect to the acylazolium starting material **1** ignoring the influence of reaction stoichiometry. Firstly, the wavelength of the light source (λ_{max}) was changed from 440 nm (blue LEDs) to 370 nm (UV-A). This resulted in an overall improvement in the reduction efficiency with the fully reduced species **2** becoming the major product formed in 38% yield alongside the *O*-benzoylated species **3** (9%, Table 1, entry 5). This result is again remarkable in that it appears the simple combination of the tertiary amine DIPEA and UV-A light irradiation is sufficient to effect complete reduction of the acylazolium species. Decreasing the equivalents of DIPEA did not have a significant influence on the overall amount of reduced products formed although the proportion of the fully reduced species **2** relative to **3** generally decreased (Table 1, entries 6–9). Employing just 1 equivalent of

DIPEA nevertheless delivered 30% of **2** alongside 9% of **3**. A survey of common organic solvents was then conducted to investigate the influence of the reaction medium. Interestingly, switching from MeCN to the chlorinated solvents DCM, DCE and chlorobenzene led to a decline in the formation of the fully reduced product **2** with *O*-benzoylated species **3** being obtained as the major product (38% in DCM, 35% in DCE, 38% in PhCl cf. 6–8% of **2**, Table 1, entries 10–12). Significant reduction of **1** was also observed in $PhCF_3$ (11% of **2**, 24% of **3**, Table 1, entry 13) and acetone (14% of **2**, 24% of **3**, Table 1, entry 14), however, relatively complex reaction mixtures were obtained in either THF (4% of **2**, 7% of **3**, Table 1, entry 15) or DMF (Table 1, entry 16). At this stage, we returned our attention to the photocatalyzed process, testing a selection of photocatalysts in the presence of 1 equivalent of DIPEA under blue light irradiation (λ_{max} = 440 nm). Notably, under these modified conditions, the photocatalyzed reaction with the originally test photocatalyst, $[Ir(dF(CF_3)ppy)_2(dtbpy)]PF_6$, resulted in clean formation of the fully reduced product **2** in 48% ^{1}H NMR yield with no intermediate species **3** being detected (Table 1, entry 17). The related iridium complex $[Ir(ppy)_2(dtbpy)]PF_6$ (ppy = 2-phenylpyridine) delivered **2** in a similar yield of 46% (Table 1, entry 18) while the organic species 1,2,3,5-tetrakis(carbazol-9-yl)-4,6-dicyanobenzene (4CzIPN), which has been commonly employed in dual NHC/photoredox-catalyzed coupling reactions, cleanly provided the fully reduced species in 50% ^{1}H NMR yield (Table 1, entry 19).

Comments on the reaction mechanism

At this stage of the study, our attention turned to a consideration of the reaction mechanism. As has been well documented in the photoredox literature [47-53], excitation of a photocatalyst ([PC]) in the presence of DIPEA can result in reductive quenching of the excited state, affording the corresponding photocatalyst radical anion ($[PC]^{\bullet-}$) and the DIPEA radical cation **D** (Scheme 1). Single-electron transfer from $[PC]^{\bullet-}$ to the benzoylazolium species **1** would then regenerate the ground-state photocatalyst and afford the Breslow radical anion **C**, which could in turn react with **D** in a hydrogen-atom-transfer (HAT) step to form the zwitterionic alkoxide **E** and the oxidized DIPEA iminium ion **F**. Notably, small signals consistent with trace amounts of the alkoxide species **E** were occasionally detected in the crude ^{1}H NMR spectra of reactions conducted both in the presence and absence of a photocatalyst (see Supporting Information File 1 for details). Finally, **E** could react in an addition/elimination process with a second molecule of the benzoylazolium starting material **1** to afford the observed *O*-benzoylated species **3**. An analogous reductive quenching cycle where the reduced photocatalyst $[PC]^{\bullet-}$ instead transfers an electron to compound **3** could explain the formation of the fully reduced species **2**. In this case, subsequent mesolysis would generate the benzyl radical cation **G**, which would deliver **2** following a HAT step with the DIPEA radical cation **D**.

To confirm whether *O*-benzoylated species is indeed an intermediate in the formation of the fully reduced product **2** under photocatalytic conditions, the independently synthesized **3** was irradiated with 1 equivalent of DIPEA and 4CzIPN under the conditions shown in Table 1, entry 16 (Scheme 1, in yellow box). After 24 h at rt, clean conversion into **2** (77% ^{1}H NMR yield) was observed, implying that a mechanistic scenario in line with that shown in Scheme 1 is plausible. Given that two molecules of the benzoylazolium starting material are required to form one molecule of **3** and, by extension **2**, the ^{1}H NMR yields of 46–50% quoted for the photocatalytic reactions in Table 1, entries 14–16, actually represent a near quantitative chemical conversion into the fully reduced species.

The successful reduction of **1** into both **2** and **3** in the absence of a photocatalyst requires an alternative mechanistic explanation. Without a sensitizer present, a question arises regarding the identity of the active light-absorbing species in the reaction mixture. UV–vis spectra of the benzoylazolium starting material **1** at different concentrations in the acetonitrile reaction solvent were accordingly measured. Although exhibiting maximum absorption at wavelengths significantly shorter than that emitted by the light sources used (latest $\lambda_{abs,max}$ = 271 nm), a significant absorption tail up to ca. λ = 400 nm was observed at higher concentrations, indicating that the starting material could potentially absorb the incident light directly. This rationale is consistent with the increase in reduction efficiency observed upon switching from blue to UV-A light irradiation. Nevertheless, alternative scenarios involving the potential formation of excited donor–acceptor (EDA) complexes between benzoylazolium species **1** and DIPEA were considered. Measurements of the UV–vis spectra in the presence of the amine, however, did not reveal any significant change in the absorption profile. To gain further insight, time-dependent density functional theory (TD-DFT) calculations were carried out (for details of the computational studies, see Supporting Information File 1). In line with the UV–vis studies, comparison of the computed vertical absorption spectrum of the benzoylazolium salt **1** with and without DIPEA did not reveal the formation of an EDA complex. We therefore propose that, even under irradiation with comparatively long wavelength blue light (λ_{max} = 440 nm), the benzoylimidazolium species **1** likely acts as the active absorbing species with its absorption band overlapping sufficiently with the emission front of the employed LEDs. Direct absorption of light by acylazolium species has indeed been previously proposed as a mechanistic pathway in light-mediated NHC-catalyzed coupling reactions [22-30]. The

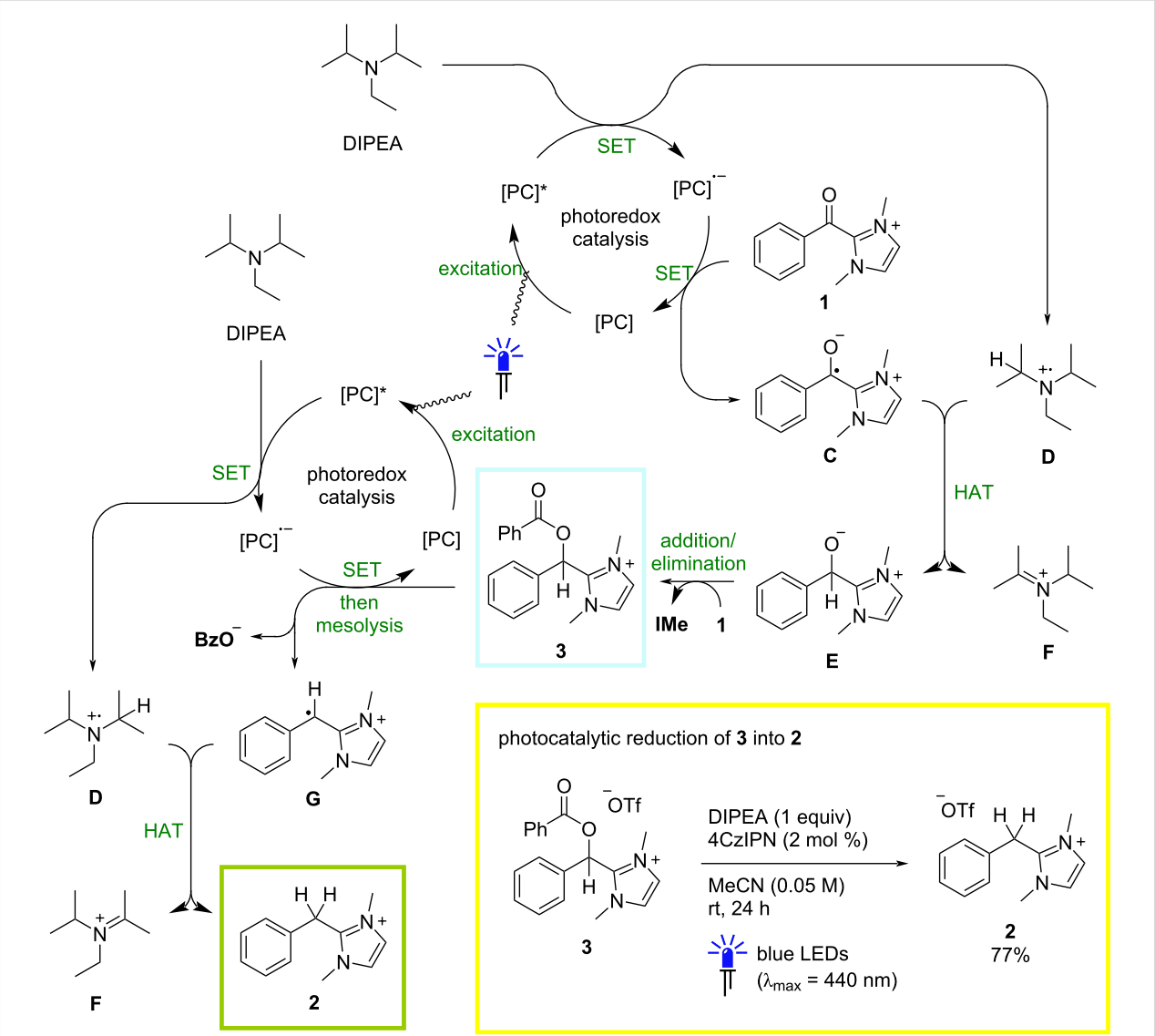

Scheme 1: Plausible mechanism for the photocatalytic reduction of benzoylimidazolium salt **1** with DIPEA. [PC] = photocatalyst; SET = single-electron transfer; HAT = hydrogen atom transfer.

TD-DFT calculations also provided insight into the nature of the subsequent mechanistic steps where the excited benzoylimidazolium **1*** is converted to the reduced zwitterionic alkoxide species **E** in the presence of DIPEA (Scheme 2). This requires the transfer of both an electron and a hydrogen atom from the amine to the excited carbonyl species, and analysis of the computed charge distributions indicates that these processes occur simultaneously in what can be best described as a formal hydride ion transfer. Addition/elimination of **E** into the carbonyl group of a second molecule of **1** then generates the *O*-benzoylated species **3**.

Determining a mechanistic rationale for the generation of the fully reduced species **2** under photocatalyst-free conditions is more challenging. The *O*-benzoylated species **3** is expected to be less susceptible to reduction than the benzoylazolium starting material **1** and, with no discernible chromophores present, it is also less likely to absorb the incident light. Indeed, when subjected to the reaction conditions shown in Table 1, entry 9 with 1 equivalent of DIPEA under UV-A light irradiation, only sluggish conversion of independently synthesized **3** into the 2-benzylimidazolium salt **2** was observed (^{1}H NMR yield = 8%) with 90% of **3** remaining unreacted after 24 h at rt (Scheme 2, in yellow box). To gain more insight into the reaction course in the absence of a photocatalyst, the reduction of **1** with DIPEA (1 equiv) under UV-A irradiation was followed by ^{1}H NMR over the course of 48 h. As shown in Figure 3, at the start of the reaction, rapid consumption of the benzoylazolium

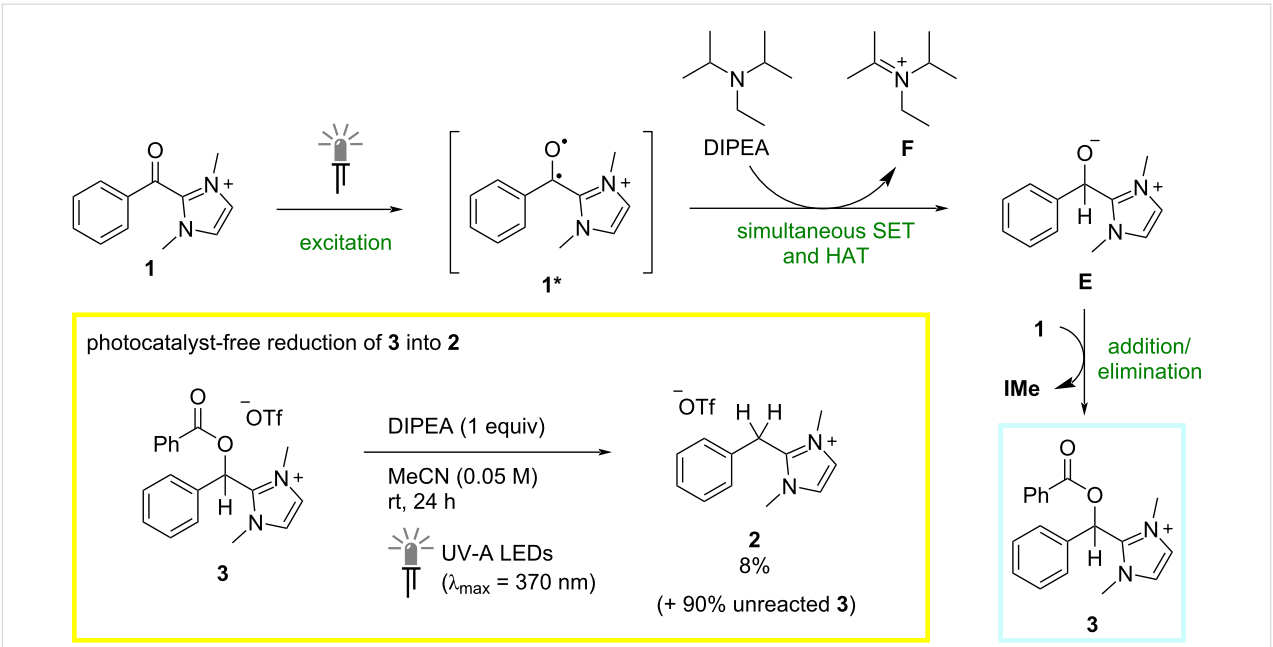

Scheme 2: Plausible mechanism for the photocatalyst-free reduction of benzoylimidazolium salt **1** into *O*-benzoylated compound **3** with DIPEA.

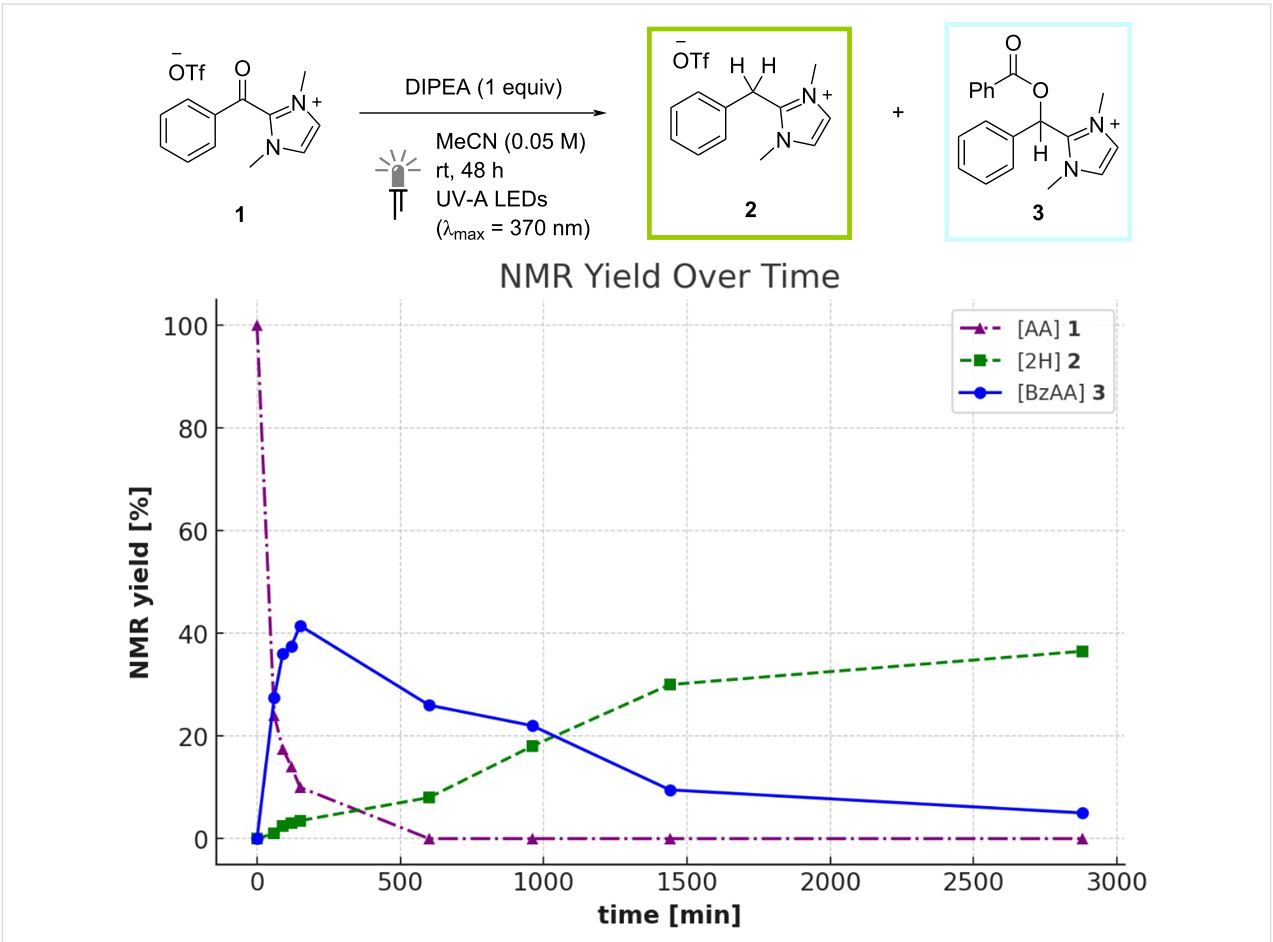

Figure 3: Reduction of 2-benzoylimidazolium triflate (**1**) under photocatalyst-free conditions monitored over 48 h by ^{1}H NMR.

starting material was observed with concomitant formation of *O*-benzoylated product **3**. The concentration of this species then slowly decreased over the remaining reaction time along with increasing formation of the fully reduced compound **2**. Taken together, these experiments seem to indicate that the *O*-benzoylated species **3** is indeed an intermediate in the formation of **2** but that the second reduction largely occurs only in concert with the initial reduction of **1**. Further studies would be needed to fully elucidate the active mechanistic pathway in this system, however, potential explanations could include activation of **3** by DIPEA-derived reaction by-products, or invoke the involvement of the strongly reducing DIPEA α-amino radical, which could feasibly be formed under the reaction conditions [54].

Photoreduction of 2-benzoylimidazolium triflate with triethylsilane

Although the DIPEA-mediated photochemical reduction of benzoylimidazolium species **1** was successful, the reaction stoichiometry where two molecules of the starting material provide only one molecule of the reduced products **2** or **3** limits the overall efficiency. To overcome this limitation, we considered whether a different approach could provide reduced products in yields greater than 50% relative to the starting material **1**. In particular, addition of chloro(trimethyl)silane (TMSCl) to the reaction mixture could provide an electrophile capable of trapping the putative alkoxide zwitterionic intermediate **E**, outcompeting *O*-benzoylation by a second molecule of **1**. Pleasingly, conducting the standard photocatalyst-free reduction of **1** with 1 equivalent of DIPEA under UV-A light irradiation (λ_{max} = 370 nm) in the presence of 1.2 equivalents of TMSCl resulted in the formation of new peaks in the crude ^{1}H NMR spectrum consistent with the desired silyl-protected species **4** (Scheme 3a). Crucially, the calculated ^{1}H NMR yield of this species (62%) is higher than the maximum of 50% possible from the mechanism discussed above.

A further intriguing result was obtained upon switching from a chlorosilane to a hydrosilane. To our surprise, irradiating benzoylimidazolium species **1** with UV-A light (λ_{max} = 370 nm) in MeCN (0.05 M) in the presence Et_3SiH (TESH, 1.2 equiv) led to smooth conversion into the silylated species **5** (^{1}H NMR yield = 62%; with 6% of **3**) even in the absence of DIPEA (Scheme 3b). This remarkable result shows that simple silanes are capable of reducing NHC-derived acylazolium species with the calculated ^{1}H NMR yield above 50% indicating that this approach is potentially higher yielding than the

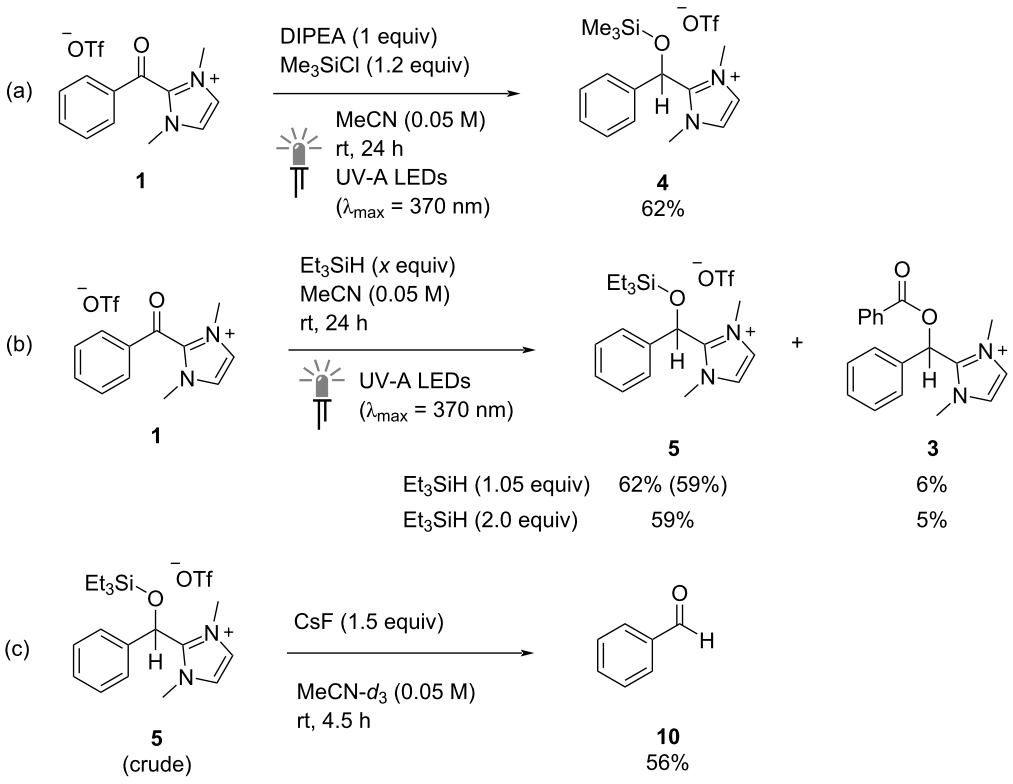

Scheme 3: (a) Reduction of 2-benzoylimidazolium triflate (**1**) under photocatalyst-free conditions with DIPEA and TMSCl. (b) Reduction of 2-benzoylimidazolium triflate (**1**) under photocatalyst-free conditions with TESH. (c) Desilylation and NHC elimination of TES-protected alkoxide **5** with CsF. ^{1}H NMR yields reported using CH_2Br_2 as an internal standard, isolated yields in parentheses.

DIPEA-mediated reduction developed above. Performing the same reaction with a selection of electronically diverse derivatives of **1** bearing 4-CF_3 (**6**), 4-CO_2Me (**7**) and 4-OMe (**8**) groups also resulted in the formation of reduced products with ^{1}H NMR spectra consistent with *O*-silylated species (^{1}H NMR yields: from **6** = 54%; from **7** = 53%, from **8** = 38%), however, a representative aliphatic species, 2-(cyclohexanoyl)-1,3-(dimethyl)imidazolium triflate (**9**) was unreactive. The lower efficiency of the reaction with the 4-methoxy-substituted azolium **8** (30% starting material remaining) is consistent with the expected higher reduction potential of this comparatively electron-rich compound. Purification of the crude reaction mixture from **1** by column chromatography allowed for the isolation of pure product **5** as a colorless oil in 59% yield. A control reaction performed under the same conditions in the dark resulted only in recovered starting material, while **5** was formed in only 5% ^{1}H NMR yield when **1** and TESH (1.2 equiv) were irradiated with blue light (λ_{max} = 440 nm) in the presence of the photocatalyst 4CzIPN (2 mol %). These results imply that the silane-mediated reduction is light-mediated and likely involves direct excitation of the benzoylazolium salt with the excited state species **1***, which subsequently reacts with TESH. Comparison of the redox potential of the silane (+1.54 V vs ferrocene) with the estimated excited-state potential of the azolium salt **1*** (+1.70 V vs ferrocene) suggest that direct electron transfer between these species affording zwitterionic radical **E** is thermodynamically feasible (for details, see Supporting Information File 1). In an alternative pathway, direct hydrogen atom transfer (HAT) from the silane to the oxygen atom of excited **1*** could occur. A similar HAT-step from **1*** was very recently proposed by Marzo and co-workers in an NHC-mediated coupling reaction with alkyl halides mediated by $(TMS)_3SiH$ [55]. The *O*-silylated product **5** could result from a subsequent radical *C*-silylation followed by a Brook-type rearrangement process [56]. Interestingly, performing the TESH-mediated reduction in the presence of additional TMSCl led to the formation of both possible *O*-silylated products with the TMS-substituted compound **4** being the major species obtained (^{1}H NMR yields: **4** = 34%; **5** = 12%). This intriguing result indicates that the *O*-silylation step is to some degree decoupled from the reduction process. Further mechanistic studies will be required, however, to fully elucidate the active pathways occurring in this system.

Finally, treatment of crude **5** with CsF (1.5 equiv) in MeCN-d_3 at rt led to efficient desilylation and elimination of the NHC, affording benzaldehyde (**10**) in 56% ^{1}H NMR yield (Scheme 3c). The successful generation of the aldehyde from the azolium species derived from the corresponding carboxylic acid highlights the potential of this two-step sequence as a method for the partial reduction of carboxyl compounds. Such transformations can be challenging in organic synthesis with complete reduction to the alcohol followed by partial re-oxidation often being conducted.

Conclusion

In conclusion, we have developed novel light-driven methodologies for the reduction of acylazolium salts using benzoylimidazolium triflate as a model substrate. In the presence of a photocatalyst under blue light irradiation, the simple tertiary amine DIPEA can serve as the terminal reductant, delivering predominantly the fully reduced benzylimidazolium species as the major product. Irradiation with UV-A light in the absence of a photocatalyst, however, also provides reduced products with an *O*-benzoylated intermediate species also being obtained under some conditions. Supported by TD-DFT studies, plausible reaction mechanisms for both processes were proposed. Moreover, further investigations employing silicon-containing additives allowed for an increase in the reduction yield beyond the maximum of 50% achievable using DIPEA. This study also led to the development of a novel silane-mediated photoreduction method where triethylsilane serves as both as terminal reductant and alkoxide trapping reagent, with subsequent treatment with fluoride providing the corresponding aldehyde. Given the importance of carboxyl reduction reactions in organic synthesis and the recent explosion in interest in light-mediated NHC-catalyzed coupling reactions, we believe this work will be of value to the community and further studies on these systems, including on the development of catalytic applications, are underway in our laboratory.

Supporting Information

Supporting Information File 1

Experimental procedures, characterization data of all isolated products, details of UV–vis, time-course and computational studies as well as copies of NMR spectra for novel compounds.
[https://www.beilstein-journals.org/bjoc/content/supplementary/1860-5397-21-153-S1.pdf]

Acknowledgements

We thank Prof. Dr. Beate Koksch and the AG Koksch (FU Berlin) for supervisory assistance and helpful discussions, as well as Andreas Mavroskoufis, Dr. Stefan Dix and Anastasia Carrano (all FU Berlin) for performing initial experiments and Haoyue Wang (Newcastle University) for providing acyl azolium salt substrates. We also thank Prof. Dr. Frank Glorius (WWU Muenster, Germany) for initial support and helpful discussions. We would like to acknowledge the assistance of the

Core Facility BioSupraMol supported by the DFG and the HPC Service of FUB-IT, Freie Universität Berlin, for computing time.

Funding

Funded by the Deutsche Forschungsgemeinschaft (DFG, German Research Foundation) - Project-IDs 420535461 & 393271229 (gefördert durch die Deutsche Forschungsgemeinschaft (DFG) – Projektnummer 420535461 & 393271229), the State of Berlin (Elsa Neumann Scholarship to M. J.) and the Dahlem Research School. Financial support from the Fonds der Chemischen Industrie (FCI, Sachkostenzuschuss) is also gratefully acknowledged.

ORCID® iDs

Michael Jakob - https://orcid.org/0000-0003-3584-8784
Hassan Abdelwahab - https://orcid.org/0009-0000-2282-1748
Janos Wasternack - https://orcid.org/0009-0002-7784-4191
Jan P. Götze - https://orcid.org/0000-0003-2211-2057
Matthew N. Hopkinson - https://orcid.org/0000-0002-0183-0466

Data Availability Statement

Data generated and analyzed during this study is available from the corresponding author upon reasonable request.

References

1. Bourissou, D.; Guerret, O.; Gabbaï, F. P.; Bertrand, G. *Chem. Rev.* **2000,** *100,* 39–92. doi:10.1021/cr940472u
2. Hopkinson, M. N.; Richter, C.; Schedler, M.; Glorius, F. *Nature* **2014,** *510,* 485–496. doi:10.1038/nature13384
3. Bellotti, P.; Koy, M.; Hopkinson, M. N.; Glorius, F. *Nat. Rev. Chem.* **2021,** *5,* 711–725. doi:10.1038/s41570-021-00321-1
4. Enders, D.; Niemeier, O.; Henseler, A. *Chem. Rev.* **2007,** *107,* 5606–5655. doi:10.1021/cr068372z
5. Bugaut, X.; Glorius, F. *Chem. Soc. Rev.* **2012,** *41,* 3511–3522. doi:10.1039/c2cs15333e
6. Flanigan, D. M.; Romanov-Michailidis, F.; White, N. A.; Rovis, T. *Chem. Rev.* **2015,** *115,* 9307–9387. doi:10.1021/acs.chemrev.5b00060
7. Menon, R. S.; Biju, A. T.; Nair, V. *Chem. Soc. Rev.* **2015,** *44,* 5040–5052. doi:10.1039/c5cs00162e
8. Zhang, C.; Hooper, J. F.; Lupton, D. W. *ACS Catal.* **2017,** *7,* 2583–2596. doi:10.1021/acscatal.6b03663
9. Chen, X.; Wang, H.; Jin, Z.; Chi, Y. R. *Chin. J. Chem.* **2020,** *38,* 1167–1202. doi:10.1002/cjoc.202000107
10. Pareek, M.; Reddi, Y.; Sunoj, R. B. *Chem. Sci.* **2021,** *12,* 7973–7992. doi:10.1039/d1sc01910d
11. Song, R.; Xie, Y.; Jin, Z.; Chi, Y. R. *Angew. Chem., Int. Ed.* **2021,** *60,* 26026–26037. doi:10.1002/anie.202108630
12. Martin, C. D.; Soleilhavoup, M.; Bertrand, G. *Chem. Sci.* **2013,** *4,* 3020–3030. doi:10.1039/c3sc51174j
13. Mahoney, J. K.; Martin, D.; Moore, C. E.; Rheingold, A. L.; Bertrand, G. *J. Am. Chem. Soc.* **2013,** *135,* 18766–18769. doi:10.1021/ja4104765
14. Mavroskoufis, A.; Rajes, K.; Golz, P.; Agrawal, A.; Ruß, V.; Götze, J. P.; Hopkinson, M. N. *Angew. Chem., Int. Ed.* **2020,** *59,* 3190–3194. doi:10.1002/anie.201914456
15. Mavroskoufis, A.; Lohani, M.; Weber, M.; Hopkinson, M. N.; Götze, J. P. *Chem. Sci.* **2023,** *14,* 4027–4037. doi:10.1039/d2sc04732b
16. Hopkinson, M. N.; Mavroskoufis, A. *Synlett* **2021,** *32,* 95–101. doi:10.1055/s-0040-1706472
    See for a highlight on Photo-NHC catalysis.
17. Guin, J.; De Sarkar, S.; Grimme, S.; Studer, A. *Angew. Chem., Int. Ed.* **2008,** *47,* 8727–8730. doi:10.1002/anie.200802735
18. Ishii, T.; Kakeno, Y.; Nagao, K.; Ohmiya, H. *J. Am. Chem. Soc.* **2019,** *141,* 3854–3858. doi:10.1021/jacs.9b00880
19. Ishii, T.; Ota, K.; Nagao, K.; Ohmiya, H. *J. Am. Chem. Soc.* **2019,** *141,* 14073–14077. doi:10.1021/jacs.9b07194
20. Man, Y.; Liu, S.; Xu, B.; Zeng, X. *Org. Lett.* **2022,** *24,* 944–948. doi:10.1021/acs.orglett.1c04317
21. DiRocco, D. A.; Rovis, T. *J. Am. Chem. Soc.* **2012,** *134,* 8094–8097. doi:10.1021/ja3030164
22. Ishii, T.; Nagao, K.; Ohmiya, H. *Chem. Sci.* **2020,** *11,* 5630–5636. doi:10.1039/d0sc01538e
23. Mavroskoufis, A.; Jakob, M.; Hopkinson, M. N. *ChemPhotoChem* **2020,** *4,* 5147–5153. doi:10.1002/cptc.202000120
24. Liu, Q.; Chen, X.-Y. *Org. Chem. Front.* **2020,** *7,* 2082–2087. doi:10.1039/d0qo00494d
25. Liu, J.; Xing, X.-N.; Huang, J.-H.; Lu, L.-Q.; Xiao, W.-J. *Chem. Sci.* **2020,** *11,* 10605–10613. doi:10.1039/d0sc03595e
26. Marzo, L. *Eur. J. Org. Chem.* **2021,** 4603–4610. doi:10.1002/ejoc.202100261
27. Liu, K.; Schwenzer, M.; Studer, A. *ACS Catal.* **2022,** *12,* 11984–11999. doi:10.1021/acscatal.2c03996
28. Tang, Q.; Du, D.; Gao, J. *Eur. J. Org. Chem.* **2023,** *26,* e202300832. doi:10.1002/ejoc.202300832
29. Wang, X.; Wu, S.; Yang, R.; Song, H.; Liu, Y.; Wang, Q. *Chem. Sci.* **2023,** *14,* 13367–13383. doi:10.1039/d3sc03274d
30. Cai, H.; Yang, X.; Ren, S.-C.; Chi, Y. R. *ACS Catal.* **2024,** *14,* 8270–8293. doi:10.1021/acscatal.4c01973
31. Bay, A. V.; Fitzpatrick, K. P.; Betori, R. C.; Scheidt, K. A. *Angew. Chem., Int. Ed.* **2020,** *59,* 9143–9148. doi:10.1002/anie.202001824
32. Ren, S.-C.; Lv, W.-X.; Yang, X.; Yan, J.-L.; Xu, J.; Wang, F.-X.; Hao, L.; Chai, H.; Jin, Z.; Chi, Y. R. *ACS Catal.* **2021,** *11,* 2925–2934. doi:10.1021/acscatal.1c00165
33. Bay, A. V.; Fitzpatrick, K. P.; González-Montiel, G. A.; Farah, A. O.; Cheong, P. H.-Y.; Scheidt, K. A. *Angew. Chem., Int. Ed.* **2021,** *60,* 17925–17931. doi:10.1002/anie.202105354
34. Bay, A. V.; Farnam, E. J.; Scheidt, K. A. *J. Am. Chem. Soc.* **2022,** *144,* 7030–7037. doi:10.1021/jacs.1c13105
35. Wang, X.; Tang, Y.; Ye, S.; Zhang, J.; Kuang, Y.; Wu, J. *Org. Lett.* **2022,** *24,* 2059–2063. doi:10.1021/acs.orglett.2c00657
36. Byun, S.; Hwang, M. U.; Wise, H. R.; Bay, A. V.; Cheong, P. H.-Y.; Scheidt, K. A. *Angew. Chem., Int. Ed.* **2023,** *62,* e202312829. doi:10.1002/anie.202312829
37. Ren, S.-C.; Yang, X.; Mondal, B.; Mou, C.; Tian, W.; Jin, Z.; Chi, Y. R. *Nat. Commun.* **2022,** *13,* 2846. doi:10.1038/s41467-022-30583-2
38. Tan, C.-Y.; Kim, M.; Hong, S. *Angew. Chem., Int. Ed.* **2023,** *62,* e202306191. doi:10.1002/anie.202306191
39. Meng, Q.-Y.; Lezius, L.; Studer, A. *Nat. Commun.* **2021,** *12,* 2068. doi:10.1038/s41467-021-22292-z
40. Wang, X.; Zhu, B.; Liu, Y.; Wang, Q. *ACS Catal.* **2022,** *12,* 2522–2531. doi:10.1021/acscatal.1c05815
41. Wang, X.; Yang, R.; Zhu, B.; Liu, Y.; Song, H.; Dong, J.; Wang, Q. *Nat. Commun.* **2023,** *14,* 2951. doi:10.1038/s41467-023-38743-8

42. Zhu, J. L.; Schull, C. R.; Tam, A. T.; Rentería-Gómez, Á.; Gogoi, A. R.; Gutierrez, O.; Scheidt, K. A. *J. Am. Chem. Soc.* **2023,** *145,* 1535–1541. doi:10.1021/jacs.2c12845
43. Huang, H.; Dai, Q.-S.; Leng, H.-J.; Li, Q.-Z.; Yang, S.-L.; Tao, Y.-M.; Zhang, X.; Qi, T.; Li, J.-L. *Chem. Sci.* **2022,** *13,* 2584–2590. doi:10.1039/d1sc06102j
44. Liu, W.-C.; Zhang, X.; Chen, L.; Zeng, R.; Tian, Y.-H.; Ma, E.-D.; Wang, Y.-P.; Zhang, B.; Li, J.-L. *ACS Catal.* **2024,** *14,* 3181–3190. doi:10.1021/acscatal.3c06027
45. Jakob, M.; Steiner, L.; Göbel, M.; Götze, J. P.; Hopkinson, M. N. *ACS Catal.* **2024,** *14,* 17642–17653. doi:10.1021/acscatal.4c03103
46. Magano, J.; Dunetz, J. R. *Org. Process Res. Dev.* **2012,** *16,* 1156–1184. doi:10.1021/op2003826
47. Narayanam, J. M. R.; Stephenson, C. R. J. *Chem. Soc. Rev.* **2011,** *40,* 102–113. doi:10.1039/b913880n
48. Tucker, J. W.; Stephenson, C. R. J. *J. Org. Chem.* **2012,** *77,* 1617–1622. doi:10.1021/jo202538x
49. Prier, C. K.; Rankic, D. A.; MacMillan, D. W. C. *Chem. Rev.* **2013,** *113,* 5322–5363. doi:10.1021/cr300503r
50. Schultz, D. M.; Yoon, T. P. *Science* **2014,** *343,* 1239176. doi:10.1126/science.1239176
51. Nicewicz, D. A.; Nguyen, T. M. *ACS Catal.* **2014,** *4,* 355–360. doi:10.1021/cs400956a
52. Marzo, L.; Pagire, S. K.; Reiser, O.; König, B. *Angew. Chem., Int. Ed.* **2018,** *57,* 10034–10072. doi:10.1002/anie.201709766
53. Petzold, D.; Giedyk, M.; Chatterjee, A.; König, B. *Eur. J. Org. Chem.* **2020,** 1193–1244. doi:10.1002/ejoc.201901421
54. DeLaive, P. J.; Foreman, T. K.; Giannotti, C.; Whitten, D. G. *J. Am. Chem. Soc.* **1980,** *102,* 5627–5631. doi:10.1021/ja00537a037
55. MacLean, I.; Grenda, D. J.; Echávarri, E.; Muth, S.; Nuernberger, P.; Marzo, L. *J. Am. Chem. Soc.* **2025,** *147,* 31324–31331. doi:10.1021/jacs.5c10923
56. Wang, T.; Wang, G.-Q.; Zhang, Y.; Liu, Y.-Y.; Zhang, Z.-B.; Han, P.; Jing, L.-H. *Eur. J. Org. Chem.* **2023,** *26,* e202301087. doi:10.1002/ejoc.202301087

License and Terms

BEILSTEIN JOURNAL OF ORGANIC CHEMISTRY

Enantioselective radical chemistry: a bright future ahead

Anna C. Renner, Sagar S. Thorat, Hariharaputhiran Subramanian* and Mukund P. Sibi*

Perspective

Open Access

Address:
Department of Chemistry and Biochemistry, North Dakota State University, Fargo, North Dakota, 58105-5516, USA

Email:
Hariharaputhiran Subramanian* - Hariharaputhiran.Sub@ndsu.edu;
Mukund P. Sibi* - Mukund.Sibi@ndsu.edu

* Corresponding author

Keywords:
chiral Lewis acid; electrochemistry; enantioselective radical reaction; organocatalysis; photoenzymatic catalysis; photoredox

Beilstein J. Org. Chem. **2025,** *21,* 2283–2296.
https://doi.org/10.3762/bjoc.21.174

Received: 08 August 2025
Accepted: 17 October 2025
Published: 28 October 2025

This article is part of the thematic issue "Modern radical chemistry".

Guest Editor: H.-M. Huang

Abstract

This perspective is focused on enantioselective free radical reactions. It describes several important catalytic asymmetric strategies applied to enantioselective radical reactions, including chiral Lewis acid catalysis, organocatalysis, photoredox catalysis, chiral transition-metal catalysis and photoenzymatic catalysis. The application of electrochemistry to asymmetric radical transformations is also discussed.

Introduction

Asymmetric catalysis plays an integral role in the enantioselective synthesis of organic compounds. A wide variety of enantioenriched catalysts ranging from chiral organometallic complexes to organocatalysts (small organic molecules) have been designed, synthesized, and successfully used in several organic transformations [1-3]. Despite these advances, catalytic methods involving radical intermediates were very rare until the 1990s. Since then, meticulous research by several research groups has led to significant advances in this area [4-8]. This perspective focuses on several important contributions to the science of asymmetric radical reactions. Pioneering work on chiral Lewis acid catalysis and iminium catalysis is discussed initially. This is followed by the recently emerging areas of transition-metal catalysis, photoenzymatic catalysis, and electrochemistry.

Perspective

Radical generation and reactions

Synthetic methods based on free radical chemistry are some of the most efficient and powerful tools for the construction of carbon–carbon and carbon–heteroatom bonds. Unlike many ionic reactions, radical reactions are often functional group tolerant and carried out under mild, neutral conditions, avoiding harsh acidic or basic conditions that can promote epimerization or decomposition of the product. Additionally, radical chemistry offers opportunities to achieve transformations that may not proceed via two-electron processes.

Radicals can be generated through several different approaches, summarized in Figure 1A. The use of organostannanes to generate carbon-centered radicals was formerly commonplace

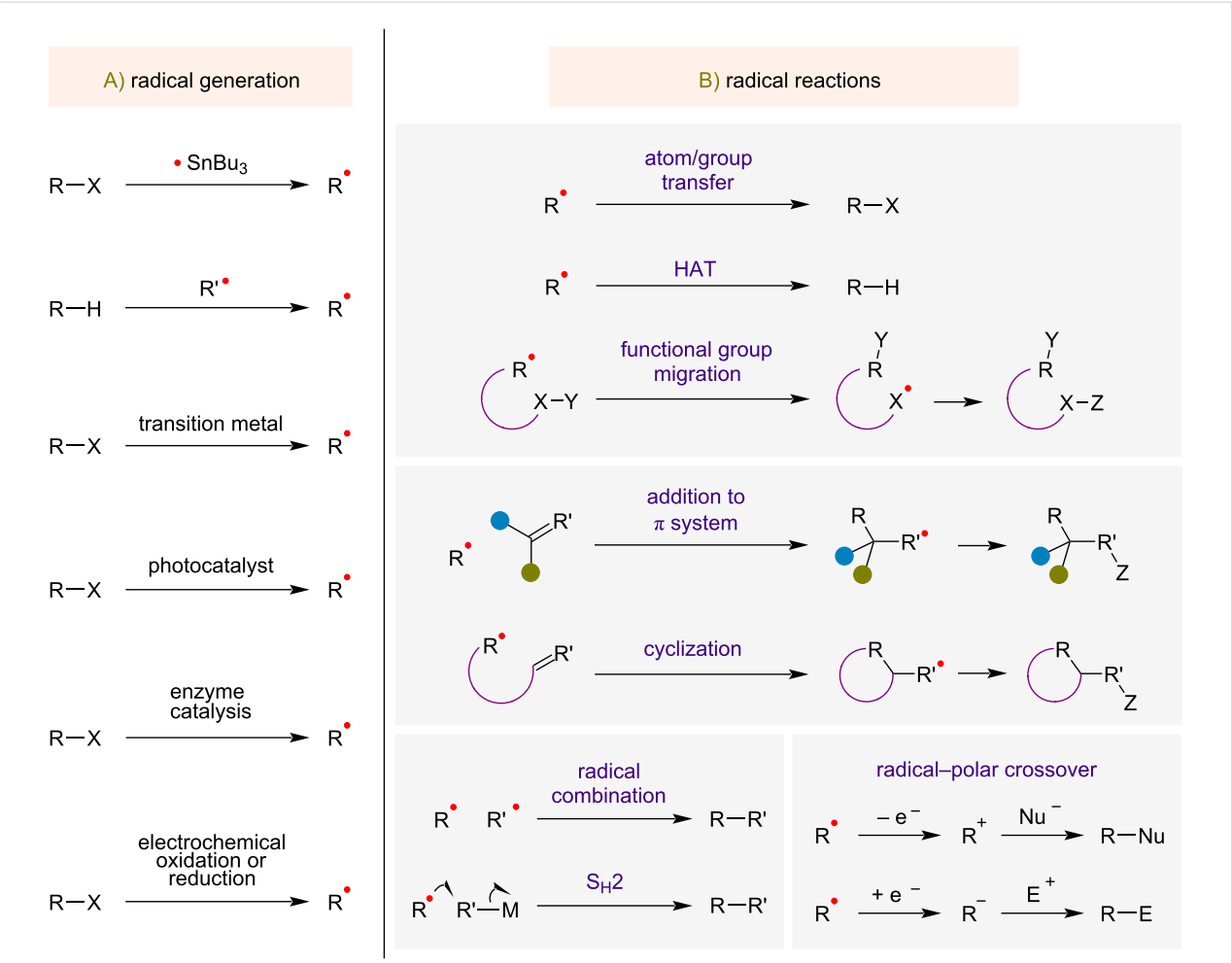

Figure 1: Methods of radical generation (A) and general types of radical reactions (B).

but has been largely supplanted by greener methods employing less-toxic reagents. Using alternative methods, radicals can be generated by hydrogen atom transfer (HAT), resulting in the homolytic cleavage of a carbon–hydrogen bond. Other approaches for radical generation in modern radical transformations include the use of transition metals or photoredox catalysts. In photoredox catalysis, radical generation often involves single-electron transfer (SET) to or from a photoexcited state of a photoredox catalyst, usually a metal complex or organic molecule. Two other notable strategies for radical generation are photoenzymatic catalysis and electrochemical oxidation or reduction.

Free radicals can undergo several types of basic reactions (Figure 1B), including atom or group transfer, addition to a π-bond, and radical–radical combination. In an atom or group transfer reaction, an atom or group is transferred to the radical. Important processes of this kind are hydrogen atom transfer (HAT) and halogen atom abstraction. An intramolecular group transfer reaction can result in the net migration of a functional group. Addition of a radical to a π-bond (carbon–carbon or carbon–heteroatom) is another common radical reaction and can occur either intermolecularly or as an intramolecular cyclization reaction. Radical coupling or combination is a possible transformation that is more feasible when one of the radicals is relatively stabilized (a persistent radical). Trapping a radical with a transition metal is one way to convert a free radical to a more stable intermediate, which can subsequently undergo coupling with another radical via an S_H2 (bimolecular homolytic substitution) mechanism. Lastly, some noteworthy radical processes proceed through a radical–polar crossover pathway, in which one-electron oxidation or reduction of the radical yields a cationic or anionic intermediate that participates in a subsequent step through a polar mechanism. An important aspect of many of these radical reactions is that they can result in the formation of new carbon–carbon bonds, a fundamental goal in organic synthesis.

Strategies for asymmetric radical reactions

Stereoselectivity in radical reactions can be challenging to control. Many radicals are highly reactive, and radicals moreover have typically low inversion barriers, resulting in no permanent chirality at the radical center. Stereochemistry in radical reactions is generally governed by the subsequent reaction with a radical trap. Most enantioselective radical strategies developed thus far include the incorporation of a chiral element into the radical species or the radical trap (either stoichiometrically or catalytically). Chiral transition-metal catalysis affords the dual advantages of introducing stereochemical discrimination on both the radical and the trap via chiral ligands.

Early research on parameters governing stereoselectivity in radical reactions was achieved with the help of radicals or radical traps appended with chiral auxiliaries. The research on auxiliary-based chiral Lewis acid catalysis inspired Porter, Sibi and others to transpose the concept to radical chemistry. A large number of enantioselective radical reactions that were reported during 1996–2007 were mainly based on chiral Lewis acid-mediated/catalyzed free radical reactions.

The past three decades have seen enormous advances in the development of enantioselective radical reactions, particularly using organocatalysts. Some of the notable chiral organocatalysts imparting enantioselectivity include chiral secondary amines, chiral Brønsted acids, and chiral H-bonding catalysts. The drawbacks of chiral Lewis acids have been overcome to an extent using organocatalysis. The use of photochemistry to generate radicals by light-induced electron transfer has resulted in elegant enantioselective radical transformations. Several transition-metal photocatalysts [9] and organo-photocatalysts [10-12] have been successfully incorporated into enantioselective radical reactions.

The use of transition metals to catalyze enantioselective radical reactions can be considered a major advancement in the field of asymmetric catalysis. Several metals such as cobalt, nickel, copper, and titanium have been employed successfully to catalyze enantioselective radical reactions. Two earth abundant transition metals that have found extensive application in enantioselective radical reactions are copper and nickel. These metals, particularly Ni, can be used in radical–radical coupling reactions which are not possible in traditional organocatalyzed reactions.

An overview of different modes of asymmetric catalysis in radical chemistry is presented in Figure 2. Of these, this perspective focuses on Lewis acid catalysis, organocatalysis (including enamine catalysis), photoredox catalysis, transition-metal catalysis, and enzyme catalysis. Progress in enantioselective reactions using these approaches is discussed with the help of one or two examples in each category to highlight the outstanding achievements in the past three decades. Other modes of catalysis relying on hydrogen-bonding [13,14], ion pairs [15], *N*-heterocyclic carbene (NHC) catalysts [16-18], or thiols [19-21] are not covered here but can also be effective for achieving high levels of enantioselectivity in radical reactions.

Lewis acid-catalyzed radical reactions

In the context of enantioselective radical reactions, initial examples of catalytic methodologies were based on chiral Lewis acid catalysis, with catalysts used in stoichiometric or sub-stoichiometric amounts [38,39]. Porter and Sibi disclosed the first enantioselective examples of conjugate additions to electron-deficient olefins by nucleophilic radicals [22,23]. In these studies, alkyl radicals underwent conjugate addition to *N*-enoyloxazolidinones. Sibi later described enantioselective tandem radical conjugate addition–trapping reactions that formed two carbon–carbon bonds and created two vicinal stereocenters in a single transformation (Scheme 1) [40]. The reactions were catalyzed by chiral Lewis acids and involved conjugate addition of a nucleophilic alkyl radical to an α,β-unsaturated substrate containing an oxazolidinone or pyrrolidinone template. The resulting α-radical was trapped with an allylstannane and the addition and trapping occurred in an *anti* fashion. Products were obtained with up to 97% ee via catalysis by complexes of magnesium or copper(II) with ligand **L1**. The absolute stereochemistry of the product could be controlled by a simple change from copper(II) to magnesium Lewis acids while using the same chiral ligand, thus obviating the need for both enantiomers of the ligand.

Although chiral Lewis acid-mediated radical reactions were groundbreaking, they suffered from major disadvantages: (a) high catalyst loadings (stoichiometric or sub-stoichiometric), (b) large amounts of the radical initiator, (c) the need for a large excess of radical precursor, (d) use of toxic H-atom sources such as tin hydride, and (e) limited variation in the nature of the radicals (mostly nucleophilic).

Organocatalyzed radical reactions

Chiral secondary amine-based catalytic systems have been used in several asymmetric transformations [41,42]. MacMillan obtained chiral free radicals by stoichiometric single electron transfer (SET) oxidation of enamines, formed by the reaction between chiral secondary amines and aldehydes. This mode of activation was called SOMO (singly occupied molecular orbital) catalysis and was employed in several organic transformations [43-48].

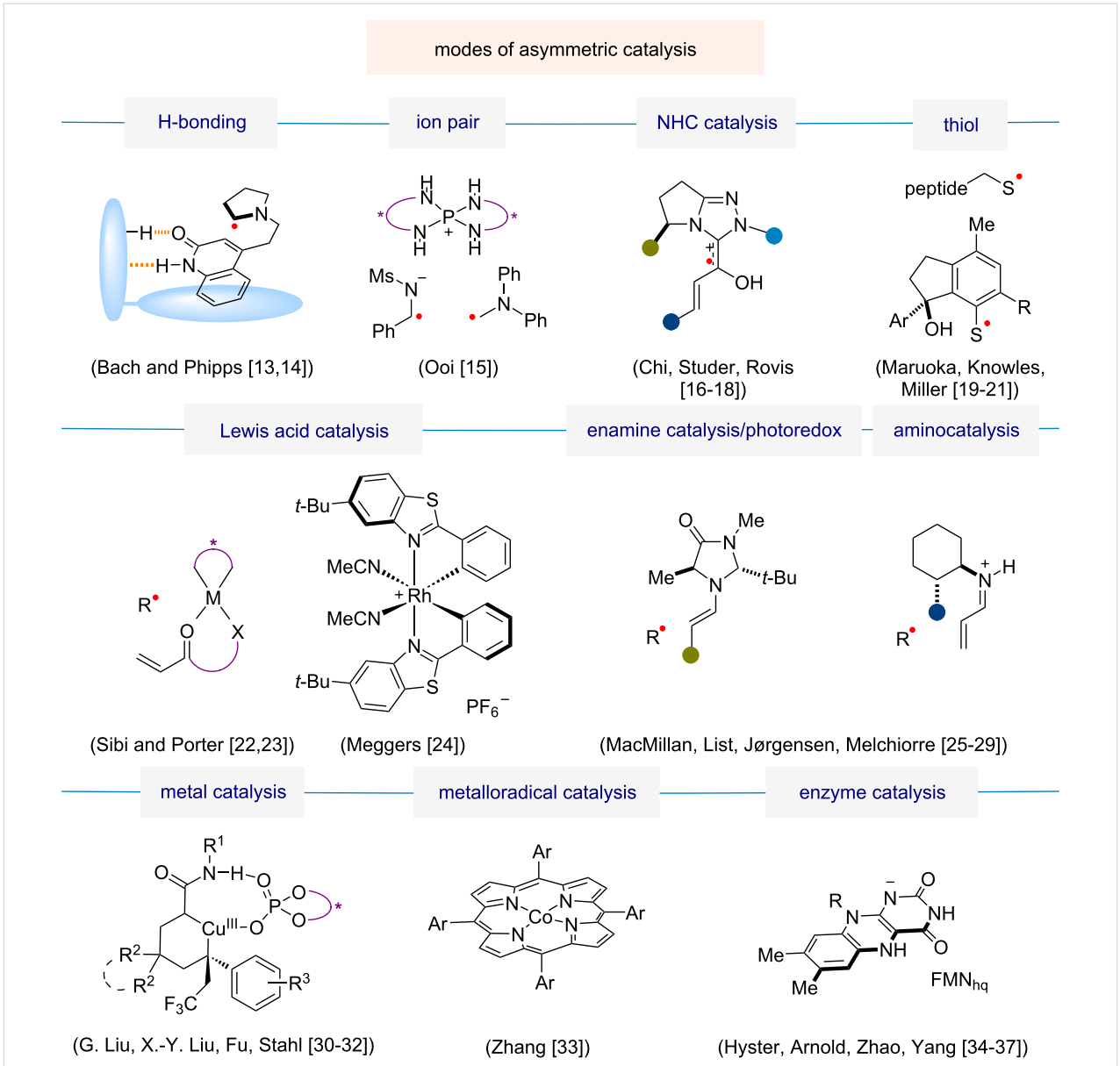

Figure 2: Chiral catalysis in enantioselective radical chemistry [13-37].

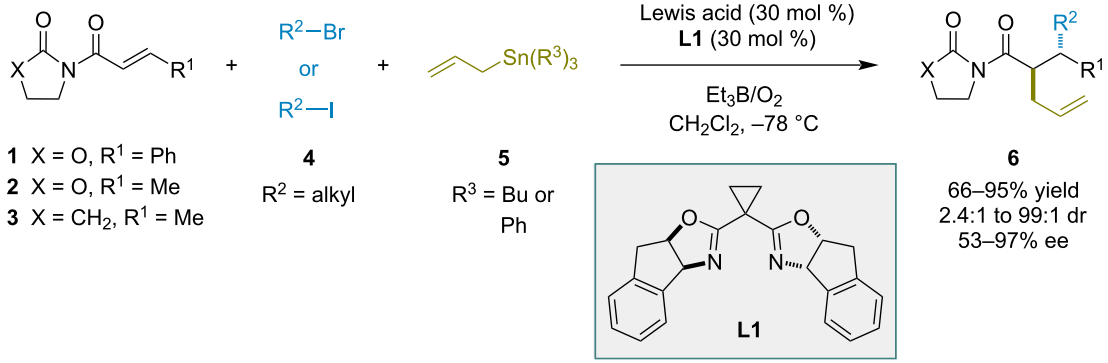

Scheme 1: Diastereo- and enantioselective additions of nucleophilic radicals to *N*-enoyloxazolidinone and pyrrolidinone electrophiles.

Using SOMO catalysis, MacMillan and co-workers developed a method for the synthesis of substituted pyrrolidines from β-aminoaldehydes and olefins in a formal [3 + 2] cycloaddition (Scheme 2) [44]. The transformation was proposed to proceed via a radical–polar crossover mechanism involving single-electron oxidation of an enamine intermediate, addition of the resulting radical to the olefin, single-electron oxidation of the adduct to form a carbocationic intermediate, and intramolecular nucleophilic attack on the carbocation to form the pyrrolidine ring. The reaction tolerated a range of substituents on the olefin, giving the products with high enantioselectivity. Reactions of chiral β-methyl-substituted aldehydes **11** and **12** with indene (**13**) yielded tricyclic products with good diastereoselectivity and particularly high optical purity (99% ee).

Organo-SOMO catalysis was applied in the development of enantioselective polyene cyclizations, which demonstrated the power of the catalytic strategy. In the presence of a chiral amine catalyst **16** (Scheme 3) and the mild oxidant $Cu(OTf)_2$, polyenes with a terminal aldehyde group underwent intramolecular cyclizations affording polycyclic products in a highly diastereo- and enantioselective manner [45]. The polyene substrates were designed to facilitate a radical cyclization process, with alternating electron-poor and electron-rich olefins so as to enable polarity matching of the olefins and radical intermediates. With this design, a relatively electrophilic radical could readily add to a nearby electron-rich olefin, and the resulting nucleophilic radical could add to an electron-poor olefin (e.g., substituted with a cyano group). In one example, polyene **15** underwent cyclization to afford hexacyclic product **17** with 93% ee in a single process that established five new carbon–carbon bonds and nine contiguous stereocenters, including four all-carbon quaternary centers (Scheme 3).

Transition-metal-catalyzed radical reactions

Recent advances in enantioselective radical reactions catalyzed by base metals (e.g., Fe, Co, Ni, Mn) should enable the development of methodologies that expand radical transformations to a larger number of substrates in green and sustainable ways.

Nickel is an earth-abundant transition metal that has been used in several organic transformations [49-52]. Chiral nickel catalysts have been demonstrated to forge $C(sp^2)$–$C(sp^2)$ as well as aliphatic $C(sp^3)$–$C(sp^3)$ bonds.

The Fu group reported a nickel-catalyzed α-alkylation of racemic secondary α-bromoamides **18** using organozinc reagents **19** (Scheme 4A) [32]. A chiral nickel complex, obtained from the mixture of chiral pyridinebisoxazoline ligand **L2** and $NiCl_2$·diglyme, was used as the catalyst to obtain the coupling products **20** in good yield and high enantioselectivity.

The first nickel-catalyzed asymmetric reductive cross-coupling reaction between acid chlorides **21** and secondary benzylic chlorides **22** was reported by Reisman and co-workers (Scheme 4B) [53]. A catalytic system consisting of a combina-

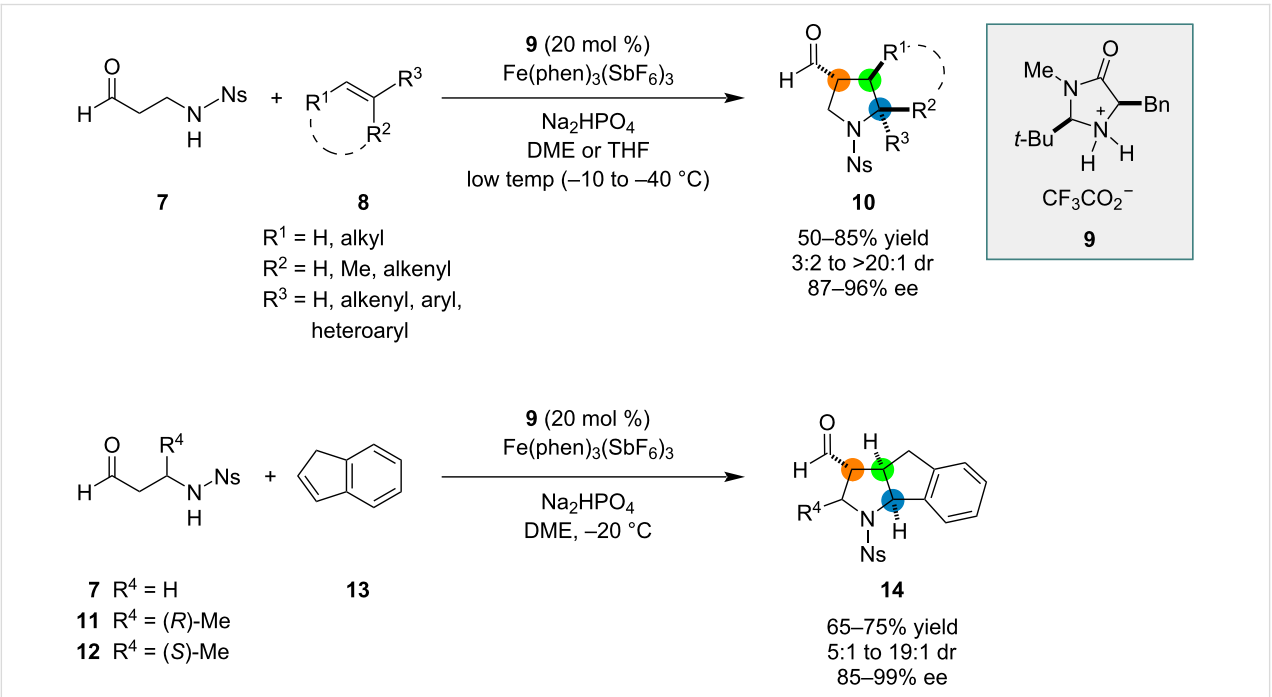

Scheme 2: Organocatalyzed formal [3 + 2] cycloadditions affording substituted pyrrolidines.

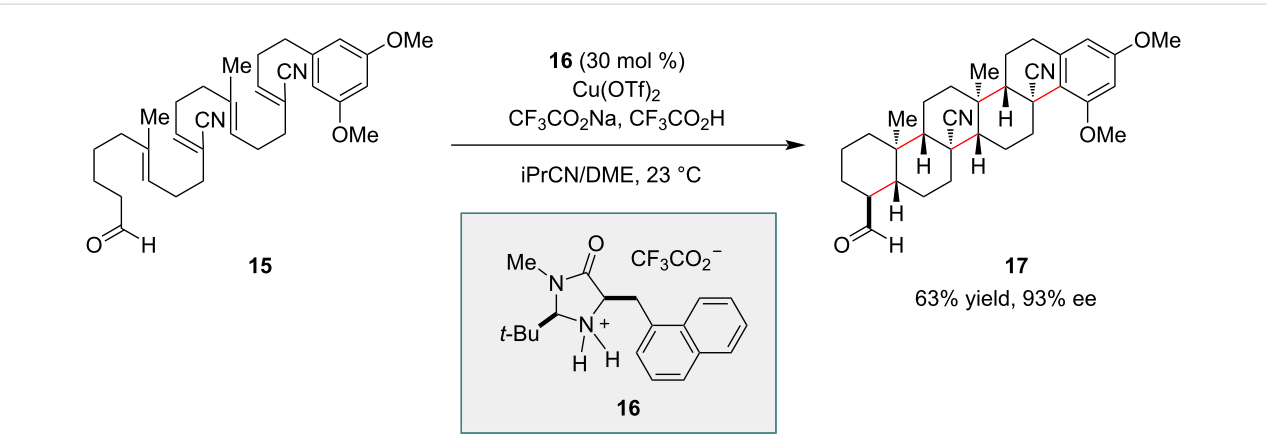

Scheme 3: Synthesis of a hexacyclic compound via an organocatalyzed enantioselective polyene cyclization.

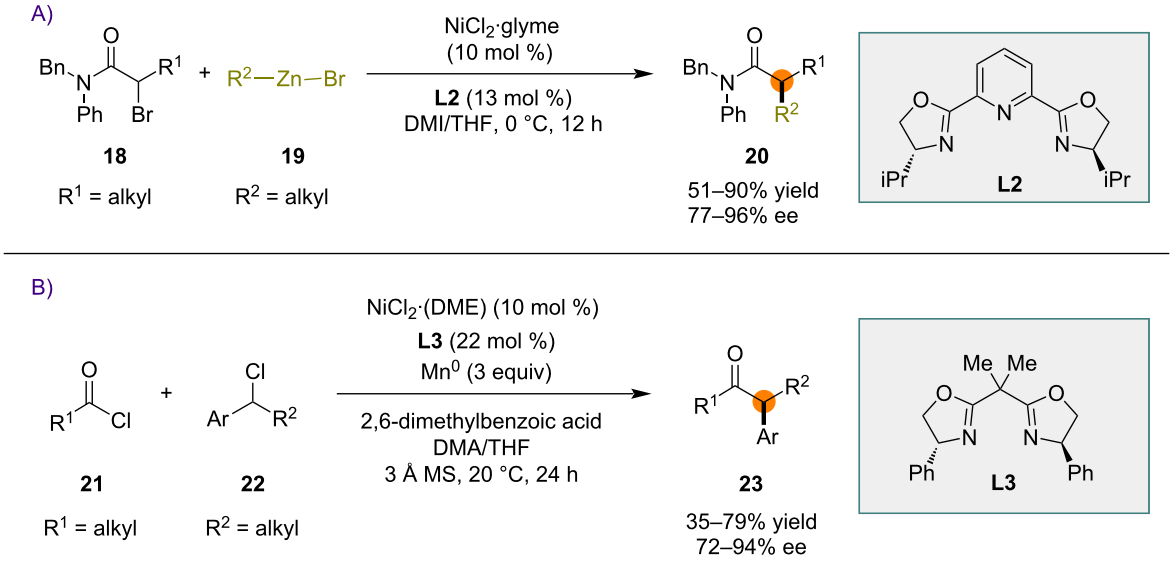

Scheme 4: Nickel-catalyzed asymmetric cross-coupling reactions.

tion of chiral bisoxazoline **L3** and $NiCl_2$·(DME) was able to catalyze the reaction between **21** and **22** in the presence of a stoichiometric amount of Mn as reductant. α,α-Disubstituted ketones **23** were obtained in moderate to good yields and up to 94% ee.

A mechanistically distinct way of achieving enantioselective radical transformations is the use of metalloradical catalysis [54]. A metalloradical is a persistent metal-centered radical species that can homolytically activate substrates without other initiators, light, or electricity. Several different transition-metal complexes have been employed in metalloradical catalysis, including porphyrin complexes of cobalt(II) [55,56] and iron(III) [57,58]. Both cobalt in oxidation state +2 and iron in oxidation state +3 can be viewed as persistent metalloradicals.

Zhang and co-workers reported a unique chiral cobalt–porphyrin complex **25** that could catalyze the conversion of diazoester **24** to lactone **26** (Scheme 5) [33]. In most cases, lactone **26** was formed with complete diastereocontrol and excellent enantioselectivity. A mechanism involving an initial reaction between Co(II) metalloradical **25** and diazoester **24** to furnish a Co(III)-bonded α-ester radical (α-Co(III)-ester radical) with extrusion of nitrogen was proposed by the authors. Further steps include (a) *5-exo* cyclization by α-Co(III)-ester radical and (b) homolytic substitution at the carbon atom by 3-*exo-tet*-cyclization to generate bicyclic lactone **26**.

The Zhang group has extended the chiral metalloradical catalysis to cyclopropanation by the intermolecular reaction between styrenes and ketodiazoacetates [59]. Cyclopropanes were ob-

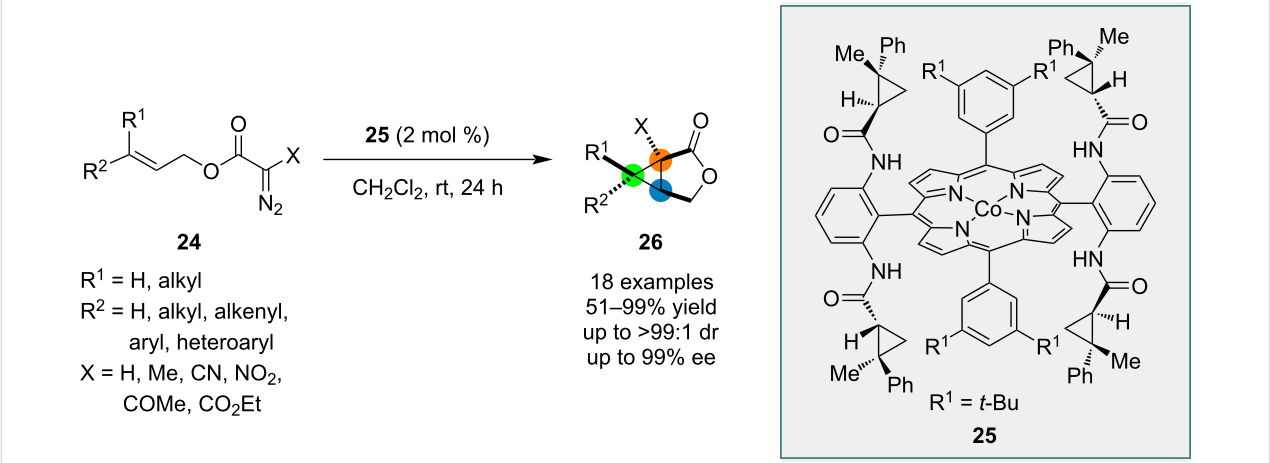

Scheme 5: Chiral cobalt–porphyrin metalloradical-catalyzed radical cyclization reactions.

tained in good yields with high relative and absolute stereocontrol.

Properties, such as relatively high earth abundance, low cost, less toxicity, and existence of multiple oxidation states (I, II, and III) make copper an essential transition metal for catalytic purposes [60,61]. The fact that copper, like other transition metals, has multiple oxidation states makes it an excellent redox catalyst. Owing to the reducing ability of copper(I), substrates can be reduced to radicals and oxidize copper(I) to copper(II) in the process. Copper(II) can oxidize other organic radicals to cations by SET or reversibly react with other radicals to form copper(III) species that can undergo fundamental organometallic steps such as reductive elimination [62].

G. Liu and Stahl disclosed an elegant methodology to functionalize benzylic C–H bonds via copper catalysis [30]. Under the catalytic conditions, alkylarenes were converted to benzylic nitriles in good yields and excellent enantioselectivities. In the proposed mechanism, a chiral Cu(III) complex forms from an achiral benzylic radical and a Cu(II)–CN species, and subsequent reductive elimination affords the enantioenriched benzylic nitrile product.

Recently, X.-Y. Liu and co-workers reported an enantioselective aminofluoroalkylation of alkenes using a Cu(I)/chiral phosphoric acid catalytic system [31]. Aminoalkenes react with Togni's reagent in the presence of a catalytic amount of CuCl and a chiral phosphoric acid to yield pyrrolidines. Using this methodology, chiral α-quaternary substituted pyrrolidines were synthesized in good yields and excellent enantioselectivities.

A radical chaperone methodology is based on a multicatalytic system in which a chiral Cu(I) catalyst, Brønsted acid (camphoric acid) and Ir photocatalyst work synergistically. An asymmetric synthetic method based on radical C–H functionalization was reported by Nagib and co-workers for the preparation of chiral β-aminoalcohols [63]. Chiral copper(I) complexes convert imidate radicals, formed transiently through energy-transfer catalysis, to oxazolines. The transformation includes a regioselective and enantioselective HAT process. Upon blue LED irradiation, oxime imidates (derived from alcohols and imidoyl chlorides) in the presence of $CuBAr^F{}_4$/bisoxazoline **L4** catalyst, an acid co-catalyst, and iridium photocatalyst form chiral oxazolines **29** in good yields and excellent enantioselectivities (82–97% ee) (Scheme 6). Chiral β-aminoalcohols **30** can be obtained by the hydrolysis of **29**.

Another transition metal that has seen extensive use in radical chemistry is titanium. Titanium(III) complexes can function as Lewis acids but can also generate carbon-centered radicals via SET to an organic substrate. In an example from Lin and co-workers, a chiral titanium catalyst promoted enantioselective isomerization reactions of cyclic *meso*-epoxides as part of a bimetallic titanium/cobalt catalytic system [64].

Photoredox catalysis in radical reactions

The ability of a photocatalyst (organic small molecule or transition-metal complex) to undergo single electron transfer (SET) to a variety of organic substrates or organometallic complexes upon photoexcitation has enabled the synthetic community to access reactive open-shell species under very mild conditions. The ability of excited photocatalysts to induce other reagents, substrates, or other catalysts to participate in new activation modes makes them a powerful tool in organic synthesis [65-70]. Over the years, many catalytic systems were developed by merging photoredox processes and other catalytic modes. Some of the disadvantages of chiral Lewis acid catalysis such as toxic

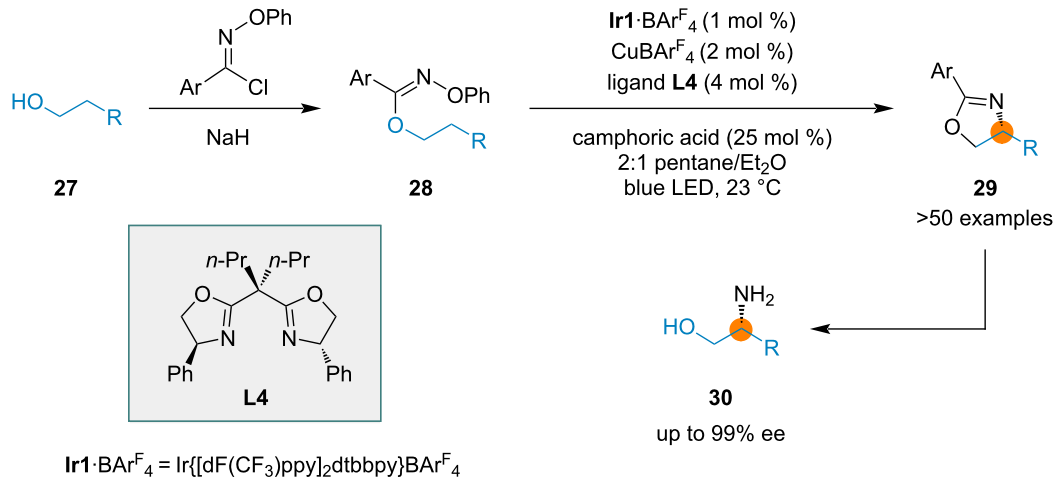

Scheme 6: Enantioselective radical chaperone catalysis.

reducing agents, high catalytic loading, and limitations in the type of radicals used can be overcome using photoredox catalysis. Synergistic photoredox and other forms of catalysis (using chiral Lewis acids, chiral Brønsted acids, H-bonding compounds, polarity reversal catalysts, etc.) expanded the scope of radical traps used and introduced alternate ways of quenching, in some cases involving radical–polar crossover processes. The photoredox catalysts used in most of the synergistic catalysis are Ir and Ru-based systems that are expensive and less readily available. This limitation can be overcome by developing green and sustainable organophotoredox systems.

Melchiorre and co-workers reported a dual catalytic system that involves photoredox and chiral organocatalysts for the construction of all-carbon quaternary centers. The authors studied radical additions to β,β-disubstituted cyclic enones (Scheme 7) [29]. The dual catalytic system of tetrabutylammonium decatungstate (TBADT) and chiral amine **33** was able to cata-

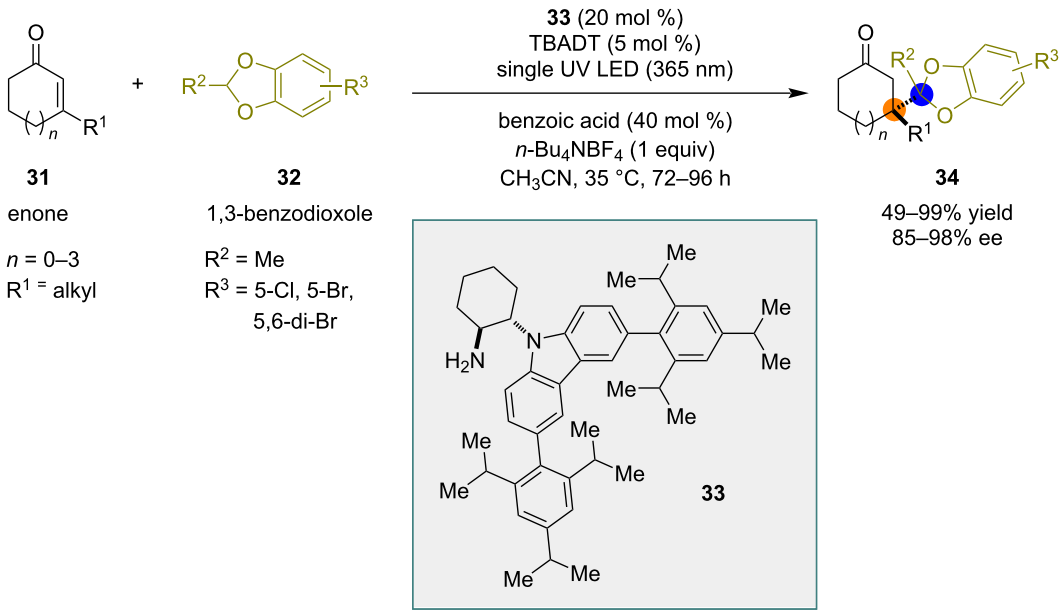

Scheme 7: Enantioselective radical addition by decatungstate/iminium catalysis.

lyze the reaction between benzodioxoles **32** and cyclic β,β-disubstituted enones **31**. Cyclic ketones **34** bearing all-carbon quaternary stereocenters at the β-position were obtained in good yields and high enantioselectivity.

Enzyme-catalyzed radical reactions

An emerging trend in the field of enantioselective radical transformations is the use of enzymatic catalysis to control absolute stereoselectivity. Some remarkable transformations have been demonstrated using this promising greener catalysis. This methodology has a bright future when used individually or synergistically with other catalytic systems. Enzymatic catalysis can pose challenges including enzyme engineering, reaction scale-up, etc. but is optimal in terms of the toxicity profile of the reaction conditions.

Biomolecules such as enzymes are attractive candidates for efficient and selective synthesis owing to their unprecedented catalytic activity and selectivity. Advances in the field of protein engineering have made enzymatic catalysis more amenable to enantioselective organic synthesis in the past decade. Recent advances in the development of synergistic catalytic systems, particularly involving photoredox catalysts, have led to the emerging area of photoenzymatic catalysis. Several new modes of activation successfully catalyzed by enzymes have been demonstrated [71-74].

Notable photoenzymatic reactions involving radical cyclizations have been reported. In one photoenzymatic transformation developed by the Hyster group, α-chloroamides were converted to enantioenriched 5-, 6-, 7-, and 8-membered lactams through an enantioselective radical cyclization followed by a diastereoselective HAT, producing contiguous stereocenters [75]. In the subsequent year, the same group reported intramolecular Giese-type radical cyclization reactions involving unstabilized alkyl radicals generated from alkyl iodides (Scheme 8) [34]. The generation of unstabilized, nucleophilic alkyl radicals from alkyl iodides was more challenging than the generation of more electrophilic alkyl radicals from α-halocarbonyl compounds as in the previous report. In this case, radical formation from the alkyl iodide was accomplished through photoexcitation of a charge-transfer complex of the substrate and flavin in the active site of the enzyme (a mutated ene-reductase). Subsequent 5-*exo-trig* or 6-*exo-trig* cyclization and HAT furnished the enantioenriched products with up to 97:3 er.

In addition to intramolecular radical reactions, intermolecular radical transformations have also been achieved using photoenzymatic catalysis, such as the addition of fluoroalkyl radicals to alkene substrates [36] and cross-electrophile coupling of alkyl halides and nitroalkanes [76]. Yang and co-workers reported photoenzymatic asymmetric $C(sp^3)$–$C(sp^3)$ oxidative cross-couplings between organoboron reagents and amino acids (Scheme 9) [37]. The authors used a synergistic system consisting of an engineered threonine aldolase, a photoredox catalyst, and an oxidizing agent. With this catalytic system, they were able to accomplish the C–H functionalization of glycine and α-branched amino acids, obtaining α-tri- and tetrasubstituted amino acids with moderate to good yields, good diastereoselectivity, and high enantioselectivity.

New catalytic methods have been developed by merging photoenzymatic catalysis with small-molecule photoredox catalysis. Enantioselective radical acylation reactions of *N*-hydroxyphthalimide esters and aldehydes, yielding α-substituted ketones, were catalyzed by a radical acyl transferase (an engineered thiamine diphosphate-dependent lyase) working together with an organic dye (eosin Y) that served as a photoredox catalyst [77]. Highly diastereo- and enantioselective three-component couplings were catalyzed by an evolved pyridoxal decarboxylase and a small-molecule photoredox catalyst (rose bengal), affording diversely substituted products [78].

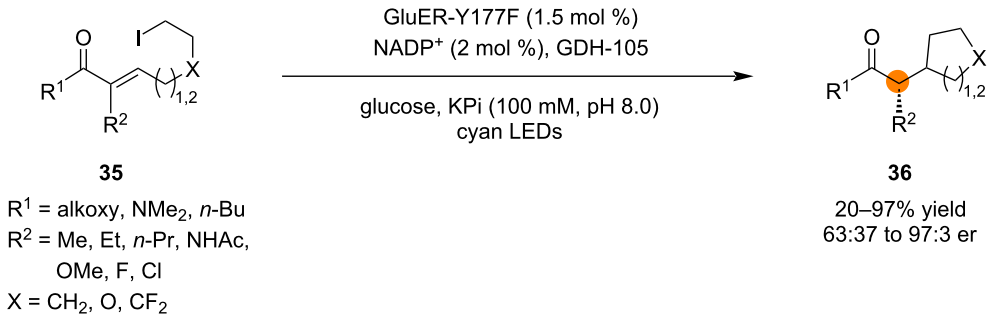

Scheme 8: An ene-reductase-catalyzed photoenzymatic enantioselective radical cyclization/enantioselective HAT process.

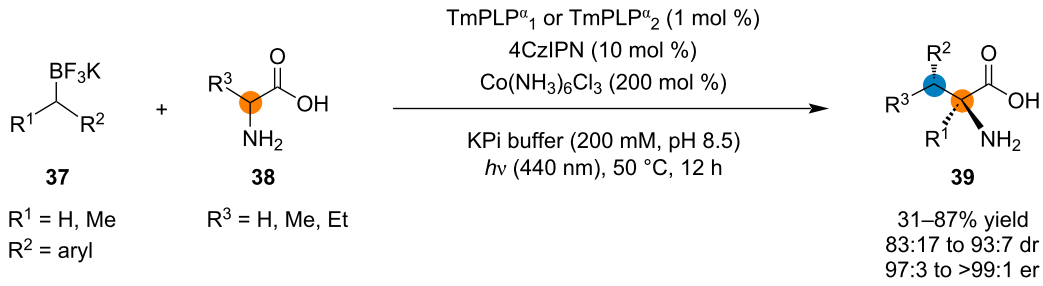

Scheme 9: Photoenzymatic oxidative C(sp^3)–C(sp^3) coupling reactions between organoboron compounds and amino acids.

Electrochemical radical reactions

The organic chemistry community has witnessed a resurgence of interest in electrochemical methods for organic synthesis [79]. Organic electrochemistry can provide mild reaction conditions, good functional group tolerance, and scalability [80]. Electrochemical methods offer the opportunity to tune reaction conditions by controlling parameters such as potential, current, electrode, and electrolyte [81], providing a sophisticated platform for attaining optimal reactivity. A variety of catalytic strategies can be employed under electrochemical conditions, and many asymmetric electrochemical transformations have been established [82-84]. Electrochemistry is well-suited to applications in one-electron processes, including transformations involving organic radicals, and can obviate the need for a stoichiometric chemical oxidant or reductant [80,85], thereby reducing toxicity and waste. With these advantages, organic electrochemistry holds significant promise for improving efficiency and sustainability while enabling the development of new transformations.

Meggers and co-workers developed an electrochemical method for the enantioselective α-C(sp^3) alkenylation of ketones containing imidazole auxiliaries (Scheme 10) [24]. The transformation was catalyzed by a chiral-at-rhodium Lewis acid **42**. A variety of ketone electrophiles **40** and alkenyl trifluoroborate nucleophiles **41** were converted to the corresponding α-alkenylated products **43** with excellent enantioselectivities. Alkenyl trifluoroborates with (*Z*) configuration gave higher product yields than the analogous (*E*)-alkenyl trifluoroborates, but the corresponding alkenyl group in the product had (*E*) configuration in all cases. A key enabling aspect of the method was the use of ferrocene as a redox mediator, which played an important role in preventing substrate decomposition under the electrochemical conditions.

An electrochemical method enabled regio- and enantioselective radical reactions of silyl polyenolates with racemic α-branched esters, yielding products with a new all-carbon quaternary stereocenter (Scheme 11) [86]. With a Ni(II)–bisoxazoline com-

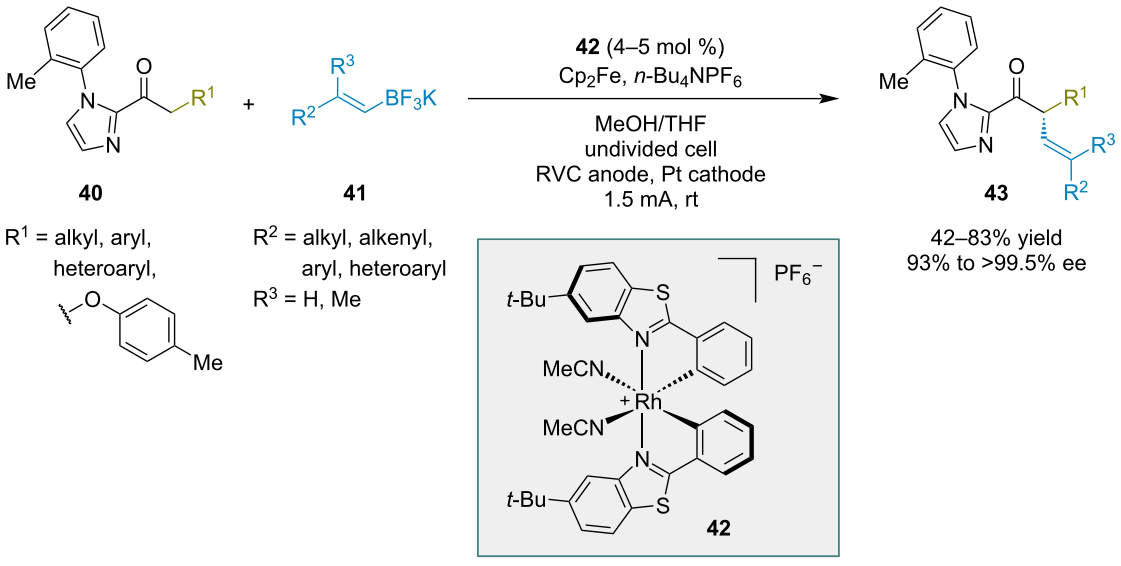

Scheme 10: Electrochemical α-alkenylation reactions of 2-acylimidazoles catalyzed by a chiral-at-rhodium Lewis acid.

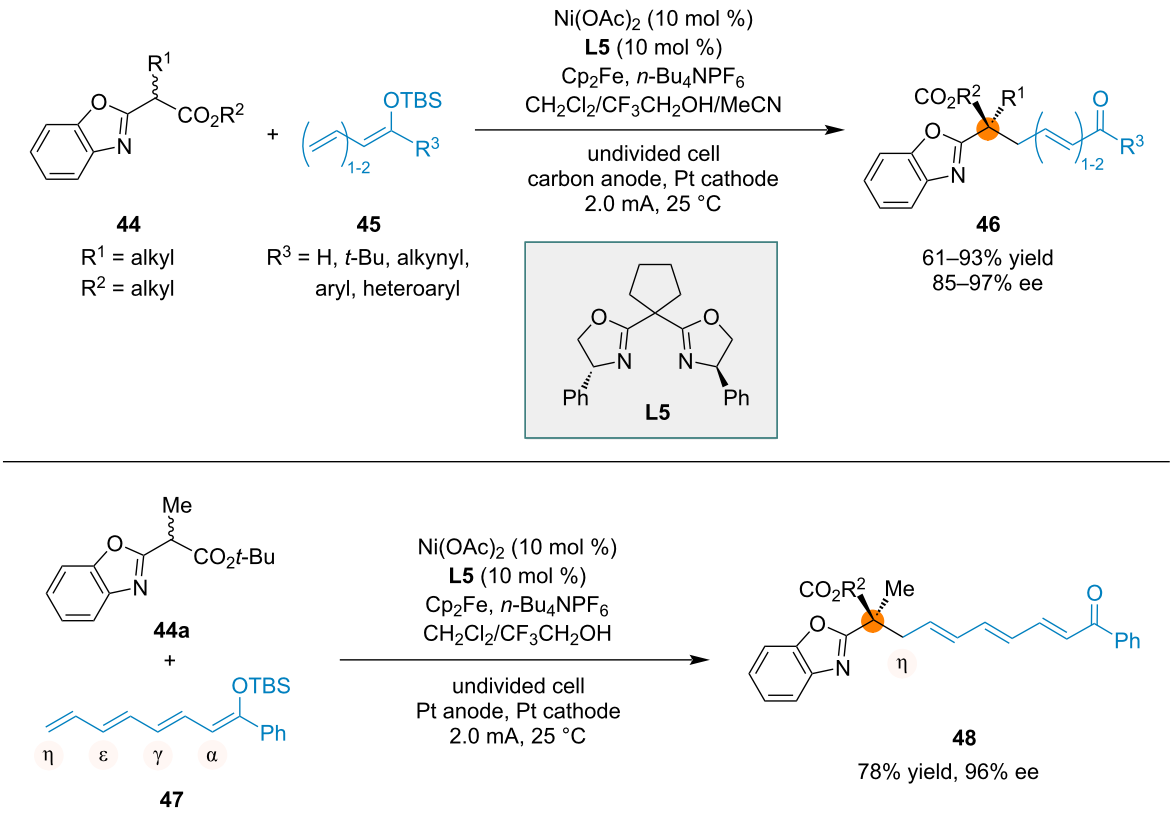

Scheme 11: Regio- and enantioselective electrochemical reactions of silyl polyenolates catalyzed by a chiral nickel catalyst.

plex as the catalyst, various substrates underwent the transformation with good to high yields and high enantioselectivities. The reactions were regioselective, resulting in the selective functionalization of the terminal carbon atom of the silyl polyenolate. In the reaction of silyl tetraenol ether **47**, selective reaction at the η position occurred, and the product **48** was obtained in 78% yield and 96% ee.

Conclusion

This perspective highlights important contributions in the area of enantioselective radical reactions. These examples demonstrate a wide variety of radical transformations, asymmetric catalytic systems, and strategies for radical generation. The selection included here not only highlights outstanding accomplishments but also draws attention to promising areas for future research.

In the past three decades, numerous advances have overcome major disadvantages of early enantioselective radical methods, including the use of tin hydrides as H-atom sources and excess quantities of radical initiator or radical precursor. A broad range of enantioselective radical transformations has been developed, allowing for the asymmetric construction of C(sp^3)–C(sp^3), C(sp^3)–C(sp^2), and C(sp^3)–C(sp) bonds and challenging motifs such as vicinal stereocenters and all-carbon quaternary centers. A diverse range of chiral catalysts has been employed to achieve enantioselectivity, including Lewis acids, organocatalysts, transition-metal complexes, and enzymes. In many cases, low catalyst loadings have been achieved, especially in transition-metal catalyzed, photoredox, and biocatalytic methods.

Photoredox catalysis has had a tremendous impact on the field of organic radical chemistry. In many modern radical methods, photoredox catalysis is used in combination with another mode of catalysis, such as organocatalysis, chiral Lewis acid catalysis, or enzymatic catalysis. Photoredox-based methods have introduced new, atom-economical approaches for radical generation, in some cases enabling direct radical generation and C–H functionalization of aliphatic substrates via HAT and thereby avoiding the use of more highly functionalized radical precursors such as organic halides.

The application of electrochemistry for enantioselective radical transformations is a highly promising approach. Electrochem-

istry provides a way to avoid the use of stoichiometric chemical oxidants or reductants and to achieve new transformations that are highly regio- and stereoselective. Though not covered in this perspective, flow chemistry and mechanochemistry are also increasingly popular areas that hold significant potential for applications in radical chemistry. Compared with conventional batch synthesis, flow chemistry can improve efficiency and facilitate reaction scale-up [87-90]. Mechanochemistry allows reactions to be conducted with no solvent or with only a small volume of added liquid, thus providing a green alternative to solution-phase chemistry [91]. Mechanical grinding or milling also provides a means to generate radicals via piezocatalysis [91], an emerging strategy that warrants investigation in the context of enantioselective radical reactions.

Future research holds the key to addressing current limitations in the scope and capabilities of enantioselective radical chemistry. The existing literature features a predominant use of nucleophilic radicals, a small number of H-atom donors, and limited application of hydrogen-bonding catalysis in radical reactions. Further studies on enantioselective transformations of electrophilic radicals, alternative H-atom sources, and additional modes of catalysis (including hydrogen-bonding catalysis) would be valuable. Additionally, the development of more efficient methods, using lower catalyst loadings, remains an important goal for ongoing research. The use of more sustainable photoredox catalysts – organic molecules or complexes of earth-abundant metals – is a key endeavor toward decreasing reliance on the iridium and ruthenium complexes commonly employed in photoredox methods.

As a whole, asymmetric radical chemistry offers significant utility for synthetic applications and great potential for further development. Building upon the significant advances of the past three decades, future research may overcome existing limitations and deliver more efficient and green methods for enantioselective radical transformations.

Author Contributions

Anna C. Renner: conceptualization; writing – original draft; writing – review & editing. Sagar S. Thorat: writing – original draft; writing – review & editing. Hariharaputhiran Subramanian: conceptualization; writing – original draft; writing – review & editing. Mukund P. Sibi: conceptualization; writing – original draft; writing – review & editing.

ORCID® iDs

Anna C. Renner - https://orcid.org/0000-0003-4971-9609
Sagar S. Thorat - https://orcid.org/0000-0003-3146-7837
Hariharaputhiran Subramanian - https://orcid.org/0000-0002-1585-5146
Mukund P. Sibi - https://orcid.org/0000-0003-1999-4167

Data Availability Statement

Data sharing is not applicable as no new data was generated or analyzed in this study.

References

1. Wen, X.; Ojima, I. Asymmetric Isomerization of Allylamines: Chapter 3 Addendum—1999. In *Catalytic Asymmetric Synthesis,* 2nd ed.; Ojima, I., Ed.; John Wiley & Sons: New York, NY, USA, 2000; pp 162–163. doi:10.1002/0471721506.ch4
2. Ohkuma, T.; Kitamura, M.; Noyori, R. Asymmetric Hydrogenation. In *Catalytic Asymmetric Synthesis,* 2nd ed.; Ojima, I., Ed.; John Wiley & Sons: New York, NY, USA, 2000; pp 1–110. doi:10.1002/0471721506.ch1
3. Akutagawa, S.; Tani, K. Asymmetric Isomerization of Allylamines. In *Catalytic Asymmetric Synthesis,* 2nd ed.; Ojima, I., Ed.; John Wiley & Sons: New York, NY, USA, 2000; pp 145–161. doi:10.1002/0471721506.ch3
4. Mondal, S.; Dumur, F.; Gigmes, D.; Sibi, M. P.; Bertrand, M. P.; Nechab, M. *Chem. Rev.* **2022,** *122,* 5842–5976. doi:10.1021/acs.chemrev.1c00582
5. Bauer, T.; Hakim, Y. Z.; Morawska, P. *Molecules* **2023,** *28,* 6252. doi:10.3390/molecules28176252
6. Sibi, M. P.; Porter, N. A. *Acc. Chem. Res.* **1999,** *32,* 163–171. doi:10.1021/ar9600547
7. Rowlands, G. J. *Tetrahedron* **2009,** *65,* 8603–8655. doi:10.1016/j.tet.2009.07.001
8. Sibi, M. P.; Manyem, S.; Zimmerman, J. *Chem. Rev.* **2003,** *103,* 3263–3296. doi:10.1021/cr020044l
9. Twilton, J.; Le, C.; Zhang, P.; Shaw, M. H.; Evans, R. W.; MacMillan, D. W. C. *Nat. Rev. Chem.* **2017,** *1,* 0052. doi:10.1038/s41570-017-0052
10. Amos, S. G. E.; Garreau, M.; Buzzetti, L.; Waser, J. *Beilstein J. Org. Chem.* **2020,** *16,* 1163–1187. doi:10.3762/bjoc.16.103
11. Vega-Peñaloza, A.; Mateos, J.; Companyó, X.; Escudero-Casao, M.; Dell'Amico, L. *Angew. Chem., Int. Ed.* **2021,** *60,* 1082–1097. doi:10.1002/anie.202006416
12. Marzo, L.; Pagire, S. K.; Reiser, O.; König, B. *Angew. Chem., Int. Ed.* **2018,** *57,* 10034–10072. doi:10.1002/anie.201709766
13. Bauer, A.; Westkämper, F.; Grimme, S.; Bach, T. *Nature* **2005,** *436,* 1139–1140. doi:10.1038/nature03955
14. Proctor, R. S. J.; Davis, H. J.; Phipps, R. J. *Science* **2018,** *360,* 419–422. doi:10.1126/science.aar6376
15. Uraguchi, D.; Kinoshita, N.; Kizu, T.; Ooi, T. *J. Am. Chem. Soc.* **2015,** *137,* 13768–13771. doi:10.1021/jacs.5b09329
16. Zhang, Y.; Du, Y.; Huang, Z.; Xu, J.; Wu, X.; Wang, Y.; Wang, M.; Yang, S.; Webster, R. D.; Chi, Y. R. *J. Am. Chem. Soc.* **2015,** *137,* 2416–2419. doi:10.1021/ja511371a
17. Guin, J.; De Sarkar, S.; Grimme, S.; Studer, A. *Angew. Chem., Int. Ed.* **2008,** *47,* 8727–8730. doi:10.1002/anie.200802735
18. White, N. A.; Rovis, T. *J. Am. Chem. Soc.* **2014,** *136,* 14674–14677. doi:10.1021/ja5080739
19. Hashimoto, T.; Kawamata, Y.; Maruoka, K. *Nat. Chem.* **2014,** *6,* 702–705. doi:10.1038/nchem.1998
20. Shin, N. Y.; Ryss, J. M.; Zhang, X.; Miller, S. J.; Knowles, R. R. *Science* **2019,** *366,* 364–369. doi:10.1126/science.aay2204
21. Ryss, J. M.; Turek, A. K.; Miller, S. J. *Org. Lett.* **2018,** *20,* 1621–1625. doi:10.1021/acs.orglett.8b00364
22. Sibi, M. P.; Ji, J.; Wu, J. H.; Gürtler, S.; Porter, N. A. *J. Am. Chem. Soc.* **1996,** *118,* 9200–9201. doi:10.1021/ja9623929

23. Sibi, M. P.; Ji, J. *J. Org. Chem.* **1997,** *62,* 3800–3801. doi:10.1021/jo970558y
24. Xiong, P.; Hemming, M.; Ivlev, S. I.; Meggers, E. *J. Am. Chem. Soc.* **2022,** *144,* 6964–6971. doi:10.1021/jacs.2c01686
25. Welin, E. R.; Warkentin, A. A.; Conrad, J. C.; MacMillan, D. W. C. *Angew. Chem., Int. Ed.* **2015,** *54,* 9668–9672. doi:10.1002/anie.201503789
26. List, B.; Lerner, R. A.; Barbas, C. F., III. *J. Am. Chem. Soc.* **2000,** *122,* 2395–2396. doi:10.1021/ja994280y
27. Das, S.; Zhu, C.; Demirbas, D.; Bill, E.; De, C. K.; List, B. *Science* **2023,** *379,* 494–499. doi:10.1126/science.ade8190
28. Næsborg, L.; Corti, V.; Leth, L. A.; Poulsen, P. H.; Jørgensen, K. A. *Angew. Chem., Int. Ed.* **2018,** *57,* 1606–1610. doi:10.1002/anie.201711944
29. Murphy, J. J.; Bastida, D.; Paria, S.; Fagnoni, M.; Melchiorre, P. *Nature* **2016,** *532,* 218–222. doi:10.1038/nature17438
30. Zhang, W.; Wang, F.; McCann, S. D.; Wang, D.; Chen, P.; Stahl, S. S.; Liu, G. *Science* **2016,** *353,* 1014–1018. doi:10.1126/science.aaf7783
31. Lin, J.-S.; Dong, X.-Y.; Li, T.-T.; Jiang, N.-C.; Tan, B.; Liu, X.-Y. *J. Am. Chem. Soc.* **2016,** *138,* 9357–9360. doi:10.1021/jacs.6b04077
32. Fischer, C.; Fu, G. C. *J. Am. Chem. Soc.* **2005,** *127,* 4594–4595. doi:10.1021/ja0506509
33. Xu, X.; Lu, H.; Ruppel, J. V.; Cui, X.; Lopez de Mesa, S.; Wojtas, L.; Zhang, X. P. *J. Am. Chem. Soc.* **2011,** *133,* 15292–15295. doi:10.1021/ja2062506
34. Clayman, P. D.; Hyster, T. K. *J. Am. Chem. Soc.* **2020,** *142,* 15673–15677. doi:10.1021/jacs.0c07918
35. Yang, Y.; Arnold, F. H. *Acc. Chem. Res.* **2021,** *54,* 1209–1225. doi:10.1021/acs.accounts.0c00591
36. Li, M.; Yuan, Y.; Harrison, W.; Zhang, Z.; Zhao, H. *Science* **2024,** *385,* 416–421. doi:10.1126/science.adk8464
37. Wang, T.-C.; Mai, B. K.; Zhang, Z.; Bo, Z.; Li, J.; Liu, P.; Yang, Y. *Nature* **2024,** *629,* 98–104. doi:10.1038/s41586-024-07284-5
38. Urabe, H.; Yamashita, K.; Suzuki, K.; Kobayashi, K.; Sato, F. *J. Org. Chem.* **1995,** *60,* 3576–3577. doi:10.1021/jo00117a003
39. Sibi, M. P.; Asano, Y.; Sausker, J. B. *Angew. Chem., Int. Ed.* **2001,** *40,* 1293–1296. doi:10.1002/1521-3773(20010401)40:7<1293::aid-anie1293>3.0.co;2-y
40. Sibi, M. P.; Chen, J. *J. Am. Chem. Soc.* **2001,** *123,* 9472–9473. doi:10.1021/ja016633a
41. Hajos, Z. G.; Parrish, D. R. *J. Org. Chem.* **1974,** *39,* 1615–1621. doi:10.1021/jo00925a003
42. Dalko, P. I., Ed. *Enantioselective Organocatalysis: Reactions and Experimental Procedures;;* Wiley-VCH: Weinheim, Germany, 2007. doi:10.1002/9783527610945
43. Beeson, T. D.; Mastracchio, A.; Hong, J.-B.; Ashton, K.; MacMillan, D. W. C. *Science* **2007,** *316,* 582–585. doi:10.1126/science.1142696
44. Jui, N. T.; Garber, J. A. O.; Finelli, F. G.; MacMillan, D. W. C. *J. Am. Chem. Soc.* **2012,** *134,* 11400–11403. doi:10.1021/ja305076b
45. Rendler, S.; MacMillan, D. W. C. *J. Am. Chem. Soc.* **2010,** *132,* 5027–5029. doi:10.1021/ja100185p
46. Comito, R. J.; Finelli, F. G.; MacMillan, D. W. C. *J. Am. Chem. Soc.* **2013,** *135,* 9358–9361. doi:10.1021/ja4047312
47. Jui, N. T.; Lee, E. C. Y.; MacMillan, D. W. C. *J. Am. Chem. Soc.* **2010,** *132,* 10015–10017. doi:10.1021/ja104313x
48. Kim, H.; MacMillan, D. W. C. *J. Am. Chem. Soc.* **2008,** *130,* 398–399. doi:10.1021/ja077212h
49. Yu, D.-G.; Li, B.-J.; Shi, Z.-J. *Acc. Chem. Res.* **2010,** *43,* 1486–1495. doi:10.1021/ar100082d
50. Li, B.-J.; Yu, D.-G.; Sun, C.-L.; Shi, Z.-J. *Chem. – Eur. J.* **2011,** *17,* 1728–1759. doi:10.1002/chem.201002273
51. Rosen, B. M.; Quasdorf, K. W.; Wilson, D. A.; Zhang, N.; Resmerita, A.-M.; Garg, N. K.; Percec, V. *Chem. Rev.* **2011,** *111,* 1346–1416. doi:10.1021/cr100259t
52. Tasker, S. Z.; Standley, E. A.; Jamison, T. F. *Nature* **2014,** *509,* 299–309. doi:10.1038/nature13274
53. Cherney, A. H.; Kadunce, N. T.; Reisman, S. E. *J. Am. Chem. Soc.* **2013,** *135,* 7442–7445. doi:10.1021/ja402922w
54. Lee, W.-C. C.; Zhang, X. P. *Angew. Chem., Int. Ed.* **2024,** *63,* e202320243. doi:10.1002/anie.202320243
55. Xu, H.; Wang, D.-S.; Zhu, Z.; Deb, A.; Zhang, X. P. *Chem* **2024,** *10,* 283–298. doi:10.1016/j.chempr.2023.09.010
56. Xu, P.; Xie, J.; Wang, D.-S.; Zhang, X. P. *Nat. Chem.* **2023,** *15,* 498–507. doi:10.1038/s41557-022-01119-4
57. Lee, W.-C. C.; Wang, D.-S.; Deb, A.; Zhu, Y.; Zhang, X. P. *J. Am. Chem. Soc.* **2025,** *147,* 24001–24013. doi:10.1021/jacs.5c07473
58. Lee, W.-C. C.; Wang, D.-S.; Zhu, Y.; Zhang, X. P. *Nat. Chem.* **2023,** *15,* 1569–1580. doi:10.1038/s41557-023-01317-8
59. Xu, X.; Zhu, S.; Cui, X.; Wojtas, L.; Zhang, X. P. *Angew. Chem., Int. Ed.* **2013,** *52,* 11857–11861. doi:10.1002/anie.201305883
60. Trammell, R.; Rajabimoghadam, K.; Garcia-Bosch, I. *Chem. Rev.* **2019,** *119,* 2954–3031. doi:10.1021/acs.chemrev.8b00368
61. Kozlowski, M. C. Organic Synthetic Methods Using Copper Oxygen Chemistry. In *Copper-Oxygen Chemistry;* Karlin, K. D.; Itoh, S., Eds.; John Wiley & Sons: New York, NY, USA, 2011; pp 361–444. doi:10.1002/9781118094365.ch11
62. Gu, Q.-S.; Li, Z.-L.; Liu, X.-Y. *Acc. Chem. Res.* **2020,** *53,* 170–181. doi:10.1021/acs.accounts.9b00381
63. Nakafuku, K. M.; Zhang, Z.; Wappes, E. A.; Stateman, L. M.; Chen, A. D.; Nagib, D. A. *Nat. Chem.* **2020,** *12,* 697–704. doi:10.1038/s41557-020-0482-8
64. Ye, K.-Y.; McCallum, T.; Lin, S. *J. Am. Chem. Soc.* **2019,** *141,* 9548–9554. doi:10.1021/jacs.9b04993
65. Douglas, J. J.; Sevrin, M. J.; Stephenson, C. R. J. *Org. Process Res. Dev.* **2016,** *20,* 1134–1147. doi:10.1021/acs.oprd.6b00125
66. Lang, X.; Zhao, J.; Chen, X. *Chem. Soc. Rev.* **2016,** *45,* 3026–3038. doi:10.1039/c5cs00659g
67. Nicewicz, D. A.; Nguyen, T. M. *ACS Catal.* **2014,** *4,* 355–360. doi:10.1021/cs400956a
68. Prier, C. K.; Rankic, D. A.; MacMillan, D. W. C. *Chem. Rev.* **2013,** *113,* 5322–5363. doi:10.1021/cr300503r
69. Romero, N. A.; Nicewicz, D. A. *Chem. Rev.* **2016,** *116,* 10075–10166. doi:10.1021/acs.chemrev.6b00057
70. Shaw, M. H.; Twilton, J.; MacMillan, D. W. C. *J. Org. Chem.* **2016,** *81,* 6898–6926. doi:10.1021/acs.joc.6b01449
71. Chen, K.; Arnold, F. H. *Nat. Catal.* **2020,** *3,* 203–213. doi:10.1038/s41929-019-0385-5
72. Reetz, M. T. *Angew. Chem., Int. Ed.* **2011,** *50,* 138–174. doi:10.1002/anie.201000826
73. Devine, P. N.; Howard, R. M.; Kumar, R.; Thompson, M. P.; Truppo, M. D.; Turner, N. J. *Nat. Rev. Chem.* **2018,** *2,* 409–421. doi:10.1038/s41570-018-0055-1

74. Emmanuel, M. A.; Bender, S. G.; Bilodeau, C.; Carceller, J. M.; DeHovitz, J. S.; Fu, H.; Liu, Y.; Nicholls, B. T.; Ouyang, Y.; Page, C. G.; Qiao, T.; Raps, F. C.; Sorigué, D. R.; Sun, S.-Z.; Turek-Herman, J.; Ye, Y.; Rivas-Souchet, A.; Cao, J.; Hyster, T. K. *Chem. Rev.* **2023,** *123,* 5459–5520. doi:10.1021/acs.chemrev.2c00767
75. Biegasiewicz, K. F.; Cooper, S. J.; Gao, X.; Oblinsky, D. G.; Kim, J. H.; Garfinkle, S. E.; Joyce, L. A.; Sandoval, B. A.; Scholes, G. D.; Hyster, T. K. *Science* **2019,** *364,* 1166–1169. doi:10.1126/science.aaw1143
76. Fu, H.; Cao, J.; Qiao, T.; Qi, Y.; Charnock, S. J.; Garfinkle, S.; Hyster, T. K. *Nature* **2022,** *610,* 302–307. doi:10.1038/s41586-022-05167-1
77. Xu, Y.; Chen, H.; Yu, L.; Peng, X.; Zhang, J.; Xing, Z.; Bao, Y.; Liu, A.; Zhao, Y.; Tian, C.; Liang, Y.; Huang, X. *Nature* **2024,** *625,* 74–78. doi:10.1038/s41586-023-06822-x
78. Zhang, C.; Zhou, J.; Xie, P.-P.; Rivera, S. M.; Alturaifi, T. M.; Finnigan, J.; Charnock, S.; Liu, P.; Yang, Y. *Science* **2025,** *389,* eadx2935. doi:10.1126/science.adx2935
79. Zhu, C.; Ang, N. W. J.; Meyer, T. H.; Qiu, Y.; Ackermann, L. *ACS Cent. Sci.* **2021,** *7,* 415–431. doi:10.1021/acscentsci.0c01532
80. Horn, E. J.; Rosen, B. R.; Baran, P. S. *ACS Cent. Sci.* **2016,** *2,* 302–308. doi:10.1021/acscentsci.6b00091
81. Yan, M.; Kawamata, Y.; Baran, P. S. *Angew. Chem., Int. Ed.* **2018,** *57,* 4149–4155. doi:10.1002/anie.201707584
82. Medici, F.; Resta, S.; Andolina, S.; Benaglia, M. *Catalysts* **2023,** *13,* 944. doi:10.3390/catal13060944
83. Ghosh, M.; Shinde, V. S.; Rueping, M. *Beilstein J. Org. Chem.* **2019,** *15,* 2710–2746. doi:10.3762/bjoc.15.264
84. Mao, K.; Liu, C.; Wang, Y.; Gu, C.; Putziger, J. M.; Cemalovic, N. I.; Muniz, C.; Qi, Y.; Lin, S. *Nature* **2025,** *643,* 1288–1296. doi:10.1038/s41586-025-09238-x
85. DeLano, T. J.; Reisman, S. E. *ACS Catal.* **2019,** *9,* 6751–6754. doi:10.1021/acscatal.9b01785
86. Zhang, J.; Liu, M.; Zhang, W.; Guo, C. *Sci. Adv.* **2025,** *11,* eadu5594. doi:10.1126/sciadv.adu5594
87. Pulcinella, A.; Bonciolini, S.; Stuhr, R.; Diprima, D.; Tran, M. T.; Johansson, M.; von Wangelin, A. J.; Noël, T. *Nat. Commun.* **2025,** *16,* 948. doi:10.1038/s41467-025-56234-w
88. Rehm, T. H. *Chem. – Eur. J.* **2020,** *26,* 16952–16974. doi:10.1002/chem.202000381
89. Garg, A.; Rendina, D.; Bendale, H.; Akiyama, T.; Ojima, I. *Front. Chem. (Lausanne, Switz.)* **2024,** *12,* 1398397. doi:10.3389/fchem.2024.1398397
90. Boselli, M. F.; Intini, N.; Puglisi, A.; Raimondi, L.; Rossi, S.; Benaglia, M. *Eur. J. Org. Chem.* **2023,** *26,* e202201309. doi:10.1002/ejoc.202201309
91. Sheikhaleslami, S.; Sperry, J. *Chem. – Eur. J.* **2025,** *31,* e202403833. doi:10.1002/chem.202403833

License and Terms